Department of Chemical Engineering

Imperial College London

Artificial Golgi reactions for targeted glycosylation

Elli Makrydaki

Supervisors: Dr. Cleo Kontoravdi and Dr. Karen Polizzi

Submitted in accordance with the requirements for the degree of

DOCTOR OF PHILOSOPHY

Declaration

I hereby certify that unless otherwise stated, the work within this document is my own. Where data or material from other sources has been used the original author has been appropriately credited.

Copyright

Abstract

N-linked glycosylation constitutes a Critical Quality Attribute for biotherapeutics. It is known to affect drug efficiency, efficacy and half-life. Glycosylation is a non-templated and complex process owning firstly to the promiscuity of the enzymes involved and secondly to enzyme and nucleotide sugar donor availability. This leads to heterogeneity amongst cell-derived glycoproteins, limiting therapeutic efficacy. Production of biotherapeutics focuses on controlling the glycosylation profile to enhance their activity and produce tailored drugs. Despite the intense efforts to control glycosylation, current methods face important limitations including simplicity, cost and lack of homogeneity. The work presented here addresses the current limitations by developing an Artificial Golgi Reactor (AGR) that allows bespoke N-linked glycosylation of glycoproteins in an artificial environment. Specifically, this novel proof-of-concept system comprises immobilised glycosyltransferase (GnTI, GalT) and glycosidase enzymes (ManII). These enzymes comprise a glycosylation pathway where promiscuity naturally exists. A method to express, *in vivo* biotinylate and immobilise GnTI and GalT was developed enabling "one-step immobilisation/purification". ManII was biotinylated using an alternative chemical approach and similarly immobilised. The immobilised enzymes were used in a sequential fashion to reconstruct the N-linked glycosylation pathway on artificial glycans and on a monomeric Fc expressed in glycoengineered *Pichia pastoris*. The spatiotemporal separation tackled enzyme promiscuity, resulting in increased glycoform homogeneity (>95% conversion). Finally, immobilised GalT was used to enhance the galactosylation profile of three IgGs, yielding 80.2 – 96.3 % terminal galactosylation. Enzyme recycling was further demonstrated for 7 cycles, with a combined reaction time greater than 140-hours. The methods and results outlined in this work demonstrate the application of the AGR as an *in vitro* glycosylation strategy applied post-expression that is easy to implement, modular and reusable. Furthermore, it has the potential to be expanded and applied for the large-scale manufacture of bespoke biotherapeutics.

Acknowledgments

Firstly, I wish to express my deep gratitude to my supervisors Dr. Cleo Kontoravdi and Dr. Karen Polizzi. Cleo, thank you for waiting 2 years, for giving me the opportunity to do a PhD and trusting me with this project. Also thank for making my experience as a PhD student, with all the opportunities for networking and your immense support, a memorable one. Karen, thank you for guiding me through the world of biology, your patience and your huge support whenever I needed it. Thank you both for your kindness, your trust, your guidance through difficult aspects of this work and for all your help with the writing. It was a great honour working with you and learning from you.

I am very grateful for all the advice and help I received from Dr. Stuart Haslam regarding the unknowns of mass spectrometry. Furthermore, I would like to thank the Haslam lab members, in particular Dr. Laura Bouché and Dr. Anja Krueger for all the hours they spent trying to help me troubleshoot and analysing my samples. Also, I am thankful for the help of Mr. Roberto Donini and all the work he did and analysis he performed with the mFc.

I wish to acknowledge Dr. David Rose and Dr. Doug Kuntz for so kindly providing DmManII, and Oskar Lange for so kindly offering his mFc plasmid.

I would also like to thank Dr. Rochelle Aw for holding my hand when entering the *Pichia* world. Thank you for all that you taught me and always offering to help in any way that you could. Special thanks also to Dr. Ignacio Moya Ramirez, for always remaining positive when I hated everything and for all your advice and support.

I also thank all my fellow lab and Imperial College London members for their help during the long lab hours and pulling each other up. In particular, I want to thank Mr. Pavlos Kotidis for not only offering his CHO cultures to me, but for all the fun we shared analysing glycans with SCIEX, for supporting me and motivating me. I am very grateful for Miss Chiara Heide, for her friendship. Finally, I am grateful for Dr. Panayiota Pissaridou for teaching me everything about proteins.

Furthermore, I would like to thank my family and especially my mother for all the sacrifices she made after our father passed away, to get me where I am today. I only hope one day I can do the same.

Finally, I want to thank Dr. Matt Haines. Thank you for all your love and support you showed me every single day of this PhD. Thank you for reading every single line of this thesis. Thank you for teaching me how to do research, for pushing me when I wanted to hide, for supporting me when I failed, for celebrating when I succeeded. I would not have done any of this if it wasn't for you. I hope I will soon join you in holding a doctorate and celebrate together somewhere in the sun.

Table of Contents

List of figures

List of Tables

List of equations

List of Abbreviations

General terms

ADCC	Antibody-Dependent Cellular Cytotoxicity
ADCP	Antibody-Dependent Cellular Phagocytosis
AGR	Artificial Golgi Reactor
Asn	Asparagine
BBCP	Biotin Carboxyl Carrier Protein
BMGY	Buffered Glycerol-Complex Medium
BMMY	Buffered Methanol-Complex Medium
CDC	Complement-Dependent Cytotoxicity
CE	Capillary Electrophoresis
CFPS	Cell-Free Protein Synthesis
CHO	Chinese Hamster Ovary
CQA	Critical Quality Attribute
CQA	Critical Quality Attribute
CSTR	Continuous Stirred Tank Reactor
DOE	Design Of Experiments
DTT	Dithiothreitol
ER	Endoplasmic reticulum
Fab	antigen binding Fragment
Fc	crystallizable Fragment
FcRn	Fc neonatal Receptor
GS	Glycine-Serine
HEK	Human Embryonic Kidney
HILIC	Hydrophilic Interaction Liquid Chromatography
HPAEC	High-Performance Anion exchange Chromatography

HPLC	High Performance Liquid Chromatography
HPV	Human Papilloma Virus
IPTG	Isopropyl β-D-1-thiogalactopyranoside
kDa	kilo Dalton
LLOs	lipid-linked oligosaccharides
MALDI-TOF MS	Matrix Assisted Laser Desorption/Ionisation Time of Flight Mass Spectrometry
MBP	Maltose Binding Protein
MW	Molecular weight
MWCO	Molecular Weight Cut Off
NANA	N-Acetylneuraminic acid
NDs	Nucleotide Donors
NGNA	N-Glycolylneuraminic acid
NSDs	Nucleotide Sugar donors
PAD	Pulse Amperometric Detector
PCR	Polymerase Chain Reaction
PTMS	Post-Translational Modifications
RPLC	Reverse Phase Liquid Chromatography
s.f.	scale factor
SDS-PAGE	Sodium Dodecyl Sulfate Polyacrylamide Gel Electrophoresis
Ser	Serine
SF	Soluble Fraction
STR	Stirred Tank Reactor
StV	Streptavidin
Thr	Threonine
Xaa	Any amino acid
αMF	Buffered Methanol-Complex Medium
µRPLC-ESI-MS	Microreverse-phase liquid chromatography-electrospray ionization-tandem mass spectrometry

Species

S. cerevisiae	*Saccharomyces cerevisiae*
E. coli	*Escherichia coli*
P. pastoris	*Pichia pastoris*
C. jejuni	*Campylobacter jejuni*
Sf	*Spodoptera frugiperda*
Dm (or S2)	*Drosophila melanogaster*
N. tabacum	*Nicotiana tabacum*
G. gallus	*Gallus Gallus*
C. hircus	*Capra Hircus*
A. pleuropneumoniae	*Actinobacillus pleuropneumoniae*

Proteins (enzymes, antibodies, etc)

ApNGT	N-linked GT from *A. pleuropneumoniae*
bnAbs	Broadly neutralising Antibodies
chIgG	Humanised IgG produced in CHO cells
DmManII	*Drosophila melanogaster ManII*
ENGases (EndoS, EndoM, EndoF etc.)	Endoglycosidases (S, M, F etc)
EPO	Erythropoietin
FucT	Fucosyltransferase
GalT	Galactosyltransferase (β-1,4- Galactosyltransferase)
GI	Glucosidase I
GII	Glucosidase II
GnTI	N-acetylglucosaminyltransferase I (N-acetylglucosaminyltransferase I)
GnTII	N-acetylglucosaminlytransferase II
GnTIII	β1,4-*N*-acetylglucosaminyltransferase III
GT	Glycosyltransferase
hGalT	Human GalT

hGnTI	Human GnTI
hIgG	IgG from human serum
IgE	Immunoglobulin E
IgG	Immunoglobulin G
mAbs	monoclonal Antibodies
ManIA	Golgi Mannosidase 1A
ManII	Golgi mannosidase II (α -1,2- Mannosidase II)
MnsI	ER mannosidase
NtGnTI	*Nicotiana tabacum* GnTI
OST	Oligosaccaryltransferase
PglB	Protein glycosylation enzyme B for bacterial N-linked glycosylation in *C. jejuni*
PnGaseF	Peptide -N-Glycosidase F
rIgG	IgG from rabbit serum
SiaT	Sialyltransferase
SrtA	Sortase A

Glycans, nucleotide sugar donors and nucleotide donors

CMP-NANA	Cytidine Monophosphate N-acetylneuraminic acid
GalGM3	$GalGlcNAcMan_3GlcNAc_2$
GalGM4	$GalGlcNAcMan_4GlcNAc_2$
GalGM5	$GalGlcNAcMan_5GlcNAc_2$
GalNAc	N-acetylgalactosamine
GlcNAc	N-acetylglucosamine
GM3	$GlcNAcMan_3GlcNAc_2$
GM4	$GlcNAcMan_4GlcNAc_2$
GM5	$GlcNAcMan_5GlcNAc_2$
LacNAc	N-acetyllactosamine

M2	$Man_2GlcNAc_2$
M3	$Man_3GlcNAc_2$
M5	$Man_5GlcNAc_2$
M6	$Man_6GlcNAc_2$
M8	$Man_8GlcNAc_2$
M9	$Man_9GlcNAc_2$
UDP-Gal	Uridine diphosphate galactose
UDP-Glc	Uridine diphosphate glucose
UDP-GlcNAc	Uridine diphosphate N-acetylglucosamine

Chapter 1: Introduction

1.1. Glycosylation and modern biotherapeutics

The use of biological molecules as therapeutics started in the 1980s with the development and use of recombinant insulin and recombinant erythropoietin (EPO)[1]. Since then, the growing knowledge of the genome and of cellular processes, coupled with the need to develop new, higher efficacy and more targeted drugs has driven research into the development and use of biopharmaceutics. Compared to conventional chemical drugs, biotherapeutics exhibit higher specificity and can be tailored based on the disease profile[2].

Glycosylation has an important effect on the properties of proteins making it an essential process in production. It can improve their pharmacological properties such as affinity, absorption, distribution, excretion, stability, response time, half-life etc.[3–11]. Because of this, efforts are made to engineer biotherapeutics carrying a desired glycan structure[5–7].

Currently, more than 50% of biotherapeutics are glycosylated proteins[4,12]. Monoclonal antibodies (mAbs) of the immunoglobulin G (IgG) family and single chain Fc fragments of IgG, lead the biotherapeutics group[1,12]. As discussed in **Section 1.1.2.1** glycosylation in the Fc domain of mAbs governs important properties such as efficacy and stability. Finally, viral glycoproteins are of increasing interest in the manufacture of glycoconjugate vaccines[13–16].

Understanding the effects of glycosylation will pave the way to design and develop new and targeted drugs.

1.1.1. Glycosylation

Glycosylation is the post-translational covalent attachment of sugar moieties to biological molecules such as proteins. It is one of the most common post-translational modifications with more than 50% of human proteins expected to be glycosylated[17]. The process begins in the rough endoplasmic reticulum (ER) and is completed in the Golgi apparatus (**Figure 1-1**). In contrast to peptide and nucleotide synthesis, there is no template to copy from and synthesise the attached glycan structure, hence a diverse and highly complex profile of glycoproteins is typically observed[18,19]. In addition, in contrast to DNA/RNA and peptides, glycan moieties can be branched within the structure[20].

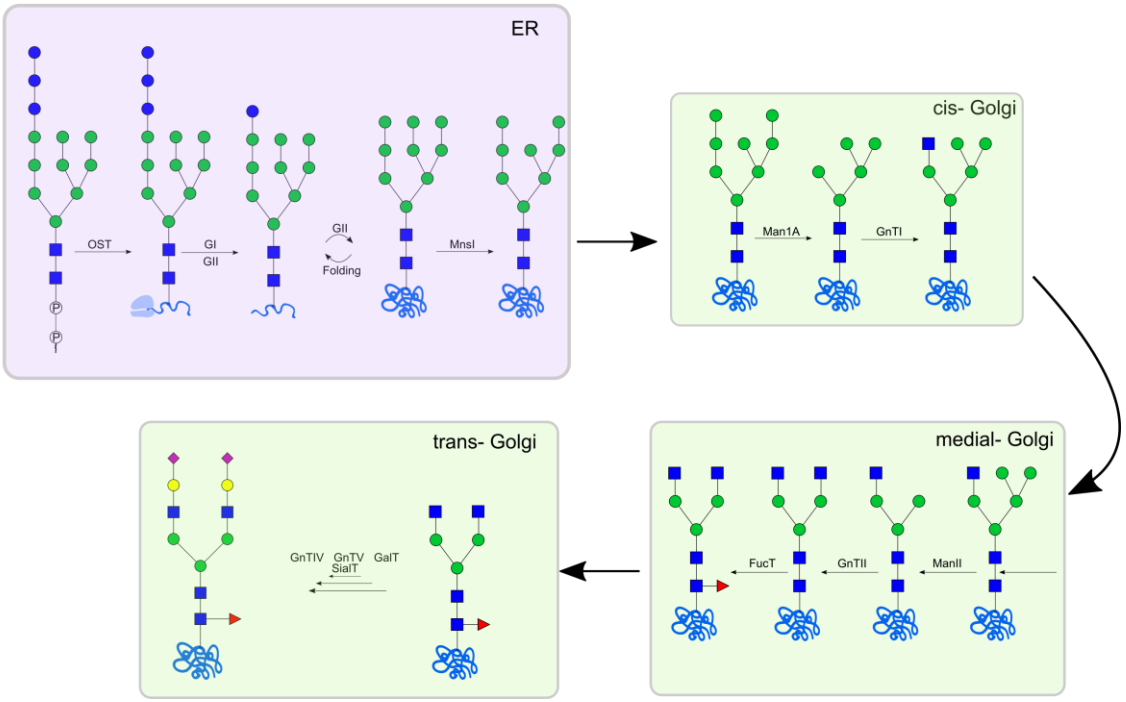

Figure 1-1: N-linked mammalian glycosylation process. It initiates in the ER with the transfer of the sugar assembly from the dolichol diphosphate to the asparagine residue of a newly formed protein. Glucosidases react sequentially to remove the remaining glucose molecules whilst the protein folds and assumes its tertiary structure. Further glycan trimming and maturation occurs in the Golgi apparatus and its various compartments in a sequential manner. OST, oligosaccharyltransferase; GI, glucosidase I; GII, glucosidase II; MnsI, ER mannosidase; Man1A, Golgi Mannosidase 1A; GnTI, N-acetylglucosaminyltransferase I; ManII, Golgi mannosidase II; GnTII, N-acetylglucosaminlytransferase II; FucT, fucosyltransferase; SiaT, sialyltransferase, GalT, galactosyltransferase.

The two main protein glycosylation classes are O-linked and N-linked glycosylation. The two differ greatly in synthesis and structure[21]. O-linked glycosylation occurs in the Golgi apparatus with the attachment of N-acetylgalactosamine (GalNAc) to a Serine/Threonine (Ser/Thr) residue. In contrast to N-linked glycosylation, any Ser/Thr residue can serve as a glycosylation site making it difficult to predict the potential sites[1]. The oligosaccharide chain is further expanded by glycosyltransferases. These are enzymes residing in the ER and Golgi apparatus, resulting in glycoproteins with highly diverse profiles[22,23].

N-linked glycosylation is the covalent attachment of oligosaccharides to Asparagine (Asn) residues following the consensus Asn-Xaa-Ser/Thr, where Xaa can be any amino acid except proline[21]. The tertiary structure does not allow all Asn residues to be glycosylation sites, enabling prediction of

which residues will be glycosylated[1]. It begins in the rough ER with a precursor $Glc_3Man_9(GlcNAc)_2$ molecule attached to a dolichol molecule which is transferred by an oligosaccharide-protein transferase to the Asn residue of the peptide[22] (**Figure 1-1**). The core glycan structure is further modified by glycosyltransferases.

N-linked glycosylation takes place in all eukaryotic cells and in some bacterial cells[24]. Glycosylation profiles from vertebrate, plant and insect cells share a core glycan structure but their final profiles differ greatly.

1.1.1.1. Enzymes in glycosylation

All steps in the glycosylation process are regulated by enzymes in a series of sequential reactions. In the ER, glucosidases and mannosidases trim down the initial glycan to create the core structure. This structure is further elongated in the Golgi by a number of enzymatic reactions catalysed by various glycosyltransferases and a mannosidase, leading to linear or branched oligosaccharides (**Figure 1-1**). The large number of glycosyltransferases and the enzyme preference for different substrates lead to a complex network of possible N-linked structures.

Glycosyltransferases (GTs) are a large group of membrane-bound enzymes that catalyse the formation of a glycosidic bond via a sugar transfer reaction to substrates such as proteins, lipids, DNA and other small molecules[25]. They are located in the ER and the Golgi apparatus in specific compartments (Cis-trans-medial- Golgi) to achieve sequential reactions (**Figure 1-1**)[25]. They are grouped into families based on their fold type i.e. GT-A, GT-B, GT-C, GT-D and GT-E, their amino acid similarities, their catalytic mechanism (retaining or inverting stereochemistry) and substrate specificity[26,27].

GTs exhibit high acceptor specificity with a few exceptions. These include galactosyltransferases which act upon any free GlcNAc; human fucosyltransferase III which can form different glycosidic bonds when attaching a fucose to the existing carbohydrate structure; and fucosyltransferases III–VII which catalyse the same bond formation, using N-acetyllactosamine as a substrate on any glycan[25,28]. In addition to the acceptor substrate, GTs also exhibit high sugar donor specificity[25]. The majority of GTs use activated nucleotide sugar donors (Leloir GTs) and some use non-activated co-substrates such as sugar phosphates (Non-Leloir GTs)[27,29]. Finally, some GTs require metal cofactors for their catalytic activity (e.g. GT-A) while others are independent (e.g. GT-B)[27].

1.1.2. Effects of glycosylation on biotherapeutics

Glycosylation has several effects on biotherapeutic proteins. As previously mentioned, glycosylation improves protein stability. Newly modified proteins carry a specific glycan structure which will act as a recognition site for proteins that mediate folding (e.g. lectins)[30]. This improves folding and overall solubilisation and stabilisation of the molecule[1,2]. The recognition sites serve as tags for trafficking of a protein which can have an effect in secretion e.g. glycosylation improves secretion of EPO[2,31]. N-linked glycosylation of certain residues also improves stabilisation as it prevents aggregation and precipitation e.g. glycosylation of α-galactosidase at Asn215[2,32] (**Table 1-1**). This is particularly important in drug development as it facilitates drug distribution and increases its efficacy once administered[2]. Stabilisation with glycosylation is extended through protection against various chemical and physical instabilities such as oxidation, deamidation, chemical crosslinking, in addition to thermal, chemical and pH denaturation[2].

Glycosylation of certain Asn residues alters the structure of the molecule protecting it from proteolytic degradation and removal from circulation, thus improving protein stability and half-life[30]. Specific glycoforms can also improve half-life. Proteins with a higher concentration of sialic acids have an improved half-life compared to proteins with a higher concentration of mannose[1,31]. A structure rich in sialic acids makes the molecule more hydrophilic thus more soluble and stable while it offers a shielding to protect from proteolytic degradation[33]. Furthermore, sialylated proteins are not targeted by asialoglycoprotein receptors and consequently are not cleared from the circulation[10,19].

Glycans on therapeutic proteins have an important role in enzyme binding properties. Certain glycosylated enzymes target and bind toxins produced by bacteria or enzymes produced by viruses, thus inhibiting their action[34]. Furthermore, the correct glycan structure allows binding of the drug to the appropriate receptors improving its uptake and subsequent action. For example terminal mannose on glycans of glucocerebrosidase enables binding to macrophage cell surface receptors enabling enzyme replacement treatments[31].

Glycosylation also plays a significant role in the manufacture of glycoconjugate vaccines. Most viruses have their surface decorated by glycoproteins called envelope proteins and they are often the target for vaccine design. Although glycosylation is of great importance to the virus itself as it can mask the antibody-binding sites, it has been shown in many cases that the glycans on the envelope proteins serve as targets for broadly neutralising antibodies (bnAbs) that bind carbohydrates[13–16,25,26]. The type and site of glycans can also have an impact on binding efficacy as in

the case of the HIV gp120 envelope protein[37–40]. Glycans in gp120 vary from high mannose to complex glycoforms and can attract different antibodies. This heterogeneity poses a challenge when identifying possible antigen targets[40].

Table 1-1: Glycoengineered drugs and the effect of glycosylation has on each of them [2,31,32,41].

Drug	**Effect of glycosylation**
Therapeutic enzymes e.g. human glucocerebrosidase	Targeting and activity
Stimulating factors e.g. Granocyte™	Protects from degradation and pH denaturation Prevents chemical cross linking which leads to deactivation
α -galactosidases e.g. Fabrazyme™, Replagal™	Protects from aggregation
Growth factors, Erythropoietin e.g. Epogen™	Protects from oxidation, pH and thermal denaturation Affects secretion
Lipases e.g. Merispace	Protects from degradation
Thyroid-stimulating hormone e.g. Thyrogen	Protects from degradation
Cytokines-Intherferones (e.g. Actimmune)	Enhanced activity, increased half-life, protects from degradation
β Interferons (e.g. Rebif™, Avovex™)	Protects from chemical crosslinking and thermal denaturation Increased solubility
mAbs	Protects from papain digestion, affects antigen binding
Urokinases e.g. Abbokinase™	Protects from thermal denaturation and degradation
Follicle-stimulating hormones e.g Gonal-F™	Protects from thermal denaturation
RNAses e.g. Onconase™	Increases toxicity against cancer cells

1.1.2.1. Effect of glycosylation on monoclonal antibodies

MAbs currently dominate the biotherapeutic market[4]. Most of the recombinant mAbs are based on immunoglobulin (IgG). They consist of four polypeptide chains, two heavy and two light, which form the crystallisable fragment (Fc) and the antigen-binding fragment (Fab).

The Fab region contains the site of antigen binding and in some cases can be decorated with complex hybrid N-linked glycans[42,43]. Although the exact role of Fab glycosylation is still a topic of research, results have shown the importance of the attached glycans to antigen recognition and subsequent binding[43]. Absence of glycans or structural heterogeneity results in significantly decreased binding[27,43,44]. Based on the glycan structure in the Fab region, the advantages of

glycosylation associated with increased half-life, activity and protection from aggregation apply in mAbs[45,46,47].

The Fc region carries the receptor binding site and the core N-linked glycosylation of mAbs[48]. Glycosylation of the Fc region is essential for binding to receptors and initiation of downstream effector functions[3,7,42]. The natural heterogeneity of glycans attached to the Fc of antibodies also determines their binding properties and efficacy as the Antibody-Dependent Cellular Cytotoxicity (ADCC), Antibody-Dependent Cellular Phagocytosis (ADCP) and Complement-Dependent Cytotoxicity (CDC), the main killing mechanisms, can be either enhanced or decreased[42] (**Table 1-2**). For example, lack of core fucose is the predominant reason for increased ADCC while in fucosylated mAbs ADCC often depends on the presence of galactose[7,49–54]. Additionally, sialic acid and galactose residues on IgGs enhance the binding to receptors (i.e FcγRIIIA), thus increasing the efficacy, whilst sialic acids are also known to offer anti-inflammatory properties[17,49,50,55–58]. Finally, the presence of oligomannose structures can reduce CDC while it increases ADCC[59].

Of interest is the impact of sialylation on the half-life of IgGs. In contrast to other proteins where sialylation prevents removal by asialoglycoproteins, this does not seem to be the case for IgGs[10,58]. This is because IgGs are removed by the FcRn receptors that are independent of glycosylation[10]. However, the presence of sialic acids, protects from aggregation and proteolytic degradations thus increasing serum half-life of IgGs.

An important drawback of glycosylated antibodies and other proteins is the potential for immunogenicity. Immunogenicity can be induced from unnatural glycans or misfolding of the overall molecule[60]. Native antibodies can then destroy or block the action of a therapeutic protein[61]. An example is the mAb cetuximab, an IgG1 molecule developed to treat colorectal cancer[60,62]. Cetuximab is recombinantly produced as a chimeric mouse-human antibody in murine cell lines (SP2/0), leading to a non-human α-1,3-galactose residue. Upon administration, it induced an immune response as native IgE antibodies reacted to the unnatural sugar, causing the development of anaphylaxis[62]. Furthermore, the absence of glycans can cause improper folding leading to aggregation and consequently immunogenicity. For example, human β-interferon produced in *E. coli* forms aggregates as it is not glycosylated, causing an immunogenic response[60,62].

Table 1-2: Effects of Fc glycosylation on monoclonal antibody properties.

Glycan type	Impact on mAb properties
Galactose	Increases CDC[7]. Increases ADCP[63]. Some positive effect on ADCC[64]. α-(1,6)- galactose has been shown to increase ADCC[63]. Increased receptor affinity[64–66]. Anti-inflammatory properties[67].
Lack of core fucose	Significantly increased ADCC[51,53] Increased receptor binding[54,7].
Mannose	High mannose structures (M5-M9) induce clearance[33,59]. M5 structures have increased ADCC[59]. M5 structures have decreased CDC[59].
Sialic acid	α-(2,6)- sialic acids are known to have anti-inflammatory properties[56,68] Increases serum half-life[57].
Bisecting GlcNAc	Offers thermal stability[69].

1.2. Glycoengineering for tailored biotherapeutics - Efforts to control glycosylation

The importance of glycosylation in the context of biotherapeutic proteins is well established and already applied in drug production[4–11,70,71]. As discussed previously, it offers desirable characteristics such as improved pharmacokinetic properties, half-life and efficacy. Furthermore, different beneficial properties arise from different glycans. These include increased sialylation for higher efficacy and half-life, galactosylation for increased CDC and hypermannosylation for specific binding as in the case of specific tumour antigens[72]. In addition, as the disease profile varies among patients, biotherapeutics with defined glycan structures are a means to develop personalised treatments[73]. Furthermore, as glycosylation enhances stability and solubility, higher titres of mAbs can be produced thus reducing their cost[42].

Glycosylation constitutes a Critical Quality Attribute (CQA) that needs to be regulated in biotherapeutic production[74]. However, glycosylation is a complex process, regulated by multiple

enzymes. Although these enzymes are located in defined compartments in the Golgi there is still competition for the same substrate. Furthermore, some enzymes can recognise multiple substrates e.g. galactosyltransferases add a galactose moiety to any free GlcNAc residue regardless of the branch[33,75]. This enzyme promiscuity as well as the substrate and the site availability lead to highly diverse glycoforms (micro-heterogeneity) and variable site-occupancy (macro-heterogeneity)[33].

It is considered desirable to minimise heterogeneity in the glycosylation profile of biotherapeutic proteins[33,76]. This is because different glycoforms have different properties, altering the efficacy and safety of the resulting biotherapeutic. Furthermore, glycan heterogeneity can cause structural changes in proteins altering their properties. For example, underglycosylation can increase proteolytic degradation and subsequent clearance[2,58] or it can alter the binding sites and lower the efficacy of antibody-drug conjugates[33,77].

Defining and controlling the glycosylation profile of drugs as demonstrated in clinical trials helps ensure the required beneficial properties in accordance with the safety and efficacy[11]. Towards this direction, various methods have been developed. Current techniques include the *in vivo* engineering of the native glycosylation pathways in mammalian cells and other hosts such as plants, insects, bacteria etc. The host is selected based on similarities to human glycosylation, flexibility for genetic modifications, production yield and ease of manipulation. Furthermore, there are various *in vitro* glycoengineering techniques for more control over the process to achieve homogeneity and bespoke glycans. Finally, metabolic glycoengineering is applied to control the culture environment and subsequently the metabolic pathways regulating glycosylation.

1.2.1. *In vivo* glycoengineering

There is an increasing interest in producing biotherapeutics with tailored glycosylation using various *in vivo* glycoengineering techniques that allow the modification and manipulation of native glycosylation pathways in host cell lines. A typical technique is gene knockout, where the genes coding for glycosyltransferases are deleted or inactivated. This results in an altered glycosylation pathway and the production of a humanised product[78–80]. Certain glycosyltransferases can also be selectively inhibited by other enzymes to avoid undesired modifications[34] or overexpressed to achieve a high concentration of the target glycan structure[18,34]. Furthermore, N-linked glycosylation heavily depends on the availability of the Nucleotide Sugar Donors (NSDs), the substrates of glycosyltransferases[81,82]. Hence, targeting the NSD biosynthetic pathway is a strategy often applied to increase their concentrations and enhance the desired glycosylation. The selected technique heavily depends on the choice of cell line and the end application.

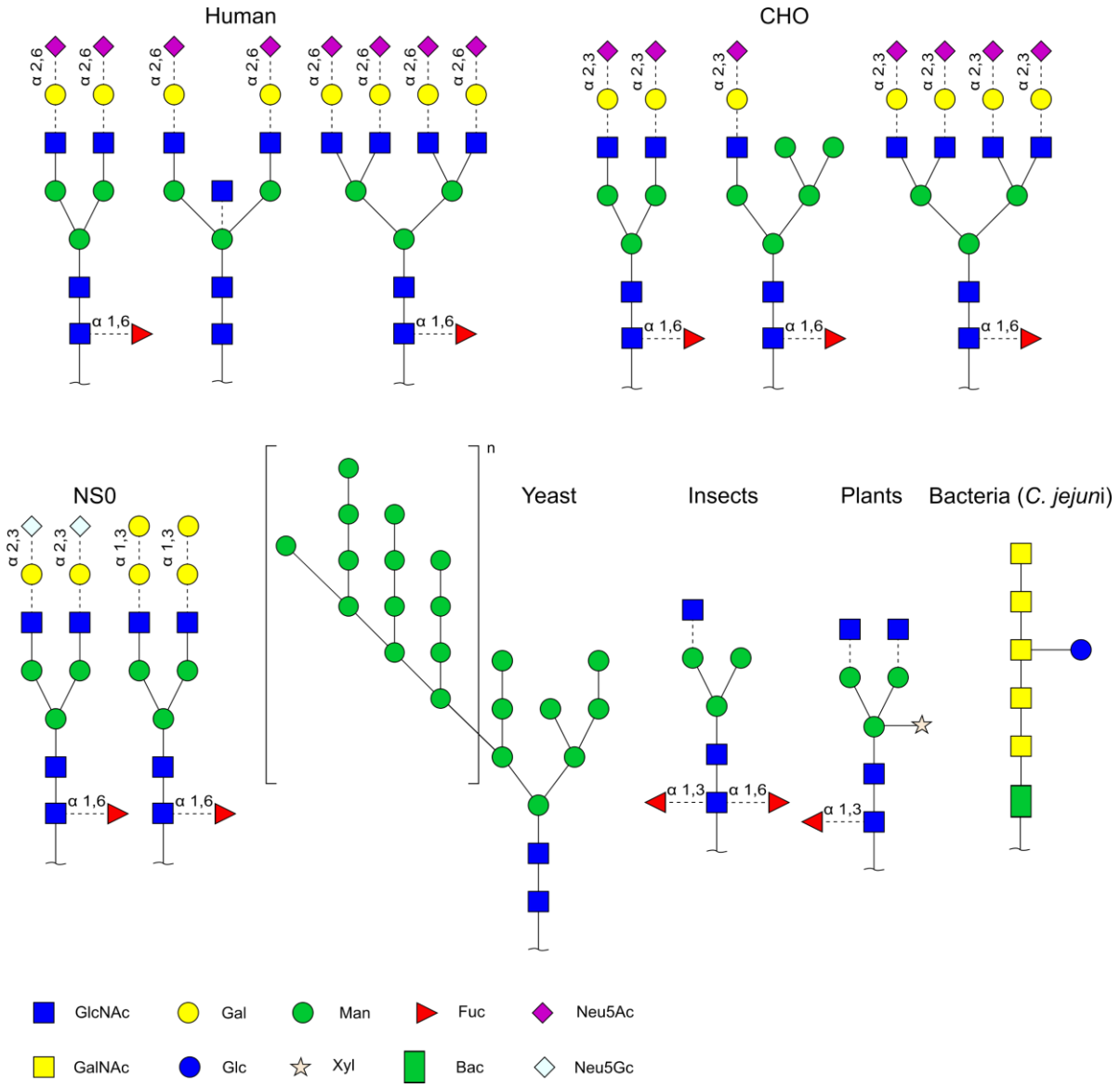

Figure 1-2: Common glycan structures of recombinant proteins produced in different organisms. The dotted lines represent variable glycans that might not be present.

1.2.1.1. Glycoengineering in mammalian cells

Mammalian cells are the preferred hosts for glycoprotein production as they can produce highly complex and human-like glycoforms (**Figure 1-2**). Common mammalian cell lines used for glycoprotein production are Chinese Hamster Ovary (CHO) cells, NS0 mouse myeloma cells and Human Embryotic Kidney (HEK) cells.

Human cell lines, e.g. HEK293, PER.C6 and HT-1080, are already used to produce recombinant therapeutic proteins and antibody fragment fusion proteins (Fc proteins). These include: Dulaglutide for type 2 diabetes (TRULICITY®, produced in HEK293), rFVIIIFc for haemophilia A (produced in HEK293) and α galactosidase (Replagal®, in HT 1080). As there is no risk for immunogenic post-translational modifications and the fact they can be grown in serum free media preventing contamination, makes them ideal hosts[83,84,85]. As such, human cell lines are attractive hosts for therapeutic protein production and glycoengineering[86,87]. An interesting approach is GlycoDelete developed by Meuris and co-workers and demonstrated in HEK 293S cells[88]. It combines the knockout out of a glycosyltransferase encoding gene with simultaneous overexpression of an enzyme to produce small sialylated oligosaccharides with high homogeneity. In particular, inactivating the gene encoding for GnTI (the glycosyltransferase that initiates N-linked glycosylation) and overexpression of endo-β-N-acetylglucosaminidase (enzyme which trims down the glycan structure to a GlcNAc residue) led to substrates suitable for galactosyltransferases and sialytransferases[88]. Similarly, HEK-293 cell lines lacking GnTI activity, allow for oligomannose structures (M5) to be produced in high yields[89,90]. Despite the progress and developed methods, genetic modifications are not always simple and production yields can be low[91]. Even with the advent of genome editing, the production of optimised human cell lines is challenging. Furthermore, they have been less commonly used for biotherapeutic production compared to alternative hosts, implying there is less experience and knowledge[83].

CHO cell lines are currently the workhorse for expression of recombinant glycoproteins and mAbs[4]. Currently, more than 60% of mAbs are produced in CHO cells[4]. As shown in **Figure 1-2**, they can produce highly complex and human-like glycosylation patterns, a key factor to avoid immunogenicity. They are well-studied cells, robust and can be scaled up. Drugs produced in CHO cells include mAbs (Rituxan™, Herceptin™), cancer treatment supportive hormones (Aranesp™) and fusion proteins (Ziv-aflibercep™)[92]. To control the glycosylation profile and improve antibody characteristics (e.g. ADCC and serum half-life), gene knockouts and overexpression of selected enzymes have been successfully applied. Notable examples of developed methods include POTELLIGENT® (Kyowa Hakko Kirin's & Lonza) where a α-1,6-fucosyltransferase (*FUT8*) knockout line produces afucosylated mAbs[93] and GlycoMAb® where β1,4-*N*-acetylglucosaminyltransferase III (GnTIII) is overexpressed and inhibits core-fucosylation[94]. These technologies resulted in the first-approved glycoengineered mAbs for cancer, mogamulizumab (POTELLIGENT®) and obinutuzumab (GlycoMAb®) as well as mAbs for asthma i.e. Benralizumab (POTELLIGENT®). Of particular interest is a glycoengineered CHO cell line to finely tune the levels of galactosylation and fucosylation[95]. Specifically, the researchers used CRISPR/Cas9 to knockout *FUT8* and *β4GalT1*, the genes encoding

for the enzymes responsible for core fucosylation and terminal galactosylation respectively, while introducing new synthetic *FUT8* and *β4GalT1* gene circuits. The latter were induced by the administration of small molecule inducers. By regulating the concentration of inducer molecules, the levels of fucosylation and/or galactosylation were modified. CRISPR/Cas9 was also used to create GnTI deficient CHO cell lines. These lines were developed in a study by Byrne and co-workers to produce HIV-like oligomannose envelope proteins for the design and study of vaccines[96]. Finally, modifying the pathway regulating the formation of nucleotide sugar transporters, can enhance the concentration of NSDs in the Golgi. This was demonstrated in the work by Wong and co-workers, where overexpression of a sialic acid transporter, increased the overall sialylation of interferon-γ[97]. Even though glycosylation in CHO cells is similar to humans, there is still risk due to undesirable immune responses (**Table 1-3**). Finally, despite successful production of glycosylated mAbs in CHO cells, the glycan structure in the Fc region is heterogeneous which decreases their half-life[18] and can compromise efficacy.

Although progress in mammalian cell line glycoengineering is evident, engineering of their complex biosynthetic pathways requires time consuming methods in order to design, construct and identify the right clone[98]. The lack of strict control over the pathway manipulation and availability of enzymes and sugar donors does not ensure homogeneity. In some cases this can lead to unpredicted and undesired structures, e.g. 9 LecR CHO mutants produced glycoforms with non-predicted N-glycans[99]. Furthermore, scaling up of mammalian cell lines is complicated by the increased concentration of growth inhibitory metabolites such as lactate and ammonium that accumulate during commonly used batch and fed-batch reactors[100,101].

1.2.1.2. Glycoengineering in transgenic animals

Transgenic animals such as goats, mice, hens and cows are currently used for therapeutic protein production[102–104]. Compared to host-cell production methods, it is a cost-effective technique due to the cheaper capital costs (cost of raising animals versus bioreactors), cheaper scaling-up and high production yields[102]. Examples of therapeutic proteins produced in transgenic animals, include Ruconest™ a type of C1 esterase inhibitor protein produced in rabbits' milk and Atryn, a recombinant antithrombin α protein produced in goats' milk[102].

To produce human-like antibodies, the animals' native antibodies have been replaced with human orthologs using various genetic manipulation techniques[104,105]. As a result, transgenic animals can produce fully human antibodies in their milk, blood or egg white. This paves the way for transgenic animals to be used as a mAb discovery platform. One application of this is the XenoMouse, a

transgenic mouse platform with a fully human antibody machinery which lead to the discovery of panitumumab, a monoclonal antibody for colorectal cancer[106]. However, the achieved antibody yields were low. To overcome this, researchers developed chimeric lines to produce humanised antibodies with a murine constant region[78,105].

Despite the upstream benefits of using transgenic animals, it is challenging and potentially harmful to alter the native glycosylation. This might not be necessary if the glycosylation is quite similar to humans, however its essential if immunogenic sugars are present such as N-acetylneuraminic acid and α 1,3 galactose in mice (**Table 1-3**). As such, genetic engineering of animals and their use for human protein production, which in some cases can also cause them to have an immunogenic response, raises a lot of ethical concerns[107,108].

1.2.1.3. Glycoengineering in yeast

Yeast strains are currently used for biotherapeutics production as they are cheaper than mammalian production platforms, easier to grow whilst achieving high production yields and purity[98,109–112]. Examples of drugs produced in yeast include growth factors for cancer treatment, recombinant hormones e.g. insulin analogues, vaccines e.g. human papillomavirus vaccine (in *Saccharomyces cerevisiae*) and antibody fragments e.g. Nanobody ALX0061[4,92,100]. However, as yeast is not a mammalian organism, "humanisation" of the native glycosylation is necessary when tailored biotherapeutics are required.

Yeast as a eukaryotic organism performs co- and post-translational modifications including N-linked glycosylation. The sugar structure of the proteins leaving the ER is identical to those of mammalian cells. However, glycan differentiation occurs in the Golgi apparatus and as a result, the final glycosylation profile in yeast is quite different to humans (**Figure 1-2**). It consists of multiple mannose residues while there are no complex or hybrid glycans. This hypermannosylation is not desired as it can lower the half-life of antibodies and might cause immunogenicity (**Table 1-3**). Despite the drawbacks, yeast is a good candidate for glycoengineering. It is a well-studied and an easy-to-grow organism, requiring simple genetic modifications to achieve glycoforms similar to humans The two main cell lines used for glycoengineering and glycoprotein production are *S. cerevisiae* and *P. pastoris*.

S. cerevisiae can add more than 100 mannose residues on the expressed proteins. This is due to multiple genes controlling hypermannosylation in the Golgi e.g. *Och1, Mnn1p, Mnn6p* etc[111,113]. Homologous recombination is used to knockout a combination of these genes and introduce

heterologous enzymes to produce human-like glycoforms. An example of this strategy is GlycodExpress™ which was used to produce humanised EPO[114].

In contrast to *S. cerevisiae,* proteins produced in *P. pastoris* have a smaller number of mannose residues (≤ 40 mannoses). This is due to hypermannosylation being controlled by the expression of one gene, *Och1*, rather than multiple ones[115]. The glycoengineering technique to humanise *P. pastoris* is quite similar to GlycodExpress™. It requires the disruption of *Och1,* the gene encoding for Och1p-mannosyltransferase, and the stepwise introduction of non-native glycoenzymes[109,110,112,114,116]. It is important to mention that the catalytic domains of these enzymes are fused with native or other retention signal peptides to allow their correct localization in the Golgi apparatus of the yeast strain (*P. pastoris* and *S. cerevisiae)*. This has led to the humanisation of the *P. pastoris* glycosylation pathway. Two prominent illustrations of this approach are GlycoFi and GlycoSwitch®. Examples of humanised proteins produced in these platforms include, sialylated EPO and a monoclonal antibody, rituximab with enhanced efficacy due to tailored glycosylation[116,117].

Despite the progress in yeast glycoengineering there are still key limitations. Disrupting the native glycosylation modifies the integrity of the cell-wall leading to constraints on cell growth[5,109,111]. This is evident in multiple cases of engineering *S. cerevisiae,* where glycoengineering produced unhealthy cell lines[111,112]. This restricts the use of yeast at a commercial scale[92]. Furthermore, O-linked glycosylation pathways are still intact and non-human and potentially immunogenic proteins are still produced[5,109]. To address this, it is important to disrupt the native O-linked glycosylation which is still a challenge as it negatively affects cell-wall formation which in turn negatively impacts cell proliferation[5]. Finally, glycoform homogeneity is not always ensured. This can be due to multiple genes involved in the hypermannosylation process (i.e. *S. cerevisiae*) requiring more genes interruptions or due to the natural enzyme competition in glycosylation pathways. Interestingly, in a GlycoSwitch® strain producing mainly M5 glycans (SuperMan5®), while homogeneity was high (>80%), off-target and non-natural glycans were detected[118]. This can also pose potential risks when health and safety are required.

1.2.1.4. Glycoengineering in bacteria

Bacteria have various mechanisms to form repeating sugar moieties known as polysaccharides. Their glycan structures are highly varied and have little similarities to their eukaryotic counterparts[119,120] (**Table 1-3** & **Figure 1-2**). They can be found on the cell surface of bacteria and can act as antigens, e.g. O-linked lipopolysaccharides[119,120]. As a result, bacteria are used for the production of antigens as is the case for glycoconjugate vaccines[121].

Some bacterial species are also able to perform protein glycosylation. The N-linked glycosylation mechanism is similar to that in eukaryotic organisms, i.e. oligosaccharides are formed on the surface of lipid carriers on the inner side of membranes then transferred by oligosaccharyltransferases to a conserved amino acid sequence on acceptor proteins and then further elongated by resident glycosyltransferases[38,122,123]. Interestingly, these bacterial enzymes are very promiscuous as they can recognise a variety of formed glycans to transfer to the acceptor protein[120,122].

The first fully characterised N-linked glycosylation system in bacteria was that of *Campylobacter jejuni* (**Figure 1-2**)[123,124]. A significant achievement is the successful transfer of the *C. jejuni's* glycosylation machinery to *E. coli*[125,126]. This was a turning point for glycoengineering in bacteria as *E. coli* is easy to manipulate genetically, has fast growth rates and produces high yields of recombinant proteins. A noteworthy example is the work by Valderrama-Rincon and co-workers as they synthesised a human like N-linked glycosylation pathway in *E. coli*. Briefly, co-expressing four yeast glycosyltransferases enabled the formation of the human-like core glycan $Man_3GlcNAc_2$[126]. This glycan was subsequently transferred by *C. jejuni's* oligosacchalytransferase PglB onto the target recombinant proteins such as the Fc domain of an IgG or a human growth hormone. The authors envisioned further modifications of this glycan by the introduction of more glycosyltransferases.

The ease of genetic manipulations and the incorporation of glycosylation machinery in bacteria such as *E. coli* has led to the development of a platform to produce bioconjugates in a fast and simple way compared to the usual semi-synthetic ways[14]. Examples include vaccine glycoconjugates and their successful use in clinical trials (e.g. S. *dysenteriae* type 1 and ExPEc) and biomarkers used in diagnostics (e.g. Brucellosis antigens)[46,128,129].

Although there have been significant advances in bacterial glycoengineering, there are still important limitations that need to be addressed. The N-linked glycosylation consensus sequence that *C. jejuni's* PglB recognises is different to the eukaryotic as it follows the Asp/Glu–X_{aa}–Asn–X_{aa}–Ser/Thr motif (X_{aa} is any amino acid except proline)[130]. Therefore, target proteins have to be engineered to carry the consensus site, which can in turn interfere with protein folding, purification and function. Alternatively, genetic engineering is required to change the specificity of the enzyme or bioinformatic tools must be used to screen for enzymes able to identify different consensus sites but similar to eukaryotes[121,131–133]. The latter steps are also necessary as it has been shown that although the bacterial oligosaccharyltransferases are promiscuous, the glycans to be transferred need to have an acetomido group in the reducing end of the sugar chain[122]. Finally, productivity and yields are low as the metabolic burden on the cell is significantly increased[126,134]. As such, further optimisation of energy sources might be required.

1.2.1.5. Glycoengineering in plants

Plants are attractive production systems with significant advantages to mammalian cells due to less maintenance costs and smaller incubation times leading to high productions and easy scale up[18,135]. N-linked glycosylation in plants is simple as it consists of oligomannose or small core glycans. Plants can also produce terminally galactosylated structures but in low abundance. Despite the simplicity, all the glycoforms include the immunogenic β-1,2 xylose and α-1,3 fucose sugars (**Figure 1-2** & **Table 1-3**). However, the lack of complexity of the native glycosylation pathway in combination with the available genetic tools, enables targeted glycoengineering.

Similarly to yeast, glycosylation pathways in plants can be altered and humanised[18]. A widely applied technique is the use of small RNA molecules (RNAi) which allows the knockdown of genes responsible for the non-human fucosylation and xylosylation[136,137]. Alternatively, only a couple of core gene deletions e.g. knockout of α1,6 fucosyltransferase gene (ΔXF) or knockout of both α-1,6 fucosyltransferase and β-N-acetylhexosaminidases genes (ΔXF, ΔHEXO), lead to the core eukaryotic glycan $GlcNAc_2Man_3GlcNAc_2$[136,137]. Another available tool, is GlycoDelete, as the deletion of the GnTI gene gives glycans lacking xylose which can be then further modified[136].

Some plant glycoengineering achievements worth mentioning include the use of *Nicotiana benthamiana* to produce a mixture of chimeric mAbs lacking core fucose and xylose against the EBOLA virus (Zmapp) and the use of *Lemna* aquatic plants to produce an afucosylated biosimilar to rituximab[138–141]. Furthermore, glycoengineered plants are used for the production of vaccines such as a vaccine against human papilloma virus (HPV)[142]. As a next step, the core glycans can be further elongated by the introduction and correct localization of human enzymes. As a result, complex human-like glycans can be produced in transgenic plants e.g. terminally sialylated IgGs, terminally galactosylated IgGs and branched structures[54,55,57,58,143].

Despite the important developments, glycoengineering in plants is not widely established. As in other production systems there are limitations regarding regulation of glycosylation to achieve the desired final product and the complexity and metabolic load of genetic modifications. Furthermore, there are ethical concerns regarding the use of genetically modified organisms (GMOs) and approval from a regulatory body has yet to be given[144]. These drawbacks, have limited the commercial use of glycoengineered plants[140].

1.2.1.6. Glycoengineering in insect cells

Insect cell lines have been considered for the production of glycosylated biotherapeutics. Their glycosylation network is different to humans as it consists of paucimannosidic structures and carries the immunogenic α-1,3 fucose sugar (**Figure 1-2**). However, this lack of complex glycosylation machinery, as with plant cells, makes insects an attractive target for *in vivo* glycoengineering.

Similarly to previously discussed cell lines, insects are easy to grow, scale-up and maintain. Recombinant proteins are secreted in a serum free media, thus increasing he safety for use in humans[141]. Amongst the preferred lines are *Spodoptera frugiperda* (sf9, sf2) and *Drosophila melanogaster* (S2 cells). Genetic manipulations are simple, especially with the use of baculovirus expression vectors, a virus infecting insects but non-harmful to humans[145,146]. Typical examples of insect glycoengineering include the knockout/knockdown of the N-acetylglucosaminidase gene (using CRISPR/Cas9) to prevent formation of the paucimannose core structure. This allows the addition of a GlcNAc residue, essential for further elongation. Subsequent introduction of glycosyltransferases (GnTII, GalT, SiaT) enables the formation of human-like complex structures[146–148]. This has been demonstrated on EPO, human IgGs, etc[147,149]. An alternative approach is targeting the nucleotide sugar donor synthesis pathways to alter glycosylation, e.g. afucosylated proteins were produced when the GDP-fucose precursor moiety was consumed by an integrated bacterial enzyme[150].

The main drawback can be the time required to produce the transgenic cells and the lack of control over the glycosylation reactions which leads to highly heterogeneous structures[147]. Furthermore, the impact of native glycosylation modifications on cell growth and viability is severe, limiting the application of this host[151].

Table 1-3: Comparison of various production systems in terms of glycan structures. Adapted from Zhong & Somers, 2012[1].

Host Cells	**Ability to make human-like glycans**	**Non-human features**	**Effect**
CHO	High	Trace amount of α-Gal, NGNA, high mannose	Immunogenic
NS0/SP2/0 mouse myeloma cells	High	Small amount of α-Gal, NGNA	Immunogenic
Yeast	Low	Hypermannosylation	Decreases serum half life
Plants	Low	Bisecting β-(1,2)-xylose α-(1,3)- fucose	Immunogenic Decreases ADCC Activity
Transgenic animals	Low	High mannose NGNA	Decreases serum half-life Immunogenic
Bacteria	Low	diNAcBac pseudaminic acid (Pse) DATDH and GATDH	Immunogenic
Insects	Low	α-(1,3)-fucose	Immunogenic

1.2.2. *In vitro* glycoengineering

The need to overcome the limitations associated with cell line glycoengineering led to the development of *in vitro* glycosylation techniques. An *in vitro* environment allows for better control over the reaction conditions and the desired modifications to create human-like and non-immunogenic glycoforms. Common *in vitro* techniques include chemoenzymatic modifications and *in vitro* enzymatic modifications.

1.2.2.1. Chemoenzymatic glycosylation

Chemoenzymatic glycosylation is the *in vitro* transglycosylation of a target protein using enzymes and chemically modified sugars (**Figure 1-3a**). The main strategy relies heavily on endoglycosidases and consists of two essential steps. Firstly, wild type endoglycosidases (ENGases) e.g. EndoM -*M. hiemalis*, endoS -*S.* pyogenes, endoF -*F. meningosepticum* etc. trim back the glycan chains to the core fucosylated or non-fucosylated GlcNAc. These core sugars serve as substrates for engineered ENGases, referred to as glycosynthases, which are able to form glycosidic bonds. Hence, they catalyse the *en bloc* transfer of new and desired N-linked glycan structures to a target site allowing site-specific modifications and homogeneous glycosylation[152–155]. The homogeneity is further ensured as the glycan structures can be chemically synthesised and assembled *in vitro* or purified from natural sources, most commonly egg yolk[152]. Finally, before their transfer and in order to be recognised by the enzymes, the glycan structures need to be derivatized with an oxazoline group[152–154,156].

The chemoenzymatic technique using endoglycosidases for transglycosylation is very commonly used to perform remodelling of mAbs. By attaching the desired glycans, efficacy and functionality are markedly improved[157–159]. As previously discussed, sialylation is a critical attribute for increased receptor binding. As such, the biantennary, sialylated glycan G2F or "universal" glycan has been successfully isolated from egg yolk, chemically derivatized and attached to IgGs. One example is the remodelling of cetuximab, where successful transglycosylation led to increased binding to the FcγrIIIa receptor[156,159]. Moreover, the target glycoform can be further modified with linkers or chemical groups which will eventually allow the site-specific conjugation of the antibody with drugs, forming ADCs[77,155,160,161]. This can be done with the use of mutated glycosyltransferases.

A significant advantage of chemoenzymatic glycosylation is the independence of host cell lines, meaning the target protein can be produced in any organism and further modified with a series of chemical or enzymatic reactions. This "plug and play" approach is a powerful tool for controlling

glycosylation of biotherapeutics. Examples include the chemoenzymatic glycosylation of mAbs produced in yeast (e.g. trastuzumab), mammalian cells (e.g. cetuximab) and recombinant proteins produced in glycoengineered *E. coli*[157,159,162,163]. In all cases, the proteins were deglycosylated leaving the innermost GlcNAc intact followed by transglycosylation using glycosynthases.

Another method is the use of chemically synthesised sugars and glycosyltransferases for site-specific modifications. Noteworthy is the "stop and go" assembly developed by Liu and co-workers to synthesise complex and bespoke glycoforms[164]. The design is based on reacting isolated glycoforms with glycosyltransferases while certain sugar residues on target branches, were chemically protected to prevent unwanted enzymatic modifications. Once the desired glycosylation on the remaining branches was completed, the protected sugars were then deprotected and separately glycosylated. This allows the selective modification of each branch creating highly complex and diverse glycoforms.

Despite the significant advantages in chemoenzymatic glycosylation, there are still important restrictions. The oxazoline derivatized sugars need to be separately developed in multiple chemical steps[18,165]. Additionally, oxazolines can be reactive and produce non-enzymatic and unwanted by-products[157]. The protection and deprotection steps require numerous reagents, multiple and lengthy reactions and often harsh chemical conditions[155,164]. Furthermore, purification is required after every chemical reaction step to remove reagents leading to a loss of material and overall yield[164]. All these limitations make chemoenzymatic synthesis a rigid, costly and time-consuming method.

1.2.2.2. Chemical Synthesis

A different and not so commonly applied method is the *de novo* chemical synthesis of glycoproteins (**Figure 1-3b**). For this, solid phase peptide synthesis is commonly used where the building blocks are amino acids and sugars which are chemically protected to avoid unwanted interactions. The synthesised peptides and glycopeptides are then ligated using most commonly Native Chemical Ligation, a linkage formed between a thioester peptide and a cysteine residue of the glycopeptide[152,154]. The key advantages are the absolute control over the glycosylation sites and sugar profiles as well as the overall homogeneity. An example is the total chemical synthesis of glycosylated EPO[166]. However, there are still significant limitations in the *de novo* chemical synthesis of glycoproteins. These include site-directed mutagenesis or chemical modification of existing amino acids to introduce multiple cysteine residues, protection and deprotection steps which can hinder the stereo- and regio- specificity, in addition to low yields[152,154,166]. Furthermore, the specialist skill set, and knowledge required to implement this technique makes it difficult to replicate and apply.

Finally, there are chemoselective and site-specific techniques where expressed proteins are tagged at cysteine residues and they are ligated to modified glycans[18]. An application is the "automated glycan assembly" where a starting oligosaccharide is attached to a solid support through a linker[20]. An automated system is used for the expansion of the chain using building blocks and protectors to stabilise the glycans. This approach is characterised by multistep chemical reactions each requiring careful design.

1.2.2.3. *In vitro* enzymatic glycosylation

Enzymatic treatment of mAbs in an *in vitro* environment is often applied to complement and enhance *in vivo* glycosylation. It requires the use of recombinant glycosyltransferases and the appropriate sugar donors for the desired outcome (**Figure 1-3c**). The reactions can occur in a one-pot system, where multiple enzymes are mixed with the target mAb or sequentially where free enzymes are supplied to the mixture once the previous enzymatic step is completed[79,133,167]. It is a simpler approach compared to the existing *in vivo* and chemical methods since it requires only a few steps incubated under mild pH and temperature. The enzymes to be used are either commercially available or they can be produced in-house. These features make *in vitro* glycosylation an attractive method to synthesise bespoke glycans.

In vitro enzymatic glycosylation has been used to increase the sialylation and galactosylation of mAbs produced in CHO cells. Examples include the *in vitro* treatment of IgG1 with recombinant β-1,4-galactosyltransferase and α-(2,6)-sialyltransferase which led to the increase of terminal galactosylation and terminal sialylation[167–169]. Furthermore, to avoid intermediate purification and to increase the final yield, Tayi and co-workers performed sequential enzymatic reactions on immobilised antibodies[170]. Similarly to the use of galactosyltransferases and sialyltransferases, recombinant fucosidases are used to remove the core fucose from IgGs e.g. in trastuzumab[158,171]. Finally, an interesting approach is the bottom-up synthesis of human-like glycans from oligosaccharides (i.e. $Man_5GlcNAc_2$, $Man_3GlcNAc_2$) produced in *S. cerevisiae* and *E. coli*[172]. Briefly, by performing sequential or one-pot reactions with recombinant glycosyltransferases (GnTI, GnTII, GalT, GnTIV etc) complex multiantennary glycans were synthesised.

As highlighted before, *in vitro* modifications offer significant advantages for controlling glycosylation. However, this approach faces some important limitations. One of these is the inability to modify the glycan complexity of proteins produced in mammalian cells[79]. This is due to the N-linked glycosylation profile being fully processed with the proteins carrying highly mature glycans. The desire to modify this glycoprofile such as adding more branches is hindered by the high specificity of

the enzymes as they will not recognise the fully developed structures. In order to do so, enzymatic remodelling or *in vivo* engineering are required to produce proteins with core glycan structures. Finally, homogeneity in one-pot reactions is not ensured as the enzyme promiscuity is not addressed. Therefore, the glycosylation profile is a mixture of structures which can lower the efficacy of the therapeutic protein. In contrast, sequential reactions, where each enzyme is only added when the previous step is complete, can address the heterogeneity. However intermediate purifications are necessary to remove the free enzymes and avoid interference in later reactions. This leads to loss of material and the inability to recover the enzyme which in turn increases the cost of the process.

1.2.2.4. Cell-free protein synthesis and glycoengineering

Cell-free protein synthesis (CFPS) involves the expression of proteins in cell extracts containing the transcriptional and translational machinery. Various CFPS extracts exist, including human, plant, CHO and bacteria. Of particular relevance is their ability to perform post-translational modifications and specifically glycosylation.

As previously discussed, CHO cells are the workhorse for therapeutic protein production. Glycosylation in eukaryotic CFPS extracts is challenging. It relies on the concentration of microsomes[173]. Enrichment of extracts with microsomes can increase glycosylation yields but heterogeneity is still an issue. However, no advances have yet been made to control glycosylation and make defined structures.

In contrast to CHO and other mammalian cell-free extracts, there are significant developments in controlling glycosylation using *E. coli* extracts (**Figure 1-3d**). Guarino and co-workers developed *E. coli* cell extracts containing purified PglB and lipid-linked oligosaccharides (LLOs). Typically these components are required to initiate N-linked glycosylation in CFPS[174]. Hence, they were separately expressed and purified from *E. coli*. They were then added to cell-free extracts along with T7 polymerase and a plasmid encoding for the target protein (a single chain variable antibody fragment (scFv) or a *C. jejuni* protein (AcrA). This resulted in glycosylated proteins in various yields. However, this was a lengthy and complicated process. To overcome these limitations, the same group prepared cell-free extracts from glycoengineered *E.coli* (already containing the necessary components) making this a simpler and faster one-pot approach[175]. To further simplify the process, Kightlinger and co-workers eliminated the need for oligosaccharyltransferase and LLOs, by introducing glycosyltransferases that can directly add glucose to a conserved consensus site[176]. An example is a N-linked glycosyltransferase from *A. pleuropneumoniae* (ApNGT). Based on this, the

authors developed a CFPS system, GlycoPRIME, enriched to screen and identify novel glycosylation pathways. Briefly, the cell-free extracts were supplied with plasmids encoding for a target protein, the ApNGT to add the first glucose and various recombinant glycosyltransferases to further extend the glycans producing terminal lactose capped with sialic acid. The result was the successful glycosylation of the targets including an influenza vaccine candidate, H1HA10. Finally, the same glycosylation pathway i.e. the series of recombinant glycosyltransferases, was then transferred to living *E.coli* cells to successfully glycosylate the Fc domain of a human IgG[176]. This demonstrated the effectiveness of CFPS systems to screen and identify novel glycosylation pathways in an artificial environment. However, simultaneous co-expression of glycosyltransferases led to heterogenous structures. Furthermore, this approach has not yet been applied to full-length IgGs or other whole mAbs.

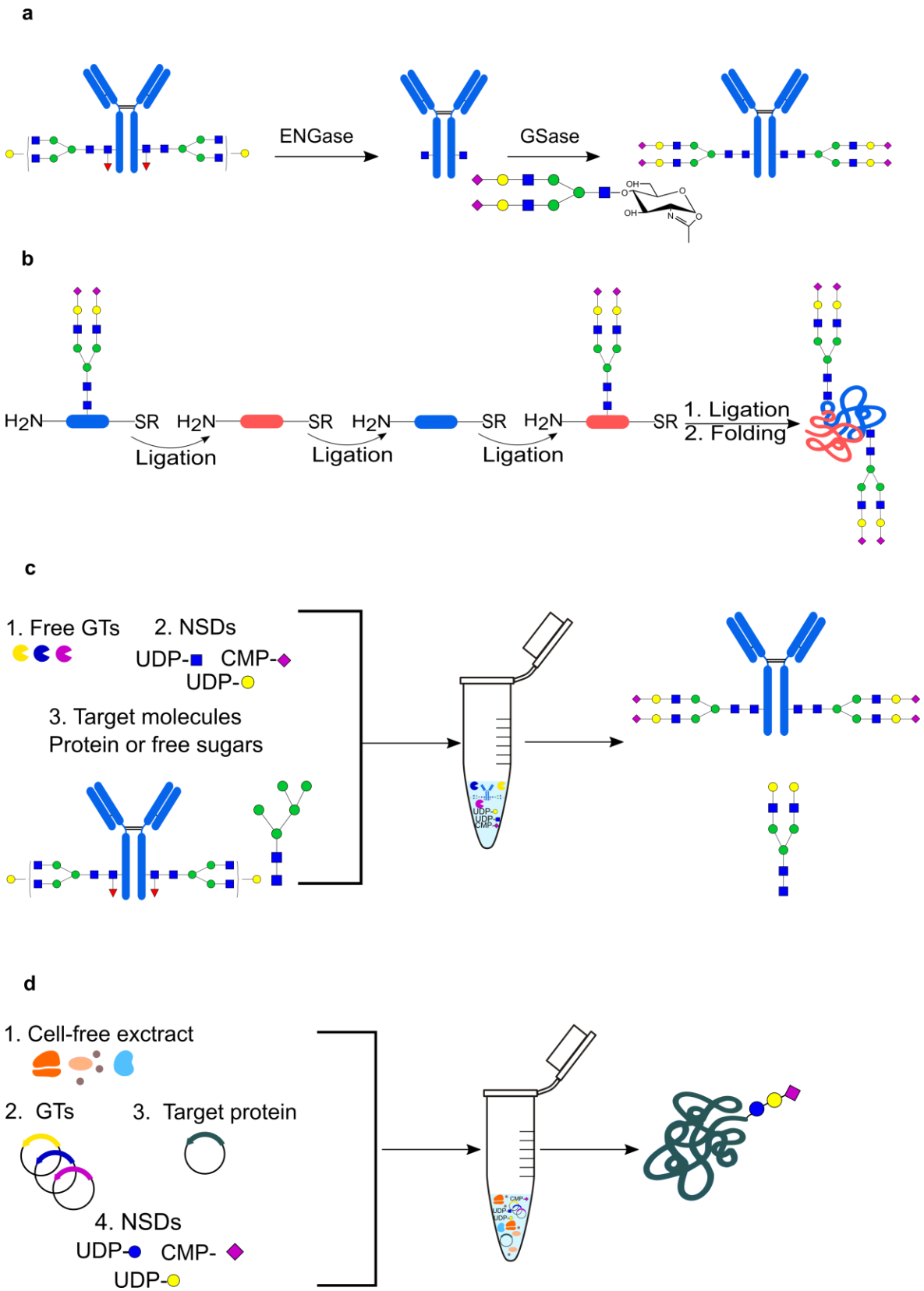

Figure 1-3. Common techniques for *in vitro* glycoengineering. a. Chemoenzymatic synthesis of monoclonal antibodies. b. Chemical synthesis and glycosylation of proteins. c. *in vitro* enzymatic glycoengineering. d. cell-free glycoengineering.

1.2.3. Metabolic glycoengineering

One key reason for the heterogeneity in the glycoprofile of proteins produced in host-cell lines, are the intracellular and extracellular conditions. These include the availability of nucleotide sugars and enzymes as well as the growth conditions such as temperature, dissolved oxygen and pH[76,177–180]. Since CHO cells are the workhorse in therapeutic protein production, they are the subject of extensive research in understanding relevant metabolic pathways and how they can affect glycosylation. As a result, metabolic glycoengineering is used to tailor glycosylation by adding the right component and controlling the fermentation environment.

One application of metabolic glycoengineering is feeding the appropriate nucleotide-sugar precursor nutrients to increase the NSD synthesis and transportation and their subsequent concentration into the Golgi[75,82,178,181]. This is often accompanied by up-regulation of the relevant enzymes[82]. These events can lead to increased glycosylation. Indeed, supplementing the growth media with nucleotides such as uridine and N-cytidine, metal cofactors such as manganese and sugars such as galactose, glucosamine and acetylmannosamine resulted in an increase in the concentrations of UDP-Gal, UDP-GlcNAc and CMP-NANA. Therefore, there was an increase in galactosylation, bisecting glycans and sialylation[82,178,181–183]. Furthermore, Wong and co-workers observed that their feeding strategy led to the up-regulation of β4GalT1 and St3GalT enzymes leading to an increase of terminal sialylation[82].

Similarly, culture media additives can be used to specifically inhibit enzymes and control glycosylation. Some cases include using fluorinated fucose sugars to inhibit core fucosylation in CHO cells, kifunensine to inhibit α-mannosidase I and produce oligomannose structures and fluorinated sialic acid sugars to inhibit the sialyltransferases and therefore allow fucosylation[178,180,184]. Finally, an interesting application of metabolic glycoengineering is the development of vaccine candidates for cancer treatment[185,186]. For instance, supplementing the media of cancer-cell cultures with sugar precursor moieties induces the production of glycan antigens that serve as epitopes for the development of neutralising antibodies[186].

In addition to media components, culture conditions also have an impact on the glycosylation profile. Low growth temperatures can negatively affect the extent of sialylation, galactosylation as well as the concentration of glycosyltransferases and NSDs[177,179,187]. pH and dissolved oxygen are also known to have an impact on glycosylation and enzyme localisation; however the effect varies based on the cell line and the end product[177,179].

The need for a better understanding of how the intracellular, (e.g. enzyme and donor availability or enzyme specificity) and extracellular conditions affect the cell metabolism and consequently the glycosylation profile led to the development of predictive mathematical models[75,76,182,188–190]. These tools are used to identify the key parameters to tune glycosylation and antibody productivity whilst indicating a suitable experimental design. One example is the work conducted by Spahn and co-workers[191]. The researchers developed a probabilistic model using Markov chain theory that minimises the need for parameter estimation and achieves high levels of accuracy in predicting glycoengineering effects. This model was applied to understand GTs specificity[192] as well as drive the design of strategies for biosimilars production with the desired glycosylation profile[193].

Another example of mathematical modelling is the work by Kotidis and co-workers[182]. The authors developed a mathematical model to describe the impact of nutrient feeding on galactosylation and on cell viability. The mathematical predictions were then experimentally validated and led to the increase in galactosylation without reduction in antibody yield.

As per every approach, the use of metabolites for controlling glycosylation has its own set of limitations. It is often the case that feeding strategies alone are not sufficient to tailor glycosylation. A synergistic approach of feeding strategies and *in vivo* glycoengineering to overexpress glycosyltransferases is then required[82]. Additionally, batch-to-batch variability can give unpredicted results regardless of the efforts to control the experimental environment[79]. It has also been shown that feeding strategies often lower antibody titres while the cost of the additives can be quite high[190]. Finally, as discussed earlier the effect of each metabolite on glycosylation heavily depends on the cell line and the end-product. As such, identifying and implementing feeding strategies remains challenging.

1.2.4. Summary of challenges and limitations

A crucial factor is the production of glycosylated biotherapeutics in a consistent and reproducible manner to ensure quality, safety and high efficacy[33,185,194,195]. This is not always ensured in *in vivo* production due to batch-to-batch variability and experimental inconsistencies. The result can be the improper glycosylation of the biotherapeutic that in turn can reduce the activity of the drug[108]. Another limitation is the difficulty in reproducing biotherapeutics with specific glycoforms. Variations in cell line, glycoengineering approach, growth conditions etc. can lead to altered glycosylation. This might result in batch failure and also adds to the cost of biosimilar development[4,31,33]. Furthermore, it is often the case that different sets of therapeutic proteins require specific glycoforms[85]. Using *in vivo* glycoengineering, requires the generation of multiple,

different strains with different glycosyltransferase profiles to achieve the desired set of products. As such it can be a rigid approach and difficult to adapt to specific requirements.

The need for drugs with higher efficacy and tailored to individual patients' needs is emerging. This requires strict control over design and production to ensure glycan homogeneity. However, this is a challenging task as naturally glycosylation is a heterogeneous process. This is because it is governed by multiple glycosyltransferases in a non-templated manner. These enzymes are known for their promiscuity which leads to a large number of possible glycan structures. Furthermore, even though the glycosylation mechanisms and pathways are well studied there is still not a clear understanding of how the proteins are being transported between the various Golgi compartments and how long they remain there[141]. Control of these processes is difficult and ensuring the quality of the final product is not always possible. Despite the developments in controlling glycosylation in *in vivo* systems and enriching for the desired featured, structural heterogeneity still remains a bottleneck.

In vitro glycoengineering allows for a strict control over the reaction conditions and subsequent control over the glycosylation profile. Chemoenzymatic methods lead the efforts as they can produce site-specific and homogeneous sugar structures. However, it is laborious, time-consuming and it is often the case that it produces undesirable chemical by-products. *In vitro* enzymatic treatment is a simple alternative with much less conditions to control. However, to ensure homogeneity purification of the target protein after each enzymatic step is essential which leads to loss of time and material.

1.3. Artificial Golgi reactions for targeted glycosylation

Currently, there is significant drive for controlling glycosylation and producing bespoke biotherapeutics. There is a need for a strategy eliminating problems associated with lack of control and heterogeneity. An *in vitro* environment allows strict and fine control over enzyme and NSD concentrations and reaction conditions so that the desired product is produced. However, one-pot *in vitro* reactions do not address the main challenges of heterogeneity, given enzyme competition and promiscuity, remains. A way to address this, is to perform sequential *in vitro* glycosylation reactions that run to completion[77,79,170,172]. However, replicating a whole glycosylation pathway with multiple enzymatic steps in this manner is inefficient given intermediate purifications are required and enzyme recovery is impossible. These lead to loss of material and increased cost.

A different approach to address the aforementioned issues is an artificial platform using enzymes in defined compartments. The target protein can pass through each compartment while the spatial and temporal segregation of enzymes allows targeted sequential reactions to take place. This design

strongly resembles the structure of the Golgi apparatus consisting of packed cisternae but in a stricter format to prevent overlap and consequently enzyme competition. Previous efforts for artificially controlling glycosylation by mimicking the Golgi structure include the design of a digital microfluidic chip to target a modification of glycosaminoglycans and specifically the oligosaccharide heparan sulfate (HS) using oligosaccharyltransferases (OSTs)[196]. The enzymes and substrates were in droplets, moved around the channel and mixed by electrowetting. The chip was tested for HS and 3-OST and achieved only a 5% conversion. This could be due to a loss of enzyme activity or unsuccessful mixing. Other examples include the use of enzymes immobilized on particles and the design of microfluidic chips for sequential reactions on synthetic oligosaccharides[197,198,199]. However, these studies did not address the issue of heterogeneous mAb glycoforms. Instead their primary focus was on biocatalysis, microfluidic chip development and performing cascade reactions.

A novel strategy was described by Klymenko and co-workers, proposing an artificial Golgi reactor (AGR) for the bottom-up synthesis of N-linked glycosylation of mAbs[200]. The described system uses target mAbs that can be produced in glycoengineered non-mammalian hosts, such as *P. pastoris*, in order to carry a homogeneous core glycan structure (e.g. $Man_5GlcNAc_2$). Then, the desired N-linked glycosylation pathway can be reconstructed *in vitro* with the continuous flow of the mAb through compartments of immobilized enzymes[200]. To better understand the requirements of the AGR, they developed a mathematical model to characterize the sequential enzymatic reactions in a targeted N-linked glycosylation pathway**.** They demonstrate the feasibility of AGR and investigated a number of possible designs helping to inform future optimizations. These were a microcapillary flow reactor (MCFR), a non-porous packed bed reactor (PBRnp) and a porous packed bed reactor (PBRp).

The purpose of the AGR is to glycosylate mAbs in an automated and effective fashion, without intermediate purification or undesired products, factors that would affect yield and drug efficacy, respectively. Furthermore, the conditions and resources required to achieve optimal yields can be determined for each step, allowing facile optimisation. A successful design can in principle mimic any pathway allowing a range of glycosylated mAbs to be produced. This is because the use of immobilized enzymes allows a modular assembly of compartments in a desired order. Finally, as immobilization commonly helps with retaining enzyme activity, such reactors can be used multiple times, reducing costs.

1.4. Aims and objectives of this thesis

In line with the work set out by Klymenko and co-workers, the goal of this PhD was to design and develop an experimental proof-of-concept system for targeted glycosylation using immobilized enzymes. Specifically, the main hypothesis was that the spatial and temporal separation can address

the enzyme promiscuity and ensure increased homogeneity when reconstructing a N-linked glycosylation pathway. Therefore, the aim was to design, build and test a system of immobilised enzymes (an AGR) to achieve sequential glycosylation reactions whilst optimising conditions to maximise homogeneity.

The system design is described in Chapter 3. Initially, a three-enzyme N-linked glycosylation pathway, GnTI-ManII-GalT, where enzyme promiscuity naturally exists was identified. This was based on the proposed pathway by Klymenko and co-workers. The next step required critically evaluating enzyme homologs and expression systems. The selection relied on the features of the chosen enzymes as well as the need for a simple immobilisation strategy that would also increase enzyme stability. Once identified, the selected techniques were implemented, and the immobilised enzymes were tested for activity.

The next stage was to apply the system to perform an enzymatic cascade to produce targeted glycoforms with increased homogeneity (Chapter 4). This involved performing and optimising sequential reactions of the three enzymes using artificial oligosaccharides as substrates. Subsequently the system of immobilised enzymes was used on a relevant protein produced in glycoengineered *P. pastoris* as a proof-of-concept for reconstructing N-linked glycosylation in cell-derived material.

Finally, an application of using enzymes *in vitro* to complement *in vivo* glycosylation can be found in chapter 5. As described earlier, galactosylation is a desired attribute as it can increase the IgG-receptor binding and drug efficacy. Therefore, immobilised GalT was used to enhance the galactosylation of an IgG produced in CHO cells. Furthermore, immobilisation allowed enzyme recovery and reusability so multiple cycles of *in vitro* modifications were performed. This can help make the system more economical for future applications.

Chapter 2: Designing and developing an Artificial Golgi Reactor

2.1. Introduction

The first objective of this work was the design of a multienzyme system for the production of targeted glycoforms, resembling the function of the Golgi Apparatus. This AGR system comprises recombinant, immobilised enzymes. To achieve this, it was essential to first identify a suitable pathway and understand the characteristics of the participating enzymes. Subsequently, available expression and immobilisation systems for the enzymes were reviewed driving the selection of techniques used in this study.

2.1.1. Target enzymes in selected glycosylation pathway

The first step towards designing an AGR was the selection of an enzymatic pathway. As described in **Section 1.4**, the pathway must involve enzyme competition which would produce heterogeneous final products without spatiotemporal separation. This would then be addressed using the AGR. A pathway previously described by Klymenko and co-workers consisted of four enzymes, GnTI, ManII, GnTII and GalT[200]. In this PhD work, the pathway was simplified to three enzymes, GnTI, ManII and GalT for time purposes. Out of the enzymes, GalT can recognise multiple substrates producing different glycoforms, satisfying the above requirement (**Figure 2-1**).

2.1.1.1. N-acetylglucosaminyltransferase I

N-acetylglucosaminyltransferase I (GnTI) is responsible for initiating the synthesis of complex N-linked glycans. This makes it a target for *in vivo* glycoengineering (e.g. GlycoDelete) in order to "shut down" the native glycosylation network[88,96,201]. It catalyses the addition of a N-Acetylglucosamine (GlcNAc) sugar onto the α-1,3 mannose (Man) branch of newly modified proteins from the ER carrying oligomannosidic glycans (**Figure 2-1**: Glycosylation reaction of selected enzymes. a. GnTI add a GlcNAc sugar in the α 1,3 mannose branch of M5, forming a β 1,2 glycosidic bond and producing GM5; b. Golgi ManII sequentially trims the α 1,3 and α 1,6 mannose residues in the α 1,6 mannose branch of GM5 producing GM4 and consequently GM3; c. GalT catalyses the addition of a galactose sugar in any available GlcNAc residue forming a β 1,4 glycosidic bond. Here it can recognise the product of GnTI (GM5) and the products of ManII (GM4 and GM3) making it a highly promiscuous enzyme.). Acceptor substrates include $Man_2GlcNAc_2$ (M2), $Man_3GlcNAc_2$ (M3), $Man_4GlcNAc_2$ (M4), $Man_5GlcNAc_2$ (M5) and $Man_6GlcNAc_2$ (M6) as well as

oligomannose structures such as mannotriose[202,203]. Out of all, $Man_5GlcNAc_2$ (M5) is the preferred starting substrate from all the possible structures[202,204,205].

Like most glycosyltransferases (GTs), GnTI is a membrane bound enzyme and it belongs in the type II membrane protein family[23,206]. It requires the use of uridine diphosphate-GlcNAc (UDP-GlcNAc) as a nucleotide sugar donor, making it a Leloir GT[200]. Finally, it requires divalent metal ion co-factors (e.g. manganese) for catalytic activity.

2.1.1.2. α -1,2- Mannosidase II

The α-1,2 mannosidase II (ManII) is a glycosidase with three different variants: lysosomal, intermediate/Golgi, and cytosolic, all structurally related but with different biochemical properties[207,208]. Golgi ManII has an integral role in the N-linked glycosylation pathway, since its hydrolytic activity creates suitable substrates for complex and branched glycans to be formed. Therefore, ManII is a target for cancer research focusing on altering the glycosylation pattern of tumours and thus slow their growth. As such there is an interest in identifying and using ManII inhibitors as potential anti-cancer treatments[207–209].

The catalytic activity of any of the three types of ManII consists of the sequential removal of the two α-1,6 and α-1,3 mannose residues on the α-1,6 branch of oligomannosidic glycans. The Golgi ManII is less promiscuous than its counterparts, requiring a GlcNAc residue on the α-1,3 branch of the acceptor moiety[209]. Therefore, it can only recognise GnTI's products. In the AGR design, it recognises $GlcNAcMan_5GlcNAc_2$ (GM5) and produces $GlcNAcMan_4GlcNAc_2$ (GM4) and $GlcNAcMan_3GlcNAc_2$ (GM3) (**Figure 2-1b**). Furthermore, as with GnTI, it is also a type II membrane protein and it requires the presence of metal ions for catalytic activity. However, it does not require a nucleotide sugar donor given it has hydrolytic activity.

2.1.1.3. β-1,4- Galactosyltransferase (GalT)

β-1,4- Galactosyltransferase is a versatile enzyme participating in various galactosylation processes within the cell and organisms. There are four isoenzymes (GalT-I, GalT-II, GalT-III, GalT-IV) which catalyse the galactosylation of N-linked glycans, with GalT-I (here referred to as GalT) having the major role[210]. Furthermore, GalT plays a major role in the O-linked milk oligosaccharides pathway as it catalyses the synthesis of lactose in the mammary glands, making it one of the most well- studied galactosyltransferases[211].

In the N-linked glycosylation network, GalT catalyses the addition of a galactose sugar to any available GlcNAc residue, including a free GlcNAc, forming a β-1,4 glycosidic bond. This makes it a highly promiscuous enzyme. Similar to GnTI, it is a type II membrane protein and requires the use nucleotide sugar donors, i.e. uridine diphosphate-Galactose (UDP-Gal) as well as divalent metal ion cofactors. In the selected pathway, GalT catalyses the addition of galactose to GM5, GM4 or GM3 producing $GalGlcNAcMan_5GlcNAc_2$ (GalGM5), $GalGlcNAcMan_4GlcNAc_2$ (GalGM4) or $GalGlcNAcMan_3GlcNAc_2$ (GalGM3) respectively (**Figure 2-1c**).

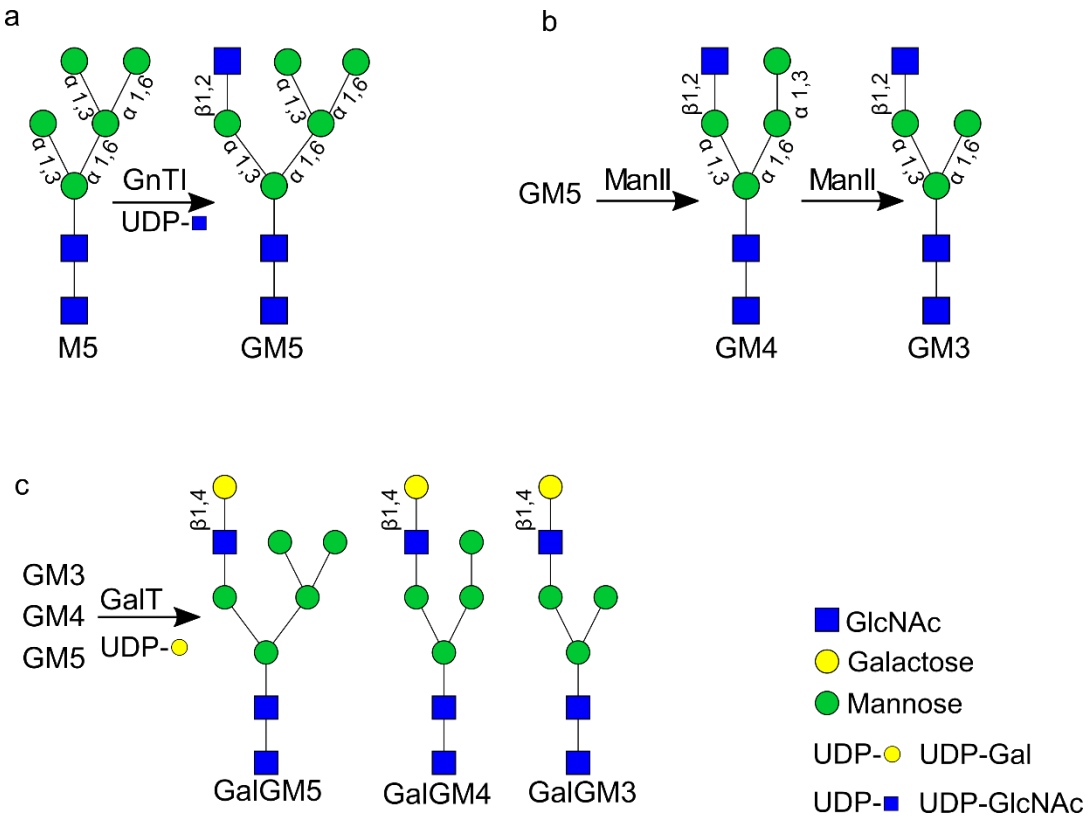

Figure 2-1: Glycosylation reaction of selected enzymes. a. GnTI add a GlcNAc sugar in the α 1,3 mannose branch of M5, forming a β 1,2 glycosidic bond and producing GM5; b. Golgi ManII sequentially trims the α 1,3 and α 1,6 mannose residues in the α 1,6 mannose branch of GM5 producing GM4 and consequently GM3; c. GalT catalyses the addition of a galactose sugar in any available GlcNAc residue forming a β 1,4 glycosidic bond. Here it can recognise the product of GnTI (GM5) and the products of ManII (GM4 and GM3) making it a highly promiscuous enzyme.

2.1.2. Enzyme expression

Having identified a pathway and associated enzymes, the next step was identifying suitable expression hosts for the enzymes. As illustrated in **Table 2-1**, there are a range of selection criteria

and identifying the appropriate hosts can be challenging. The selected cell type will define all the future steps to be taken to achieve high yields of soluble protein for further analysis and subsequent immobilisation. The following section reviews possible options for producing or obtaining the target enzymes.

Table 2-1: Criteria for host selection

Criteria for host selection
Supports post translational modifications
Size of target proteins
Enables folding
Ease of genetic modifications
Ease of handling
Scale-up
Production yield
Maintenance needs, cost and time

2.1.2.1. Review of expression systems

There is a large variety of available host cells i.e. mammalian, bacteria, yeast, insects etc., each with their own advantages and limitations. The selected host should be able to produce active enzymes. Mammalian cells can be attractive hosts since they support PTMs and enable the production of functional enzymes[12,18,212,213]. For instance, human GnTI and human ManII have been successfully expressed in CHO or COS cells, respectively[214,215]. Other hosts that support PTMs and have been used for successful expression of the target enzymes include *P. pastoris* (recombinant *C. hircus* ManII)[216,217], Sf9 insect cells (recombinant *D. melanogaster* GnTI)[205], *N. tabacum* (recombinant *G. gallus* GalT)[218] and *S. cerevisiae* (recombinant human GalT)[219] (**Appendix Table 8-1**, **Table 8-2**, **Table 8-3**). Finally, genetically modified *E. coli,* with an oxidising instead of reducing cytoplasm, supports disulphide bond formations and has been successfully used for the expression of recombinant human GnTI and GalT[172,220].

An additional factor to consider, is modifying the enzyme to increase solubility. For example, it is often necessary to add solubility tags or truncate the enzyme so that it does not contain the transmembrane domain (**Appendix Table 8-1**, **Table 8-2**, **Table 8-3**). This makes the enzyme more soluble, enabling expression in hosts where it would not be possible otherwise. This is particularly relevant for bacteria such as *E. coli*, as demonstrated in expression of truncated GnTI and GalT with different solubility tags (e.g. MBP, His_6-tag etc.) (**Appendix Table 8-1**, **Table 8-3**). Similar

modifications are also made to increase solubility in eukaryotic hosts such as insect or CHO cells (**Appendix Table 8-1, Table 8-2, Table 8-3**). Furthermore, as later discussed in **Section 2.1.3**, solubility tags can also facilitate affinity immobilisation.

Finally, different enzyme orthologs have also been explored to identify the most active or easier-to-express forms. This is important for human and other mammalian ManII as the size (~125kDa) and range of PTMs make it challenging to express. Therefore, alternative expression systems and enzyme origins have been explored (**Appendix Table 8-2**). The most successful example, is the expression of *D. melanogaster* ManII (DmManII) in insect cells[209]. DmManII is not glycosylated, only carrying multiple disulphide bonds, thus making it a relatively easy target for expression.

2.1.3. Enzyme immobilisation

In the context of this work, immobilisation was necessary for the spatial and temporal separation of enzymes. Nevertheless, there are other benefits of enzyme immobilisation: it helps retain enzyme activity and structural stability, a critical step in achieving optimum conversion and enzyme reusability[221,222]. The latter can be achieved due to the facile enzyme recovery.

2.1.3.1. Review of immobilisation techniques

There is a multitude of immobilisation techniques available. The selection criteria include the structure of the expressed enzymes, the ease of handling and the strength of binding to the solid support. The latter is important to enhance stability without compromising the enzyme's catalytic activity. There are two binding types that are considered when immobilising enzymes: irreversible and reversible. The former, consisting mainly of covalent bonds, offers very strong interactions enabling long-term storage and increased stability[221,223]. Careful design is required to achieve the correct orientation and protect the enzyme's catalytic site. For example, covalent binding has been used to immobilise human GalT (hGalT) on activated sepharose solid supports through the enzyme's primary amine residues[224]. Another example is the sortase-mediated covalent immobilisation of GTs including GalT, facilitating enzyme orientation without compromising the active site[220]. In contrast, reversible binding, such as ionic and affinity binding, has weaker interactions but offers more flexibility in design and enzyme recovery. Therefore, it is commonly used for enzyme immobilisation. As GTs are often fused to solubility tags facilitating affinity purification, affinity binding can be used for enzyme immobilisation and subsequent reactions. Examples include the immobilisation of the Maltose Binding Protein (MBP)-GnTI fusion protein on amylose[203] and the immobilisation of the 6X

histidine (His_6-tag)-GalT fusion protein on magnetic Nickel beads[198]. Similarly, DmManII was expressed as a Protein A fusion and subsequently immobilised on IgG-Sepharose beads[225].

A widely used immobilisation technique based on affinity is the biotin-streptavidin system. Biotinylated enzymes are immobilised on streptavidin (StV) solid supports through strong non-covalent bonds allowing high specificity and stability[222]. Furthermore, the bond can form spontaneously without the use of harsh chemical conditions. For biotinylation of enzymes, it is often common to use commercially available chemical reagents. However, this requires the prior purification of the protein and there is a risk of affecting the enzymatic activity[226]. In addition, it is rigid approach targeting free residues such as primary amines, carboxyls and carbohydrates[227]. As a result, there are multiple possible interactions between the biotinylated protein and the solid support. In contrast, enzymatic biotinylation allows for site-specific immobilisation while allowing *in vivo* biotinylation[228,229]. This method makes use of BirA, a native biotin ligase enzyme in *E. coli*[229]. This enzyme is responsible for biotinylation of Biotin Carboxyl Carrier Protein (BCCP) in *E. coli*. It can also act on various peptide tags ranging from 15-75 amino acids, with AviTag (15 amino acids) being the most commonly used[229,230]. Conveniently, there are commercially available strains and plasmids encoding BirA and AviTag to simplify this approach. Based on this, enzymes can be fused to AviTag and achieve site specific biotinylation either *in vitro* with the addition of BirA or *in vivo* by co-expressing BirA.

2.1.4. Experimental strategy and objectives

The techniques required to develop the AGR were selected based on the review of enzyme expression and immobilisation systems in the context of the target enzymes. *E. coli* was selected for the expression of human GnTI (hGnTI) and human GalT (hGalT) as it meets the criteria outlined in **Table 2-1**.

The immobilization strategy was based on biotin-streptavidin as it offers the strongest non-covalent bond available, increased stability and it forms under mild conditions. It was decided to test and implement *in vivo* biotinylation by co-expressing BirA and fusing AviTag to the enzymes. This is a novel system for GTs and once established would be impactful and allow several future applications. Here, the *in vivo* biotinylation system was tested on hGnTI, NtGnTI and hGalT. All enzymes were engineered to carry AviTag at the C-terminus. As biotinylation can mask the catalytic site, it is recommended to add flexible linkers e.g. Glycine-Serine (GS) residues[226]. Therefore, a small two-residue linker was also added between the enzyme and AviTag to ensure enzymatic activity (**Figure 2-2a**). Finally, the biotinylated enzymes were immobilised on streptavidin-coated beads (**Figure 2-2**:

In vivo biotinylation and immobilisation. a. *In vivo* biotinylation strategy. The catalytic domain of a target enzyme is fused to a Maltose Binding Protein (MBP) on the N-Terminus and AviTag on the C-terminus. To ensure functionality, a small two-residue Glycine-Serine (GS) linker was inserted before the AviTag. The biotin ligase BirA recognises AviTag and can perform enzymatic biotinylation; b. Biotinylated enzyme is subsequently immobilised on streptavidin coated solid supports.**b**).

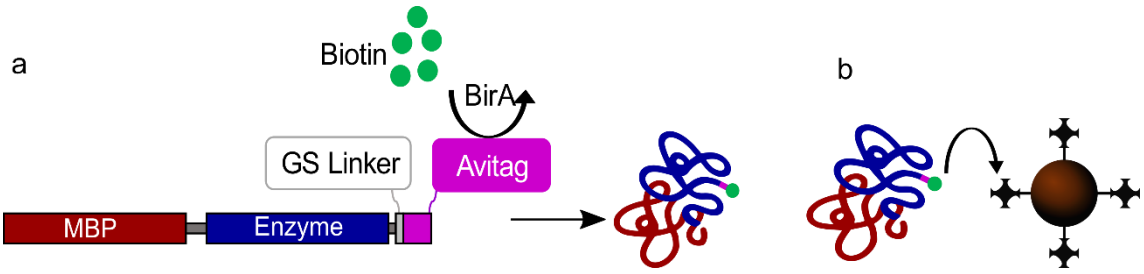

Figure 2-2: *In vivo* biotinylation and immobilisation. a**.** *In vivo* biotinylation strategy. The catalytic domain of a target enzyme is fused to a Maltose Binding Protein (MBP) on the N-Terminus and AviTag on the C-terminus. To ensure functionality, a small two-residue Glycine-Serine (GS) linker was inserted before the AviTag. The biotin ligase BirA recognises AviTag and can perform enzymatic biotinylation; b. Biotinylated enzyme is subsequently immobilised on streptavidin coated solid supports.

DmManII was chosen to perform the second step in the enzymatic pathway as it is a stable enzyme with high activity. Human ManII expression was attempted by a previous lab member and ruled out (data not shown). Pure DmManII was kindly provided to us by our collaborators Dr. David Rose and Dr. Doug Kuntz, from the University of Waterloo. As the enzyme was already expressed without an AviTag, it was not possible to apply the enzymatic biotinylation system. To maintain the same immobilisation principle for all enzymes, *in vitro* chemical biotinylation using commercially available reagents was applied.

To confirm the activity of immobilised enzymes two techniques with different principles were tested. The first one was a commercially available colorimetric assay to detect released nucleotide diphosphates (NDs e.g. UDP). This technique relies on the principle that Leloir GTs follow a sequential ordered bi-bi catalytic mechanism[231]. According to this, GTs bind sequentially to the NSD followed by the sugar acceptor. The NDs are released only after the sugar transfer is complete (**Figure 2-3**), thus making it a target of activity assays. In this colorimetric assay, the NDs are broken down by a phosphatase and the amount of released inorganic phosphate is detected and measured. The inorganic phosphate directly corresponds to the amount of released NDs and hence the specific activity (µmol of inorganic phosphate x min^{-1} x mg of $enzyme^{-1}$) can be quantified[232]. The second

technique used was MALDI-TOF MS, commonly applied for the detection and identification of glycoforms[172,202,203,233]. This method relies on the ionisation of samples and the subsequent detection of the mass-to-charge (m/z) ratio of the charged molecules. It can be applied to detect the product of all glycosylation reactions.

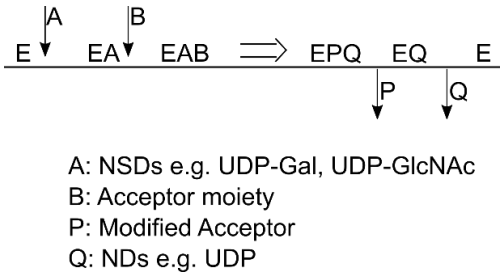

Figure 2-3: Ordered Sequential Bi-Bi mechanism

Based on the above, the objectives of this chapter were:

- **Objective 1**: a. Expression, biotinylation and immobilisation of both hGnTI and NtGnTI; b. Confirmation of immobilised enzyme activities.
- **Objective 2**: a. Expression, biotinylation and immobilisation of hGalT; b. Confirmation of immobilised enzyme activity.
- **Objective 3**: a. Chemical biotinylation and immobilisation of DmManII; b. Confirmation of immobilised enzyme activity.

2.2. Results

As discussed in the introduction section, GnTI (hGnTI and NtGnTI) and GalT (hGalT) were fused to an MBP tag at the N-terminus for enhanced solubility and an AviTag at the C-terminus to allow *in vivo* biotinylation catalysed by BirA (**Figure 2-2**: *In vivo* biotinylation and immobilisation. a. *In vivo* biotinylation strategy. The catalytic domain of a target enzyme is fused to a Maltose Binding Protein (MBP) on the N-Terminus and AviTag on the C-terminus. To ensure functionality, a small two-residue Glycine-Serine (GS) linker was inserted before the AviTag. The biotin ligase BirA recognises AviTag and can perform enzymatic biotinylation; b. Biotinylated enzyme is subsequently immobilised on streptavidin coated solid supports.). To enhance biotinylation, the growth media was supplemented with free d-biotin. Similar to the use of tags for affinity purification, it was hypothesised the AviTag-Streptavidin bond could be used for a one-step immobilisation/purification. Therefore, the process outlined in **Figure 2-4** was developed and applied for the expression and one-step immobilisation/purification of hGnTI, NtGnTI and hGalT. Desalting of the samples prior to binding on StV beads was considered necessary to remove any free biotin that could bind on the solid supports and consequently hinder enzyme immobilisation.

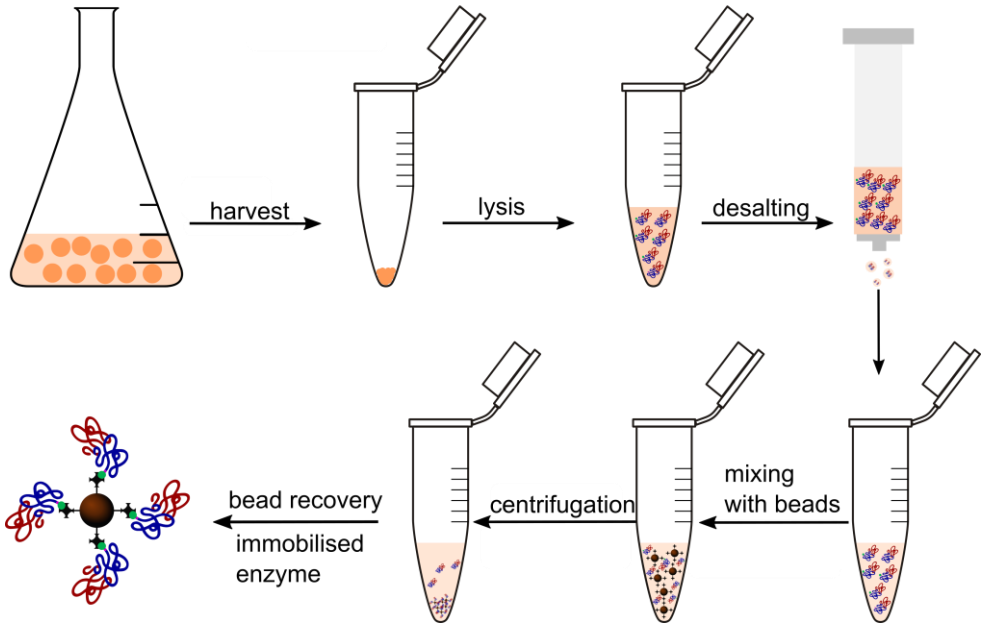

Figure 2-4: Experimental process for one-step immobilisation/purification of GnTI variants (hGnTI and NtGnTI) and hGalT. Following cell harvest, cells are lysed via sonication and the soluble content including the enzymes was extracted via centrifugation. A desalting step was necessary to remove any free biotin. The desalted solution was mixed with StV beads to capture the biotinylated enzyme. A final centrifugation step allowed the recovery of the immobilised enzyme whilst the unbound material was discarded. The specific conditions are described in **Chapter 6:**.

2.2.1. Objective 1a. Expression, biotinylation and immobilisation of GnTI

As reviewed in **Section 2.1**, the *E. coli* strain Origami, which supports the formation of necessary disulphide bonds, was selected for the expression of hGnTI and NtGnTI. Both of these enzymes are transmembrane proteins, which in their native form would not fold correctly when expressed in bacteria. To overcome this limitation, the enzymes were truncated, removing the transmembrane domain as previously described[202,203]. The resulting catalytic domains were fused to either or both MBP and AviTag resulting in the enzyme variants described in **Table 2-2.** Furthermore, as mentioned earlier, a small GS linker was added between each enzyme and AviTag. This is to ensure biotinylation would not mask the catalytic site and cause any undesired steric hindrance. Expression cassettes were generated via restriction enzyme digestion. The backbone expression vector was the commercially available pMAL-c5X (New England Biolabs) which encodes for the MBP. Enzyme constructs were subsequently cloned into (**Chapter 6:**) Origami 2 (DE3).

Table 2-2: Fusion enzyme variants

Enzyme	Truncation	Backbone plasmid	Fusion enzyme	Molecular weight (in kDa)
hGnTI	Δ103	pMAL-c5X	MBP- hGnTI	83.4
			MBP- hGnTI-AviTag	85
NtGnTI	Δ29	pMAL-c5X	MBP- NtGnTI	92.2
			MBP- NtGnTI-AviTag	93.8
hGalT	Δ128	pMAL-c5X	MBP- hGalT-AviTag	76.4

The expression of all fusion proteins was confirmed using SDS-PAGE analysis, where bands corresponding to the expected MW were detected (**Figure 2-5**). Furthermore, there was no apparent change in solubility amongst fusion proteins, indicating that the addition of AviTag in the C-terminus did not affect protein folding. Finally, MBP-hGnTI-AviTag and MBP-NtGnTI-AviTag were each co-expressed with BirA to achieve *in vivo* biotinylation. The solubility of the biotinylated enzymes was also verified via SDS-PAGE analysis and the addition of BirA (indicated by arrows) does not have a negative effect on expression or solubility (**Figure 2-5**).

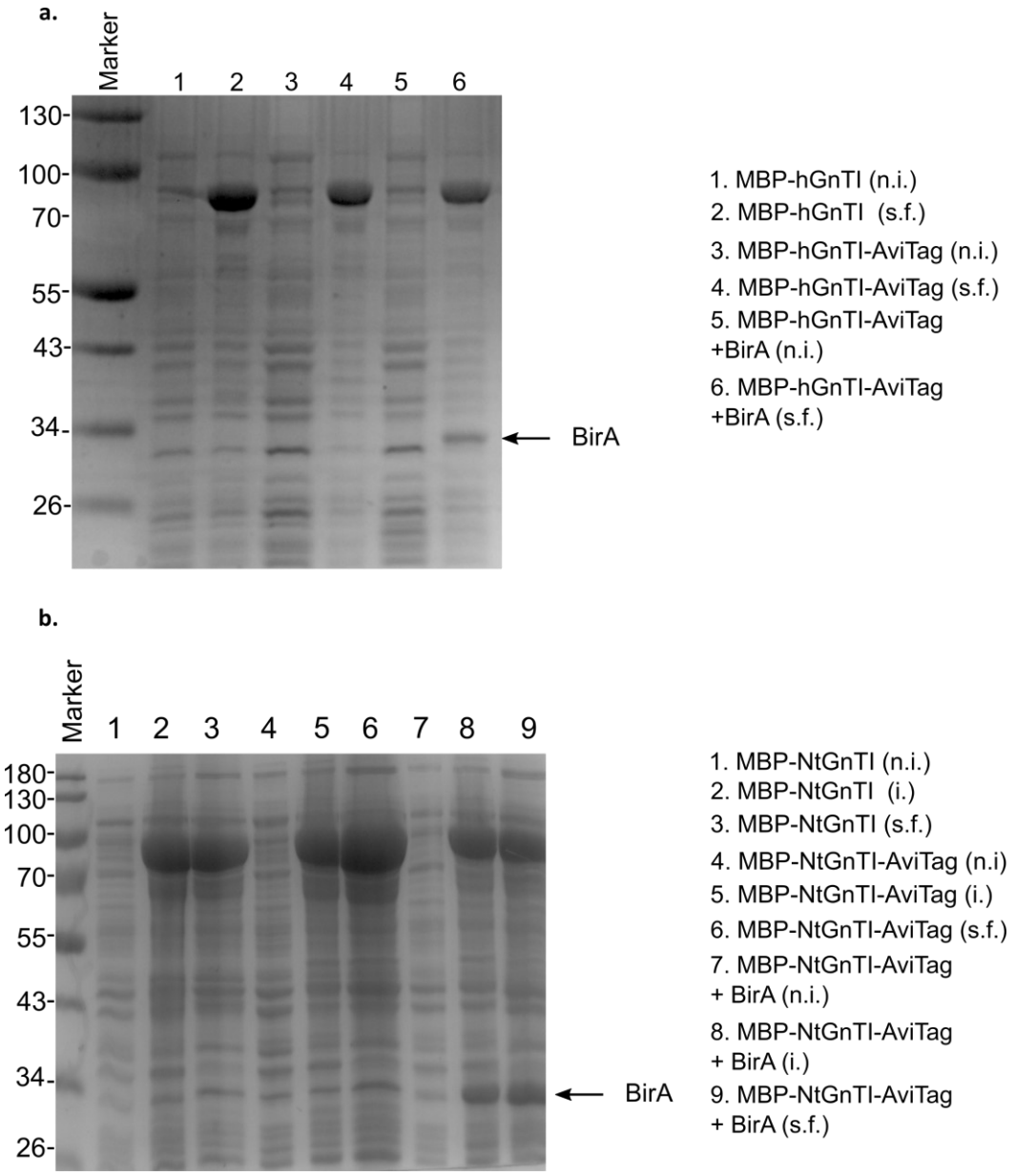

Figure 2-5 : Solubility check of GnTI orthologs and variants. a. Solubility check of hGnTI fusions; b. solubility check of NtGnTI fusions. n.i.: non-induced; s.f.: soluble fraction.

To confirm biotinylation of expressed enzymes, a previously implemented gel shift assay was used[226], with the modification that it was performed on crude soluble fractions rather than a purified protein. Briefly, the crude soluble fractions were incubated with streptavidin (StV) in the absence of a reducing agent. The latter is important for StV to maintain its natural conformation, facilitating binding to biotin conjugates. StV is expected to bind to biotinylated fusion proteins and the complex appears as a new band at a greater molecular weight (MW). As a result, the bands corresponding to biotinylated hGNTI (~85kDa) and biotinylated NtGnTI (~94 kDa) were noticeably decreased (**Figure**

2-6). Image analysis and densitometry were used to calculate the decrease in band intensity and therefore estimate the extent of biotinylation at ~62% for both enzymes (**Chapter 6:**). Furthermore, two new distinct bands were detected for each biotinylated enzyme as indicated by arrows (**Figure 2-6**). Specifically, these bands appear at ~120kDa/~180kDa for biotinylated hGnTI and ~120kDa/~200kDa for biotinylated NtGnTI. The appearance of multiple bands can be explained by the valency of streptavidin as it naturally exists as a tetramer. It is worth noting that similar gel shifts were not observed in the absence of BirA. These events combined suggest that the shifted bands likely correspond to the StV-hGnTI and StV-NtGnTI complex. Interestingly, although the expected MW of StV is ~55kDa, in the gel-shift assay it appears at ~65kDa. This is also observed in the shifted bands, where the MW does not match the expected MW of the complexes (~140kDa and ~150kDa for StV-hGnTI and StV-NtGnTI respectively). It is plausible that this result is caused by the absence of a reducing agent, enabling disulphide bond formation and the generation of non-linear structures. This would result in a non-homogeneous charge distribution, altering their migration through the SDS-PAGE gel.

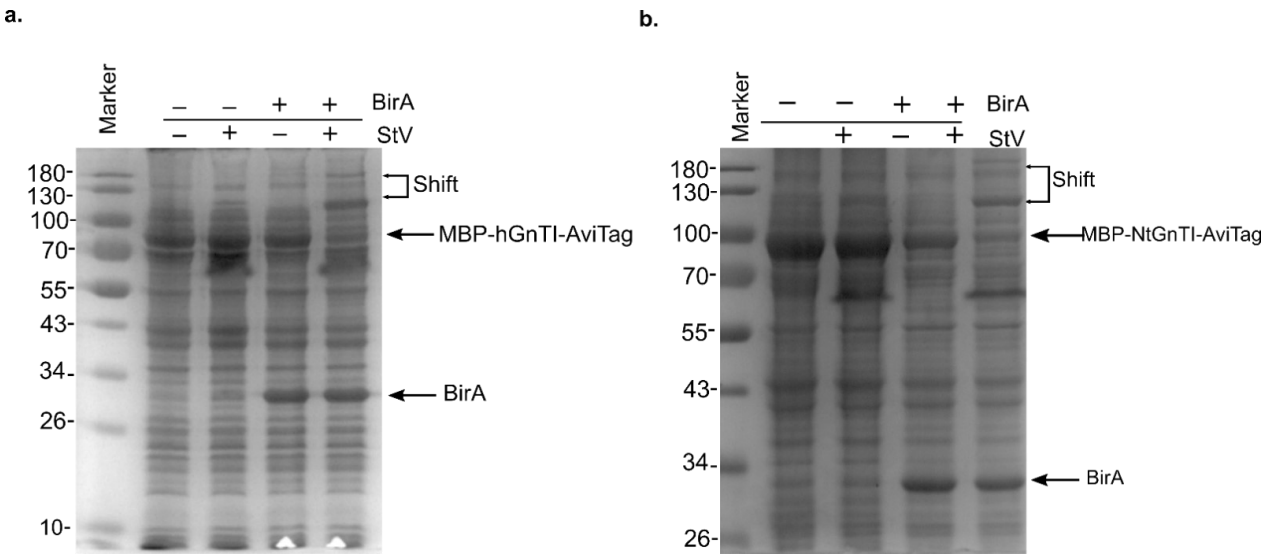

Figure 2-6: Biotinylation confirmation using a gel shift assay. Each lane was loaded with and without BirA and StV in the absence of reducing agent. A. Confirmation of biotinylation for MBP-hGnTI-AviTag; b. Confirmation of biotinylation for MBP-NtGnTI-AviTag; StV: streptavidin

Following expression and soluble fraction extraction, it was reasoned it would be necessary to remove any remaining d-biotin from solution that could compete with biotinylated enzyme for StV binding sites on the solid support. To achieve this, gravity-flow desalting columns were used (PD-10, GE Healthcare). To maximise enzyme recovery, different NaCl concentrations in the equilibration/elution buffer were tested (**Figure 2-7**). Interestingly, varying results were observed as biotinylated hGnTI required a high salt concentration of 500mM for maximum recovery while for NtGnTI, the same result was achieved with 200mM.

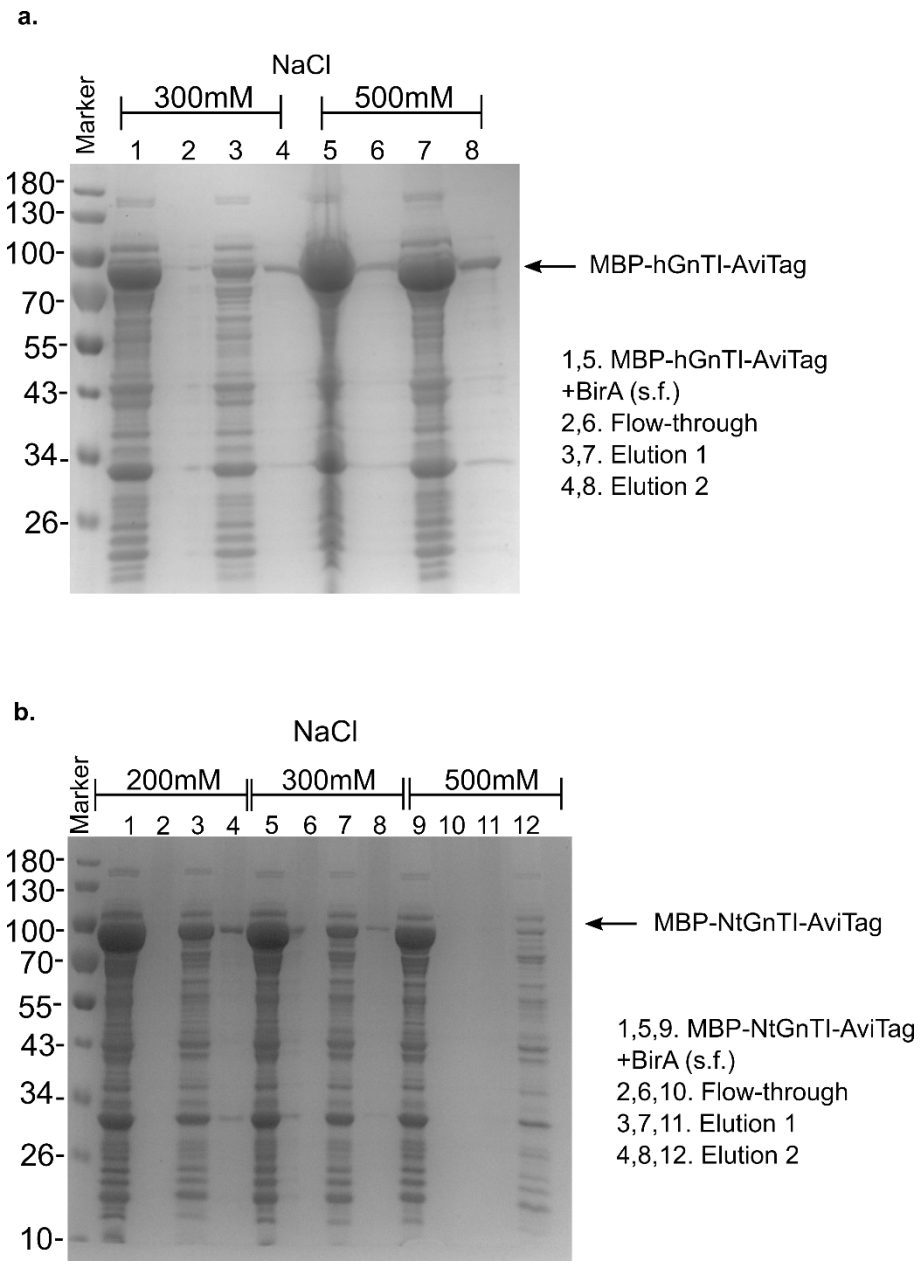

Figure 2-7: Soluble fraction desalting of GnTI orthologs to remove any free d-biotin. Buffers with different NaCl concentrations were tested. a; desalting of hGnTI; b. desalting of NtGnTI

Following desalting and removal of d-biotin, the samples were incubated with StV-coated beads attempting a one-step immobilisation/purification. Specifically, the soluble fractions were incubated at 4°C for 1h with StV-coated silica beads to allow one-step immobilisation/purification. To confirm binding, the beads were stripped by boiling them for 10 min in 1X SDS and DTT (reducing agent). The supernatant fractions were tested using SDS-PAGE analysis. Biotinylated hGnTI and NtGnTI were successfully extracted from the soluble fraction and immobilised on StV-Beads (**Figure 2-8**). Interestingly, BirA also binds to the beads, possibly due to the formation of a complex with its substrate AviTag. To further elucidate the nature of binding, 2% SDS was included in the washes following immobilisation. Indeed, washing in the presence of a strong detergent removes BirA, indicating non-specific binding. Furthermore, different ratios of soluble fraction to StV bead volumes were tested to attempt to improve immobilisation efficiency (**Figure 2-9:** Immobilisation of desalted hGnTI. Different soluble fraction (s.f.): StV-beads ratios are indicated.. However, no apparent difference was observed in the intensity of bands, suggesting the binding sites were saturated. Similar results were observed for immobilised NtGnTI (data not shown).

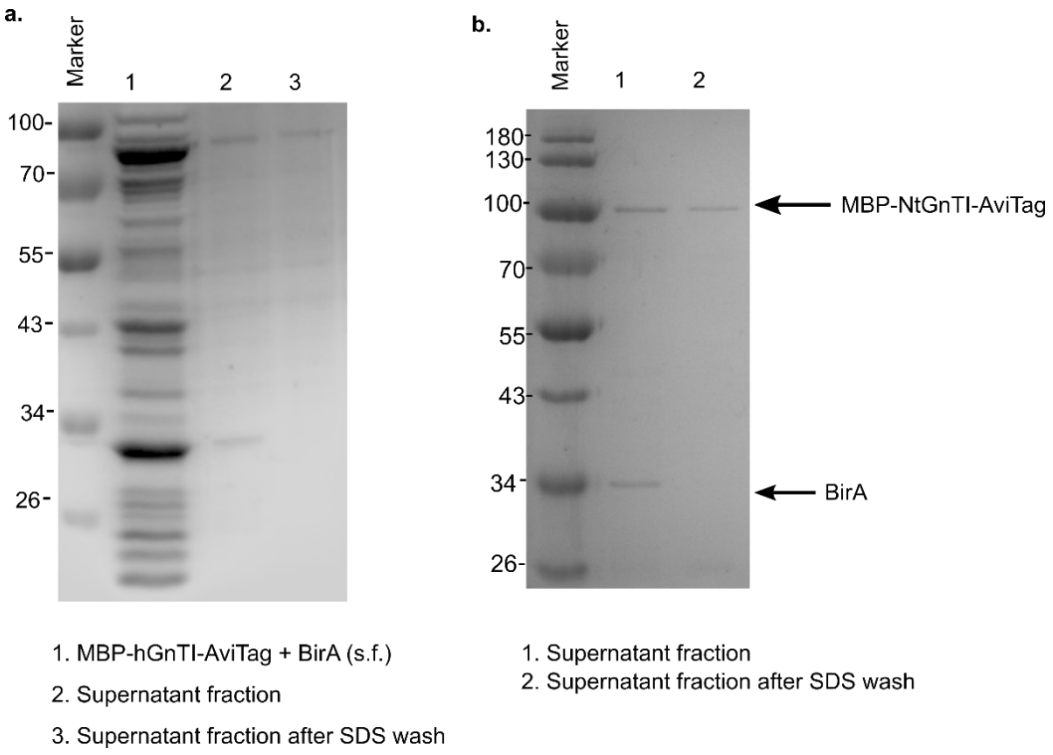

Figure 2-8: Immobilisation of desalted soluble fractions of GnTI orthologs on StV beads and confirmation of non-specific binding following detergent (SDS) washes post-immobilisation. Beads were stripped after boiling with SDS detergent and the supernatant fractions were analysed. a. Immobilisation of hGnTI; b. Immobilisation of NtGnTI.

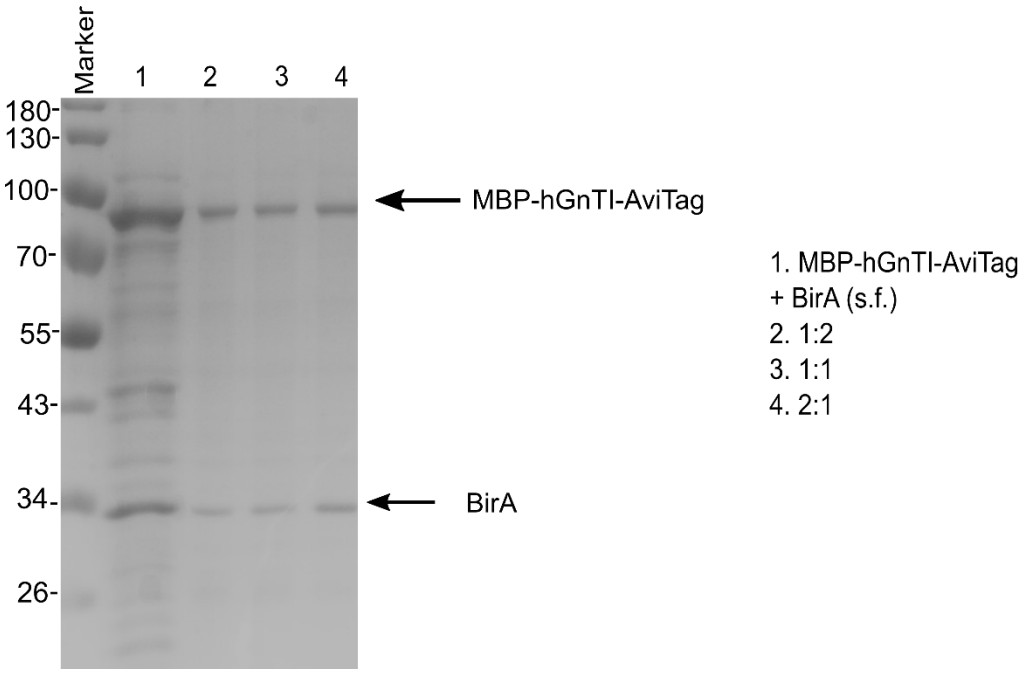

Figure 2-9: Immobilisation of desalted hGnTI. Different soluble fraction (s.f.): StV-beads ratios are indicated.

Finally, an estimation for the amount of enzyme bound on StV beads was performed, by using the binding capacity of the particles and assuming maximum occupancy and no steric hindrance. Specifically, for a binding capacity of 0.3 nmoles/mg of solid particles and for 50µl of StV beads, the enzyme retention was 0.25 mg/ml for hGnTI and 0.28 mg/ml for NtGnTI.

2.2.2. Objective 1b. Confirmation of activity of immobilised hGnTI and immobilised NtGnTI

Following one-step immobilisation/purification, hGnTI and NtGnTI were tested for activity using a commercially available colorimetric activity kit for GTs (R&D systems). Their activity was compared to that of free hGnTI and NtGnTI, respectively, to understand the effect of immobilisation on activity. To investigate if the impurities from the one-step immobilisation/purification have an effect, purified hGnTI and NtGnTI were immobilised and tested for activity. As described in section 2.1.4, this is a coupled assay where UDP generated from the activity of GnTI is degraded by a phosphatase, releasing inorganic phosphate which is subsequently detected using Malachite green. The intensity of malachite green functions as a proxy for enzymatic activity. This assay was conducted using freshly prepared immobilised fractions of hGnTI and NtGnTI which were incubated as described by the manufacturer of the activity kit: for 1h with a reaction mixture containing the sugar acceptor mannotriose (3 mannose sugars), the NSD UDP-GlcNAc and $MnCl_2$ at pH 6.5. The optimum

temperature differs between the two enzymes, hence hGnTI was reacted at 37°C while NtGnTI at 25°C[202,203].

As shown in **Figure 2-10**, both enzymes tested positive for activity, while 3x more inorganic phosphate, was detected for NtGnTI compared to hGnTI. The negative control showed an increased amount of released inorganic phosphate which can be explained by the natural degradation of UDP-GlcNAc to UDP. Unexpectedly, the free enzymes showed no measurable activity as the concentration of inorganic phosphate corresponding to UDP matched the negative control. These results were also replicated using an in-house HPLC method, developed to measure the concentration of NSDs and NDs directly (data not shown).

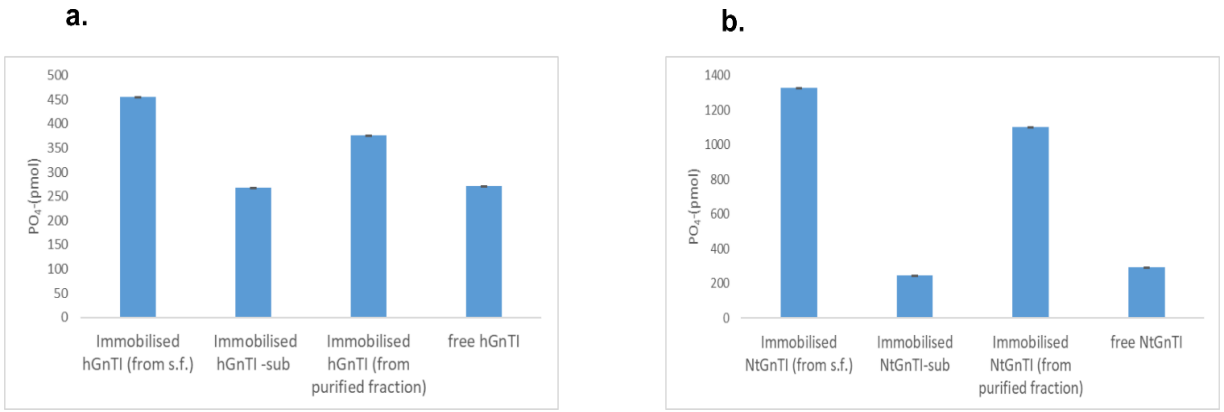

Figure 2-10: Colorimetric activity assay for GnTI. a. results for hGnTI; b. results for NtGnTI. -sub denotes the negative control, where no acceptor substrate was included in the reaction mixture; s.f.: soluble fraction.

Rather than inferring activity from this data, it was decided to further investigate and test the samples using MALDI-TOF MS. Surprisingly, the desired product (GlcNAcMan3- expected m/z 926) was not detected for any of the immobilised enzyme candidates (**Figure 2-11**, data only shown for immobilised NtGnTI), contradicting the positive activity results obtained using the colorimetric assay.

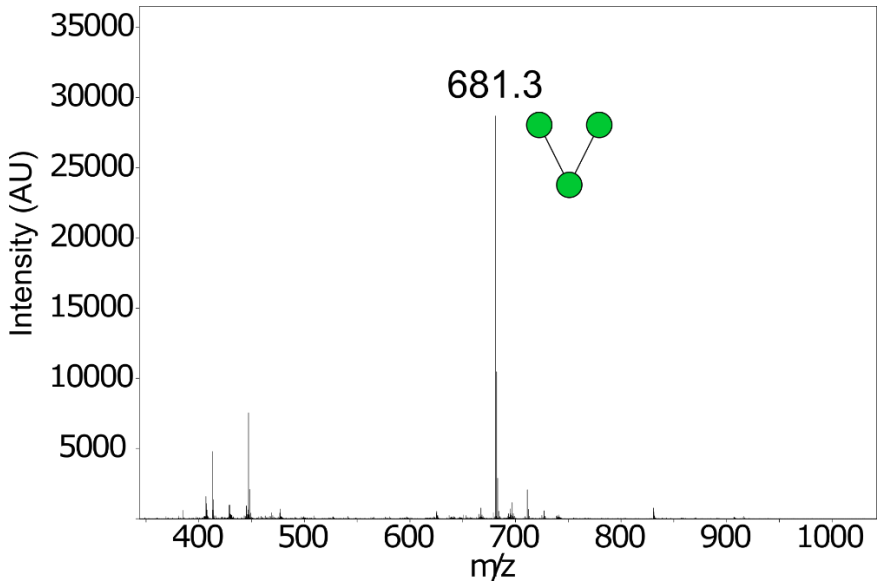

Figure 2-11: MALDI-TOF MS results for immobilised NtGnTI. m/z of acceptor substrate (Man3) is 681.3; m/z of expected product (GlcNAcMan3) is 926.5 (not detected).

Considering the high specificity towards the acceptor substrate, it was decided to re-test for enzymatic activity but using the preferred substrate $Man_5GlcNAc_2$ (M5). Furthermore, only NtGnTI was selected due to ease of handling and because higher cell growth rates were achieved (data not shown). Immobilised NtGnTI was reacted overnight with UDP-GlcNAc and commercially available M5, in the presence of 1mM $MnCl_2$, 100mM MES at pH 6.5 and 25°C as described previously[202]. The expected product GM5 was successfully detected, confirming the activity of immobilised NtGnTI (**Figure 2-12b**). Furthermore, GM5 was in abundance suggesting the reaction was near completion. Similar results were also achieved for free, biotinylated NtGnTI and NtGnTI immobilised after purification (data not shown). Finally, enzyme activity was also checked using commercially available $Man_3GlcNAc_2$ (M3) as the acceptor glycoform (**Figure 2-12c**). Compared to mannotriose used previously, M3 differs as it has two additional GlcNAc residues. There was successful production of GM3 but the relative intensities indicate less than 50% conversion (**Figure 2-12d**).

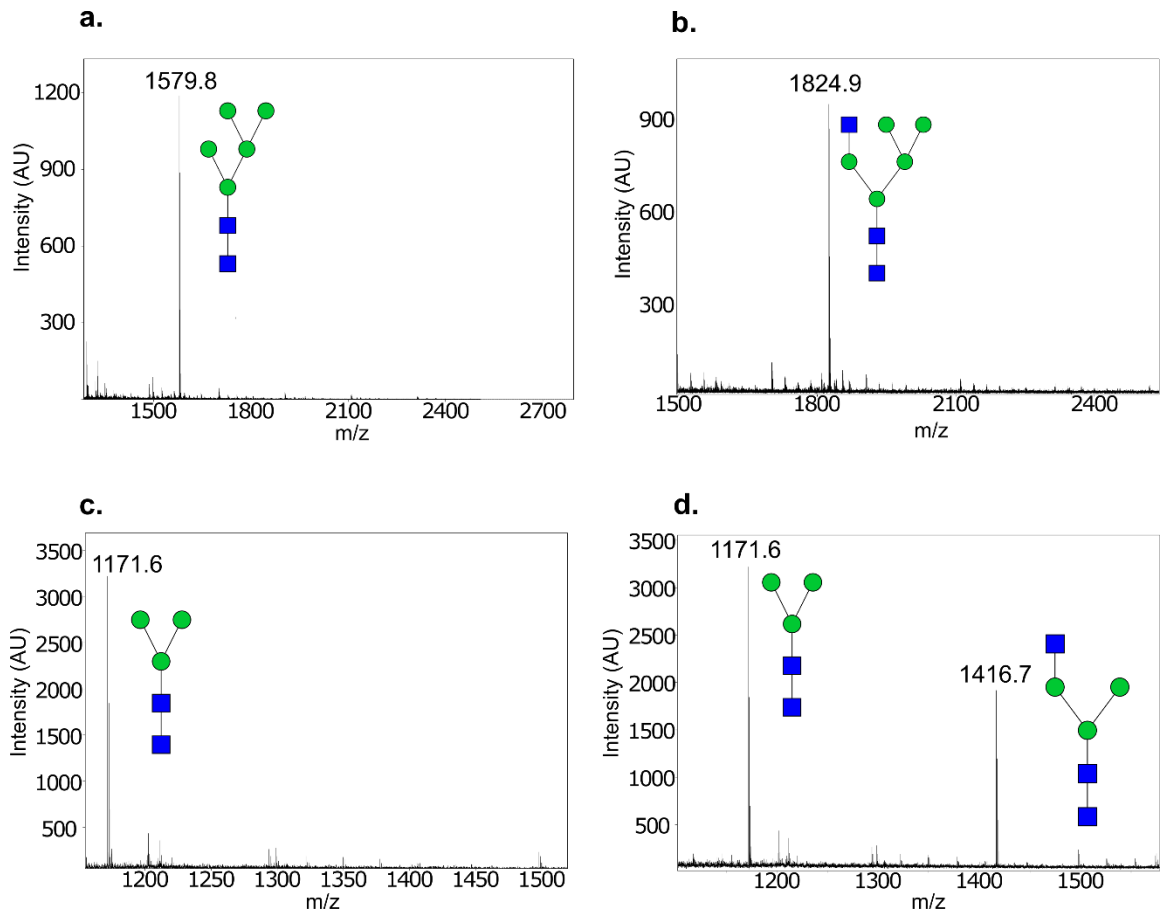

Figure 2-12: Reactions of immobilised NtGnTI as monitored by MALDI-TOF MS. a. 0h, acceptor sugar M5 b. overnight reaction, product GM5 c. 0h, acceptor sugar M3; d. overnight reaction, product GM3.

2.2.3. Objective 2a. Expression, biotinylation and immobilisation of hGalT

The methods developed for GnTI were also applied for the expression and immobilisation of hGalT, the final enzyme involved in the selected pathway. Specifically, the catalytic domain of hGalT was used to make the fusion MBP-hGalT-AviTag (~76 kDa) (**Table 2-1**). Solubility was confirmed using SDS-PAGE analysis, where bands corresponding to the expected MW were detected (**Figure 2-13a**). Furthermore, the enzyme remained soluble following co-expression with BirA and *in vivo* biotinylation.

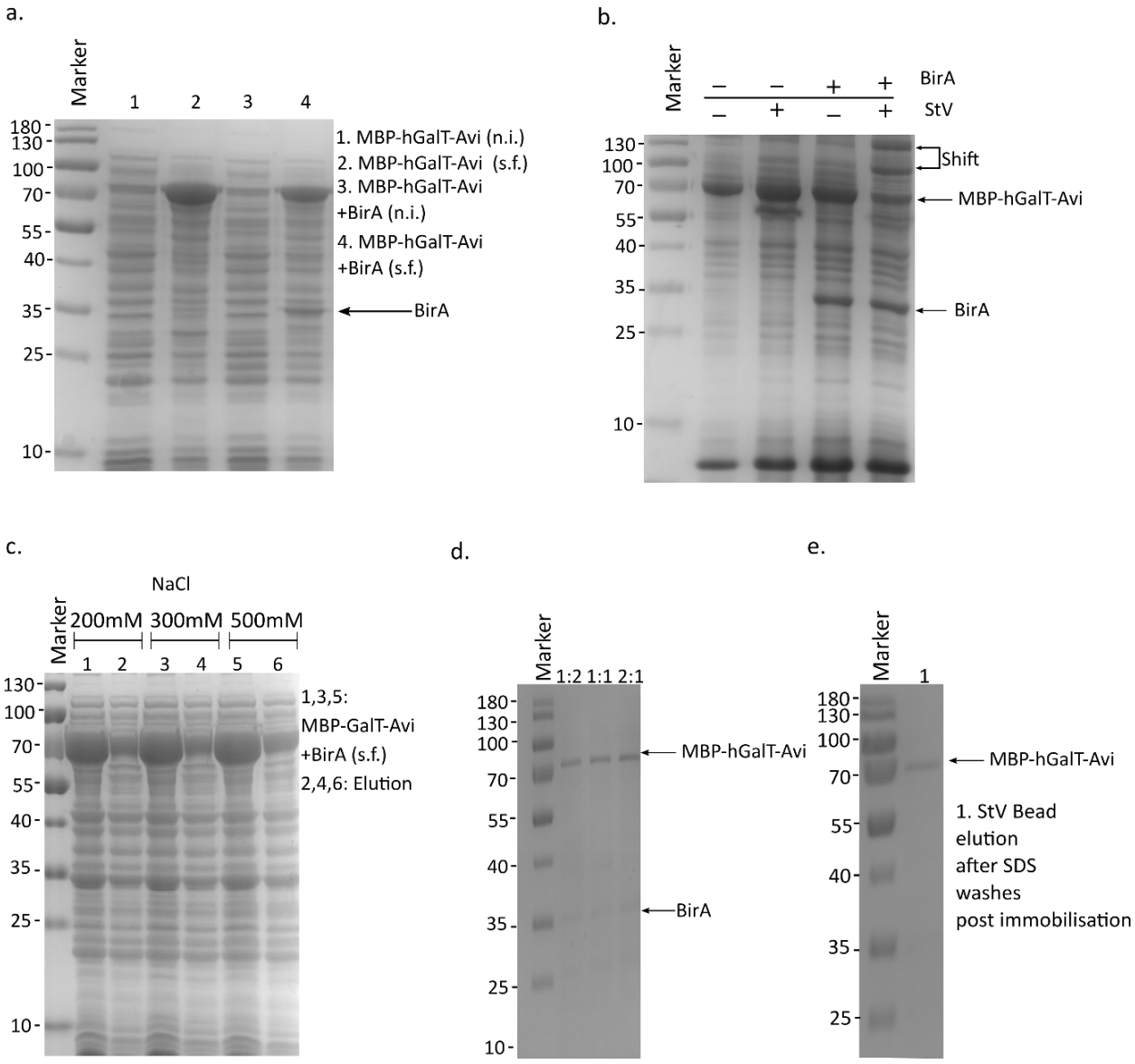

Figure 2-13: Expression and immobilisation of hGalT. a. Solubility check of hGalT with and without in vivo biotinylation; b. Biotinylation confirmation using a gel shift assay; c. Crude soluble fraction desalting. Buffers with 200/300/500mM NaCl concentrations were tested; d. Immobilisation of desalted crude soluble fraction on beads. Different s.f.: StV beads ratios were tested as indicated; e. confirmation of non-specific binding using detergent (SDS) wash post-immobilisation. Beads were stripped after boiling with SDS; n.i.: non-induced; Avi: Avitag; s.f.: soluble fraction; StV: streptavidin.

The gel shift assay applied previously to GnTI was also applied here. The crude soluble fraction of MBP-hGalT-AviTag produced in cells with and without BirA was incubated with StV in the absence of a reducing agent. There is a distinct decrease in the band intensity corresponding to MBP-hGalT-AviTag, which was estimated to be ~72% using image analysis and densitometry. Furthermore, two

new distinct bands were detected as indicated by the arrows in **Figure 2-13b**. However, due to the improper migration of StV it is not certain which complex each band represents.

Following expression and soluble fraction extraction, a desalting step was performed to remove free d-biotin from solution, which, as mentioned, may interfere with immobilisation. To achieve this, gravity-flow desalting columns were used (PD-10, GE Healthcare). To maximise enzyme recovery, different NaCl concentrations in the equilibration/elution buffer were tested (**Figure 2-13c**). In contrast to the results for the GnTI variants, no difference was observed amongst the NaCl concentrations tested. For convenience, 200mM NaCl was selected. Biotinylated hGalT was subsequently immobilised/purified from the crude soluble fraction by incubation with StV-conjugated beads. Eluting bound protein bound to the StV-conjugated beads confirmed successful binding, as there was a distinct band at ~76kDa, corresponding to the molecular weight of MBP-hGalT-AviTag (**Figure 2-13d**). Interestingly, there appears to be less non-specific binding when compared to hGnTI and NtGnTI as the band corresponding with BirA was weaker (**Figure 2-13d** & **e**). Furthermore, different ratios of soluble fraction to StV-beads volumes were tested but there was no apparent improvement in binding efficiency, suggesting bead saturation under the conditions used.

Finally, an estimation for the amount of enzyme bound on StV beads was performed, by using the binding capacity of the particles and assuming maximum occupancy and no steric hindrance. Specifically, for a binding capacity of 0.3 nmoles/mg of solid particles and for 50µl of StV beads, the enzyme retention was 0.23 mg/ml.

2.2.4. Objective 2b: Confirmation of activity of immobilised GalT

The activity of immobilised hGalT was confirmed using an existing protocol for commercially available hGalT (R&D systems). Specifically, the immobilised enzyme was incubated with a reaction mixture containing the acceptor GlcNAc, UDP-Gal and $MnCl_2$ overnight at pH 7.5 and 37^{o}C. Commercially available hGalT was used as a reference (R&D Systems). The expected product GalGlcNAc was successfully detected for both samples, thus confirming enzymatic activity (**Figure 2-14**). It is worth mentioning that it is not easy to detect single sugars such as GlcNAc with MALDI-TOF MS. Hence it was not feasible in this experimental set-up, to quantify the extent of the reaction and determine whether it was near completion.

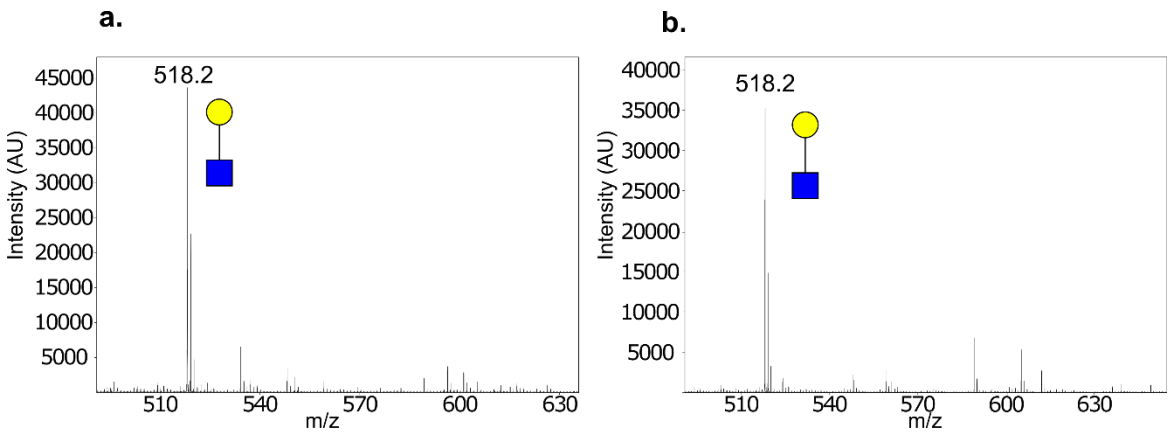

Figure 2-14: hGalT reactions with GlcNAc after overnight reaction as monitored by MALDI-TOF MS. Expected product is GalGlcNAc. a. commercially available free hGalT; b. immobilised hGalT produced in *E. coli*.

2.2.5. Objective 3a: Chemical biotinylation immobilisation and of dmManII

The remaining enzyme required to implement the selected glycosylation pathway is dmManII. As it was already expressed and purified, commercially available reagents for chemical biotinylation (Lightning-Link, Expedeon) were used. The resulting biotinylated enzyme was immobilised on streptavidin beads. SDS-PAGE analysis of the bead elution fraction confirmed successful immobilisation since there is a distinct band at the expected MW (~116 kDa) (**Figure 2-15**). The remaining bands are either impurities or the result of enzyme fragmentation. Interestingly, following immobilisation, the amount of StV beads after centrifugation was significantly decreased suggesting losses during the washes or some interference from the chemical biotinylation reagents. The enzyme retention, 0.3 mg/ml, was calculated based on the StV beads capacity and the concentration of DmManII used for immobilisation (1mg / ml).

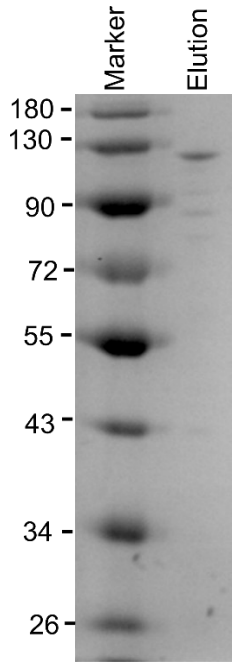

Figure 2-15: SDS-PAGE analysis of bead elution fraction following immobilisation of chemically biotinylated DmManII.

2.2.6. Objective 3b: Confirmation of activity of immobilised DmManII

The activity of immobilised DmManII was confirmed using its substrate GM5, the product of the immobilised NtGnTI's reaction, produced in this work (**Figure 2-12**). The reaction took place at 37°C overnight, at pH 5.6 and in the presence of the metal donor $ZnSO_4$. The expected product GM3 was successfully detected using MALDI-TOF MS thus confirming enzymatic activity (**Figure 2-16**). Furthermore, only the expected product was detected suggesting the reaction was near completion.

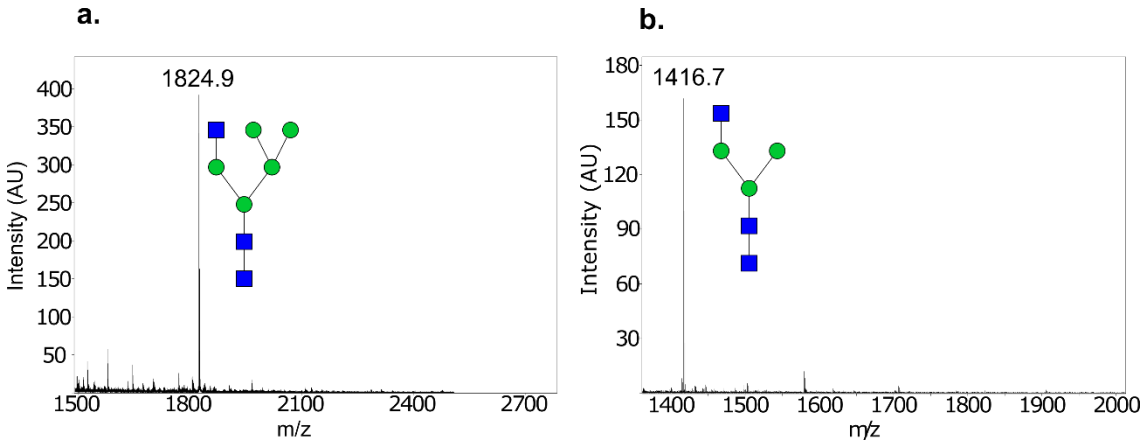

Figure 2-16: Reactions of immobilised DmManII as monitored by MALDI-TOF MS. a. 0h, starting sugar GM5 b. Overnight reaction, product GM3.

2.3. Discussion

2.3.1. Expression, biotinylation and immobilisation

In line with the objectives of this chapter, methods for the expression, biotinylation and immobilisation of functional GnTI and GalT and immobilisation of functional ManII were developed. The origin of each enzyme and expression conditions were selected based on available literature data. Two orthologs of GnTI, NtGnTI and hGnTI, in addition to hGalT were selected for expression in *E.coli* Origami as previously demonstrated[172,198,202,203,220,234]. Although all enzymes derive from eukaryotes, they have been successfully expressed in bacterial hosts, demonstrating that the lack of certain PTMs does not affect functionality. This demonstrates that certain strains of bacteria are suitable expression platforms for these GTs, enabling scale-up in an affordable way. As for the mannosidase, purified DmManII was available to use from our collaborators in the University of Waterloo, Canada whose group has extensive experience with this enzyme[209,225,235].

A crucial step of this work was the selection of an immobilisation method. The overall scope of this PhD was to establish a method to address enzyme promiscuity in glycosylation reactions by means of spatial and temporal separation. In contrast to traditional methods such as *in* vitro one-pot reactions or *in vivo* glycoengineering that fail to address promiscuity and ensure homogeneity, enzyme immobilisation is a simple and attractive solution. It enables the facile handling and recovery of enzymes after each reaction thus preventing undesired competition. Amongst the factors that drove the method selection was the strength of binding to the support. Strong interactions are essential to prevent enzyme leaching which can lead to undesired enzyme cross-reactivity and require intermediate purification steps. Notably, biotin/streptavidin is the strongest, natural non-covalent interaction which forms spontaneously without the need for harsh chemicals[223]. Furthermore, contrary to commonly used affinity-based immobilisation methods, it is not susceptible to changes in reaction conditions e.g. salt concentration or pH, that might break the bond[221,223,227].

Of great importance is the type of biotinylation to appropriately modify the enzymes and consequently bind them onto streptavidin-coated solid supports. Here, an *in vivo* enzymatic biotinylation system was selected, requiring the fusion of the GnTI and GalT enzymes to AviTag, a substrate of the biotin ligase BirA. To our knowledge, enzymatic biotinylation using BirA and AviTag has never been tested on glycosyltransferases before. Amongst the advantages of using enzymatic biotinylation is the simplicity and versatility of the method as it can be applied either *in vivo*, with co-expression of BirA, or *in vitro*, where all components are previously purified[229]. This simplicity was a

decisive element for method selection as it does not require excessive enzyme engineering that might negatively affect structure or activity. Furthermore, the versatility makes the system compatible with multiple expression platforms such as bacteria or mammalian-based systems[226,230,236,237], thus allowing for the potential of a multitude of glycosyltransferases to be biotinylated regardless of their specific requirements. In addition, the ability to perform *in vivo* biotinylation enables a one-step production and modification process while enabling a one-step purification/immobilisation strategy. Moreover, a significant advantage is the ability to achieve oriented and site-specific immobilisation. Biotin is added on a single site on the target tag thus non-specific interactions with the solid supports are prevented. This is in contrast to traditional chemical biotinylation methods where biotin is added in multiple sites.

There are various alternative techniques that also enable site-specific immobilisation with varying reported yields[220,238–245]. Amongst these, a notable method is the Sortase A (SrtA) mediated covalent immobilisation technique which has been successfully used to immobilise human GalT and *H. pylori* FucT[220]. It requires the fusion of the enzyme with a suitable peptide which is subsequently attached to the solid support by SrtA through a transpeptidase reaction. It would be interesting to perform a comparison study of the two methods for immobilising glycoenzymes, the *in vivo* enzymatic biotinylation for binding on Stv supports developed here and the SrtA mediated covalent immobilisation. The factors to consider can be the conditions required for immobilisation, the enzyme retention on the solid supports and whether it can be applied to enzymes derived from different cell-based systems. Such a study can inform future endeavours for immobilising functional GTs of similar structure, which would be expected to behave in a similar manner.

To establish the novel *in vivo* biotinylation system for the selected GTs, a few factors required consideration. Firstly, the selection of the target tag. Although other peptides of varying sizes and sequences exist and can act as substrates to BirA, AviTag remains the most widely used tag for increased biotinylation yields[226,230]. Furthermore, to ensure biotinylation does not cause unwanted steric hindrance, a small two-residue flexible glycine-serine (GS) linker was added before the AviTag[226]. Interestingly, AviTag can be added on either the N- or the C-terminus of proteins without a negative effect on biotinylation yields[230]. However, in this work, since the enzymes are fused to an MBP on the N-terminus and to ensure the immobilisation of the enzyme rather than of the solubility tag, AviTag was inserted on the C-terminus.

The designed *in vivo* biotinylation scheme was subsequently tested on three enzymes, two orthologs of GnTI (NtGnTI and hGnTI) and hGalT. All enzymes were estimated to be >60% biotinylated. This can be further improved either by optimising the concentration of added biotin or by optimising the

expression levels of BirA[226,229,230]. Alternatively, *in vitro* biotinylation with purified BirA can be performed. This can allow optimisation of the reaction conditions, i.e. concentration of BirA and biotin, to ensure maximum biotinylation yield.

A challenge faced upon development of the *in vivo* biotinylation system concerned the detection method. The gel shift assay is often recommended as it is cost-effective, easy and semi-quantitative. As first demonstrated here, the gel shift assay does not require purified protein. As seen in the obtained results, multiple shifts were observed across all tested enzymes, (NtGnTI, hGnTI, hGalT) which do not correspond to the expected molecular weight of the StV-enzyme complex. Although this altered migration is explained by the absence of oxidising reagents, it complicates the precise quantitation using standard image analysis. As recommended by the authors who described this technique[230], densitometry analysis was used to quantify the intensity of each band. Nevertheless, this was still an estimation. Therefore, if strict biotinylation quantification is required, a more sensitive detection method is necessary. One example is a commercially available Biotinylation Reaction Titration Assay (BRTA) (Avidity, LLC), an ELISA-like assay used to detect the biotinylation of purified MBP-AviTag fusion proteins.

Following confirmation of biotinylation, a one-step purification/immobilisation of the enzymes (hGnTI, NtGnTI and hGalT) was accomplished. However, additional work is required to further optimise this process. Firstly, although the target enzymes were in abundance, there were still some persistent impurities mostly caused by BirA. The gel shift assays demonstrated that BirA is not covalently bound to biotin, although there could be a weak interaction between BirA and biotin. Alternatively, BirA's presence might be due to it still being attached to AviTag. In the future and if required, BirA-related impurities can be addressed by optimising the buffer and detergent conditions.

Another aspect that requires work is calculating the immobilisation yield. This can be demanding since the enzymes are not purified and their concentration is unknown. It would be possible to perform a protein concentration assay on the crude samples before and after immobilisation. However, such a calculation would be inaccurate as the samples are significantly diluted for immobilisation and it does not consider possible losses caused by centrifugation or shaking. One solution is to perform titrations of StV beads and gel-shift assays on the unbound material until maximum recovery of biotinylated enzyme is confirmed. Furthermore, it can also be challenging to accurately calculate the amount of enzyme bound on StV beads. Theoretically, it can be estimated indirectly based on the binding capacity of StV beads, assuming maximum occupancy, as demonstrated here. Although this assay appears a simple way, it is subject to variability as it

operates under the assumption the enzyme expression and immobilisation yields remain constant as well as there is no steric hindrance. Therefore, calculating the amount of bound enzyme in the aforementioned way should ideally be performed after every reaction, thus complicating implementation.

Finally, further work is necessary to apply the same biotinylation system to DmManII and maintain a uniform production process. DmManII, a kind gift from our collaborators in the University of Waterloo, was expressed without carrying an AviTag, thus enzymatic biotinylation using BirA was not feasible. Future work would consist of either expressing a DmManII-AviTag fusion in insect cells followed by *in vitro* enzymatic biotinylation or attempt expression in *E. coli*. Since the enzyme does not carry any glycosylation sites, bacteria can in principle support the production of functional enzyme variants[209]. However, there are no literature data to demonstrate the feasibility, thus making it a novel endeavour.

2.3.2. Confirmation of activity

Following successful implementation of the biotinylation and immobilisation schemes, all enzymes were tested for activity. The main objective was to determine if the enzyme expression and immobilisation strategies had a negative effect on enzyme functionality. Activity was confirmed for three immobilised enzyme candidates, NtGnTI, hGalT and DmManII, thus demonstrating the success of the biotinylation/immobilisation scheme. The main challenge encountered was identifying a suitable analysis technique.

Initially, NtGnTI and hGnTI were tested for activity using a commercially available colorimetric kit specific to GTs. It relies on detecting released inorganic phosphate from UDP. In principle it is an accurate method as UDP is released only when the sugar transfer is complete. However, the results obtained with this technique were in contrast to those obtained using MALDI-TOF MS, given no product was detected. A possible explanation for this discrepancy could be that the various modifications conducted on these enzymes have altered their mode of action. Typically, after binding onto the NSDs, GnTI and all Leloir GTs undergo natural conformational changes that prevent them from degrading the donor prematurely[27,246]. Perhaps immobilising the enzymes created non-predicted structures that allow the enzymatic degradation of UDP-GlcNAc prior to transferring to the acceptor. To support this hypothesis, structural data could be collected during future studies.

In the case of hGnTI and NGnTI, no product was detected when these enzymes were incubated in the presence of mannotriose. The absence of formed product is most likely the result of the high

specificity of GTs towards the acceptor substrate[27,246]. Despite mannotriose being the supplier's recommendation, it is not the preferred substrate for GnTI[202,203,205,247]. Indeed, when repeating the experiment for NtGnTI with M5, activity was successfully confirmed with MALDI-TOF MS for both the free and the immobilised enzyme. Significantly, the product GM5 was in high abundance showing the reaction was near completion. Moreover, GnTI substrate specificity[202] was confirmed using M3 as a substrate, where, after an overnight incubation, the reaction extension yields were significantly less than the reaction with M5. It is worth mentioning, that these experiments were not performed for hGnTI. It was decided to advance with NtGnTI, given higher yields were achieved. Interestingly, though mannotriose and M3 share the same number of mannose residues, there was no product detected in the reaction with the former. It is possible that the presence of the two extra GlcNAc residues in M3 serve as docking for the enzyme thus allowing the sugar transfer.

In conclusion, the observations made in this work illustrate the limitations of techniques detecting released NDs. As such, they should not be the sole analysis method in studies focusing on understanding the activity or the substrate specificity particularly when identifying novel substrates. It is important to use a technique that can successfully detect product formation rather than focus on by-product detection, which might be misinterpreted. MALDI-TOF MS is an appropriate technique but faces certain limitations which are discussed later on[7,233]. MALDI-TOF MS was used for sample analysis in subsequent experiments.

Immobilised hGalT was tested for activity using MALDI-TOF MS following a reaction with free GlcNAc as a substrate. Our analysis using MALDI-TOF MS confirmed the activity of hGalT immobilised using the methodology developed in this chapter. hGalT has previously been immobilised at the C-Terminus using SrTA mediated site-specific immobilisation[220]. Our data is in-line with this previous result, supporting this strategy as a viable option hGalT immobilisation.

One challenge faced during analysis of hGalT activity was the inability to detect the substrate of the reaction (GlcNAc) using MALDI-TOF MS. This was likely due to the high noise level at a low m/z range. Therefore, there is no indication of the extent of the reaction. Other techniques that can be used and have been previously demonstrated to work well in similar assays are High Performance Liquid Chromatography (HPLC) for the detection of neutral metabolites or scintillation provided the sugars are radioactively labelled[248,249]. However, since the main objective was to only confirm activity, optimisations to estimate conversion were not necessary at this stage. Furthermore, when the multi-enzyme pathway is implemented, the substrate will be the polysaccharide GM3, which is easier to detect using MALDI-TOF MS given it has a larger m/z ratio. GM3 was not available to test it

on hGalT when performing the experiments described in this chapter, as DmManII which produces it, was developed last.

The final enzyme that was tested for activity following immobilisation was DmManII. This was particularly interesting, since it was thought that chemical biotinylation might have damaged the catalytic site and consequently the activity. However, the functionality of the immobilised DmManII was successfully confirmed thus showing a highly robust enzyme. Significantly, the reaction was conducted using NtGnTI's product, hence this is the first step towards completing the cascade of glycosylation reactions of the three-enzyme pathway (NtGnTI-DmManII-hGalT).

A final point that is worthy of discussion is the conditions and the technique applied to demonstrate activity. All enzymatic reactions were monitored with MALDI-TOF MS were performed overnight to ensure a positive signal. In addition, though the specific conditions of temperature, pH, donor concentration and buffer composition were selected based on available literature on the free enzymes, the amount of enzyme was still an estimate. Furthermore, as MALDI-TOF MS is not commonly used for absolute quantitation it is not possible to accurately calculate the specific activity[250,251]. Although the intensities of the peaks do not change between runs, thus allowing a relative comparison, there are variations associated with instrument response, surface modifications and ionisation efficiency related to the sugar structures[250]. Furthermore, the vast range of glycan structures and the difficulty in obtaining pure material in sufficient amounts, complicates the use of internal standards that would allow quantitation. Though there has been progress in quantifying glycans using MALDI-TOF MS, techniques that do not rely on the structure of the components are most often used. Such techniques depend on labelling, e.g. fluorescence or chromatographic interactions. Some examples are capillary electrophoresis, High Performance Anion Exchange Chromatography (HPAEC) or HPLC[251–257]. Therefore, these results obtained here are a confirmation of functionality but not indicative of specific enzymatic activity. Future work would entail the use of quantitative techniques to quantify kinetic parameters such as K_m and k_{cat}. Additionally, Design of Experiments (DoE) can be used to identify the right conditions for enhanced activity. These will facilitate modelling of the multi-enzyme pathway and elucidate the conditions required to achieve optimal conversions.

2.4. Summary and Conclusions

The aim of this results chapter was to conceive and implement methods for the expression and immobilisation of enzymes regulating a target glycosylation pathway i.e. GnTI-ManII-GalT. The development of such methods would assist with controlling enzyme promiscuity and ensuring

homogeneity when performing glycosylation reactions. To this end, a literature review assisted with identifying suitable expression platforms and an appropriate immobilisation technique. An enzymatic biotinylation was selected and an experimental strategy was designed. This strategy was applied for the first time on three glycosyltransferases, specifically on hGnTI, NtGnTI and hGalT. This demonstrates the potential of this novel platform to be applied on multiple GTs of similar structure. Furthermore, a simple biotinylation detection assay was used on crude soluble fraction while a one-step purification/immobilisation was achieved, eliminating the need for additional purification steps. Activity post-immobilisation was confirmed for NtGnTI, hGalT and chemically biotinylated DmManII using MALDI-TOF MS. The experiments conducted here, and the observations made, shine some light on the importance of an appropriate detection method. More work is required to understand immobilisation efficiencies and optimising the cost of the method. Future work also includes the application of quantitative methods and DOE to optimise the reaction parameters. Hence, kinetic values can be obtained and used in the mathematical model developed by Klymenko and co-workers. As a result, optimal conditions for maximum conversion in each enzymatic step can be identified. Finally, the functional immobilised enzymes will be used to perform an enzymatic cascade and re-construct a human-like glycosylation pathway, achieving the overarching aim of this thesis.

Chapter 3: Immobilised-enzyme cascade for homogeneous glycosylation

3.1. Introduction

As reviewed in Chapter 1, there are various techniques available to control and tailor glycosylation. *In vivo* glycoengineering requires the genetic modification of host cell lines to either overexpress native GTs or to knock-out native GTs and/or knock-in GTs of different origin to produce human-like glycans[10,79,27]. Additionally, feeding strategies are also implemented to drive the production and availability of NSDs[179,181–183,188]. However, homogeneity is impossible due to the complex glycosylation network and enzyme promiscuity. Furthermore, *in vivo* glycoengineering is a slow and laborious approach, susceptible to bioprocess conditions and native metabolism[79]. In contrast, *in vitro* chemoenzymatic strategies allow homogeneity due to the *en bloc* transfer of the desired glycoform on an appropriately modified protein[27,79,154,161,164,258]. Nevertheless, it consists of multiple chemical steps hindering its implementation and making it a rigid approach.

An alternative method is the *in vitro* use of GTs to drive glycosylation to the desired profile, such as the use of recombinant GalT or SiaT to enhance galactosylation or sialylation respectively[167,172]. It is an attractive method as it allows strict control over the reaction conditions such as enzyme concentration and NSD availability. However, since GalT or SiaT function on already mature glycans, it is difficult to alter the profile and create complex glycans. An extended enzyme library and antibody remodelling would thus be required. To this end, a noteworthy example of *in vitro* glycoengineering is the work by Hamilton and co-workers. The authors used various GTs in a one-pot set-up to modify precursor glycans derived from microbial hosts *in vitro* and create complex structures[172]. However, the authors observed enzyme cross-reactivity and thus intermediate purifications were required. Another notable application was demonstrated by Witte and co-workers, where they performed sequential glycosylation reactions, without intermediate enzyme purification, to produce RNaseB with the SLe^x glycoform[259].

Despite progress in *in vitro* enzymatic glycosylation reactions, the challenge of enzyme promiscuity and cross-reactivity remains, particularly when a long enzymatic pathway has to be reconstructed[172]. An attractive idea is the spatiotemporal separation of glycosylation reactions. A theoretical design was described by Sears and Wong[260], where immobilised enzymes are kept in separate reactors and the substrate of interest flows through each compartment. An implementation of spatiotemporal separation was demonstrated by Ono and co-workers, where immobilised enzymes were used to

catalyse the production of a target glycosaminoglycan tetrasaccharide on a microfluidic chip[197]. Another noteworthy example is the use of a digital microfluidics chip to create an artificial Golgi[196]. Specifically, the authors kept the glycosylation enzymes in separate compartments and immobilised the substrate, heparan sulfate, which moves through each compartment with electrowetting. Finally, Heinzler and co-workers developed a microfluidic microreactor where immobilised GalT and β1,3-glucuronyltransferase were used to produce the human natural killer cell-1 glycan epitope[198]. Their purpose was to create a compartmental microfluidic reactor and demonstrate the potential of immobilised enzyme cascades in automated processes. Furthermore, they immobilised enzyme-complexes for the regeneration of the NSDs UDP-Gal and uridine 5'-diphospho-α-d -glucuronic acid (UDP-GlcA). Interestingly, the authors also demonstrated the reusability of the enzymes and specifically of GalT by performing multiple reaction cycles.

The aforementioned studies and applications of spatiotemporal separation in glycosylation reactions are pioneering in the development of enzymatic cascades and for automated glycan synthesis[198,260]. However, the main focus was the development and optimisation of the microfluidic or reactor platforms rather than addressing glycosyltransferase promiscuity to produce homogeneously glycosylated proteins. To that end, Klymenko and co-workers described a linear, continuous flow microreactor design with immobilised enzymes occupying different sections to achieve targeted glycosylation reactions[200]. The protein of interest, in this case a mAb, flows through the reactor allowing for a continuous modification process, whilst in principle addressing promiscuity and producing homogeneous glycoforms. In line with this work, Chapter 3 focused on using immobilised enzymes to tackle promiscuity and achieve the desired glycosylation profile. Furthermore, since the designed platform enables GTs to be recycled, reuse of enzymes has been explored.

3.1.1. Hypothesis and Experimental Strategy

In Chapter 2, a method for the expression and *in vivo* enzymatic biotinylation of GTs was developed and implemented. It was shown that it is possible to yield >60% of biotinylated NtGnTI and hGalT as estimated by a gel-shift assay when a one-step purification/immobilisation was achieved. It was demonstrated that this method is capable of producing functional enzymes, immobilised on StV solid supports. Additionally, DmManII was chemically biotinylated and similarly immobilised while retaining its functionality.

The next stage was to apply the system of immobilised enzymes, (the AGR), to perform sequential and tightly controlled glycosylation reactions. Naturally, the three-enzyme pathway of GnTI-ManII-GalT, is subject to enzyme competition yielding multiple possible structures (**Figure 3-1a**). The facile

recovery of immobilised enzymes can prevent this undesired competition while allowing for the desired product to be formed (**Figure 3-1b**). This is in line with the hypothesis of spatiotemporal separation addressing enzyme promiscuity and ensuring homogeneity.

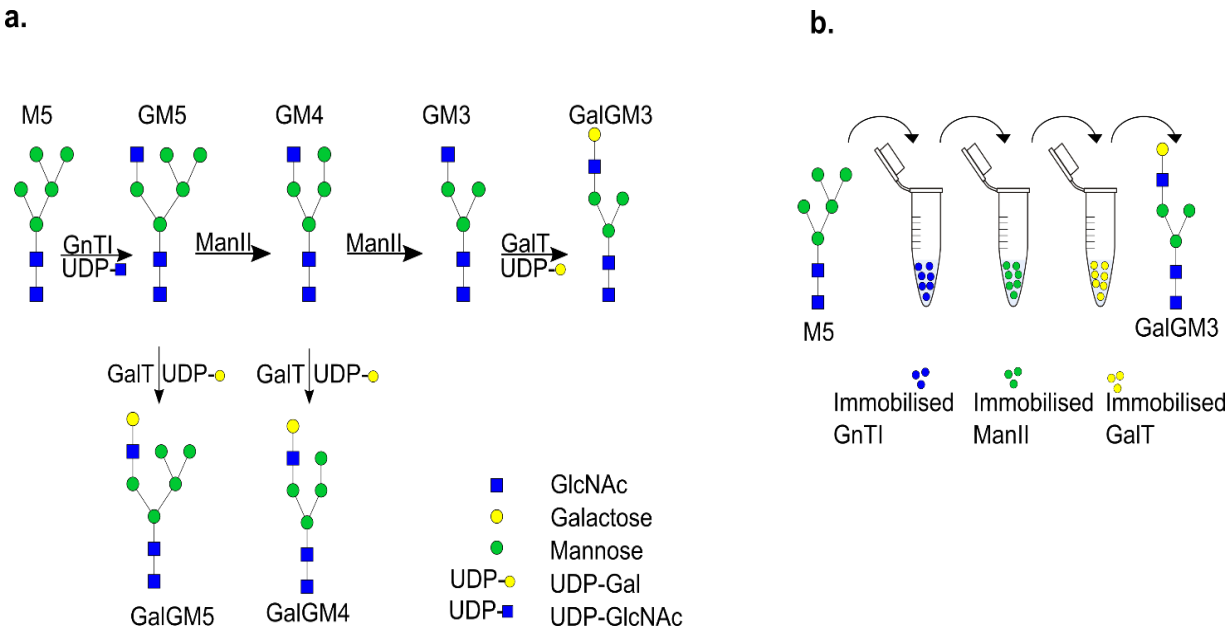

Figure 3-1. Strategy for sequential glycosylation reactions. a. N-linked glycosylation pathway as regulated by GnTI, ManII and GalT. GalT simultaneously recognises the products of GnTI and ManII, making it a highly promiscuous enzyme; b. Sequential glycosylation reactions using immobilised enzymes. The facile enzyme recovery and thus the spatiotemporal separation will yield the desired product, GalGM3, in increased homogeneity.

To test the hypothesis of spatiotemporal separation and the feasibility of AGR, sequential glycosylation reactions were performed on artificial glycans as a proof-of-concept. The aim was to produce the final glycan, GalGM3, in increased homogeneity (**Figure 3-1b**). Optimisation of the enzymatic reactions was performed to ensure each step approached completion (i.e. >95% conversion). MALDI-TOF MS was used to monitor each reaction.

Following successful implementation of the AGR on artificial glycans, the sequential reactions were applied on a model, therapeutically relevant protein. This was the monomeric Fc fragment (mFc) of a mAb (**Figure 3-2**). mFc has been explored as a potential substitute for the full-length Fc when developing drug conjugates for delivery through the FcRn circulatory pathway[261,262]. Furthermore, the mFc has a single glycosylation site facilitating analysis and optimisation and thus enabling its use as a model protein for multiple enzymatic reactions. Here, the mFc was expressed in the

glycoengineered *P. pastoris* strain SuperMan5, a product of the GlycoSwitch® technology, producing only M5 structures (**Figure 3-2b**)[109,110]. M5 is the preferred substrate of GnTI, the enzyme that initiates N-linked glycosylation. Achieving homogeneity after sequential enzymatic reactions demonstrates the potential of the AGR to reconstruct human-like N-linked glycosylation on cell-derived glycoproteins.

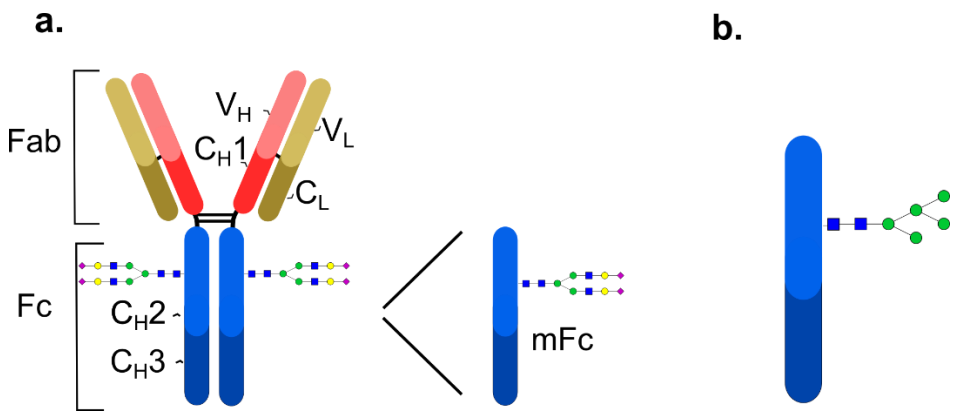

Figure 3-2*:* a. Structures of full-length IgG monoclonal antibody and monomeric Fc (mFc); b. mFc produced in *P. pastoris* SuperMan5 strain to produce mainly M5 structures. V_H: variable heavy chain; V_L: variable light chain, C_H1: constant heavy chain 1; C_L: constant light chain; C_H2: constant heavy chain 2; C_H3: constant heavy chain 3; Fab: antigen binding fragment; Fc: crystallizable fragment.

3.1.2. Objectives

The specific objectives of this chapter were as follows:

- **Objective 1:** Perform sequential reactions on artificial glycans to reproduce the enzymatic pathway of GnTI-ManII-GalT. The participating enzymes were immobilised to facilitate recovery. Each step was optimised to ensure final homogeneity. Reactions were monitored with MALDI TOF MS.
- **Objective 2:** Express mFc in the glycoengineered *P. pastoris* strain SuperMan5, to carry mainly M5 glycoforms. Glycoform distribution was confirmed with MALDI-TOF MS/MS
- **Objective 3:** Perform sequential reactions on mFc to reproduce the enzymatic pathway of GnTI-ManII-GalT. The participating enzymes were immobilised to facilitate recovery. Each step was optimised to ensure final homogeneity. Reactions were monitored with MALDI TOF MS.

- **Objective 4:** Demonstrate reusability of immobilised enzymes. StV beads were recovered with centrifugations, washed and supplemented with fresh reaction reagents. Reactions were monitored with MALDI-TOF MS.

3.2. Results

3.2.1. Objective 1: Sequential reactions of immobilised NtGnTI, DmManII and hGalT on artificial glycans.

3.2.1.1. Reaction of immobilised NtGnTI

Immobilised NtGnTI (estimated 14µg of enzyme assuming maximum site occupancy of StV beads and no steric hindrance) was reacted with M5 overnight, to produce GM5. The experimental conditions were identical to the conditions described in Chapter 2: 2.5mM UDP-GlcNAc, 0.5µM M5, 100mM MES pH 6.5, 1mM $MnCl_2$, 25°C. Interestingly, the experimental results did not match the initial estimated conversion of >95% achieved in method development in Chapter 2 (**Figure 3-3**). There is a distinct peak of remaining M5, while the conversion this time was estimated to be ~75% (**Figure 3-3a**). This was calculated by dividing the peak intensity of M5 with the sum of the intensity of M5 and GM5. The ionisation efficiency does not change significantly thus allowing a relative comparison[250]. Although the experiment was repeated multiple times using fresh batch of enzymes, the results matched the one shown in **Figure 3-3a**, but the initial result was not reproduced.

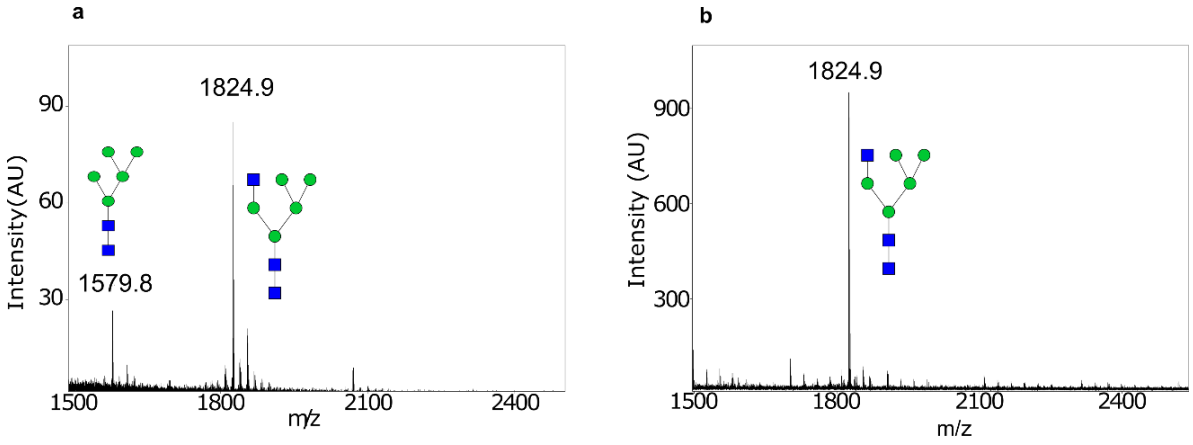

Figure 3-3*:* Overnight reactions of immobilised NtGnTI with M5, under identical conditions: 2.5mM UDP-GlcNAc, 0.5µM M5, 100mM MES pH 6.5, 1mM $MnCl_2$, 25°C. Reactions were monitored with MALDI-TOF MS; a. Recent reaction of immobilised NtGnTI; b. Earlier reaction of immobilised NtGnTI (Chapter 2).

A simple optimisation approach was undertaken to try and achieve a higher conversion. All experiments were performed in duplicates. Initially, the concentration of $MnCl_2$ metal donor was increased from 1mM to 10mM which helped to slightly increase the conversion to an estimated 80% and thus it was used in all subsequent experiments. Furthermore, in an attempt to increase the enzyme concentration, the immobilisation experiment was scaled-up by a factor of 2 (estimated 28µg enzyme assuming maximum site occupancy of StV beads and no steric hindrance). Crucially, the ratio of 1:2 of S.F. to StV beads was kept the same to avoid changes in the immobilisation efficiency. The results achieved indicated that the conversion increased approaching ~85% (**Figure 3-4a**). Furthermore, different concentrations of UDP-GlcNAc ranging from 2.5mM-10mM were tested. Out of all, 10mM gave the highest conversion of ~85% (**Figure 3-4b**).

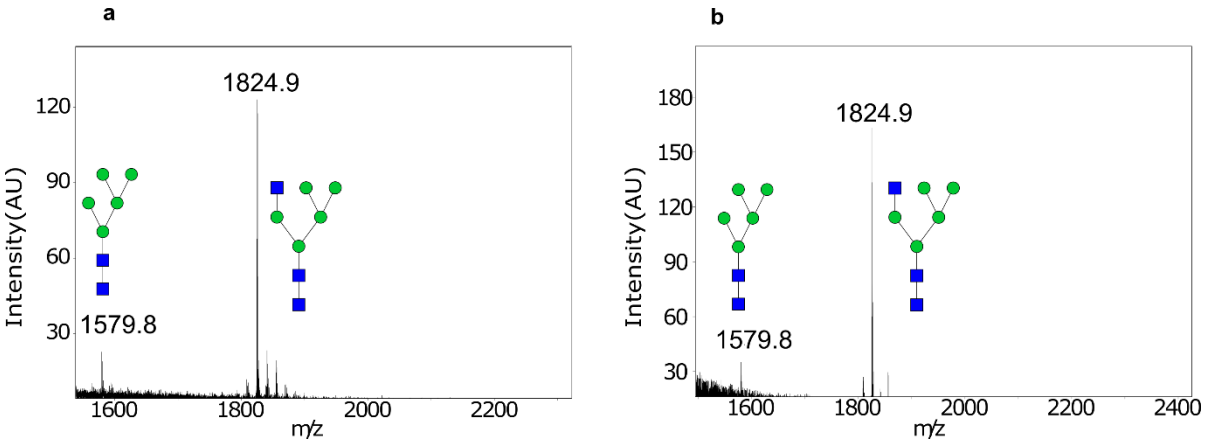

Figure 3-4*:* Optimising reaction of immobilised NtGnTI with M5 and UDP-GlcNAc. Reactions were performed overnight and were monitored with MALDI-TOF MS. a. reaction of immobilised NtGnTI where enzyme concentration and StV was doubled (Experiment A); b. reaction of immobilised NtGnTI and 10mM UDP-GlcNAc (Experiment B).

It was hypothesised that the determining factor of activity was the enzyme concentration. Therefore, the reactions depicted in **Figure 3-4** (*Experiment A*: reaction of immobilised NtGnTI where enzyme concentration and StV was doubled; *Experiment B*: reaction of immobilised NtGnTI and 10mM UDP-GlcNAc) were repeated under the same conditions and then subsequently retreated with freshly immobilised enzyme (25µl S.F : 50 µl StV beads, estimated 14µg of enzyme, assuming maximum site occupancy and no steric hindrance) to drive the reaction to completion. Furthermore, 2.5mM UDP-GlcNAc were added to *Experiment A*. No sugar donor was added to *Experiment B* since it was assumed that the initial 10mM UDP-GlcNAc was a sufficient excess. Both reactions took place

overnight. MALDI-TOF MS on the samples confirmed that both reactions approached completion with more than ~95% conversion to GM5 being achieved (**Figure 3-5**).

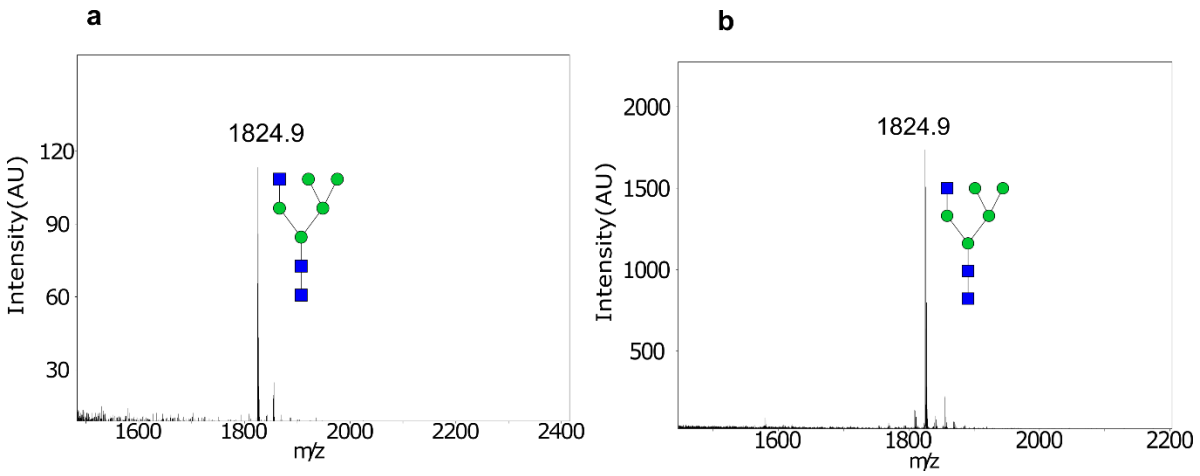

Figure 3-5: Reactions of immobilised NtGnTI following addition of fresh enzyme. Reactions took place overnight and results were monitored with MALDI-TOF MS. a. Retreated Experiment A; b: Retreated Experiment B.

Interestingly, brown precipitation was observed upon long term storage at -20°C. This could be caused by oxidation of $MnCl_2$, which was increased compared to the initial experiments. Nevertheless, it did not seem to cause any interference with the process of permethylation for glycan analysis with MALDI-TOF MS.

3.2.1.2. Reaction of immobilised DmManII

As described in Chapter 2, following chemical biotinylation and immobilisation of DmManII, recovery of immobilised enzyme was challenging. Losses occurred during washes and centrifugation. This could be a result of insufficient biotinylation and immobilisation and thus unoccupied StV beads were removed during the centrifugation steps. Therefore, to increase the likelihood of successful biotinylation and binding and hence facilitate recovery, the number of beads and enzyme used was increased by a factor of 4. Immobilised DmManII (17.5µg assuming maximum site occupancy and no steric hindrance) was reacted with GM5, NtGnTI's product. GM5 was produced by retreating the reaction mixture (10mM UDP-GlcNAc, 0.5µM M5 as a starting substrate) with freshly immobilised NtGnTI. The reaction of DmManII was reproduced in duplicates as described in chapter 2: 37°C overnight, 0.4µM GM5, 0.1mM $ZnSO_4$, 50mM MES pH 5.6. The reaction yielded the desired product GM3 in abundance with increased homogeneity (>95% conversion) (**Figure 3-6a**). The intermediate product GM4 was detected at trace levels, while the starting substrate GM5 (m/z 1824.9) was not

detected. These results suggest the reaction approached completion; thus no optimisation was undertaken. As was the case for the NtGnTI reactions, brown precipitation was observed following the overnight incubation, however it did not appear to have an effect on sample preparation for MALDI-TOF MS or the quality of the spectra.

3.2.1.3. Reaction of immobilised hGalT

Immobilised hGalT (estimated 11.3µg assuming maximum site occupancy and no steric hindrance) was reacted with GM3, DmManII's product. GM3 was produced as described earlier. Briefly, DmManII reacted overnight with NtGnTI's product (retreated *Experiment B:* reaction of immobilised NtGnTI and 10mM UDP-GlcNAc). Reaction conditions were: 37°C overnight, 0.3µM GM3, 10mM $MnCl_2$, 10mM UDP-Gal and 20mM Tris-HCl pH 7.5. MALDI-TOF MS analysis was performed on the sample. The expected product GalGM3, has a m/z ratio of 1620.8. Interestingly, this is the same m/z ratio as GM4, DmManII's intermediate product. When comparing the spectra of the reactions of DmManII and hGalT (**Figure 3-6**), no significant increase was observed in the peak corresponding to m/z 1620.8, following reaction with immobilised hGalT (**Figure 3-6b**). This suggests that the expected product GalGM3, was not formed.

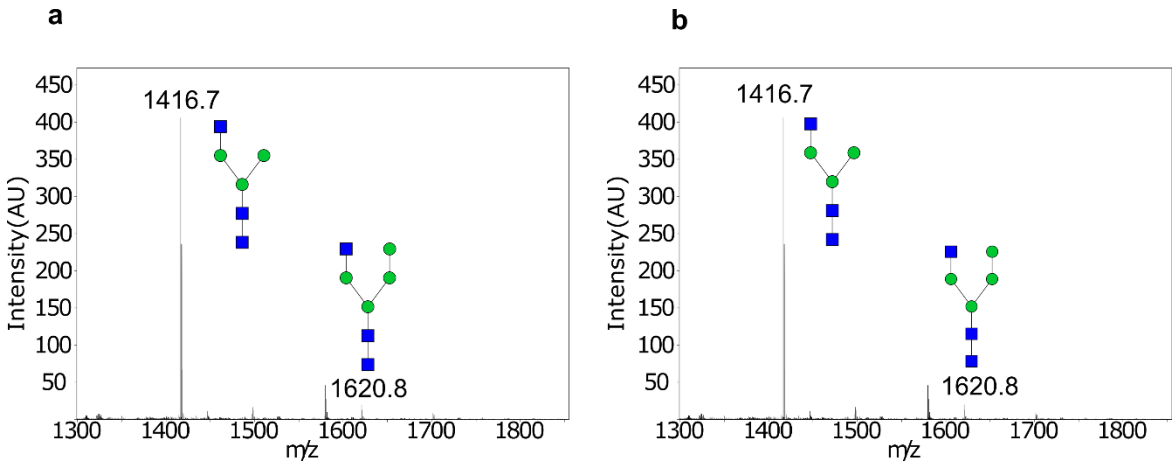

Figure 3-6: Reaction of immobilised DmManII and hGalT as monitored by MALDI-TOF MS. a. Reaction of immobilised DmManII with GM5 (m/z 1824.9). The reaction is a step-wise removal of 2 mannose residues yielding initially GM4 (m/z 1620.8) and finally GM3 (m/z 1416.7). Peak corresponding to GM3 is in abundance, suggesting reaction approached completion; b Reaction of immobilised hGalT with GM3, DmMAnII's product. Expected product, GalGM3, has an m/z ratio at 1620.8. No significant increase was observed suggesting no peak at 1620.8 corresponds to GM4 and thus no GalGM3 was formed.

To ensure increased conversion and homogeneity, optimisation of the reaction conditions was undertaken. Initially, the pH of the reaction was checked and found to be at 6.5. Although a pH of 6.5 has been reported to work for hGalT[263], the majority of the published data suggest the optimum pH to be above 7[220,248,264–266]. Since the reactions take place sequentially in a continuous fashion, there was no buffer exchange or purification of the product after each reaction step and prior to adding the next enzyme in the cascade. Therefore, titrations of various Tris-HCl concentrations and pH were performed in a bid to identify the appropriate combination and raise the pH to 7.5. It was found that 80mM Tris-HCl pH 9 is sufficient to approach the desired pH.

The reaction of immobilised hGalT and GM3 was repeated under the following conditions: 37°C overnight, 0.3µM GM3, 10mM $MnCl_2$, 80mM Tris-HCl pH 9, under continuous shaking. Furthermore, different concentrations of UDP-Gal ranging from 0.15mM-6mM were tested. In addition, the remaining UDP following the sugar transfer form UDP-Gal is known to inhibit the activity of the galactosyltransferase[198,267,268]. Therefore, the alkaline phosphatase FastAP was added to remove any inhibitory by-products. All reactions were monitored with MALDI-TOF MS. As seen in **Figure 3-7** , there is a linear increase in the estimated percentage conversion when increasing the concentration of UDP-Gal. Furthermore, the addition of the alkaline phosphatase had a positive effect on overall conversion.

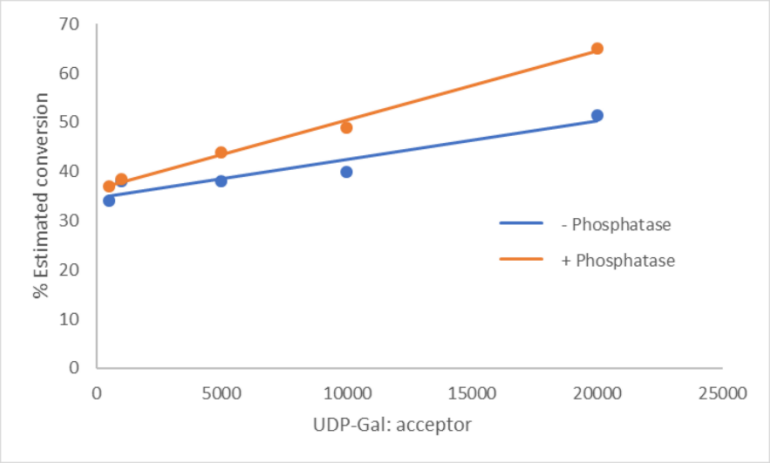

Figure 3-7: Reaction of immobilised hGalT with and without the addition of alkaline phosphatase and 0.3µM GM3 with varying UDP-Gal concentrations (n=1). Reactions were monitored with MALDI-TOF MS. Here the different rations of UDP-Gal : acceptor are depicted. Estimated conversions were calculated by dividing the peak corresponding to the product GalGM3 by the sum of the substrate and product peak. Reaction conditions: 37°C overnight, 0.3µM GM3, 10mM $MnCl_2$, 80mM Tris-HCl pH 9, under continuous shaking.

A problem faced upon analysing the samples was the increased brown precipitation. This precipitation was observed in NtGnTI's product mixture, after long-term storage, and in DmManII's product mixture, after overnight incubation at 37°C. However, in hGalT's product mixture it appeared to be significantly increased. This precipitation interfered with the quality of the samples and thus hampered permethylation and sample handling. Indeed, glycan clean-up to remove the non-permethylated material as well as any chemical reagents was challenging leading to loss of material. Furthermore, after mixing the permethylated samples with the matrix DABP and spotting on the plate for MALDI-TOF MS, the spots appeared significantly wet suggesting a hygroscopic element was present. Troubleshooting approaches included desalting of samples prior to permethylation using membranes with a suitable Molecular Weight Cut Off (MWCO) or Sep-Pak purification post-permethylation. However, either all the material was lost, or no improvement was observed (data not shown). Finally, increasing the volume of MeOH when resuspending the lyophilised permethylated samples, appeared to have a positive effect on spotting and spectrum quality. Additionally, it was observed that increasing the laser power contributed into acquiring better quality spectra (data not shown).

Following the results shown in **Figure 3-7**, the activity of hGalT was evident since there was a linear increase in the peak at m/z of 1620.8, corresponding to GalGM3, with increasing UDP-Gal. The next step in the optimisation of the activity of immobilised hGalT, was increasing the amount of enzyme. In a similar approach to NtGnTI, the immobilisation experiment was scaled up by a factor of 4 to increase the enzyme concentration (~45µg of enzyme assuming maximum site occupancy and no steric hindrance). This amount was selected after titrations performed in the reactions of immobilised hGalT and IgG, described in Chapter 4. The reaction conditions were: 37°C overnight, 0.3µM GM3, 10mM $MnCl_2$, 3mM UDP-Gal and 80mM Tris-HCl pH 9, under continuous shaking. Significantly, when the sequential reaction was repeated, the desired product GalGM3 of the enzymatic pathway NtGnTI-DmManII-hGalT was produced in increased homogeneity, suggesting all enzymatic steps were near completion. Interestingly, there was no alkaline phosphatase added suggesting the increase in the pH and the increase in the enzyme amount were sufficient for the reaction to reach completion (**Figure 3-8**). However, it was difficult to estimate the exact conversion after the hGalT reaction since there was increased noise in the m/z area of the substrate (GM3 m/z 1416.7). This reduced quality could be the result of the aforementioned precipitation. Although diluting the re-suspended samples had a positive impact, the quality of the spectra, this was still was reduced when compared to the spectra of NtGnTI and DmManII.

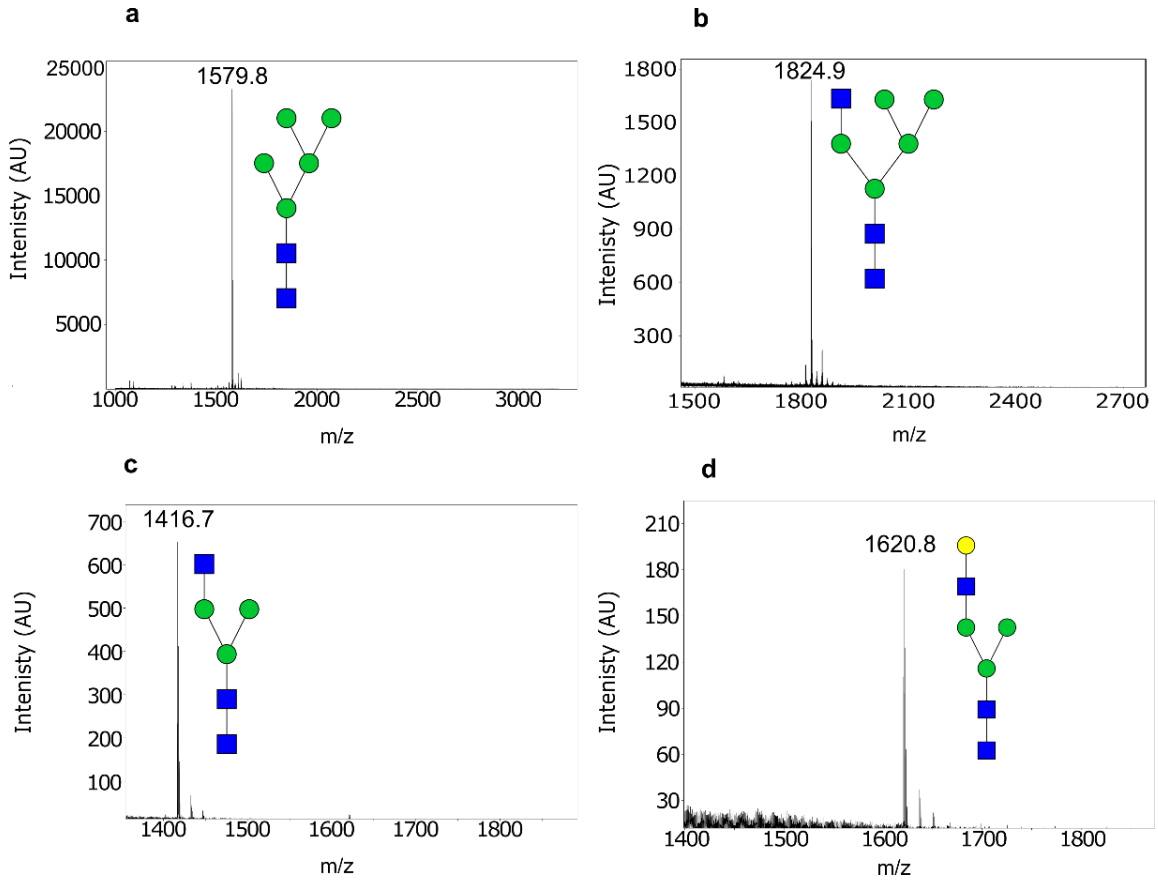

Figure 3-8: Sequential reaction of immobilised NtGnTI-DmManII-hGalT as monitored by MALDI-TOF MS. Each step was performed overnight. a. Starting substrate M5; b. Conversion of M5 to GM5 by immobilised NtGnTI with 10mM UDP-GlcNAc at 25°C. Freshly immobilised enzyme was added to drive reaction to completion; c. Conversion of GM5 to GM3 by immobilised DmManII at 37°C. Reaction approached completion; d. Conversion of GM3 to GalGM3 by immobilised hGalT at 37°C. Reaction approached completion.

3.2.2. Objective 2: Expression of mFc in the glycoengineered *P. pastoris* strain SuperMan5

To acquire the coding sequence of the mFc for expression in *P. pastoris*, an *E. coli* vector containing this sequence was kindly provided by Oskar Lange, a PhD student in the Polizzi lab. To facilitate purification, a 3-residue GS linker and a His_6 tag were originally included on the C-terminus of the protein.

Polymerase Chain Reaction (PCR) was used to amplify the mFc fusion from the *E. coli* vector, which was subsequently cloned into the pPICZα A, a *P. pastoris* methanol-inducible backbone, using Gibson assembly. The pPICZα A-mFc-His_6 was transformed via electroporation into *P. pastoris* SuperMan5 competent cells. Multiple clones were picked and screened to identify the highest expression clone.

No difference was observed and therefore a clone was arbitrarily picked for expression. Following a 3-day expression at 20°C in Buffered Methanol-Complex Medium (BMMY), the supernatant was collected, and protein expression was checked using SDS-PAGE analysis (**Figure 3-9a**). Interestingly, the expected size of mFc is ~26 kDa, however a product of ~34kDa was observed. This might be explained by the unsuccessful cleavage of the α-Mating Factor (αMF) secretion peptide (~9 kDa)[269,270]. Following expression, the supernatant was loaded on a column containing Ni-NTA resin for protein purification, following washing, the mFc was eluted with imidazole, yielding a titre of 5 mg/mL. To confirm that the detected band corresponds to mFc-His_6, the purified fraction was checked with Western Blot analysis using an Anti-His_6 antibody. Signal detected at the expected molecular weight indicates the purified protein is mFc-His_6 (**Figure 3-9b**). The presence of two distinct bands could be explained by the presence of partially uncleaved α-MF or by the presence of hypermannsoylated glycans.

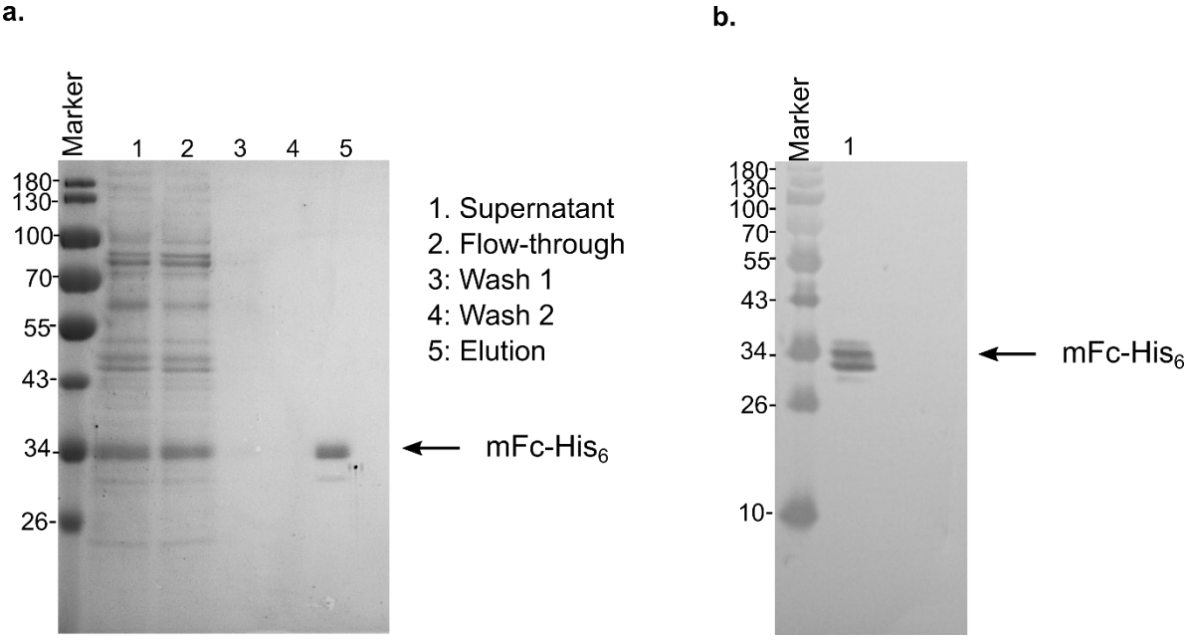

Figure 3-9: Expression of mFc-His_6 fusion in *P. pastoris*. a; Expression of mFc and purification using Ni-NTA resin. Loaded samples per lane are depicted on the right of the figure; b. Western blot analysis on purified fraction.

The glycosylation profile of mFc was checked with MALDI-TOF MS, which confirmed the M5 glycan was in abundance (**Figure 3-10**). However, hypermannosylated glycans M6-M12 were also detected.

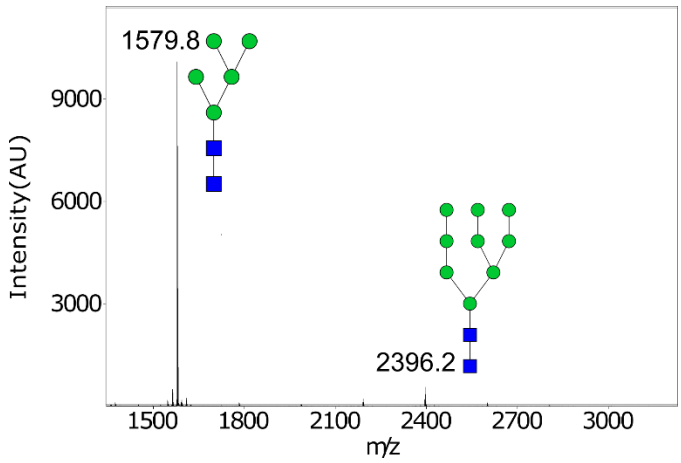

Figure 3-10: Glycosylation profile of mFc produced in *P. pastoris* SuperMan5 strain. The expected M5 glycan (m/z 1579.8) is in abundance. M6-M12 were also present in low abundance, with M9 being the highest (m/z 2396.2).

Interestingly, there have been reports in the literature, that the glycan with m/z corresponding to M9 (m/z 2396.2), was an unpredicted glycan carrying a linear, 4-residue long structure consisting of β-(1,2) / β-(1,3)-mannose residues capped by α- (1,2)-glucose or mannose[271,272]. To confirm the identity of this glycan, Mr. Roberto Donini (Haslam Lab) carried an investigation using α-(1-2,3,6)-mannosidase, that catalyses the hydrolysis of mannose residues. MALDI/TOF analysis showed successful digestion of the glycan with m/z 2396.2, confirming that it consisted of mannose rather than glucose residues and thus corresponding to M9.

3.2.3. Objective 3: Sequential reactions of immobilised NtGnTI, DmManII and hGalT on mFc.

The enzymatic cascade developed in Objective 1 was repeated for the mFc. The desired process is depicted in **Figure 3-11**.

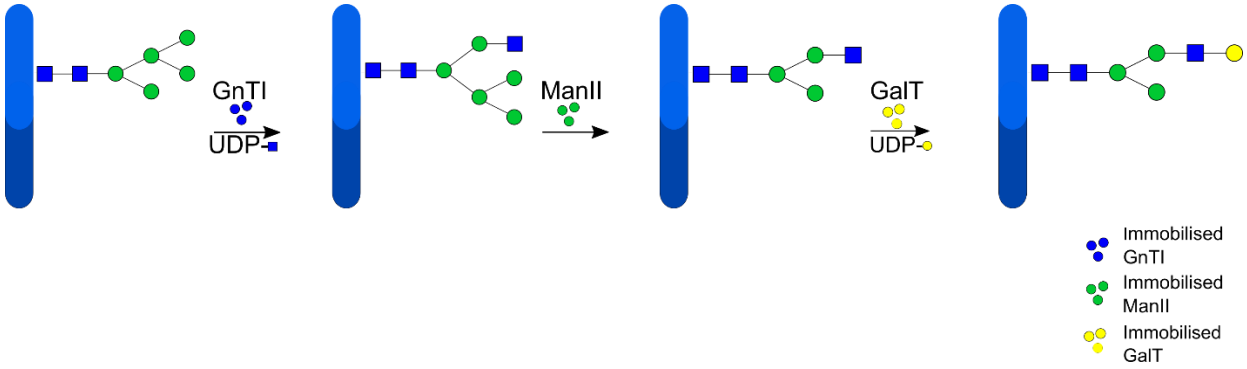

Figure 3-11: Desired enzymatic cascade using immobilised enzymes on mFc.

Upon developing the NtGnTI step, it was important to retreat the reactions with freshly immobilised enzyme to drive the reaction to completion, suggesting the amount of enzyme was the limiting factor (objective 1). Therefore, for the reaction with mFc, the amount of enzyme was increased 4-times by increasing the initial volume of soluble fraction and StV beads maintaining the 1:2 S.F to StV beads ratio (estimated 56µg assuming maximum site occupancy and no steric hindrance). The experiment was performed in duplicates and the reaction conditions were as follows: overnight reaction under continuous shaking, 10 mM UDP-GlcNAc, 100mM MES pH 6.5, 10mM $MnCL_2$, 25°C and 100 µg mFc. 20 µg of mFc was removed, and the extent of the reaction was checked with MALDI-TOF MS. Since the glycans are attached on the protein, rather than free in solution, a glycosylation cleavage step was performed prior to permethylation using a Peptide -N-Glycosidase F (PNGase F). **Figure 3-12a** illustrates that the reaction approached completion since the product GM5 was in abundance (estimated >95% conversion).

The DmManII step was repeated with 80 µg mFc as described in objective 1: 37°C overnight, 0.1mM $ZnSO_4$, 50mM MES pH 5.6. 20 µg were removed, and the extent of the reaction was checked with MALDI-TOF MS. As seen in **Figure 3-12b**, the reaction approached completion with the product GM3 being in abundance (estimated conversion of >95%).

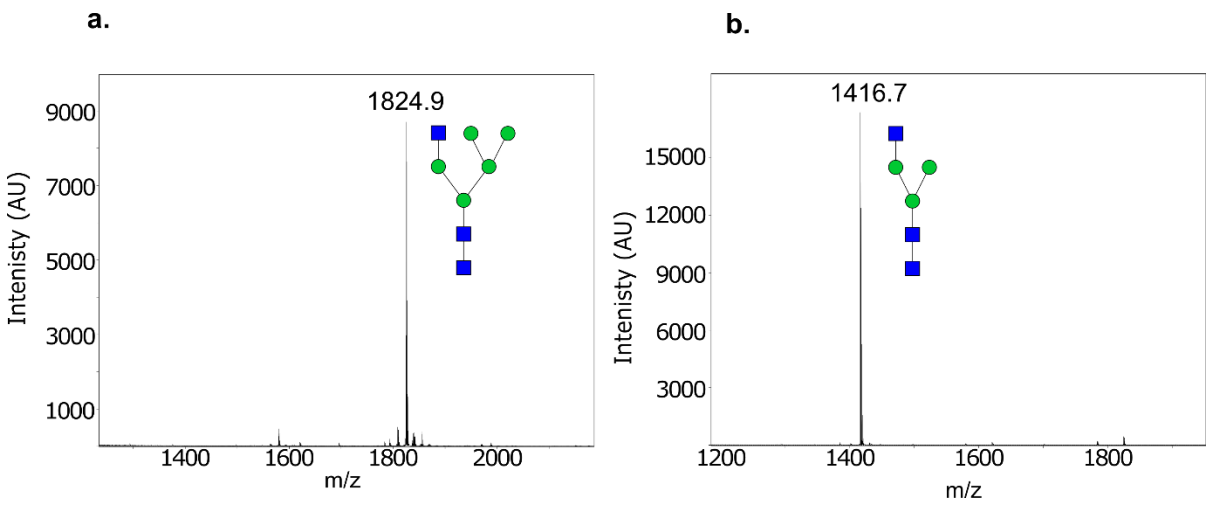

Figure 3-12: Sequential enzymatic reactions on mFc. Sequential reaction of immobilised NtGnTI-DmManII on mFc as monitored by MALDI-TOF MS. Each step was performed overnight. a; Conversion of M5 to GM5 by immobilised NtGnTI with 10mM UDP-GlcNAc at 25°C. Reaction approached completion; c. Conversion of GM5 to GM3 by immobilised DmManII at 37°C.

The final step was the reaction of mFc (60 µg with immobilised hGalT). The conditions were as developed in Objective 1: 37°C overnight, 10mM $MnCl_2$, 80mM Tris-HCl pH 9, under continuous shaking. Furthermore, UDP-Gal was increased to 6mM as identified from the immobilised hGalT-IgG experiments (Chapter 4). However, no data was obtained via MALDI-TOF MS analysis and significant brown precipitation was observed (**Figure 3-12**).

There were two possible scenarios that caused the inability to detect the glycans, either the mFc formed aggregates and was removed upon centrifugation for recovery of the immobilised enzyme or there was a by-product inhibiting the activity of PNGase F. To investigate further, a series of visual experiments were performed to identify which component was responsible for the brown precipitation. Specifically, two conditions were explored, where either the NSDs or the $MnCl_2$ were removed from the buffers (**Table 3-1**). The reaction conditions were replicated for each step of the enzymatic cascade but in absence of the enzymes, i.e. overnight incubations in the buffer of the corresponding enzyme.

Table 3-1: Conditions of visual investigations for brown precipitations. Each investigation was performed under the exact reaction conditions of the actual cascade.

Investigation	1	2	3
Enzyme	×	×	×
Sugar donor (UDP-GlcNAc & UDP-Gal)	✓	✓	×
$MnCl_2$	✓	×	✓
Precipitation	✓	×	✓

In the end, no precipitation or brown discolouration were observed in the sample containing NSDs, in contrast to to the sample containing $MnCl_2$ where both events were observed. To detect if there is any mFc still in solution, the samples were centrifuged for 5 min at 3000g, to replicate the conditions applied for enzyme recovery. The supernatants were analysed with SDS-PAGE where it was confirmed that all the protein precipitated. This result supports the hypothesis that under the conditions of the hGalT reaction, the mFc precipitated out of solution and was removed with the StV beads, preventing analysis via MALDI-TOF MS.

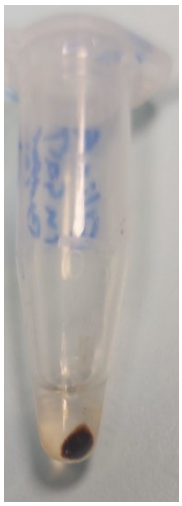

Figure 3-13: Brown precipitation observed after the overnight reaction at 37°C of immobilised hGalT and mFc

Due to time constraints this was not pursued any further.

3.2.4. Objective 4: Demonstrate reusability of immobilised enzymes.

3.2.4.1. Reusability of NtGnTI

Following an overnight incubation of NtGnTI with mFc, the beads were recovered by centrifugation and rigorously washed in enzyme storage buffer (20mM Tris pH 7.4, 200mM NaCl and 5% glycerol). Fresh mFc and reaction buffer (100mM MES pH 6.5, 10mM UDP-GlcNAc, 10mM $MnCl_2$) were added and the overnight incubation was repeated. As seen in **Figure 3-14**, immobilised NtGnTI significantly retained its activity as in both reaction cycles, more than 95% conversion was achieved.

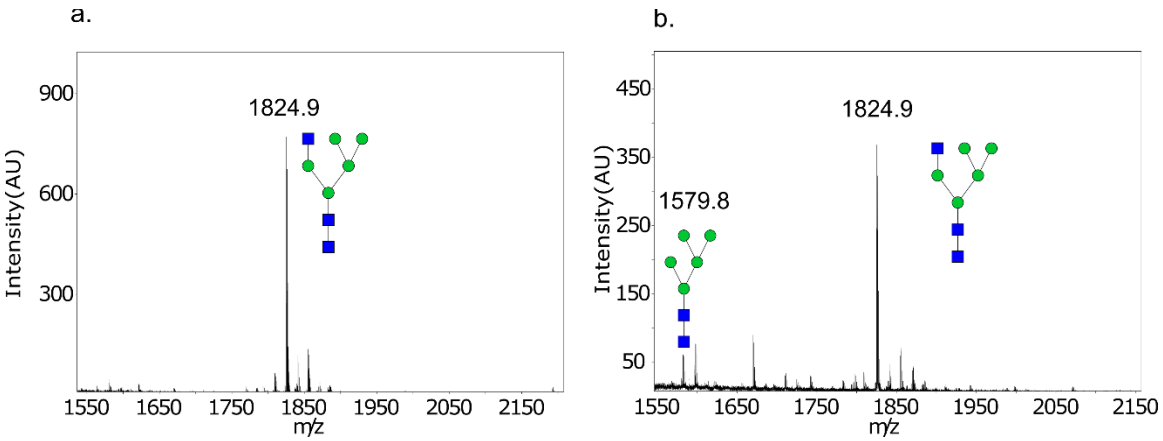

Figure 3-14: Reusability of immobilised NtGnTI with mFc. Each reaction was performed overnight. Beads were recovered with centrifugation and fresh reaction mixture containing UDP-GlcNAc and mFc were added. a. First reaction cycle; b. Second reaction cycle using recycled enzyme.

3.3. Discussion

In line with the objectives outlined in the introduction of this chapter, sequential reactions using immobilised NtGnTI, DmManII and hGalT were performed recreating a model N-linked glycosylation pathway that normally takes place in the Golgi apparatus of mammalian cells. The immobilisation enabled facile enzyme recovery at the end of each reaction step allowing for the necessary spatiotemporal separation to address enzyme promiscuity and produce the desired glycan structure in increased homogeneity.

Initially, the immobilised enzyme cascade was performed on free glycans, with the commercially available M5 being the starting substrate. Each reaction was performed overnight, and simple optimisation steps were undertaken to ensure each reaction approached completion. These sequential experiments serve as a proof of principle, demonstrating the feasibility of the design to

achieve targeted and homogeneous glycosylation whilst supporting the spatiotemporal hypothesis. However, in depth reaction optimisations need to be performed to identify optimum conditions for each enzyme. A DOE approach could be used to identify important parameters and variables to optimise enzymatic reactions. Improved reaction conditions should facilitate multiple reaction cycles using recycled immobilised enzymes[198,200], a desirable feature.

Interestingly, the hGalT reaction was near completion without the addition of alkaline phosphatase. This could be a direct result of the overnight incubation and the increase of the amount enzyme. The UDP inhibition of GTs and particularly of GalT, is well known in the glycosylation community[198,267,268]. Although here it was not a problem since all reactions were performed overnight and the inhibition was not observed, it could have a significant impact on the rate of the reaction. Therefore, a thorough kinetic analysis should be performed to fully understand and describe this reaction. The latter would also allow large scale industrial applications.

Following the successful implementation of sequential reactions on artificial glycans, the cascade was repeated on the mFc produced in glycoengineered *P. pastoris*. This experiment was performed in a bid to demonstrate that the developed AGR system can be used to modify cell-derived proteins and produce homogeneous glycosylation structures. The mFc is a therapeutically relevant protein, attracting attention to be used in protein fusions for drug delivery as an alternative to full length Fc domains[278]. In addition to the smaller size compared to the Fc (~54 kDa), the mFc lacks the typical dimerization of the Fc and carries only a single glycosylation site[261,262].

The use of yeast and specifically *P. pastoris,* a non-mammalian host, as a protein expression host has significant advantages. It is known for the fast and high protein production yields, low maintenance cost and the ease of scale-up[135]. The glycoengineered strain enables the bottom-up reconstruction of human-like N-linked glycosylation pathway which would be impossible in proteins produced in mammalian cells due to a high content of highly mature glycans[110]. Most importantly, combining a cheap and robust expression host with an *in vitro* glycosylation system allows for the development of a novel and cost-friendly modification platform. An alternative cell line that can be used in a similar way to SuperMan5, is the commercially available HEK 293S GnTI deficient line producing only M5 glycan structures. However, there are drawbacks associated with mammalian cell lines, for instance the high maintenance cost, often the introduction of serum contaminants[274] as well as low yields[79,86,275].

Here, mFc was successfully expressed in glycoengineered *P. pastoris* SuperMan5[109,110,114] producing mainly M5 structures which serve as a substrate for GnTI. The SuperMan5 strain was created by the

knockout of *Och1*, to stop the hypermannosylation at M8 structures, and the simultaneous expression of recombinant Man1A, to digest M8 and create the desirable M5. However, MALDI-TOF MS analysis showed that the mannosylated M6-M12 structures remained but in much lower concentration when compared to M5. This demonstrates the lack of strict control in *in vivo* glycoengineering, where unpredicted cell mechanisms result in a heterogenous final product. Furthermore, it has been shown that glycan structures, referred to as $Hex_9GlcNAc_2$, in glycoengineered *P. pastoris*, have been misrepresented as M9 due to the same m/z. Interestingly, there have been contradictory reports in the literature concerning the type of glycans constituting the $Hex_9GlcNAc_2$. Specifically, Gomathinayagam and co-workers[272] reported that $Hex_9GlcNAc_2$ consisted of a linear glycan (Manα-(1,2)-Manβ-(1,2)-Manβ-(1,2)-Manα-(1,2)-Man 4) in the α-(1,3)-mannose branch while Laukens and co-workers[271] reported a linear glycan in the same branch but of different residues (Glcα-(1,2)-Manβ-(1,2)-Manβ-(1,3)-Glcα1-Manα1). In contrast, here it was demonstrated that the $Hex_9GlcNAc_2$ was M9. The underlying mechanism causing the formation of these non-human glycans is not well-understood and it is unclear if it is strain or clone specific. In addition, it is not known if these glycans are potentially immunogenic which could hinder large scale applications. An investigation is thus required to identify the mechanism behind the formation of these glycans and potential troubleshooting techniques.

As seen in **Section 3.2.1**., both immobilised NtGnTI and DmManII were successfully used to alter the glycosylation profile, specifically M5, of the mFc. High conversions (>95%) were achieved after each step allowing the target glycans to be produced in homogeneity. This demonstrates the applicability of an AGR deign to alter cell-derived material and achieve homogeneous glycosylation. Unfortunately, it was not possible to characterise the reaction of hGalT since no glycans were detected. Significant brown precipitation was observed, and it was discovered that the protein, mFc, formed aggregates and was consequently removed from solution after centrifugation while recovering the StV beads. Notably, though similar brown precipitation was observed when using free glycans, since they are not attached on a protein, they were not removed with centrifugation and thus were successfully detected. A visual investigation, where different components were examined, led to the conclusion that $MnCl_2$ was the underlying cause of precipitation. $MnCl_2$ is known to form oxides when the environment is oxidative or upon a pH change[276]. It is not clear what caused this phenomenon, and to our knowledge there is no available literature or research were similar observations were made. This is to be expected as the sequential experiments performed here were a novel endeavour. Therefore, additional work and perhaps a DOE approach is required to address this issue. Example optimisation experiments would include different $MnCl_2$ concentrations or different buffer components that might be incompatible with $MnCl_2$. Furthermore, a desalting or

dialysis step after the ManII reaction might be essential. Finally, though there is no indication of the extent of the hGalT reaction, since both NtGnTI and DmManII reactions approached completion eliminating the possibility of multiple substrates for hGalT, the spatiotemporal hypothesis is still demonstrated.

An important result was enzyme reusability which was successfully demonstrated for NtGnTI. Specifically, after two overnight reactions with mFc, the enzyme retained its activity, since the desired product GM5 was in abundance and increased homogeneity was achieved. Future work would involve multiple reusability cycles as well as demonstration of reusability for DmManII and hGalT. Reusability of hGalT was explored in Chapter 4:.

Based on the observations made so far, it is apparent that optimisation of the enzymatic reactions is necessary. A robust and high-throughput analytical technique is thus essential. Although MALDI-TOF MS is beneficial for detecting and characterising glycans, it is a labour-intensive method mainly due to the required lengthy permethylation procedure[277]. As a result, under its current format it is challenging to perform multiple experiments which would aid a DOE approach. Interestingly, there are commercially available permethylation kits in a 96-well format (Ludger, Ltd) allowing the possibility for large scale preparation[277]. Alternative techniques that allow analysis of a large sample population include glycan separation methods such as capillary electrophoresis[233,257,278,279](CE), hydrophilic interaction liquid chromatography (HILIC)[280] or HPAEC[233,254]. Some of these methods, such as CE or HILIC, often require the derivatisation of the glycans with a fluorophore e.g. 9-Aminopyrene-1,4,6-trisulfonic acid (APTS) or 2-aminobenzoic acid (2-AA)[233,257,278]. Notably, these methods can be automated allowing the fast and high-throughput analysis[278].

3.4. Summary and conclusions

The aim of this results chapter was to perform sequential glycosylation reactions using immobilised enzymes. This was in line with the hypothesis of spatiotemporal separation to address enzyme promiscuity and achieve a homogeneous final product. Initially, simple optimisation was undertaken to ensure that each step in the NtGnTI-DmManII-hGalT pathway approached completion, enabling the synthesis of a homogenous product. Once the desired conditions were identified, the reaction cascade was performed on free glycans. Each step approached completion and the final product, GalGM3, was produced with high homogeneity. These experiments constitute a proof-of-principle, proving the potential of the AGR to produce human-like N-linked glycans. The next step was repeating the enzymatic cascade on mFc, a therapeutically relevant protein. mFc was produced in SuperMan5, a *P. pastoris* strain, glycoengineered to produce only M5 structures. Successful results

were obtained for the sequential two-enzyme cascade of NtGnTI and DmManII, since the product of DmManII yielded a highly homogeneous glycoform. However, it was impossible to detect the product of hGalT due to interference from accumulated by-products and specifically $MnCl_2$. Therefore, additional work is required to optimise this step. Notably, the strategy applied here can, in principle, be adapted to any glycosylation pathway by changing the identity of the immobilised enzymes. Furthermore, the use of immobilised enzymes makes this a sustainable approach since facile recovery and reusability is enabled. The latter was shown with the successful reusability of immobilised NtGnTI without a significant loss in activity after two overnight incubations. Future work would entail demonstrating reusability of the remaining enzymes and achieving a continuous modification of glycoproteins. Furthermore, different reactor set-ups could be explored with different beneficial properties, in addition to developing a system for the *in situ* regeneration of NSDs.

Chapter 4: Driving galactosylation of IgGs and demonstration of hGalT reusability

4.1. Introduction

As discussed in Chapter 1, mAbs of the IgG family, dominate the biopharmaceutics sector[4]. They are used as therapeutics for cancer, auto-immune disorders as well as bacterial and viral infections[4]. N-linked glycosylation in the Fc domain of mAbs is a key quality attribute known to affect their efficacy and activity[4,5,7,8,10,11,70,71,194,281]. The properties of mAbs directly affected by glycosylation include folding[7,11,30], trafficking[30,32,42], protection from aggregation[2,45] as well as increased half-life[2,3,11,30,57]. Furthermore, the Fc glycans mediate activity and effector function since they are known to control receptor binding[53,79,167,282,283]. In addition, the presence or absence of certain glycans can significantly impact Antibody-Dependent Cellular Cytotoxicity (ADCC), Antibody-Dependent Cellular Phagocytosis (ADCP) and Complement-Dependent Cytotoxicity (CDC). One particular example that attracts attention is the effect of galactosylation. Galactose is known to offer anti-inflammatory properties whilst enhancing receptor affinity[55,64,67]. Furthermore, the presence of galactose increases CDC, ADCP and, in some cases, ADCC[64,66,67]. Additionally, terminal galactose serves as the substrate for sialyltransferases, yielding sialic acid products. It is known that sialic acids offer anti-inflammatory properties, increase protein stability and protect from proteolytic degradation thus increasing serum half-life[7,49,50,55–58]. Therefore, the presence of galactose is highly desirable to ensure these beneficial properties whilst facilitating downstream sialylation[5,7,281,21].

Currently, IgGs are primarily produced in cell-based systems, mainly Chinese Hamster Ovary (CHO) cells, and there is great glycan heterogeneity especially amongst the galactosylated structures[33,141,177,284,285]. Specifically, ~30-50% of the glycans are agalactosylated[52,280], while single galactose structures are ~40% and two galactose structures ~20-40%[64,280]. Hypogalactosylation is sometimes linked to steric hindrance in the Fc site[286] or availability of GalT[210]. Efforts to control galactosylation heterogeneity include cell line engineering, an example of which is genome engineering using CRISPR/Cas9 to modify galactosylation in CHO cells[95]. This was demonstrated by Chang and co-workers, who developed a *FUT8 / β4GalT1* deficient CHO cell line and reintroduced recombinant versions of FucT and GalT. Crucially, the recombinant enzymes could be constitutively expressed, or expression was controlled by small inducer molecules. As a result, they identified conditions to achieve up to 80% terminal galactosylation. However, such a platform is subject to batch-to-batch variability. Furthermore, glycosylation and consequently galactosylation is protein specific. *In vivo* modulation would then require multiple iterations to identify the conditions required

to produce a stable cell line thus making it a labour-intensive approach[95]. Another approach was presented by Stach and co-workers, whereby using synthetic and systems biology tools they developed a platform to model and consequently drive glycoengineering[287]. Specifically, by fitting experimental data and multiple parameter estimation in their model, they identified combination of genes necessary for a desired outcome. Furthermore, they developed a platform for the fast generation of constructs which would be used for the generation of stable or transient cell lines. As a result, terminal galactosylation in a CHO cell line increased to ~90%. Similar examples can be found in non-mammalian hosts such as the glycoengineered yeast *P. pastoris* where the glycosylation machinery was humanised by the introduction of multiple enzymes and biosynthetic pathways to produce the relevant NSDs[117]. Crucially, GalT was also introduced so that the target proteins can carry the required terminal galactose, recognised by SiaT. As a result, sialylated EPO was produced[117]. Despite the promising results, cell line engineering is a laborious approach, which often negatively impacts cell viability[5,79,109] and might lead to unwanted structures[5,99]. The latter can also be seen in the glycoengineered strain of *P. pastoris*, SuperMan5, where unpredicted structures carrying multiple glucoses were detected[271].

Another method to enhance galactosylation is controlling the bioprocess conditions such as pH, temperature and media additives[177–180,288]. For instance, the addition of galactose and uridine, the pre-cursors of UDP-Gal, have been shown to increase the production of the sugar donor and of GalT, thus leading to increased galactosylation[181,182]. Although, such efforts have enhanced galactosylation, there is still lack of control, highlighted by batch-to-batch variability[79]. Additionally, it is often the case that the addition of metabolites can lower antibody yield and it has also been shown that feeding strategies can be costly[190].

The last method used to enhance galactosylation of mAbs is the use of recombinant galactosyltransferases *in vitro*[52,64,79,167–169,283,289,290]. This allows strict control over the reaction conditions and is independent of the host allowing for a range of antibodies to be modified[52,167]. GalT can be produced in house using recombinant production[64,283] or it can be purchased as it is commercially available (e.g. Roche, Sigma etc)[167–169,289]. A limitation of the *in vitro* enzymatic modification is the cost associated with the use of NSDs and of the enzymes which can hinder its large scale industrial application[5].

The use of immobilised enzymes in bioprocesses is a cost efficient and sustainable method[291]. Immobilisation is known to increase enzyme stability while enabling reusability. The latter can aid with lowering the cost of downstream enzyme treatment allowing its large scale application in pharmaceutical applications[291]. Examples include the use of immobilised Lipase B from *Candida*

antarctica to produce drugs for the treatment of hepatitis C[292] and the use of immobilised Penicillin G Amidase for the manufacture of Amoxicillin/ampicillin[293]. Enzyme reusability has been demonstrated on many occasions and for multiple repetition cycles[220,244,245,294,295]. For example, Elling and co-workers have demonstrated reusability of immobilised GalT in producing LacNAC, by using it in up to 7 cycles[198].

Consistent with the above, Chapter 4 focuses on increasing galactosylation on IgGs of different origins, by using the in-house produced and immobilised hGalT. Furthermore, enzyme reusability was demonstrated, paving the way for future large scale, economical processes.

In Chapter 2, expression, *in vivo* biotinylation and one-step purification/immobilisation was achieved for hGalT. Furthermore, activity was confirmed using the artificial glycan GlcNAc. In chapter 3, immobilised hGalT was successfully used in a cascade of immobilised enzymatic reactions to reconstruct a mammalian N-linked glycosylation pathway.

The next stage was to apply the immobilised hGalT to increase the levels of galactosylation on three different mAbs of the IgG1 family (here referred to as IgG). Selection was mostly based on differences in galactosylation levels as reported in the literature[280,296,297]. The IgGs were: a) a humanised IgG produced in-house in a CHO cell line kindly provided by MedImmune. This antibody was also selected for its industrial relevance, since the majority of mAbs are produced in CHO cells; b) a commercially available IgG from human serum and c) a commercially available IgG from rabbit serum.

4.1.1. Objectives

The specific objectives of this chapter were as follows:

- **Objective 1:** Increase galactosylation levels in three different IgGs using the in-house produced and immobilised hGalT. The IgGs were a) humanised IgG produced in CHO cells (chIgG); b) IgG from human serum (hIgG); c) IgG from rabbit serum (rIgG). Extent of galactosylation was monitored with CE (C100HT, SCIEX).

- **Objective 2:** Demonstrate reusability of immobilised hGalT. Condition identified from objective 1 were applied. Immobilised enzymes were recovered, thoroughly washed and reacted with fresh substrate. Multiple reusability cycles were attempted. Galactosylation levels were be monitored with CE (C100HT, SCIEX).

4.1.2. Experimental Strategy

To monitor and quantify the extent of galactosylation, Capillary Electrophoresis (CE) was used as a detection method. CE is often used to quantify and identify glycans[278,279,298]. The latter is enabled by coupling CE with an MS module to perform structural analysis of the glycoforms[279,298]. The basic principle of CE relies on the rapid migration through an electrical field and subsequent separation of free glycans. The glycan release from the protein backbone occurs with the use of a glycosidase such as PNGaseF. Another prerequisite is for the glycans to be labelled with common fluorophores such as aminopyrene trisulfonic acid (APTS), to obtain the necessary charge. This is because, with the exception of sialic acids, most glycans are neutral and thus require labelling for migration during the electrophoresis as well as detection[298]. Notably, CE is characterised by the high-throughput analysis allowing large sample sizes to be assessed in relative short times and in a simple way[278]. As a result semi-automated or automated platforms have been developed[278]. Here, the C100HT platform developed by SCIEX was used. The main principles are the fast denaturation, glycan cleavage and labelling steps occurring in the presence of magnetic beads to facilitate glycan recovery. Sample preparation and analysis takes place in 96-well plates, allowing large-scale application.

The structures and nomenclatures[299] of the target IgG glycoforms in the experiments performed in this chapter are shown in **Figure 4-1**. hGalT catalyses the addition of a galactose molecule in any free GlcNAc. Notably, this addition occurs sequentially making the glycoforms G1'/G1/G1'F/G1F intermediates of the reaction whilst G2/G2F represent the full conversion and thus final glycoforms.

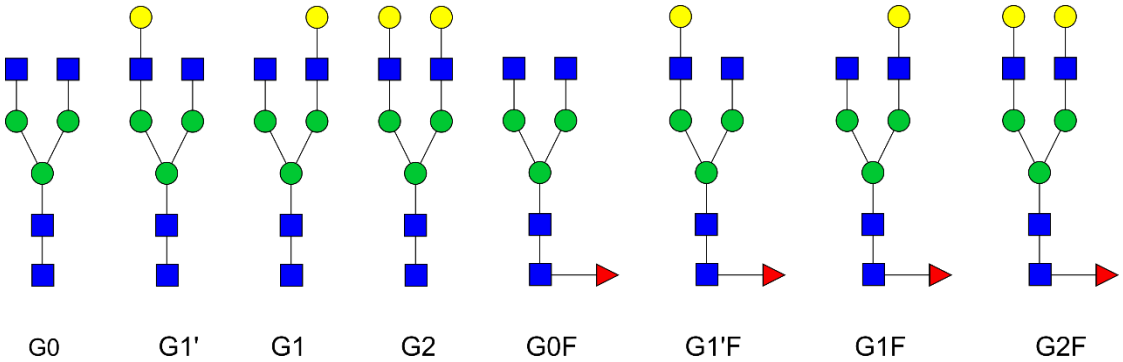

Figure 4-1: Nomenclature and structures of IgG glycoforms described in chapter 4. G: Galactose; F: Fucose; 0-2: number of galactose residues in each structure.

The following terms are mentioned throughout the analysis of results:

1. **Overall galactosylation**: a measurement of the galactose molecules, present in the glycoforms. This was normalised for the maximum number of galactose molecules and calculated by:

$$Overall\ galactosylation: \sum^{i=n} \frac{x_i}{x_m} P_i \quad (4.1)$$

   - x_i is the number of galactose molecules on i^{th} species
   - x_m is the theoretical maximum number of galactose molecules. Here x_m=2, as the structures studied are biantennary (**Figure 4-1**).
   - P_i is the percentage of i^{th} species in ensemble of species

2. **Terminal galactosylation**: the sum of percentages of all structures carrying terminal galactose:

$$Terminal\ galactosylation = G1 + G1' + G2 + G1F + G1'F + G2F \quad (4.2)$$

All glycoforms are given as a percentage, calculated as follows:

$$P_i = \frac{Area\ under\ curve}{Sum\ of\ all\ areas} * 100\%, \quad (4.3)$$

where each area is the average of independent measurements.

Finally, statistical analysis was performed using Excel and consisted of calculation of averages, standard deviation and calculation of Pearson correlation coefficient.

4.2. Results

4.2.1. Objective 1

4.2.1.1. Enzymatic galactosylation of humanised IgG produced in CHO cells (chIgG)

The culture supernatant containing the chIgG was kindly provided by Mr. Pavlos Kotidis (Kontoravdi Lab). The chIgG was subsequently purified using Protein A affinity chromatography.

Immobilised hGalT was reacted overnight with chIgG. The reaction conditions applied were: 20mM Tris-HCl pH 7.4 and 6mM UDP-Gal, at 37°C under constant shaking. The concentration of $MnCl_2$ (20mM) was selected based on available literature[54]. In contrast to the results presented in Chapter 3, there was no brown precipitation observed in any of the experiments performed here. This is

probably because there were no reaction by-products carried over from previous steps which would subsequently cause the oxidation of $MnCl_2$.

The immobilisation using silica StV beads was performed as described in the Materials and Methods section. Furthermore, to test different enzyme amounts and identify the best conditions, the immobilisation experiments were scaled up. This was done by increasing the volume of StV beads and soluble fraction used, while maintaining the ratio StV beads : soluble fraction. The scale factors (sf) used were 2 and 4. Experiments were monitored by CE (**Figure 4-2**). Interestingly, the glycoforms G0, G1, G1' were not detected, possibly due to being below the limit of detection or due to some interference from a buffer component that led to decreased sensitivity. Therefore, all calculations were performed using only the observed glycoforms. The data obtained showed galactosylation increasing linearly with an increasing amount of enzyme (**Figure 4-2**). Specifically, for the condition where the immobilisation was scaled up by a factor 4 (estimated 45µg hGalT, assuming maximum site occupancy and no steric hindrance), there was 145% increase in overall galactosylation, from 25% to 62%. Specifically, G0F decreased from ~56% to ~14.5% while G2F increased from ~4% to ~32%. Notably, untreated chIgG from different culture batches had different G0F concentrations, ranging between 40-60% (data not shown). However, heterogeneity in galactosylation did not appear to have a noticeable effect on overall conversion. Furthermore, G1F increased linearly with increasing enzyme amount. Finally, there was variation observed in the change in G2 and G1'F. Increasing the number of repeats should address these variations and obtain a clear result.

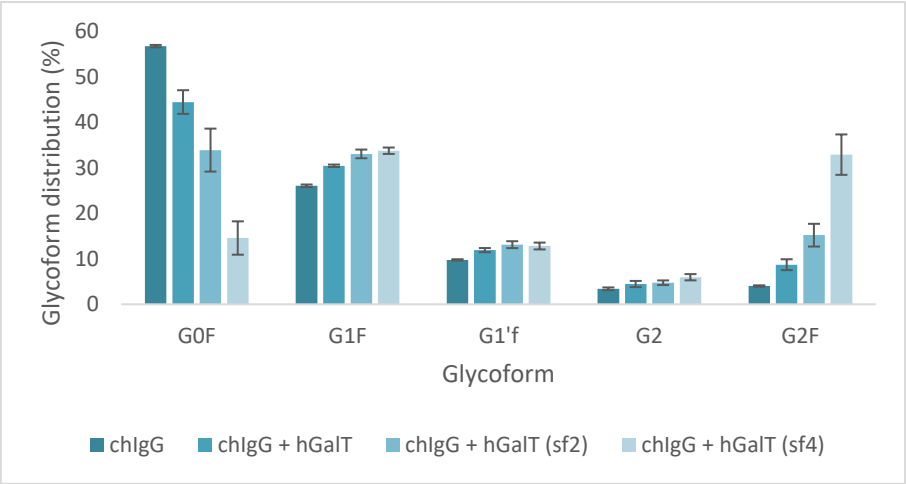

Figure 4-2: Glycoform distribution in chIgG pre- and post-treatment with hGalT immobilised on silica StV beads. Different immobilisation experiments are represented based on the different scale factors (sf) applied. Error bars represent standard deviations between independent experiments (n ≥ 2).

Surprisingly, when the experiment was repeated under the exact same conditions, there were significant variations (G2F range 15%-70%) in the galactosylation change amongst all experiments (**Figure 4-3a**). Notably, the trend amongst the different scale factors remained the same (data not shown). It was hypothesised that this variance was caused by variabilities in the amount of enzyme following the immobilisation experiment (e.g. washing steps and bead recovery).

To counteract this, hGalT was immobilised using magnetic StV beads instead of silica StV beads to facilitate washing and robust recovery. Furthermore, since the binding capacity of magnetic StV beads is 2.5 nmoles / mg beads, ~8 times more than silica StV beads, less volume of resuspended particles was required enabling scale-up whilst facilitating handling. In addition, the time required for removing unbound material post-immobilisation was significantly reduced, given centrifugation steps could be avoided. Therefore, chIgG was treated with hGalT immobilised on magnetic StV beads (estimated 76µg of hGalT assuming maximum site occupancy and no steric hindrance).

Interestingly, the variability of the results was reduced (G2F range ~45%-60%) (**Figure 4-3**: Comparison of immobilisation carriers. a. Distribution of G0F and G2F following treatment with hGalT immobilised on either silica StV beads or magnetic StV beads (n≥4)) Furthermore, it appears that this variability was not caused by the glycoform distribution in the starting chIgG, given its tight distribution as illustrated in **Figure 4-3b**. This could support the hypothesis that the use of magnetic StV beads leads to less errors e.g. due to less losses and ease of handling, when compared to silica StV beads. Therefore, all subsequent experiments were performed using magnetic StV beads.

a.

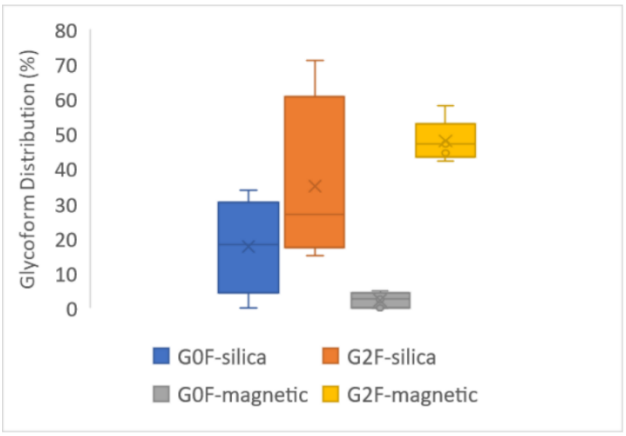

b.

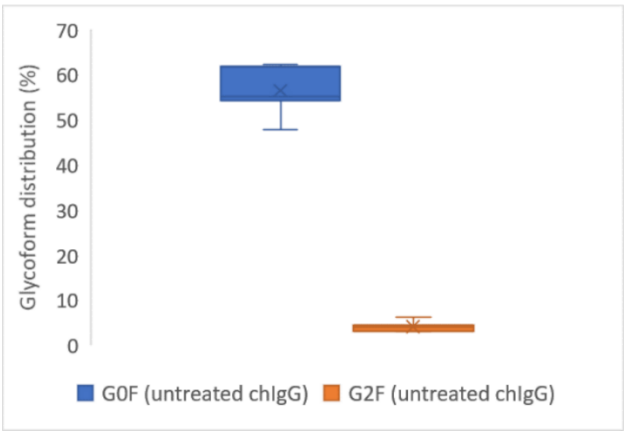

Figure 4-3: Comparison of immobilisation carriers. a. Distribution of G0F and G2F following treatment with hGalT immobilised on either silica StV beads or magnetic StV beads (n≥4); b. Distribution of G0F and G2F in untreated chIgG (n=6).

The reaction conditions of chIgG treatment with immobilised hGalT were as described earlier: 20mM Tris-HCl (pH 7.4) and 6mM UDP-Gal, 20mM $MnCl_2$, at 37°C under constant shaking. Results were monitored by CE (**Figure 4-4**, **Table 4-1**). Overall galactosylation was increased by 192% reaching 62% whilst terminal galactosylation reached ~97% As observed earlier, there was a large conversion of glycoforms to G2F. Specifically, G0F decreased from ~54% to ~4% whilst G2F increased from ~4% to 48%. As before, the glycoforms G0, G1 and G1' were not detected whilst there was no significant change in the galactosylation levels of G2.

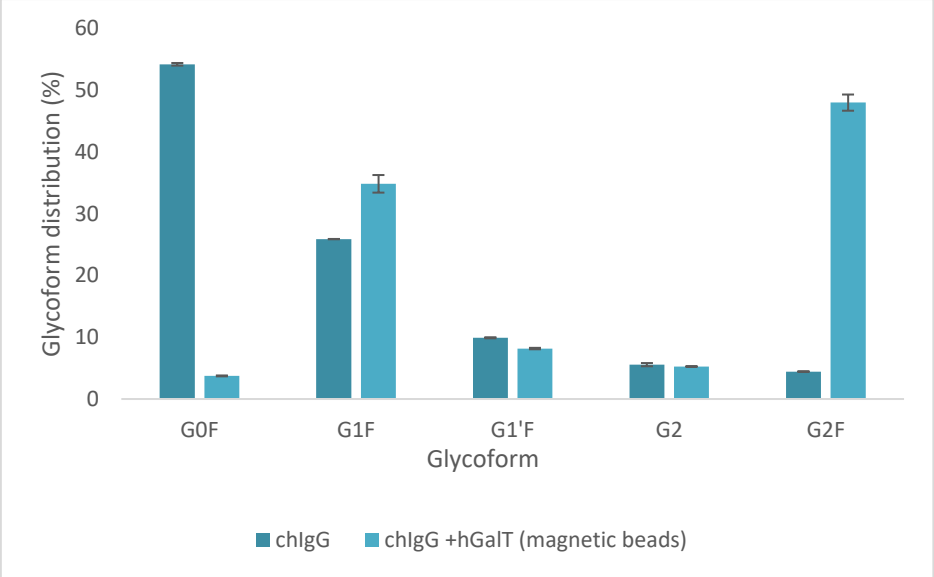

Figure 4-4: Glycoform distribution in chIgG pre- and post-treatment with hGalT immobilised on magnetic StV beads. Error bars represent standard deviations between independent experiments (n = 2).

4.2.1.2. Enzymatic galactosylation of IgG from human serum (hIgG)

hIgG was reacted with hGalT immobilised on magnetic StV beads. The reaction conditions were identical to the experiment for chIgG. Results were monitored by CE (**Figure 4-5** and **Table 4-1**). The galactosylation profile of untreated hIgG was significantly enhanced compared to the chIgG. For instance, G2F in hIgG was ~23% compared to ~4% in chIgG. Terminal galactosylation increased from ~70% to ~84%, an increase of approximately 15%. Similar to chIgG, the biggest change was observed for G2F, which reached ~38%. The glycoform G1 was not detected whilst there was no observable change in the galactosylation levels of G2 and G0. Interestingly, G1' decreased. However, no considerable change was observed in the quantity of G2, which could justify the decrease in G1'. It could be the case that the measurement of G1' is close to the limit of detection and thus the difference reported might be inaccurate. Increasing the statistical power by running more repeats may lead to a detectable or accurate change.

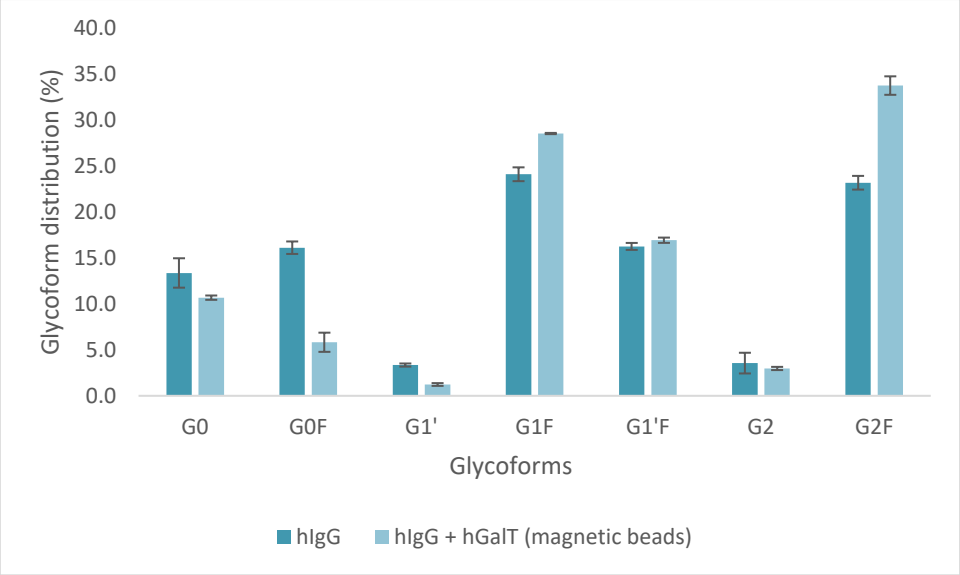

Figure 4-5*:* Glycoform distribution in hIgG pre- and post-treatment with hGalT immobilised on magnetic StV beads. Error bars represent standard deviations between independent experiments (n = 2). Overall galactosylation was increased by 20%.

4.2.1.3. Enzymatic galactosylation of IgG from rabbit serum (rIgG)

rIGg was reacted with hGalT immobilised on magnetic StV beads. The glycosylation profile as monitored by CE, showed multiple unidentified glycoforms (**Figure 8-3**). However, all the target glycoforms (**Figure 4-1**) were successfully identified and subsequently analysed (**Figure 4-6**, **Table 4-1**). The galactosylation profile of untreated rIgG contains predominantly agalactosylated structures (G0) and to a lesser extent monogalactosylated structures. Furthermore, the afucosylated structures were in abundance compared to both hIgG and chIgG. Following treatment with immobilised hGalT, the overall galactosylation levels increased by 90%. Terminal galactosylation reached ~91% from ~60%. Interestingly, the preferred substrates were the agalactosylated glycans, regardless of the presence or absence of fucose. Specifically, G0 was largely converted to G2 and G0F was no longer detected, while decreases in G1F and G1'F were observed, suggesting complete conversion of G0F to G2F or G0F dropped below the limit of detection. The difference in the remaining glycoforms as shown in **Figure 4-6** was negligible.

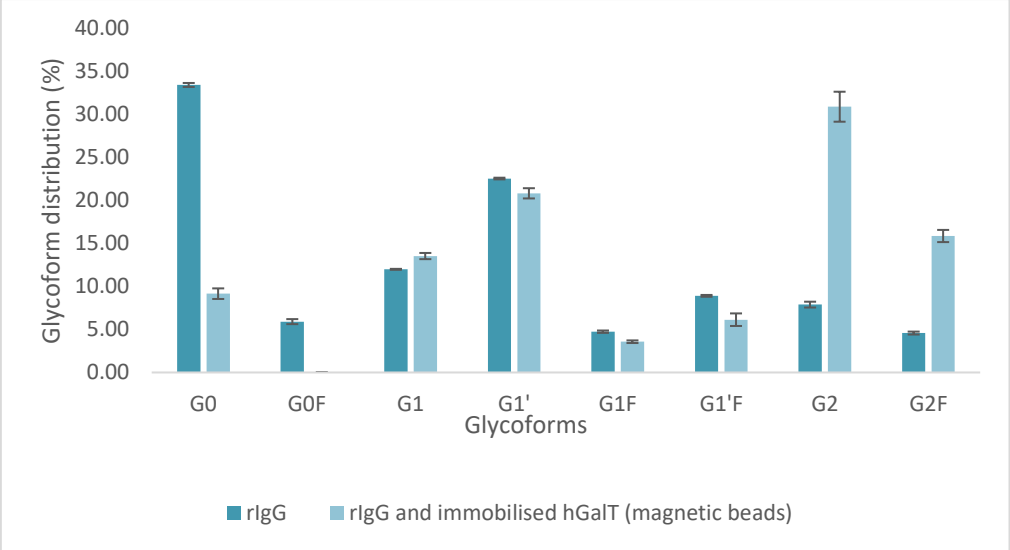

Figure 4-6: Glycoform distribution in rIgG pre- and post-treatment with hGalT immobilised on magnetic StV beads. Error bars represent standard deviations between independent experiments (n = 2). Overall galactosylation was increased by 88%.

Table 4-1: Summary of glycoforms of different IgGs pre-and post-treatment with hGalT. Distribution is depicted as percentage of total peaks and as an average of replicate measurements (n≥2).

	IgGs					
	chIgG		hIgG		rIgG	
hGalT / Glycoform	-	+	-	+	-	+
G0	ND	ND	13.4	10.7	29.0	8.2
G1	ND	ND	ND	ND	10.4	12.0
G1'	ND	ND	3.4	1.2	19.6	18.5
G2	5.6	5.3	3.6	3.0	6.9	27.1
G0F	54.2	3.7	16.1	5.8	5.1	ND
G1F	25.9	34.8	24.1	28.6	4.1	3.2
G1'F	9.9	8.2	16.3	16.9	7.7	5.5
G2F	4.4	48.0	23.2	33.8	4.0	13.9
Overall galactosylation	27.9	74.6	48.6	60.1	31.8	60.6
Terminal galactosylation	45.8	96.3	70.5	83.5	52.7	80.2

4.2.2. Objective 2

4.2.2.1. Reusability of immobilised hGalT

The highest conversion of galactosylation levels was observed for chIgG and thus it was selected for the enzyme reusability experiments. To demonstrate reusability of immobilised hGalT, chIgG was first treated with immobilised enzyme under the same conditions described in Objective 1, i.e. overnight incubation (20h) at 37°C under constant shaking with 20mM Tris-HCl pH 7.4, 20mM $MnCl_2$

and 6mM UDP-Gal. The magnetic StV beads were then separated from solution and recovered, before being thoroughly washed for subsequent incubations. The experiment was repeated for a total of 7 incubations and results were monitored with CE. Reusability and enhanced galactosylation was successfully demonstrated for all 7 cycles (**Figure 4-7**). Experiments were performed in duplicates with the exception of cycles 5-7. Unfortunately, due to an unforeseen experimental mishap it was impossible to recover the enzymes of the replicate experiment and thus cycles 5-7 were performed in single measurements. Due to Covid-19 it was impossible to repeat this experiment. Distribution of glycoforms is depicted in **Table 4-2**.

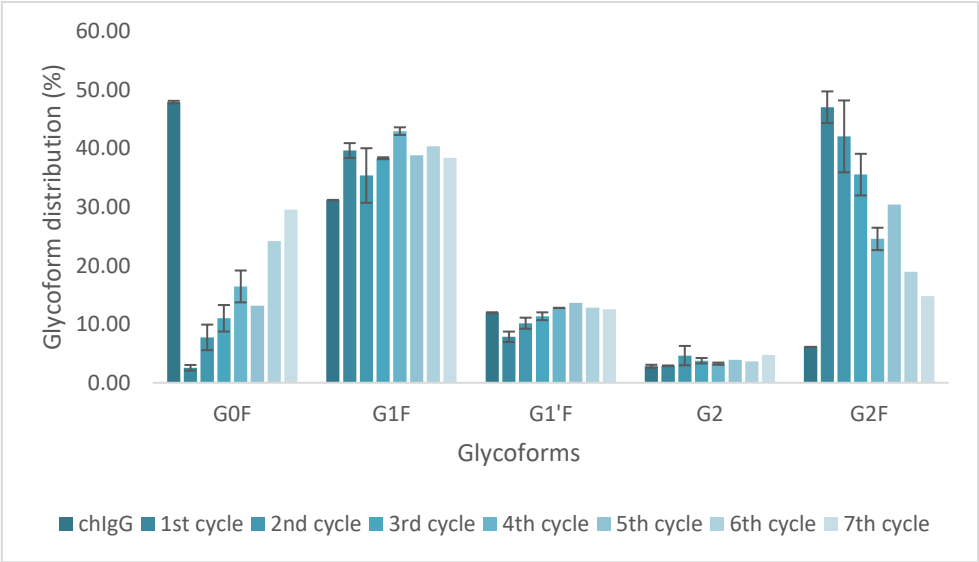

Figure 4-7: Reuse of immobilised hGalT and glycoform distribution of chIgG in multiple cycles. Error bars represent standard deviations between independent experiments (n = 2). There are no replicate experiments for cycles 5-7. Change in galactosylation depict a linear decrease with each cycle (Pearson correlation coefficient for G0F = 0.94).

The results of the reusability cycles show a reasonably linear decrease (Pearson correlation coefficient = 0.94) in galactosylation, which could be due to the loss of enzymatic activity or potential loss of material in the surrounding environment during shaking. Specifically, overall galactosylation increased by ~140% after the first cycle with the terminally galactosylated structures increasing to ~97% (**Table 4-2**). After the seventh and final cycle, terminal galactosylation was at 70%, a 35% increase compared to the untreated chIgG.

In all cycles, G0F was the substrate of preference which, as seen in previous experiments, was largely converted to G2F. There was no considerable change observed in G1'F or G2. This was consistent with the previously established behaviour of hGalT.

Table 4-2: Summary of galactosylation levels in hGalT reusability experiments. Distribution is depicted as percentage of total peaks and as an average of replicate measurements (n≥2). There are no replicates for cycles 5-7.

GalT treatment / Glycoforms	untreated chIgG	1st cycle	2nd cycle	3rd cycle	4th cycle	5th cycle	6th cycle	7th cycle
G0F	47.9	2.6	7.7	11.0	16.4	13.1	24.2	29.6
G1F	31.2	39.7	35.4	38.3	43.0	38.9	40.4	38.4
G1'F	11.9	7.9	10.2	11.4	12.8	13.6	12.8	12.5
G2	2.8	2.9	4.6	3.8	3.3	3.9	3.6	4.7
G2F	6.1	47.1	42.1	35.5	24.6	30.5	18.9	14.8
Overall galactosylation	30.5	73.7	69.5	64.1	55.7	60.6	49.2	45.0
Terminal Galactosylation	52.1	97.4	92.3	89.0	83.6	86.9	75.8	70.4

4.3. Discussion

In line with the objectives of this chapter, the in-house immobilised hGalT was applied on three IgGs, chIgG, hIgG, rIgG to successfully enhance galactosylation. The presence of galactose offers beneficial properties in IgGs such as some anti-inflammatory activity, increased receptor binding and increased ADCP and CDC. Furthermore, galactose functions as a substrate for sialytransferases, generating sialylated glycoforms which have multiple desirable properties. Therefore, galactosylation is a critical attribute and its enhancement is highly sought and often attempted[52,64,95,167–169,280,283,289,290].

As mentioned in section 4.1, the candidate IgGs were selected based on the different galactosylation levels. As seen in the glycan distribution obtained by CE, untreated chIgG showed increased agalactosylation (e.g. G0F ~40-60%) compared to hIgG (G0F~23%). In contrast, rIgG had a broad range of structures with the main ones (>60%) being afucosylated (G0, G1, G1', G2) and specifically agalactosylated (G0). Furthermore, batch-to-batch variations in the galactosylation levels of chIgG were detected. This is quite common and often observed[52]. However, it demonstrates the lack of control over the glycosylation profile in cell-based systems whilst making the need for *in vitro* treatment essential.

As seen in Section 4.2.1.1 and the *in vitro* galactosylation experiments performed, there was a distinct change in the galactosylation of fucosylated structures as has previously been reported[52,64,167–169,289]. For instance, overnight treatment of the chIgG with hGalT yielded ~96% terminal galactosylation, a ~2-fold increase, with 48% being G2F. Similarly, treatment of hIgG with hGalT yielded ~34% G2F and ~84% terminal galactosylation from 70%. In addition, there was no

considerable change observed in the concentration of G2 or G0 in any of the candidate IgGs. Although this demonstrates lack of enzymatic activity, it is not possible to comment on substrate preference between fucosylated and afucosylated structures. This is because there was no considerable change in G0, G1 and G1', or they were not detected, which could shine some light on reaction progression. Crucially, the afucosylated structures have also not been presented or discussed in similar research[52,64,95,167–169,280,283,289,290], probably due to their low concentration. In the case of rIgG, there was a preference for agalactosylated structures (~35% pre-hGalT treatment), regardless of fucose presence. Specifically, terminal galactosylation reached ~80% from ~50%, a 1.5-fold increase. Furthermore, the fully galactosylated glycans G2 and G2F increased significantly (~300%) reaching 30% and 16% respectively.

Collectively, the results obtained here demonstrate the applicability of the in-house hGalT to increase galactosylation of full length IgGs. Furthermore, it was an easy-to-implement experiment, the enzyme can be produced in a bacterial host in large quantities, whilst maximum control over the reaction conditions was allowed. For example, a single overnight treatment of chIgG with hGalT yielded >96% terminal galactosylation. In contrast, an *in vivo* glycoengineered platform, which would require multiple months of experimentation, yielded ~80% of terminal galactosylation[95].

The differences in galactosylation levels as well as in substrate specificity observed here could be a direct result of structural differences amongst the IgGs. For example, rIgG is known to be heavily glycosylated in the Fab region which is more accessible to enzymes, while carrying afucosylated structures[296,297]. It would also be interesting to understand the role of fucose in substrate specificity of hGalT. Future work could thus entail *in vitro* galactosylation using mainly afucosylated structures. These structures can be produced either *in vivo* in glycoengineered CHO cells (e.g. in a *FUT8* deficient line[52,93,300] or a GnTIII overexpressing line[52,94]) or *in vitro* with the use of a fucosidase to remove the core fucose[301]. An experiment to understand the specificity of hGalT can also inform future research regarding the order of reactions, i.e. galactosylation and defucosylation, and elucidate reaction rates. The latter would be necessary in understanding enzyme kinetics and in constructing kinetic models.

An observation made in the experiments performed here was the distribution of the mono-galactosylated structures across all three IgGs. Following incubation with GalT, the apparent change in G1/G1'/G1F/G1'F was not considerable. It is unclear whether the observed G1/G1'/G1F/G1'F after treatment with hGalT correspond to the starting material in untreated IgGs, i.e. no conversion took place, or they represent reaction intermediates. In chIgG and hIgG there was a slight increase in G1F potentially corresponding to an intermediate formed during conversion of G0F to G2F. No change

was detected in G1'F. In rIgG, there was only a slight decrease in mono-galactosylated structures suggesting they were converted to G2/G2F. A time course experiment might elucidate whether the pre-existing G1F/G1'F gets converted to G2F prior to G0F being converted to G1F/G1'F. Whether mono-galactosylated structures are substrates for immobilised hGalT could be investigated by performing separate control experiments where immobilised hGalT is reacted with commercially available G0F and G1F/G1'F (e.g. Ludger Ltd). Furthermore, it might be the case that immobilisation changed the structural conformation of the enzyme and could have affected its specificity. Computational tools such as molecular dynamics simulations are often used[246,302–305] and, could be applied to elucidate the effect of immobilisation on the structure and function of hGalT. Finally, it could be that more time was required to fully convert the mono-galactosylated structures. In similar research, reaction times are lengthy and typically require 2-4 days to achieve >80% G2F[37,39,55,58]. However, these experiments were all performed using free GalT.

A central aspect of the experiments performed, was the use of immobilised hGalT. Enzyme reusability was demonstrated for 7 cycles, with hGalT retaining its activity for over >140 hours. Furthermore, there was a linear decrease in enzymatic activity. Possible causes of the activity reductions include enzyme denaturation, degradation due to mechanical stress e.g. stirring might have created undesirable foaming which in turn can deactivate the enzyme, enzyme leaching upon storage, loss of material in the surroundings or instability of the streptavidin supports[220,288]. Interestingly, after 7 cycles the terminal galactosylation reached ~70%, a ~1.5-fold increase, with the galactosylation profile after the final cycle was similar to hIgG. Consequently, it was demonstrated that after several cycles human-like galactosylation can still be achieved.

Reusability of GalT has also been demonstrated by Heinzler and co-workers, where they were synthesising LacNAc[198]. Interestingly, they observed a different trend in loss of enzymatic activity. Specifically, significant loss was observed in the second cycle while it remained relatively constant in the remaining cycles. A reason behind the variation in the activity trend, probably lies with the reaction kinetics as well as the use of a different substrate.

Demonstration of reusability is a crucial element for large-scale industrial applications. As discussed in section 4.1, immobilised enzymes are commonly used in the biopharmaceutical sector in large scale[291]. Warnock and co-workers, demonstrated the use of GalT to modify up to 1kg of IgG, thus highlighting the potential for scale-up[169]. An industrial set-up using continuous packed-bed reactors should ensure consistency amongst the galactosylation levels, an essential requirement in the production of drugs[306,307]. Finally, recycling of the enzymes can significantly reduce costs associated

with downstream processes[27,245,291]. Therefore, the use of immobilised hGalT is an attractive alternative to using free enzymes.

Despite achieving increased galactosylation after multiple reusability cycles, the loss of enzymatic activity poses a challenge when homogeneity of the final product is required. As discussed previously, glycosylation and consequently galactosylation is a CQA and it is therefore essential to attain proteins with reliable and consistent galactose content. The latter is crucial to ensure the safety and efficacy of drugs as outlined by regulatory bodies[4,307,308]. Consequently, kinetic characterisation of the immobilised hGalT would be desirable for an understanding of enzyme activity and limiting factors. Furthermore, heterogeneity caused by loss of immobilised enzyme activity might be further addressed by a continuous-flow reactor setup, where fresh substrate is continuously fed, as demonstrated elsewhere[309]. Tuning the reaction conditions to ensure glycan homogeneity in reusability cycles, can offer a platform for the rapid and consistent modification of glycosylated biotherapeutics. Crucially, such a platform has the potential to be used for the production of biosimilars whilst ensuring efficacy, safety and accordance with regulatory requirements. Similar efforts in *in vivo* platforms are often time-consuming, expensive while strict control is not always ensured[31,60,308,310].

One challenge faced upon method development and experimentation was selecting the appropriate immobilisation carrier. As discussed in Section 4.2.1.1, considerable variability was observed in the experiments using silica StV beads. This could be a result of loss of material during reaction or washing steps. This variability was addressed by using magnetic StV beads which also reduced the timing of experiments through the absence of centrifugation steps. Furthermore, experiments were performed in 8-strip PCR tubes, compatible with the magnetic stand, allowing the parallel handling of multiple samples. In addition, magnetic StV beads have a higher binding capacity than silica StV beads. Therefore, it was possible to scale-up immobilisation experiments using smaller reaction volumes, a result of a smaller volume of beads. Specifically, by using 40µl of magnetic StV beads it was possible to capture an estimated 75µg of hGalT. An equivalent result using silica StV beads would require 10-times more particles whilst significantly increasing the reaction volumes.

An issue observed during this work that requires attention, was the use of CE to analyse the glycosylation profile of rIgG. rIgG is known to also have triantennary structures that can serve as substrates to hGalT[296,297]. The CE module applied here had a library of the major glycoforms, however it was impossible to identify the remaining structures. This is a known limitation of CE and it is often recommended to be coupled with an MS module[279,298,311]. A full characterisation of glycans can aid with understanding the specificity of the enzyme and inform future studies.

The results demonstrated here are promising and additional optimisation experiments could be conducted to further improve overall galactosylation. Conditions that can be optimised include the amount of enzyme and concentration of IgG. For example, Warnock and co-workers did a thorough investigation of reaction conditions, focusing on the required enzyme and IgG concentrations[169]. Additionally, the ability to perform and analyse multiple samples in parallel enables the use of a DOE approach and can facilitate optimisation. Finally, following optimisation of galactosylation levels, future work can involve the sialylation of the IgGs and specifically chIgG, the most industrially relevant antibody. It would require the expression and immobilisation of SiaT. This would facilitate the economical modification of cell-based material at an industrial scale, for commercial applications.

4.4. Summary and conclusions

The aim of this chapter was to demonstrate the applicability of the in-house immobilised hGalT to enhance the galactosylation levels of three full-length IgGs. This was in line with the increasing interest to enhance the galactosylation of antibodies and thus improve their therapeutic properties. Overnight reactions yielded significant increases in terminal and overall galactosylation. Specifically, >96% terminal galactosylation was achieved for chIgG, >93% for hIgG and >80% for rIgG. A significant achievement was demonstrating enzyme reusability, highlighting the application of immobilisation. Immobilised hGalT was successfully used up to 7 times, for a total incubation time greater than 140 hours, whilst galactosylation of the same molecule (i.e. G2F) was increased after each cycle. Further optimisation experiments could be utilised to maximise conversion and potentially minimise the required time to achieve the desired outcome. Furthermore, the next step could be the sialylation of the IgGs thus accomplishing the *in vitro* modification in an efficient and simple approach. Reusability makes enzymatic galactosylation a cost-effective approach with the potential for large scale applications as demonstrated in various industrial set-ups using immobilised recombinant enzymes.

Chapter 5: Final discussion

5.1. Introduction

Glycosylation has a significant effect on the properties of protein-based biotherapeutics, including trafficking, proper folding, increased half-life and improved functionality[2,3,31]. In the case of mAbs it is well-known that N-linked glycosylation in the Fc domain has a direct impact on immune cell activation via ADCC, CDC and ADCP[42,45,48]. Therefore, glycosylation constitutes a Critical Quality Attribute (CQA)[74] and as a result it is often a target for biotherapeutic engineering[4,5,9,31,70,79,312], aiming producing tailored drugs with enhanced efficacy.

Within the cell, glycosylation is a complex process, with no template and promiscuous enzymes catalysing multiple steps, leading to great glycan heterogeneity[18,19]. This heterogeneity can complicate the large-scale and bespoke application of proteins for use as therapeutics whilst their beneficial properties are not fully harnessed. Efforts to control glycosylation include cell line glycoengineering to produce human-like glycoforms, and chemoenzymatic or *in vitro* enzymatic approaches. However, these methods have key limitations associated with lack of simplicity, cost and lack of homogeneity.

The central focus of this PhD research was to develop a novel AGR comprising immobilised enzymes for the implementation of sequential reactions in an *in vitro* environment. It was hypothesised that the spatiotemporal separation achieved via immobilisation would address existing limitations associated with enzyme promiscuity allowing bespoke N-linked glycosylation of glycoproteins in increased homogeneity. The findings and implications of this thesis are first discussed followed by recommendations for future work and an overall summary.

5.2. Findings and their implications

5.2.1. Method development

5.2.1.1. Key findings

In testing the spatiotemporal separation hypothesis, the N-linked glycosylation pathway regulated by GnTI-ManII-GalT, where enzyme competition naturally exists, was selected. A system to express and immobilise functional enzymes was developed. In line with this, an evaluation of available expression platforms, enzyme orthologs and immobilisation techniques was performed. This led to the design of a method comprising of expression in the *E. coli,* Origami strain, to facilitate disulphide

bridges, with simultaneous enzymatic *in vivo* biotinylation for GnTI and GalT. Specifically, the design for both enzymes consisted of an MBP-tag for solubility at the N-terminus and an AviTag at the C-terminus, enabling site-specific enzymatic biotinylation following co-expression with BirA. The system was applied on two orthologs of GnTI, (hGnTI and NtGnTI) and hGalT with their successful *in vivo* biotinylation and subsequent one-step immobilisation / purification on StV beads. To the very best of my knowledge, this methodology has never been applied before to GTs.

Finally, activity was confirmed for all enzymes, including DmManII which was biotinylated using commercial reagents. Initially, two activity detection techniques with different principles were used: a commercially available colorimetric kit to detect and quantify the by-product UDP and MALDI-TOF MS to detect the formed product. It was identified that a technique relying solely on the detection of by-products might lead to contradictory or misleading results. These observations provide guidance for future studies characterising similar enzymatic reactions.

There are important advantages in using the methodology developed here. Firstly, it enabled the expression, biotinylation and immobilisation of functional enzymes. Specifically, activity was confirmed for both NtGnTI and hGalT. Secondly, it was a simple method that did not require extensive optimisation. It was shown that it can be successfully applied in the case of two enzymes, hGalT and two orthologs of GnTI, thus demonstrating the potential to modify an array of enzyme candidates. If required there is sufficient literature for troubleshooting advice thus further simplifying its application[226,229,230]. Furthermore, the benefit of using such a method was that it allowed the one-step immobilisation / purification on StV beads. As a result, the experimental time was reduced while fewer resources were required compared to protocols requiring purification and concentration steps[313]. Considering as well that expression occurs in a cheap microbial host with high yields, the developed system has the potential to reduce process cost. To the best of our knowledge, this approach has not previously been implemented.

5.2.1.2. Limitations

While the method demonstrated several desirable properties, it was found to have certain limitations. Initially, the one-step immobilisation / purification did not enable exact quantification of the enzyme concentration and immobilisation efficiency. Instead, an estimation, based on the assumption of maximum occupancy of the StV beads and no steric hindrance was performed. One potential issue could relate to the reproducibility of activity between batches of immobilised enzyme. However, this was not explored as kinetic studies were not performed. Furthermore, it was concluded that structural changes might have occurred upon biotinylation and/or immobilisation,

which consequently impacted the mechanism of action. It is unclear whether these changes also impacted catalytic activity e.g. rate of action, and substrate specificity. Finally, though free enzymes were used as a positive control to confirm activity, comparison studies regarding activity pre- and post-immobilisation were not performed as they were deemed irrelevant to the aims of this study. Therefore, if full characterisation of the developed system is required, including immobilisation efficiency and understating impact of immobilisation on activity, additional work is necessary. The nature of this work will be discussed in the Future Work section.

5.2.2. Glycosylation reactions using immobilised enzymes

5.2.2.1. Key findings

The main focus of this PhD was to perform sequential glycosylation reactions using the immobilised enzymes developed in Chapter 2, with the aim of addressing enzyme promiscuity. The latter can be achieved by the facile recovery of the immobilised enzymes at the end of each reaction. This was successfully demonstrated in Chapter 3, where the NtGnTI-DmManII-hGalT enzyme cascade was initially performed on artificial glycans. Each step approached completion with more than 95% conversion achieved after individual reactions (**Figure 5-1a**). This highlights how enzyme immobilisation can be used to address promiscuity, yielding near-homogenous mixtures of products. In addition, it was demonstrated that an artificial environment allows for the conditions to be fully controlled and thus achieve a high conversion after each enzymatic step. Crucially, only a few parameters require optimisation such as enzyme concentration, time and buffer composition for meaningful results.

The same enzyme cascade (NGnTI-DmManII-hGalT) was applied on an mFc, produced in the glycoengineered SuperMan5 *P. pastoris*. This choice of host strain was crucial for the target protein to carry the required starting glycoform (M5). The first two enzymatic reactions (NtGnTI and DmManII) approached completion (>95% conversion) thus demonstrating that it is possible to modify proteins post-expression and achieve homogeneous glycosylation (**Figure 5-1b**). However, the final step, the hGalT reaction, was not detected due to by-product build up, possibly because of the oxidation of $MnCl_2$. Nevertheless, the successful implementation of NtGnTI and DmManII demonstrated the potential of the AGR to reconstruct mammalian N-linked glycosylation pathways on therapeutic proteins expressed in glycoengineered (mammalian or non-mammalian) hosts. This results to complementing *in vitro* the natural process of glycosylation, enabling a continuous bioprocess. This was further stressed by the successful reusability of NtGnTI, without a significant

loss in activity. Crucially, the ability to reuse/recycle enzymes also enables the large-scale modification of proteins[27,260,314,315] as well as their application in multiple reaction cascades.

An additional application of immobilised enzymes on modifying glycoproteins was presented in Chapter 4. Specifically, immobilised hGalT was used to enhance the galactosylation profile on three full-length IgGs. Driving galactosylation of IgGs *in vitro* has been demonstrated on multiple occasions, highlighting the importance of such endeavour[52,64,167–169,280,283,290]. However, the use of immobilised hGalT, enabled enzyme reusability for 7 cycles, demonstrating activity over a timespan of >140 hours. This result established the applicability of the in-house immobilised hGalT to alter the galactosylation profile of IgGs while enabling its potential implementation in large-scale industrial set ups for continuous modifications. To the very best of our knowledge the use of immobilised hGalT to modify a full-length antibody for multiple reaction cycles has not previously been demonstrated.

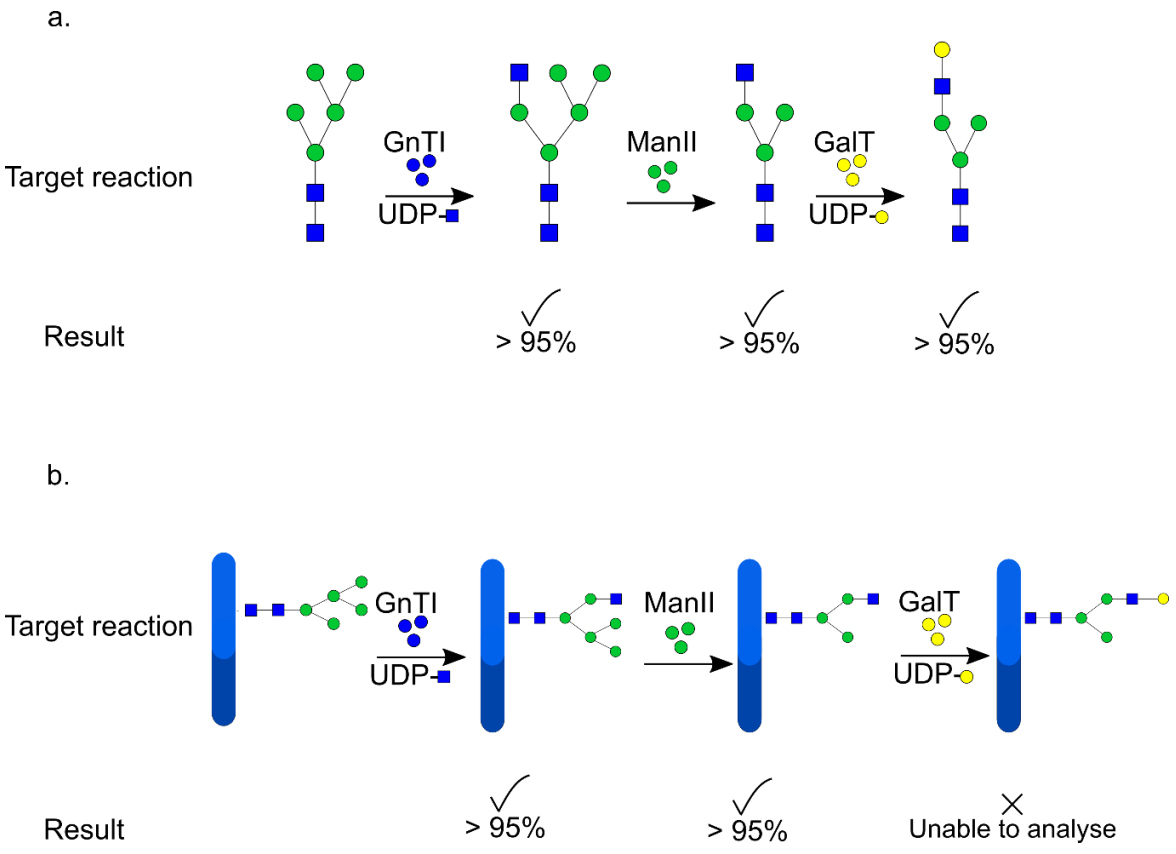

Figure 5-1: Summary of results after sequential reactions using immobilised enzymes to replicate the N-linked glycosylation pathway of GnTI-ManII-GalT. The enzyme used were NtGnTI, DmManII and hGalT. a. Sequential reactions on artificial glycans. Each step approached completion while every glycan was successfully detected; b. Sequential reactions on mFc produced in SuperMan5. The first 2 steps approached completion while glycans were detected after each step. The final step was not analysed as the glycan was not detected.

In addition to the aforementioned benefits, there are significant advantages of applying a system of immobilised enzymes, the AGR, for targeted glycosylation. In contrast to chemoenzymatic methods, where multiple protection and de-protection steps are required to pre-synthesise the glycan structure to be transferred[53,152,153,155,156,158,284], the set-up here avoids the need for many steps making it easier to apply. Furthermore, the use of enzymes makes this a sustainable approach offering important advantages as they are efficient, easy to produce and require mild reaction conditions[316,317]. Avoiding chemical processes reduces undesired by-product formation, e.g. CO_2 emissions, making our platform an environmentally friendlier approach[314]. Finally, the target enzymes can be produced in a microbial host such as *E. coli*, lowering the overall cost of the process. The latter is further accentuated by the ability to re-use the enzymes as demonstrated by the reusability of NtGnTI (Chapter 3) and hGalT (Chapter 4).

Another advantage is that in principle the AGR enables implementation of multiple pathways, allowing strict control over the order of reactions, thus making it a modular approach. As a result, such a system can also be used for the on-demand synthesis of homogeneous glycan structures that are otherwise difficult to obtain[312]. Similar modularity and strict control can, in principle, be achieved by immobilising the substrate and sequentially adding it in different pools of enzymes. This method has been demonstrated by Tayi and Butler for various mAbs immobilised via affinity on Protein A or Protein G and sequentially modified *in vitro* by GalT and SiaT[170]. Similarly, Martin and co-workers, immobilised HS on magnetic particles and was subsequently moved through different enzyme compartments of the digital microfluidic chip[196]. Although immobilising the substrate is an elegant method and can in principle address heterogeneity, it faces certain limitations. Mainly, substrate immobilisation might cause undesired steric hindrance, creating inaccessible sites and thus inhibiting enzymatic activity[27,79,259,29]. Furthermore, there is a possibility for free enzyme to remain attached to the substrate, preventing the formation of homogenous product. A similar example was observed in Chapter 2, when BirA remained attached to AviTag and washing with strong detergents was essential. Finally, it is not possible to reuse free enzymes.

Finally, a system of immobilised enzymes may address undesired cross-reactivity, e.g. competitive inhibition since it is reduced via spatiotemporal separation. Such limitations have been observed in one-pot glycosylation reactions[172]. For example, Hamilton and co-workers observed the inhibition of GnTII by GnTIV and thus intermediate purifications were necessary[172].

5.2.2.2. Limitations

Despite the desirable traits observed here, there are some drawbacks regarding the use of immobilised enzymes for *in vitro* glycosylation reactions. Initially is the increased cost associated with the use of NSDs as well as the cost of the solid supports. Although the potential for enzyme reusability as well as the use of the cheaper non-mammalian expression platforms can significantly lower the cost, the essential use of the expensive NSDs as well as the often expensive StV beads is an important limitation.

Another drawback of *in vitro* enzyme glycosylation reactions is the by-product build up that can interfere with the progress of reactions. This was encountered in Chapter 3 and the reaction of immobilised hGalT with mFc. The possible oxidation of $MnCl_2$ caused protein precipitation and thus it was impossible to comment on the extent of the reaction. This limitation can hinder large-scale applications leading to loss of valuable material, particularly of an antibody or relevant biotherapeutic. Furthermore, it might negatively impact efforts to reconstruct whole N-linked glycosylation pathways since multiple enzymes and reaction conditions are required. It might be possible that optimisation of the reaction conditions can address this limitation, or a buffer-exchange step might be necessary. Finally, one important by-product is released UDP from the NSDs. It is often the case that UDP inhibits or slows the action of GTs[169,198,268,318–320]. However, this was not observed here since all reactions were performed overnight and no study of the kinetics was performed. Nevertheless, it might be necessary to resolve the built-up and potential inhibition of UDP, particularly when characterising the reactions. Ways to address this are discussed in the future work section (**Section 5.3**).

5.3. Recommendations for future work

5.3.1. Optimisation of system

One important feature of this work is that experiments were performed to establish a proof-of-concept system and support the hypothesis of spatiotemporal separation to tackle enzyme promiscuity. Immobilisation characterisation as well as enzyme and reaction characterisation were not performed as it was beyond the scope of this study. However, optimisation of the reaction conditions as well as understanding enzyme kinetics can significantly aid with identifying essential parameters to achieve maximum conversion. This can lead to the construction of mathematical models to help design future experiments. A DOE approach using available platforms, e.g. JMP, can be helpful when optimising the system. Conditions that should be considered have been suggested

throughout the individual discussion sections of the results chapters. They include the concentration of enzyme and target protein, concentration of NSDs and metal donors as well as the incubation times. Here, all reactions were performed overnight to ensure conversion. However, in an industrial set-up a quicker turnover might be more desirable. Furthermore, as thoroughly discussed in Chapters 2 and 3, the amount of enzyme was a theoretical estimation. An accurate calculation should improve method implementation. Example ways to achieve this include purification of the enzyme and concentration determination prior to immobilisation or accurately defining immobilisation efficiency. This can be achieved by using pure enzymes and performing a material balance i.e. calculating the concentration of enzyme in solution pre- and post-immobilisation.

One factor that needs to be considered is the by-product build-up which might interfere with the integrity of the target protein, as seen in Chapter 3. Solutions to this include optimisation of reaction conditions and / or a buffer exchange. Interestingly, an online buffer exchange approach has been demonstrated by Sun and co-workers[321]. Specifically, the authors developed a system of immobilised enzymes for the online buffer exchange, protein digestion and separation by Reverse Phase Liquid Chromatography (RPLC) and finally online detection with microreverse-phase liquid chromatography-electrospray ionization-tandem mass spectrometry (µRPLC-ESI-MS/MS). Such a system has the potential to address the challenge posed by by-product built-up observed here whilst maintaining a continuous modification platform.

Finally, it is essential to address the cost associated with the use the expensive NSDs. Initially, there are enzyme complexes available for the *in situ* generation of NSDs[27,198,268,322]. An example is the generation of UDP-Gal from D -(+) -galactose through α-D -galactose-1-phosphate using a galactokinase and UDP-sugar pyrophosphorylase as demonstrated by Elling and co-workers[268]. Crucially, all the participating enzymes were immobilised in a compartmental microfluidic reactor. Similar examples also exist for other NSDs such as UDP-GlcNAc[322,323]. Notably, as the NSDs can be enzymatically produced, they can also be regenerated from the released UDP[26,27,29]. One example enzymatic pathway suitable for the regeneration of UDP-Gal was described by Bülter and Elling where sucrose synthase is used to turn UDP and sucrose to UDP-Glc and fructose[322]. Subsequently, UDP- Glc is converted to UDP-Gal by UDP-Glc 4-epimerase. Crucially, a regeneration system can also be used to address potential inhibition by UDP and thus increase the rate of the reaction whilst lowering the cost of the reagents[200]. Finally, similar to NSDs, an aspect requiring attention is the increased cost of StV beads. It might be necessary to explore bead regeneration techniques as demonstrated elsewhere to reduce their overall cost[325]. A techno-economic analysis can shed some light as of the aforementioned costly elements is the most important to tackle.

5.3.2. Applications

One interesting endeavour would be to attempt the bottom-up synthesis of mature N-linked Fc glycosylation, for example fully sialylated structures and / or multi-antennary structures. For this, it would be necessary to complete the enzyme library required for the synthesis of fully human glycans e.g. expression of functional GnTII, FucT and SiaT. The expression and immobilisation methodology developed here is in principle widely applicable thus allowing its facile implementation. Crucially, a complete system can allow the on-demand synthesis of antibodies enabling its future application for the development of personalised treatments. Therefore, following immobilisation of these new enzymes, synthesis of glycans can be either performed on the already expressed mFc or a full-length IgG expressed in glycoengineered *P. pastoris*, as previously demonstrated[157]. Because of a complete enzyme toolbox, different glycoforms can be synthesised, such as fucosylated or afucosylated structures, and thus efficacy studies can be performed e.g. effect on ADCC or receptor binding. Significantly, a complete AGR can also be used for the on-demand synthesis of homogeneous glycan structures that are otherwise difficult to obtain[312]. As a result, it could be used to study the role of individual glycoforms in biological processes and to understand the catalytic activity and specificity of GTs.

Finally, reactions with full-length IgGs can also shine some light on site-selectivity and the impact of enzyme activity. Specifically, the Fc-site has 2 N-linked glycosylation sites, and this is often presented as a potential limitation of *in vitro* modification systems[312]. It is possible that with optimisation of the conditions and characterisation of the enzymes, modification of both sites might be achieved.

One additional experiment arising from expanding the enzyme library, and consequently the library of glycan structures, is studying the specificity of individual enzymes and potential cross-reactivity. Naturally, this would be a challenging endeavour due to the limited understanding of enzymatic interactions *in vivo*[192]. However, performing the enzyme reactions *in vitro* with different homogeneous structures should allow better understanding of substrate preference. These experiments should aid with understanding substrate specificity and GT activity which in turn can help comprehend their role in glycan heterogeneity and thus inform future *in vivo* or model-based studies. Furthermore, an interesting experiment would be to perform sequential one-pot glycosylation reactions and identify unwanted enzyme cross-reactivity. An example of such cross-reactivity was the inhibition of GnTII from GnTIV as identified by Hamilton and co-workers[172]. Crucially, the use of immobilised enzymes and their recovery after each step can address these issues and thus serve as another advantage of the AGR developed here.

5.3.3. Potential for scale-up

In addition to expanding the enzymatic toolbox and characterising the reactions, the scalability of the system could also be explored. Immobilised enzymes are often used in large industrial applications as discussed in the Introduction of Chapter 4. Examples include the use of immobilised Penicillin G Amidase for the production of Amoxicillin/ampicillin[293] and immobilised glucose isomerase for the production of high-fructose syrup, a large industrial process where over 10 million tons of syrup are produced annually[314,315]. From these examples it is clear that implementation in large scale-process would require consideration of factors such as cost associated with immobilisation, cost of carriers, effect of immobilisation on catalytic activity (molecular dynamic simulations might be required[314]) and the potential for reusability which will affect the enzyme's shelf-life[291,314,315]. Therefore, a techno-economic analysis will need to be performed to explore the potential of the AGR developed here for similar industrial scale-up. Here, enzyme reusability was demonstrated in Chapter 3 and Chapter 4 thus supporting the hypothesis of retaining activity[221,288,291,326]. However, further experiments are necessary to understand how much of the decrease in the activity of hGalT was due to the loss of beads, and consequently enzyme, upon recovery and how much was due to loss of activity.

In line with the aforementioned endeavour to explore scalability, a possible reactor design can also be studied and subsequently applied. Here, the experiments were performed in a set-up resembling a Stirred Tank Reactor (STR). STRs are often used for bioprocesses using immobilised enzymes such as the use of immobilised cyclodextrin glycosyltransferase to produce β- cyclodextrin[27,327]. However, there can be some limitations associated with the use of STRs including enzyme denaturation due to limited mixing and insufficient mass transfer which can negatively impact the rates of the reactions[27]. Alternative designs include flow microreactors[198,268], capillary film microreactors[200,328] and packed-bed microreators[200,327]. These reactor designs have in common continuous flow, which allows the removal of the products and addition of fresh substrate simultaneously, allowing maximum yields to be achieved[200,317]. The latter is also enabled by the increased stability of immobilised enzymes as they can maintain enzyme activity for longer[198,221,223,227,316,317,329]. Continuous flow microfluidic reactors also benefit from higher mass transfer permitting higher enzyme rates[27,317], whist the high volume to surface ratios enable highly efficient reactions due to the increased interactions. In addition, they can also be scaled-up either by increasing the size of the channels or by using multiple channels in parallel[316]. A disadvantage of continuous-flow microreactors and specifically packed-bed reactors is that significant pressure drops are often observed[27]. Klymenko and co-workers performed an in-depth analysis of possible designs including

microcapillary flow reactors and packed bed reactors using porous or non-porous particles[200]. The authors focused on identifying conditions to achieve highest conversion such as residence time, size of particles and velocity and overcome design limitations such as pressure drop. Their study led to the conclusion that a packed bed reactor using non-porous particles is most suited for increased conversion whilst increasing the radius of the reactor and the particles can decrease the pressure drop. Another design was implemented by Rakmai and Cheirsilp, where they combined CSTR with packed-bed reactor to increase the concentration of the formed product and thus enhance the overall conversion[327]. Finally, there are reactor designs that also enable the automation of the process[198,268]. Elling and co-workers developed a compartmental microfluidic reactor where apart from the aforementioned NSD regeneration, they also integrated an online photometric detection system to monitor in real time the progress of each reaction[268].

5.4. Summary and conclusions

The key objective of this thesis was to design and develop an AGR, a novel system of immobilised enzymes to address enzyme promiscuity and achieve homogeneous glycosylation. Initially, a method for the expression, *in vivo* biotinylation and immobilisation of functional enzymes was developed and applied on GnTI (NtGnTI and hGnTI) and hGalT. Specifically, the enzymes were expressed in *E. coli* fused to MBP at the N-terminus and to AviTag at the C-terminus. Co-expression with the biotin ligase BirA allowed the *in vivo* biotinylation and direct immobilisation from the soluble fraction thus omitting the need for additional chromatography steps. Furthermore, DmManII was biotinylated using commercially available kits and similarly immobilised. Activity was successfully confirmed for each immobilised enzyme prior to building the reaction cascade. During this step, issues with the analysis techniques were identified which can instruct future characterisations.

Following enzyme immobilisation, the spatiotemporal hypothesis to address promiscuity was tested upon reconstructing a N-linked glycosylation pathway through performing a reaction cascade. Initially, the reaction cascade comprising of NtGnTI-DmManII-hGalT was applied on artificial glycans. Over 95% conversion was achieved after every step, thus successfully confirming the initial hypothesis and achieving the central aim of this PhD. Furthermore, the same cascade was applied on an mFc expressed in the glycoengineered *P. pastoris* strain: SuperMan5. Again, over 95% conversion was accomplished with the exception of the hGalT step. The latter was caused by by-product build-up which prevented analysis. This enzymatic step requires additional work to restore the chosen glycosylation pathway on this therapeutically relevant substrate. Finally, enzyme reusability was demonstrated for NtGnTI, highlighting a key benefit of immobilisation.

The final application was the use of immobilised hGalT to enhance the galactosylation profile of three full-length antibodies i.e. chIgG, hIgG and rIgG. Significant enhancement was observed in all cases thus demonstrating the functionality of the in-house immobilised hGalT in such experiments. Crucially, enzyme reusability was demonstrated for 7 cycles, further emphasizing the benefit of reusability caused by immobilisation.

The achievements presented in this thesis provide a framework to synthesise bespoke and homogeneous glycoproteins. Specifically, the presented results can serve as a model for the design and implementation of a larger pipeline which will allow the production of human-like glycoproteins derived from cell-based material. Crucially, as this strategy is applied post-expression, it can be, in principle, adapted to any glycosylation pathway by changing the identity of enzymes used, allowing for a range of glycoproteins to be produced. Furthermore, it is an economical method making use of microbial hosts while allowing for enzyme reusability. As a result, there is true potential for large scale application that in turn can lead to the development of much-desired personalised therapeutics.

Chapter 6: Materials and Methods

6.1. General molecular biology methods

6.2. Strains

Table 6-1: Strains used in this study

Name	Description	Source
E. coli DH5 α	Cloning and plasmid generation	NEB®
E. coli Origami™ 2 DE3 (competent cells)	recombinant expression of glycosyltransferases (i.e. hGnTI, NtGnTI and hGalT).	Novagen®
E. coli strain AVB99	Used for pBirAcm isolation	Avidity, L.L.C.
Pichia pastoris (syn. *Komagataella phaffi*) CBS 7435	Recombinant protein expression (mFc)	ATCC®
Pichia pastoris (syn. *Komagataella phaffi*) GlycoSwitch SuperMan5 (his4-)	Recombinant protein expression (mFc)	Biogrammatics, Inc.

6.2.1. Growth conditions

E. coli strains were cultured in Luria Broth Base (Miller's LB Broth Base) ™ (LB) medium (1% peptone from casein, 0.5% yeast extract, 1% NaCl) at 37°C. Antibiotics have been supplemented for selection (ampicillin, 100 µg/ml; kanamycin, 50 µg/ml; chloramphenicol, 10 µg/ml). Expression was carried out in LB medium supplemented with 20% sterile glucose and the appropriate antibiotics. For generation of pPICZα A mFC, *E. coli* strains were grown in low salt LB medium (0.5% NaCl) supplemented with 10 µg/ml zeocin. LB agar (Miller, Agar 15g/L, Tryptone 10g/L, NaCl 10g/L, Yeast Extract 5g/L was used for bacterial growth on agar plates at 37°C. Antibiotic concentrations used were the same as for liquid cultures. For generation of pPICZα A-mFC, *E. coli* strains were grown in low salt LB agar (0.5% NaCl) supplemented with 10 µg/ml zeocin.

P. pastoris strains were cultured in rich yeast peptone dextrose (YPD) medium (2% peptone from casein, 1% yeast extract, and 2% dextrose) at 30°C. Antibiotics have been supplemented for

selection (zeocin 100 µg/ml). *P. pastoris* strains were cultured in baffled glass flasks or in 50 ml Falcon tubes at a volume of no more than 20% of the total volume. YPD agar (2% peptone from casein, 1% yeast extract, 2% dextrose, 2% agar) was used for yeast growth on agar plates at 30°C. Antibiotic concentrations used were the same as for liquid cultures. Expression was carried out in buffered glycerol/methanol-complex medium (BMGY/BMMY; 1% yeast extract, 2% peptone, 100 mM potassium phosphate, pH 6.0, 1.34% yeast nitrogen base, 4 × 10−5% d-Biotin, 1% glycerol or 0.5% methanol).

6.2.2. Chemically synthesised cDNA

Chemically synthesised cDNA of NtGnTI (Genbank accession no. Y16832) was ordered from GeneArt® Gene synthesis, by ThermoFisher Scientific UK. The sequence was codon optimised for expression in *E. coli*, lacked the first 29 amino acids (Δ29) and carried enzyme restriction sites for *NdeI* (N-terminus) and *EcoRI* (C-terminus) (**Section 8.3.1**).

6.2.3. Chemically synthesised oligonucleotides and annealing

Chemically synthesised AviTag oligonucleotides were ordered from Invitrogen, by ThermoFisher Scientific UK (**Table 6-2**). For oligonucleotides annealing, equal volumes were mixed (100 µM stock), heated at 100°C for 5 min in a heat block and left *in situ* for 2-3 hours. The annealed oligonucleotides encode the AviTag peptide sequence GLNDIFEAQKIEWHE[229], carry a GS linker (N-terminus) and recognition sites for *EcoRI* (N-terminus) and *HindIII* (C-terminus).

Table 6-2: AviTag oligonucleotides

Name	Sequence
AviTag forward	AATTCGGTTCTGGTCTTAATGATATTTTTGAAGCTCAGAAGATTGAATGGCATGAAA
AviTag reverse	AGCTTTTCATGCCATTCAATCTTCTGAGCTTCAAAAATATCATTAAGACCAGAACCG

6.2.4. Plasmids and Primers

Table 6-3: Plasmid inventory

#	Name	Description	Source
1	pCri1b-huGnTI	Expression vector with Δ103 hGnTI (Genbank accession no. P26572), producing N-terminal His6-MBP and C-terminal His6 fusion protein;	Polizzi lab inventory (Dr. Kate Royle).

		kanamycin resistance, IPTG inducible, generated using *NdeI* and *EcoRI*.	
2	pCri1a-huGalT	Expression vector with Δ128 hGalT (Genbank accession no. P15291), producing N-terminal His6-MBP and C-terminal His6 fusion protein; kanamycin resistance, IPTG inducible, generated using *NdeI* and *EcoRI*.	Polizzi lab inventory (Dr. Kate Royle).
3	pMAL-c5X	pMAL-c5x expression vector producing N-terminal MBP fusions; ampicillin resistance, IPTG inducible.	NEB®
4	pMAL-c5X-AviTag	Derivative of pMAL-c5X with AviTag generated using *EcoRI* and *HindIII.*	This study
5	pMAL-c5X-hGnTI-AviTag	Derivative of pMAL-c5X-AviTag with hGnTI, generated using *NdeI* and *EcoRI*.	This study
6	pMAL-c5X-NtGnTI-AviTag	Derivative of pMAL-c5X-AviTag with NtGnTI, generated using *NdeI* and *EcoRI*.	This study
7	pMAL-c5X-hGalT-AviTag	Derivative of pMAL-c5X-AviTag with hGalT, generated using *NdeI* and *EcoRI*.	This study
8	pMAL-c5X-hGnTI	Derivative of pMAL-c5X with NtGnTI, generated using *NdeI* and *EcoRI*.	This study
9	pMAL-c5X-NtGnTI	Derivative of pMAL-c5X with NtGnTI, generated using *NdeI* and *EcoRI*.	This study
10	pMAL-c5X-hGalT	Derivative of pMAL-c5X with hGalT, generated using *NdeI* and *EcoRI*.	This study
11	pBirAcm	Plasmid expressing BirA; IPTG inducible, chloramphenicol resistance (10µg/mL)	Avidity, L.L.C.
12	pPICZα A	Cloning and expression vector with α-mating Factor secretion signal, AOX1 methanol inducer promoter and C-terminal His_6 tag; zeocin resistance.	Life Technologies, Thermofisher scientific, UK
13	pPICZα A-mFc	Derivative of pPICZα A with a mFc, C-terminal 3-residue GS linker and C-terminal His_6 tag, generated by Gibson assembly	This study

14	pCK304-mFc	Rhamnose inducible expression vector with mFc, ampicillin resistance.	Polizzi lab inventory (Oskar Lange)

Table 6-4: List of primers. All primers were ordered from Invitrogen, by ThermoFisher Scientific UK

#	Name	Sequence	Description
1	c5X hGnTI RV	GAAGCTTATTTAATTACCTGCAGG	Reverse primer used in sequencing of pMAL-c5X-hGnTI
2	c5X NtGnTI RV	CTTTCGACTGAGCCTTTCGTTTTATTTG	Reverse primer used in sequencing of pMAL-c5X-NtGnTI
3	AviTag Reverse	AGCTTTTCATGCCATTCAATCTTCTGAGCTTCAAAAATATCATTAAGACCAGAACCG	AviTag reverse oligonucleotide used in sequencing of pMAL-c5X-AviTag, pMAL-c5X-hGnTI-AviTag, pMAL-c5X-NtGnTI-AviTag and pMAL-c5X-hGalT-AviTag
4	EM1_Gib mFC F	GTATCTCTCGAGAAAAGAGAGGCTGAAGCTGCACCGGAACTGTTAGG	Forward primer used for PCR amplification of mFc from pCK304-mFc (annealing temperature 72^{o}C)
5	EM2_Gib mFC R	TGAGGAACAGTCATGTCTAAGGCTACAAACTCAATGGTGATGGTGATGG	Reverse primer used for PCR amplification of mFc from pCK304-mFc (annealing temperature 72^{o}C)
6	EM3_Gib pPICZa_mFC F	TCCGGCTCCCACCATCACCATCACCATTGAGTTTGTAGCCTTAGACATGACTG	Forward primer used for PCR amplification of pPICZa A (annealing temperature 72^{o}C)
7	EM4_Gib pPICZa_mFC R	AACGCTCGGACCACCTAACAGTTCCGGTGCAGCTTCAGCCTCTCTTTTCTC	Reverse primer used for PCR amplification of pPICZa (annealing temperature 72^{o}C)
8	001-AOX1F	GACTGGTTCCAATTGACAAGC	Forward primer used in colony PCR and sequencing of pPICZa A-mFc
9	002-AOX1R	GCAAATGGCATTCTGACATCC	Reverse primer used colony PCR and sequencing of pPICZa A-mFc
10	MalE	GGTCGTCAGACTGTCGATGAAGCC	Eurofins standard sequencing primer forMBP-Fusion proteins

6.2.5. Polymerase Chain Reaction

Polymerase Chain Reaction (PCR) was used to either amplify specific areas on a plasmid (e.g. amplification of mFc from pCK304-mFc) or to confirm clones of plasmid constructs. Standard PCR reactions were performed using Phusion® High-Fidelity DNA Polymerase, NEB®. Bacterial colony PCR was performed using REDTaq® ReadyMix™ PCR Reaction Mix, Sigma-Aldrich. Reaction conditions are depicted in **Table 6-5** and thermocycler conditions in **Table 6-6**. Yeast colony PCR was performed using Thermo Scientific™ Phire Green Hot Start II DNA Polymerase.

Yeast colony PCR (**Table 6-5**) was a "touchdown PCR", where the annealing temperature was gradually decreased to increase specificity. Initial annealing temperature used were several degrees higher than Tm (~6-8^{o}C) of the primers and then decreased to the Tm for at least 25 cycles.

Table 6-5: PCR conditions for polymerases used in this project

Component and stock concentrations	**Phusion reaction (50 µl)**	**Yeast colony PCR- Phire Green Hot Start II (20 µl)**	**Bacterial colony PCR – REDTaq (20 µl)**
5X Polymerase buffer	10 µl (1X)	4 µl (1X)	10 µl Red REDTaq® ReadyMix™ 1 µl 10µM Forward primer 1 µl 10µM Reverse primer 8 µl nuclease free water
10µm Forward Primer	2.5 µl (0.5 µM)	1 µl (0.5 µM)	
10µm Reverse primer	2.5 µl (0.5 µM)	1 µl (0.5 µM)	
1M Betaine (optional)	N/A	4 µl (0.2 M)	
10mM dNTPs	1 µl (200 µM)	1 µl (200 µM)	
Vector DNA (1 µg)	Variable	Colony resuspended in 20mM NaOH	
MilliQ (nuclease free) water	Variable	7.2 1 µl	
DNA Polymerase*	0.5 µl (1 unit)	0.4 1 µl	

* Add last to prevent primer degradation.

Table 6-6: Thermocycling Conditions for routine PCR.

Step	**Temperature (°C)**	**Time**	**Number of cycles**
Initial denaturation	98	30s	1
Denaturation	98	10s	25-35
Annealing	50-72 (primer specific)	30s	
Extension	72 (Polymerase	20-30s/kb (DNA template size and	

	specific)	polymerase specific)	
Final Extension	72 (Polymerase specific)	2-10min	1

Table 6-7: Yeast colony PCR conditions conducted in this study

Step	Temperature (°C)	Time	Number of cycles
Initial denaturation	98	2min	1
Denaturation 1	98	30s	8
Annealing 1	68 (primer specific)	30	
Extension 1	72 (polymerase specific)	20-30s/kb (Target DNA size and polymerase specific)	
Denaturation 2	98	30s	25-35
Annealing 2	60 (primer specific, Tm)	30s	
Extension 2	72 (polymerase specific)	20-30s/kb (Target DNA size size and polymerase specific)	
Final extension	72	2-10min	1

6.2.6. Agarose Gel electrophoresis

DNA fragments from PCR or from digests have been evaluated on a 0.8-1% agarose gel made using agarose powder (UltraPure™ Agarose, Invitrogen) and 1x TAE (Tris Acetate EDTA) (50X TAE Fisher BioReagents). The percentage of the gel depended on the size of the bands expected e.g. for fragment size more than 1kb, 0.8% was used. DNA samples were mixed with pre-mixed 6X Gel Loading Dye, Purple, No SDS (NEB®). HyperLadder 1kb (Bioline) was used as a marker. DNA fragments were then separated by electrophoresis at 100V-120V for 45 minutes. The gels were subsequently stained (SYBR safe, Invitrogen) and visualised using NuGenius GelDoc from SYNGENE.

6.2.7. DNA gel extraction

In the case of multiple bands from a PCR reaction and of restriction digests, DNA of interest was purified from an agarose gel, following gel electrophoresis, using the Zymoclean Gel DNA recovery kit as specified by the manufacturer.

6.2.8. Plasmid construction

6.2.8.1. Gibson assembly

The pPICZα A-mFc plasmid was generated by Gibson Assembly. The backbone vector pPICZα A was linearised using *BamHI*. In order to make the expression vector, desired fragments (backbone and insert) were PCR amplified with 30 bp of homology (primers **Table 6-4**). Gibson assembly was performed using a ready-made master mix (Gibson Assembly® Master Mix) and an equimolar ratio (1:1 ratio) of the insert and backbone. The purified PCR fragments were assembled at 50 °C for an hour.

6.2.8.2. Restriction digestion and DNA ligation

Restriction digestion was used to construct all remaining plasmids (**Table 6-3**). Enzymes used were purchased by NEB® can be seen in **Table 6-3**. For restriction digests, 500ng-2000ng of DNA was used and the restriction enzymes with the appropriate buffers for up to 3 hours at 37°C, according to the manufacturer's instructions. Calf Intestine Phosphatase (CIP) was added to the backbone to prevent linearization and incubated for an additional 1h at 37°C. After completion, the reactions were run on an agarose gel and gel extracted as previously discussed. Concentration of DNA samples was measured using the Biodrop (BioDrop DUO+ (Biodrop, UK).

Ligations were performed using a 1:3 ratio of vector to insert (or 1:50 when the insert is small in size, e.g. AviTag), containing 1x T4 ligase buffer and T4 ligase (NEB®). The ligation was incubated overnight at 10°C. After completion, the reactions were run on an agarose gel and gel extracted as previously discussed. Concentration of DNA samples was measured using the Biodrop.

6.2.9. Cell transformation

Heat shock transformation of bacterial competent cells (25-50µL) was performed by mixing the cells with the plasmids of interest (1-2µL) incubating for 30 minutes on ice, followed by 45 sec at 42°C (heat block or water bath) and back on ice for 2 min. 400µl of SOC outgrowth medium (provided

with competent cells) were added to the cultures and incubated for 1hour at 37°C, in a shaking incubator. Cultures were then plated on LB agar plates with the appropriate antibiotics.

Competent *P. pastoris* cells were prepared and transformed by electroporation as described by Royle and Polizzi 2017[330], with the exception that 50-100ng linearised DNA (here pPICZα A-mFC linearised with *PmeI*) were used instead of 200ng. Transformations were recovered in YPD medium at 30 °C in a shaking incubator for 1 hour and plated onto YPD agar plates with the appropriate antibiotics.

6.2.10. Cell Lysis

To prevent protein degradation all lysis steps were performed on ice. *E. coli* cell pellets were thawed and resuspended in an appropriate volume (~5 ml for every gram of cells) of storage buffer (20mM Tris-HCl pH7.4, 200 mM NaCl and 5% glycerol) supplemented with 0.1 mM phenylmethylsulfonyl fluoride (PMSF) and 1mg/mL lysozyme from chicken egg (Sigma-Aldrich). Note, that in the case of hGnTI, NaCl concentration in storage buffer was 500mM. To lyse the cells the samples were sonicated for 5 min, 30% amplitude and 10 sec on/off pulses (Fisherbrand). The lysate was centrifuged (12000 *xg*, 30 min, 4 °C) to remove the lysed bacteria using rotor. 100µl were collected from the supernatant for SDS page analysis. The supernatant (here refer to as soluble fraction, SF) was filtered using 0.2µm filters and either desalted (**Section 6.3.2**) or used for purification (**Section 6.3.3.1**).

6.2.11. Plasmid DNA purification

Plasmid purification was performed using QIAprep Spin Miniprep Kit (Qiagen) as specified by the manufacturer. DNA concentrations were measured using the BioDrop DUO+ (Biodrop, UK) spectrophotometer.

6.2.12. SDS-PAGE and Western Blot analysis

Sodium dodecyl sulfate polyacrylamide gel electrophoresis (SDS–PAGE) was performed with Mini-PROTEAN® Tetra Vertical Electrophoresis Cells (Biorad) using 10%-12%Tris-HCl SDS-PAGE gels (running gel) and 5% Tris-HCl stacking gel (**Table 6-8**). Depending on the percentage of each gel the amount of water and acrylamide varied. The percentage of acrylamide in the running gel was determined by the size of the target protein. The general rule is that the smaller the MW of the target protein, the higher the percentage of acrylamide in the SDS-PPAGE should be.

Table 6-8: Typical recipe for SDS-PAGE gels

Component for running gel	**Volume**	**Component for stacking gel**	**Volume**
Deionised H2O	Variable	Deionised H2O	3.64mL
40% Acrylamide/Bis-Acrylamide	Variable	40% Acrylamide/Bis-Acrylamide	625µL
1.5M Tris-HCl (pH 8.8),	2.5mL	1M Tris-HCl (pH 6.8),	630µL
10% SDS	150µL	10% SDS	50µL
10 % APS (Ammonium Persulfate)	150µL	10 % APS (Ammonium Persulfate)	50µL
TEMED (add last)	9 µL	TEMED (add last)	5µL
Final volume	10mL	Final volume	5mL

Liquid samples (e.g. fractions from purifications and supernatants) were diluted with 5x SDS-loading dye (5X SDS loading dye 0.225 M Tris-HCl, pH 6.8; 50% glycerol; 5% SDS; 0.05% bromophenol blue; 0.25 M DTT) to a final concertation of 1X SDS-loading dye. Samples consisting of pellets (i.e. samples from expression) were resuspended in an appropriate volume of 1X SDS-loading dye calculated by normalising cultures to $OD600_{nm}$ of 10. All samples were denatured by heating them for 10 minutes at 95^{o}C. For loading the gel, 10-15µl of each protein samples were used as well as 5µl of the Thermo Scientific™ PageRuler™ Prestained Protein Ladder (10–180 kDa) for the identification of the band size. Gels were run at constant amplitude (25mA/gel) for 40-60 minutes, with 1X 10xTris Glycine SDS buffer (0.25M Tris, 1.92M Glycine, 1% SDS, pH 8.6).

For SDS-PAGE analysis the gels were washed 2-3 times with 100ml of deionised H2O by heating up in a microwave for 1 min and shaking at room temperature for an additional 1 min. After washing was completed, SimplyBlue™ SafeStain was added for staining the gel, heated up for 10-20 sec in a microwave and placed on a shaking platform. After 10-15 min the stain was removed, the gels were rinsed multiple times in deionised H2O and incubated in fresh water overnight.

For western blot analysis a Novex® semi-dry blotter was used for electroblotting the gels to an Immobilon®-FL PVDF membrane (Millipore Ltd, Herfordshire, UK). The arrangement of the semi-dry western blot involved 3 Whatman ® 3MM filter papers (cut to gel size) placed at the bottom, the gel, the PVDF membrane and 3 filter papers on top. All components were previously soaked in transfer buffer (per litre: 3.03g tris base, 14.27g glycine, 20% methanol). The PVDF membrane was activated as follows: the membrane was incubated in methanol for 30 seconds, then in deionised H2O for 2min, and finally in transfer buffer for a minimum of 5 minutes. The gels were washed multiple times with deionised H2O before placing to transfer buffer. The transfer was run for 45 minutes at 24

Volts/0.35 A.

For the blotting the following buffers were used: 0.05% TBS-T (0.05% Tween-20, 1X TBS); 0.5% TBS-T (Washing Buffer: 0.5% Tween-20, 1X TBS); blocking buffer (5% skimmed milk in 0.05% TBS). 10X TBS stock, per litre, autoclaved prior to use: 80 g NaCl, 2 g KCl, 30 g Tris Base, pH 8.0 with HCl). All the blotting tspes took place at room temperature and on a shaking platform.

After the transfer the PVDF membrane was blocked in blocking buffer. An hour of primary antibody incubation (diluted in blocking buffer) followed i.e. anti-MBP 1:10000 dilution (NEB®), or anti-His 1:5000 dilution (Biolegend). Residual primary antibody was washed off using TBS-T washing buffer. A secondary antibody (Goat anti-Mouse IgG (H L) Secondary Antibody from Life technologies) was incubated for 30min (1:5000 dilution in blocking buffer). Residual secondary antibody was removed with TBS-T washing buffer. The membrane was washed 3 x 5 minutes with TBS-T (0.5%), followed by a 2 x 2 minutes wash with deionised H2O. Finally, bands were developed with 5mL of alkaline phosphate substrate BCIP/NBT kit (Thermofisher scientific).

6.3. Protein manipulation methods

6.3.1. Protein expression

6.3.1.1. Expression of glycosyltransferases (GTs) in *E. coli* Origami 2 DE3

All glycosyltransferases (NtGnTI, hGnTI, hGalT) were expressed as MBP-fusion proteins in *E. coli* Origami 2 DE3. Plasmids used were derivatives of pMAL-c5X (**Table 6-3**).

A colony of *E. coli* transformed with the plasmid encoding for the GT of interest was inoculated into 5 mL LB media containing 100µg/mL ampicillin and incubated at 37˚C with shaking overnight (~16 hours). 1 L of LB containing ampicillin and 20% sterile glucose was inoculated with 1:100 dilution of the starter 5mL culture and placed in a shaking incubator at 37˚C until the $OD600_{nm}$ was 0.6-0.8. A sample of 1 mL of culture was collected, pelleted (12,000 xg, 5 min) and stored at -20°C for SDS-PAGE analysis (**Section 6.2.12**). GT expression was then induced by the addition of isopropyl β-D-1-thiogalactopyranoside (IPTG) to a final concentration of 0.1 mM and incubated overnight at 20°C. The following day, the $OD600_{nm}$ was measured, a sample of 1 mL of culture was collected pelleted (12,000 xg, 5 min) and stored at -20°C. Remaining cells were harvested by centrifugation at 4000 x g for 30 min. Cell pellets were stored at -80°C until cell lysis (**Section 6.2.10**).

6.3.1.2. Expression of mFc in *Pichia pastoris* CBS 7435 and GlycoSwitch SuperMan5

Small scale expression was carried out in 24 deep-well plates in 3 mL of BMGY/BMMY medium and sealed with Breathe-Easy® sealing membrane (Sigma Aldrich). Single colonies were used to inoculate BMGY and cells were incubated at 30 °C, 216 rpm for 24 h to allow growth. Cells were harvested by centrifugation at 4000 rpm for 5 min. Cell pellets were resuspended in BMMY to induce expression. Induced cultures were incubated at 20 °C, 216 rpm for 72 h before being harvested. Every 24 h the culture was supplemented with 0.5% (v/v) methanol. Samples were collected and analysed with SDS-PAGE to identify clones with high expression levels. Large scale expression was performed under the same conditions, in glass baffled flasks (250mL-2L) at 10% of maximum volume. The supernatants were collected (centrifugation, 3000xg, 4°C, 15min) and immediately purified (**Section 6.3.3.2**).

6.3.2. Desalting of soluble fraction SF

To prevent protein degradation all desalting steps were performed at 4°C.

Desalting of the SF was necessary to remove any unreacted d-biotin from the SF that could hinder immobilisation

Desalting of SF was performed using PD-10 desalting columns (GE healthcare) and by following the protocol described by the manufacturer. Briefly, columns were equilibrated 5 times in storage buffer (20mM Tris-HCl pH7.4, 200 mM NaCl and 5% glycerol, except for hGnTI where 500mM NaCl was used), then 2.5 mL of SF were loaded and once completely entered the column, 3.5 mL of storage buffer was added. The flow-through was collected, aliquoted, flash-frozen (dry ice and EtOH bath) and stored at -80°C until the one-step purification/ immobilisation (**Section 6.4**). 100µL were kept for SDS-PAGE analysis.

6.3.3. Protein Purification

6.3.3.1. Purification of MBP-fusion proteins

To prevent any protein degradation, all purification steps were performed at 4°C.

Amylose affinity chromatography was used for purification of MBP-fusion proteins, as described in the pMAL™ Protein Fusion & Purification System Instruction Manual, from NEB®. Briefly, the SF fraction was loaded onto a column containing amylose pre-equilibrated with storage buffer (20mM Tris-HCl pH7.4, 200 mM NaCl and 5% glycerol, except for hGnTI where 500mM NaCl was used). The

bed volume (i.e. amount of resin) was determined based on binding capacity as specified by the manufacturer. The column was subsequently washed with 2X 10mL of storage buffer to remove non-specifically bound proteins. Specifically, bound proteins were then eluted with 5mL storage buffer containing 10mM maltose and collected in 1mL fractions. All the fractions were analysed by SDS-PAGE. Protein concentration was measured using the Biodrop and storage buffer as blank. Purified fractions when then buffer exchanged (**Section 6.3.3.4**) to storage buffer, aliquoted, flash-frozen using a dry ice / EtOH bath and stored at -80^{o}C.

6.3.3.2. Purification of mFc-His$_6$ from *P. pastoris* supernatant

To prevent any protein degradation, all purification steps were performed at 4^{o}C.

Initially, Ni-NTA resin was equilibrated by resuspending in buffer (20mM Tris-HCl pH 9, 10mM imidazole, 200mM NaCl and 5% glycerol) and centrifuging at 700xg, 4^{o}C, for 5 min. The process was performed 2 times. Amount of resin depends on binding capacity as specified by manufacturer.

The supernatant from the *P. pastoris* cultures (**Section 6.3.1.2**) was immediately collected in 50mL falcon tubes. One tablet of cOmplete™ EDTA-free Protease Inhibitor Cocktail/per 50 ml was added. The pH was then increased to pH 9 (protein specific) by using 5N KOH to precipitate salts. The samples were centrifuged for 15 min, at 3000 *xg* and 4 ^{o}C. Clarified supernatants were filtered using 0.2µm filters, transferred to new 50 mL falcon tubes containing the equilibrated Ni-NTA resin and placed on a shaking platform in a cold cabinet for 1 hour to allow protein binding. The resin was recovered by centrifuging at 700xg, 4^{o}C for 5 min. If multiple falcons were used, the resins were collected in one falcon. The resin was subsequently washed to remove non-specifically bound proteins with 50 mL of buffer (20mM Tris-HCl pH 9, 200mM NaCl and 5% glycerol) containing 20 mM imidazole by gently agitating for 10 min while on ice. The resin was recovered by centrifuging at 700xg, 4^{o}C for 5 min. The process was repeated one more time. The resin was then transferred in a gravity column, washed for one more time and then the protein was eluted with 5mL elution buffer (20mM Tris-HCl pH 9, 200mM NaCl, 250mM Imidazole and 5% glycerol). The fractions were analyzed by SDS-PAGE. The protein was then buffer exchanged as described in **Section 6.3.3.4**.

6.3.3.3. Purification of chIgG from CHO culture supernatant

The CHO culture supernatant was kindly provided by Mr. Pavlos Kotidis (Kontoravdi lab).

To prevent protein degradation, all purification steps were performed at 4^{o}C.

For protein purification the Amicon® Pro-Affinity Concentration Kit Protein A with 100kDa Amicon® Ultra-0.5 Device, from Merck Millipore was used as described by the manufacturer.

6.3.3.4. Buffer exchange

The Amicon® Ultra Centrifugal units from Merck Millipore (0.5-15mL) were used for buffer exchange of proteins. The size and Molecular Weight Cut Off (MWCO) of the buffer exchange units were determined by the starting volumes and the size of the target protein. The steps followed were as described by the manufacturer. The storage buffer was 20mM Tris-HCl 7.4, 200mM NaCl and 5% glycerol for all proteins.

6.3.4. Protein biotinylation

6.3.4.1. Expression and *in vivo* biotinylation of GTs in *E. coli* Origami 2 DE3

For *in vivo* biotinylation of MBP-GT-AviTag proteins, the exact expression conditions described in **Section 6.3.1.1** were applied with the following additions: a. The colony of *E. coli* used for culture inoculation was transformed with the plasmid encoding for the GT of interest as well as pBirAcm, the plasmid encoding for BirA; b. Chloramphenicol (10 µg/mL) was included for pBirAcm selection; c. Upon induction, d-biotin (20µM final concentration) was also added.

6.3.4.2. Confirmation of biotinylation-Gel shift assay

The gel shift assay applied was described by Fairhead and Howarth[226] with the modification that here the whole SF was used rather than a purified protein. Specifically, 7.5 µL of SF were mixed with 8.25µL of 2X SDS loading dye without DTT (2X SDS loading dye 0.09 M Tris-HCl pH 6.8; 20% glycerol; 2% SDS; 0.02% bromophenol blue;) and incubated for 5min at 95^{o}C. After reaching room temperature, 0.75uL streptavidin (5mg/ml) were added and incubated for 5-10 min at room temperature. Samples were run on a 12% SDS-PAGE gel.

6.3.4.2.1. Densitometry analysis and % biotinylation calculation

To measure the % biotinylation of proteins in the gel shift assay, the intensity of the corresponding bands was measured using TOTALLAB CLIQS 1D Gel Image Analysis software. Background subtraction was performed using the rolling ball method.

The band intensities were directly used. The % biotinylation was calculated from the obtained band intensities as follows:

$$\% \, \boldsymbol{biotinylation} = \frac{\sum \boldsymbol{intenstites\ of\ enzyme\ band\ shifts}}{\sum \boldsymbol{intensities\ of\ enzyme\ bands}} * \mathbf{100} \qquad (6.1)$$

6.3.4.3. Chemical biotinylation of DmManII

DmManII was kindly provided by Dr. David Rose and Dr. Doug Kuntz (University of Waterloo, Ontario Canada) in 10mM Tris-HCl pH 7.5 and 100mM NaCl. DmManII was subsequently diluted to 1mg/ml.

The Lightning-Link® Rapid Biotin Type B Labelling Kit - 3 x up to 200µg Ab, from Expedeon, Ltd, was used for the chemical biotinylation of DmManII. Steps followed were as described by the manufacturer.

6.4. Enzyme immobilisation

For enzyme immobilisation, Streptavidin silica particles 1% w/v. 1.0-1.4 µM from Spherotech or the Dynabeads C1, streptavidin coated magnetic beads, 1% w/v from ThermoFisher, were used. The storage buffer of the beads was removed either by centrifugation (5min, 5000 xg for silica beads) or by the use of a magnet. The particles were subsequently washed 3 times with 0.1M Tris-HCl pH 7.4 by resuspending and centrifuging / magnet separation.

The immobilisation for silica particles was performed as follows: desalted SF (**Section 6.3.2**) was mixed with the washed and pelleted beads, prepared as described earlier. Here, a volumetric ratio of 1:2 (SF: StV beads) was used e.g. 25µL of SF to 50µL of StV beads (volume corresponds to volume of particles before washing and pelleting). For DmManII, since the concentration was known (1mg/mL) an appropriate volume based on the binding capacity of beads, as specified by the manufacturer, was used. The samples were then diluted with 0.1M Tris-HCl, pH 7.4 at a final immobilisation volume of 1mL and incubated in a rotary shaker for 1 hour at 4^{o}C. To scale up experiments, larger volumes of SF and StV beads were used, while keeping the 1:2 ratio. Note, that the immobilisation volume was always 1mL (make up with 0.1M Tris). Following immobilisation, the samples were centrifuged for 10min at 3000 xg, the supernatant was removed, and the pelleted beads were resuspended in storage buffer (20mM Tris pH 7.4, 200mM NaCl and 5% glycerol). The centrifugation steps were repeated, and the washing process was performed 3 times in total. At the end of the washes, the immobilised enzyme was used in the glycosylation reactions described in **section 6.5**.

The ratio of SF to StV beads was determined by testing various volumes of SF (and a constant 50µL of beads) and performing SDS-PAGE analysis. Specifically, following immobilisation and washes, beads were “stripped” by resuspending in 100µL of 1XSDS loading buffer (5X SDS loading dye 0.225

M Tris-HCl, pH 6.8; 50% glycerol; 5% SDS; 0.05% bromophenol blue; 0.25 M DTT) and incubating for 10min at 95°C. The samples were briefly centrifuged to remove the particles and 10 µL of the elutions were used for SDS-PAGE analysis (**Section 6.2.12**).

Similarly, the immobilisation for magnetic particles occurred by mixing SF with prepared StV beads in a volumetric ratio of 1: 0.4. The magnetic beads were used at a smaller volume due to the higher binding capacity compared to silica particles. The final immobilisation volume was 250µL. For DmManII, since the concertation was known (1mg/mL) an appropriate volume based on the binding capacity of beads, as specified by the manufacturer, was used. The washes were performed 3 times by resuspending in storage buffer (20mM Tris pH 7.4, 200mM NaCl and 5% glycerol). The immobilised enzyme was then used in the reactions described in the following section.

6.4.1. Calculation of immobilised enzyme amount and enzyme retention

The amount of enzyme immobilised on StV beads was calculated based on the binding capacity of beads according to the manufacturer (i.e. 0.3nmoles / mg of beads for silica and 2.5nmoles / mg beads for magnetic) and under the assumption of maximum site occupancy and no steric hindrance. Specifically, for each enzyme, the MW was used to calculate the µg of protein as follows:

$$\boldsymbol{For\ a\ protein\ of\ X\ kDa, 1nmole = X\ \mu g} \qquad (6.2)$$

Enzyme retention was calculated as follows: amount enzyme / volume of beads

$$\frac{\boldsymbol{enzyme\ amount}}{\boldsymbol{volume\ of\ beads}} \qquad (6.3)$$

6.5. Glycosylation reactions

6.5.1. Confirmation of activity of immobilised enzymes (Specific to Chapter 2)

6.5.1.1. Colorimetric activity assay for Confirmation of activity of immobilised GnTI

Initially, activity of immobilised NtGnTI and hGnTI was assessed using a commercially available colorimetric kit for activity of glycosyltransferases (Glycosyltransferase Activity Kit, R&D biosystems). The protocol used was as described by the manufacturer and specific for GnTI. Briefly the activity assay consisted of 0.4mM UDP-GlcNAc (Sigma Aldrich, resuspended in deionised H2O and stored in -20°C), 2 mM alpha 1-3, alpha 1-6 Mannotriose (Dextra laboratories, resuspended in deionised H2O), 25 mM MES pH 6.5 and 10 mM $MnCl_2$, for 1 hour on a shaking platform (note: tube was placed vertically). Reaction took place at 25°C for NtGnTI and 37°C for hGnTI. The same activity assay was

performed using free, purified NtGnTI and hGnTI using 0.5µg of enzyme as specified in the protocol. After the end of the reactions, the immobilised enzyme was removed by centrifugation (5min, 5000xg). In samples where free enzyme was used, the reaction was ceased by treatment at 100°C for 5 min and heat denatured enzymes were removed by centrifugation (1min, 10000xg).
The samples were then transferred in 96-well plates (clear bottom, Sigma Aldrich) and prepared using Malachite Green reagents as described in the protocol. 620 nm (absorbance) in endpoint mode was measured using a POLARsar Omega (BMG Labtech, UK). Activity was calculated as follows:

$$\text{Activity (pmol/min)} = \frac{\textbf{Phosphate released} * (\textbf{nmol}) \textbf{ x } (\textbf{1000 pmol/nmol})}{\textbf{Incubation time}} \quad (6.4)$$

6.5.1.2. NtGnTI activity assay subsequently analysed by MALDI-TOF MS

The activity assay of immobilised NtGnTI consisted of 0.5µM M5 glycan (Sigma-Aldrich, resuspended in water and stored in aliquots at -20°C), 2.5mM UDP-GlcNAc, 100mM MES pH 6.5 and 1mM $MnCl_2$, at 25°C overnight on a shaking platform (note: tube was placed vertically). After the end of the reactions, the immobilised enzyme was removed by centrifugation (5min, 5000xg). The samples were then processed for MALDI-TOF MS (**Section 6.7.1**).

6.5.1.3. Confirmation of activity of immobilised ManII

The activity assay of immobilised DmManII consisted of 0.1mM $ZnSO_4$, 50mM MES, pH 5.6 and 0.4mM substrate from immobilised NtGnTI's reaction. Reaction was performed overnight at 37°C on a shaking platform (note: tube was placed vertically). For a positive control, free enzyme was used (amount used equivalent to amount used in immobilisation) and the assay consisted of the same conditions as before, with the addition of 100mM NaCl. After the end of the reactions, the immobilised enzyme was removed by centrifugation (5min, 5000xg). In samples where free enzyme was used, the reaction was ceased by treatment at 100°C for 5 min and heat denatured enzymes were removed by centrifugation (1min, 10000xg). The samples were then processed for MALDI-TOF MS (**Section 6.7.1**).

6.5.1.4. Confirmation of activity of immobilised hGalT

The activity assay of immobilised hGalT consisted of 0.16mM UDP Gal (Merck, resuspended in deionised H2O and stored at -20°C), 16mM GlcNAc (Sigma-Aldrich), 25mM Tris-HCl pH 7.5 and 10mM $MnCl_2$. Reaction was performed overnight at 37°C on a shaking platform (note: tube was placed vertically).

For the free enzyme assay, commercially available hGalT was used (R&D biosystems). The reaction components were as specified by the manufacturer (0.75mg/mL hGalT,25mM Tris-HCl pH 7.5, 150mM NaCl, 10mM $MnCl_2$ and 10mM $MgCl_2$) with the exception that 0.16mM UDP-Gal and 16mM GlcNAc were used instead. Reaction was performed overnight at 37°C. After the end of the reactions, the immobilised enzyme was removed by centrifugation (5min, 5000xg). In samples where free enzyme was used, the reaction was ceased by treatment at 100°C for 5 min and heat denatured enzymes were removed by centrifugation (1min, 10000xg). The samples were then processed for MALDI-TOF MS (**Section 6.7.1**).

6.5.2. Sequential glycosylation reactions (specific to Chapter 3)

6.5.2.1. Reactions on artificial glycans

The activity assay of immobilised NtGnTI consisted of 0.5µM M5 glycan, 2.5mM UDP-GlcNAc, 100mM MES pH 6.5 and 1mM $MnCl_2$, at 25°C overnight on a shaking platform (note: tube was placed vertically). The immobilisation experiment (**Section 6.4**) was scaled up by a factor of 4 (i.e. 100µL SF and 200µL silica StV beads) After the end of the reactions, the immobilised enzyme was removed by centrifugation (5min, 5000xg). The supernatant was aliquoted and used for MALDI-TOF MS analysis and as a substrate for the reaction of DmManII.

The activity assay of immobilised DmManII consisted of 0.1mM $ZnSO_4$, 50mM MES, pH 5.6 and 0.4mM substrate from immobilised NtGnTI's reaction. Reaction was performed overnight at 37°C on a shaking platform (note: tube was placed vertically). After the end of the reactions, the immobilised enzyme was removed by centrifugation (5min, 5000xg). The supernatant was aliquoted and used for MALDI-TOF MS analysis and as a substrate for the reaction of DmManII.

The activity assay of immobilised hGalT consisted of 6mM UDP-Gal, 80mM Tris-HCl pH 9, 10mM $MnCL_2$ and 0.3mM substrate from immobilised DmManII's reaction. Where described, 1µl of the alkaline phosphatase FastAp (Thermofischer scientific) was added to remove inhibitory products. Immobilisation experiment was scaled by a factor of 4 (i.e. 100µL SF and 200µL silica StV beads). Reaction was performed overnight at 37°C on a shaking platform (note: tube was placed vertically). After the end of the reactions, the immobilised enzyme was removed by centrifugation (5min, 5000xg). The supernatant was aliquoted and used for MALDI-TOF MS analysis.

6.5.2.2. Reactions on mFc

The reaction conditions were the same as described in **section 6.5.2.1**. Instead of 0.5µM artificial glycans, 100µg of mFc were used. At the end of each reaction and after removing the immobilised enzymes, 20µg of mFc were removed and kept for MALDI-TOF MS analysis.

6.5.2.2.1. Reusability of NtGnTI

Following completion of the overnight reaction of immobilised NtGnTI and mFc, the immobilised enzyme was recovered by centrifugation (5min, 5000xg). The beads were resuspended in protein storage buffer (20mM Tris-HCl pH 7.5, 200mM NaCl and 5% glycerol) and recovered by centrifugation (5min, 5000xg). The washing step was performed 3 times in total. Finally, recovered beads were used for a new reaction set up as previously discussed (**Section 6.5.2.2**). At the end of the reaction and after removing the immobilised enzymes, 20µg of mFc were removed and kept for MALDI-TOF MS analysis.

6.6. Driving galactosylation with immobilised hGalT (specific to Chapter 4)

hGalT was immobilised on either silica StV beads (100µL SF and 200µL silica StV beads) or magnetic StV beads (i.e. 100µL SF and 40µL silica StV beads) (**Section 6.4**).

The antibodies used were a) purified chIgG (**Section 6.3.3.3**); b) IgG from human serum (Sigma-Aldrich, resuspended in deionised H2O and stored at 4°C); c) IgG from human serum (Sigma-Aldrich, resuspended in deionised H2O and stored at 4°C)

The reaction consisted of the following components: 110µg IgG (chIgG / hIgG / rIgG), 20mM $MnCl_2$, 20mM Tris-HCl pH 7.5, 6mM UDP-Gal. The reaction took place overnight at 37°C on a shaking platform (note: tube was placed vertically). After the end of the reactions, the immobilised enzyme was removed by centrifugation (5min, 5000xg). The supernatant was used for CE analysis (**Section 6.7.2**).

6.6.1.1. Reusability of immobilised hGalT

Following completion of the overnight reaction of immobilised hGalT and chIgG, the immobilised enzyme was recovered by centrifugation (5min, 5000xg). The beads were resuspended in protein storage buffer (20mM Tris-HCl pH 7.5, 200mM NaCl and 5% glycerol) and recovered by centrifugation (5min, 5000xg). The washing step was performed 3 times in total. Finally, recovered beads were used for a new reaction as described in **Section 6.6**. At the end of each reaction and

after removing the immobilised enzymes, the supernatant containing chIgG was removed and used for CE analysis (**Section 6.7.2**).

6.7. Glycan analysis

6.7.1. MALDI-TOF MS

6.7.1.1. Permethylation of glycans

Artificial glycans (pure or product of a reaction as described in **Section 6.5**) were lyophilised overnight. Permethylation was performed using a sodium hydroxide (NaOH) method[331]. Briefly, NaOH pellets were crushed to form a powder and mixed with dimethyl sulfoxide (DMSO) to form a slurry. A 1 mL aliquot of this slurry was added to the lyophilised glycans, followed by the addition of 500µL of methyl iodide (CH_3I). The mixture was vigorously mixed on an automatic shaker for 1hour at room temperature. The reaction was terminated by the addition of 2 mL of water. 1mL of chloroform was added to recover permethylated glycans. The chloroform layer was washed several times with Milli-Q water in order to remove impurities and was then dried under a gentle stream of nitrogen. Dried permethylated N-glycans were resuspended by adding 20µL of 100% MeOH and subsequently mixed with 3,4-diaminobenzophenone (DABP, Acros Organics) matrix in 1:3ratio (i.e. 0.5µL glycans and 1.5 µL matrix). The matrix-glycan mixture was spotted on a MALDI-TOF plate and dried at room temperature.

Instrument calibration and MALDI-TOF analysis was performed by Dr. Anja Krueger (Haslam lab) and Dr. Laura Bouché (Haslam lab). The analysis was performed in the reflector positive-ion mode using a 4800 MALDI-TOF/TOF (Applied Biosystems, Foster City, CA) mass spectrometer. MS spectra were assigned and annotated with the help of the GlycoWorkbench software[332].

6.7.1.2. Buffer exchange to remove excess salt

Where described (Chapter 3), a buffer exchange was performed to remove excess salt amount from artificial glycan reaction products. A cellulose acetate membrane (500Da, Sigma-Aldrich) and a biodialyzer (Sigma-Aldrich) were used for dialysis as described by the manufacturer. The dialysis buffer consisted of 50mM Ammonium Bicarbonate (AMBIC).

6.7.1.3. Sep-Pak purification

Where described (Chapter 3, section,) purification of glycans was performed using Sep C18 Sep-Pak® cartridges (Waters, USA). Briefly, the Sep-Pak cartridges were conditioned successively with

methanol, 5% acetic acid (aq., v/v), propan-1-ol, and 5% acetic acid. The sample was dissolved in 5% acetic acid, loaded onto the cartridge, and eluted successively with 5% acetic acid followed by 20%, 40%, 60% and 100% propan-1-ol in 5% acetic acid (v/v). The organic solvent was removed on a Savant Speed-Vac concentrator (ThermoFisher Scientific Inc.) and samples were lyophilized prior to permethylation (**Section 6.7.1.1**)

6.7.1.4. Analysis of mFc

The sample preparation, (i.e. glycan removal and glycan permethylation), and MALDI-TOF analysis of the mFc were performed by Mr. Roberto Donini (Haslam lab).

N- linked glycomics – The N-linked glycomic analysis is based on a previous protocol[333]. Briefly, N-glycans were released from 20 µg per sample of mFc using Rapid PNGase-F (NEB®). The glycans were separated from peptides using. Prior to MALDI-TOF MS analysis, the purified N-glycans were permethylated (**Section 6.7.1.1**). The MALDI-TOF MS data was acquired in the positive ion mode using a 4800 MALDI-TOF/TOF mass spectrometer (Applied Biosystems, USA). The structural assignments are based on previous knowledge of biosynthetic pathways after analysis with Data Explorer (Applied Biosystems) and GlycoWorkBench[332].

6.7.1.4.1. Mannosidase treatment for analysis of $Hex_9GlcNAc_2$

The mannosidase treatment of mFc to investigate the nature of $Hex_9GlcNAc_2$ was performed by Mr. Roberto Donini (Haslam Lab).

Briefly, 20 µg of mFc were treated with α-(1-2,3,6)-mannosidase from NEB® following the manufacturer's protocol. N-glycomics where then performed as described in **Section 6.7.1.4**.

6.7.2. Capillary electrophoresis (CE)

For CE, the C1000HT platform from SCIEX was used. IgGs were concentrated using Vivaspin® 500 ultracentrifugation spin columns 100 kDa.

The SCIEX C100HT Glycan Labeling and Analysis kit was used for sample preparations and the steps followed were as described by the manufacturer. Briefly, the protocol involved protein denaturation, enzymatic N-linked glycan release (using PNGase F, glycerol free, NEB®), fluorophore labelling (8-aminopyrene-1,3,6-trisulfonate, APTS) and excess dye removal with consecutive washing steps. All steps occurred at 60°C, in the presence of magnetic beads, to capture released glycans. Finally

labelled glycans were eluted from the beads and separated by CE with detection of LED-induced fluorescence.

Analysis of the capillary electrophoresis separation results to identify the type of glycans in the samples followed by review of the results was performed with the C100HT build-in DataReviewer software.

6.8. Statistical analysis

Any statistical analysis was performed using Excel and built-in functions. It consisted of calculation of averages, standard deviation (STDEV.P) and calculation of Pearson correlation coefficient.

Chapter 7: Bibliography

1. Zhong, X. & Somers, W. Recent Advances in Glycosylation Modifications in the Context of Therapeutic Glycoproteins. in *Integr. Proteomics.* 187–188 (InTech, 2012).

2. Solá, R. J. & Griebenow, K. Effects Of Glycosylation On The Stability Of Protein Pharmaceuticals. *J. Pharm. Sci.* **98**, 1223–45 (2009).

3. Varki, A. Biological Roles of Glycans. *Glycobiology* **27**, 3–49 (2017).

4. Walsh, G. Biopharmaceutical Benchmarks 2018. *Nat. Biotechnol.* **36**, 1136–1145 (2018).

5. Van Landuyt, L., Lonigro, C., Meuris, L. & Callewaert, N. Customized Protein Glycosylation to Improve Biopharmaceutical Function and Targeting. *Curr. Opin. Biotechnol.* **60**, 17–28 (2019).

6. Vong, K., Yamamoto, T. & Tanaka, K. Artificial Glycoproteins as a Scaffold for Targeted Drug Therapy. *Small* **16**, e1906890 (2020).

7. Wang, Z., Zhu, J. & Lu, H. Antibody Glycosylation: Impact on Antibody Drug Characteristics and Quality Control. *Appl. Microbiol. Biotechnol.* **104**, 1905–1914 (2020).

8. Batra, J. & Rathore, A. S. Glycosylation of Monoclonal Antibody Products: Current Status and Future Prospects. *Biotechnol. Prog.* **32**, 1091–1102 (2016).

9. Solá, R. J. & Griebenow, K. Glycosylation of Therapeutic Proteins: An Effective Strategy to Optimize Efficacy. *BioDrugs* **24**, 9–21 (2010).

10. Jefferis, R. Recombinant Antibody Therapeutics: The Impact of Glycosylation on Mechanisms of Action. *Trends Pharmacol. Sci.* **30**, 356–62 (2009).

11. Li, H. & D'Anjou, M. Pharmacological Significance of Glycosylation in Therapeutic Proteins. *Curr. Opin. Biotechnol.* **20**, 678–684 (2009).

12. Walsh, G. Biopharmaceutical Benchmarks 2014. *Nat. Biotechnol.* **32**, 992–1000 (2014).

13. Dowling, W. *et al.* Influences of Glycosylation on Antigenicity, Immunogenicity, and Protective Efficacy of Ebola Virus GP DNA Vaccines. *J. Virol.* **81**, 1821–1837 (2007).

14. Costantino, P., Rappuoli, R. & Berti, F. The Design of Semi-Synthetic and Synthetic Glycoconjugate Vaccines. *Expert Opin. Drug Discov.* **6**, 1045–1066 (2011).

15. Cipollo, J. F. & Parsons, L. M. Glycomics and Glycoproteomics of Viruses: Mass Spectrometry Applications and Insights Toward Structure–Function Relationships. *Mass Spectrom. Rev.* **39**, 371–409 (2020).

16. Bagdonaite, I. & Wandall, H. H. Global Aspects of Viral Glycosylation. *Glycobiology* **28**, 443–467 (2018).

17. Walsh, G. Biopharmaceutical benchmarks 2010. *Nat. Biotechnol.* **28**, 917–924 (2010).

18. Wang, L.-X. & Lomino, J. V. Emerging Technologies for Making Glycan-Defined Glycoproteins. *ACS Chem. Biol.* **7**, 110–22 (2012).

19. Sinclair, A. M. & Elliott, S. Glycoengineering: The Effect of Glycosylation on the Properties of Therapeutic Proteins. *J. Pharm. Sci.* **94**, 1626–1635 (2005).

20. Seeberger, P. H. The Logic of Automated Glycan Assembly. *Acc. Chem. Res.* **48**, 1450–1463 (2015).

21. Easton, R. Glycosylation of Proteins - Structure, Function and Analysis. *Life Sci. - Tech. Bull.* **1**, 1–5 (2011).

22. Lodish, H., Berk, A., Zipursky, S. & Al, E. Glycosylation in the ER and Golgi Complex. *Mol. Cell Biol.* section 17.7 (2000).

23. Rini, J., Esko, J. & Varki, A. A. A. Glycosyltransferases and Glycan-processing Enzymes. in *Essentials of Glycobiology* 1–7 (2009).

24. Young, N. M. *et al.* Structure of the N-linked glycan present on multiple glycoproteins in the Gram-negative bacterium, Campylobacter jejuni. *J. Biol. Chem.* **277**, 42530–9 (2002).

25. Varki, A. *et al. Essentials of Glycobiology*. *Essentials of Glycobiology* (Cold Spring Harbor Laboratory Press, 2009).

26. Breton, C., Šnajdrová, L., Jeanneau, C., Koča, J. & Imberty, A. Structures and Mechanisms of Glycosyltransferases. *Glycobiology* **16**, 29R-37R (2005).

27. Mestrom, L. *et al.* Leloir Glycosyltransferases in Applied Biocatalysis: A Multidisciplinary Approach. *Int. J. Mol. Sci.* **20**, 5263 (2019).

28. Kim, P. J., Lee, D. Y. & Jeong, H. Centralized Modularity of N-linked Glycosylation Pathways in Mammalian Cells. *PLoS One* **4**, (2009).

29. Bojarová, P., Rosencrantz, R. R., Elling, L. & Křen, V. Enzymatic Glycosylation of Multivalent Scaffolds. *Chem. Soc. Rev.* **42**, 4774–97 (2013).

30. Helenius, A. & Aebi, M. Roles of N-Linked Glycans in the Endoplasmic Reticulum. *Annu. Rev. Biochem.* **73**, 1019–1049 (2004).

31. Walsh, G. Post-translational modifications of protein biopharmaceuticals. *Drug Discov.Today* **15**, 773–780 (2010).

32. Ioannou, Y. A., Zeidner, K. M., Grace, M. E. & Desnick, R. J. Human Alpha-Galactosidase A: Glycosylation Site 3 is Essential for Enzyme Solubility. *Biochem. J.* **332 (Pt 3**, 789–97 (1998).

33. Beck, A. & Liu, H. Macro- and Micro-Heterogeneity of Natural and Recombinant IgG Antibodies. *Antibodies* **8**, 18 (2019).

34. Dalziel, M., Crispin, M., Scanlan, C. N., Zitzmann, N. & Dwek, R. A. Emerging Principles for the Therapeutic Exploitation of Glycosylation. *Science (80-.).* **343**, 1235681–1235681 (2014).

35. Cao, L. *et al.* Global Site-Specific N-glycosylation Analysis of HIV Envelope Glycoprotein. *Nat. Commun.* **8**, 14954 (2017).

36. Daniels, C. C., Rogers, P. D. & Shelton, C. M. A Review of Pneumococcal Vaccines: Current Polysaccharide Vaccine Recommendations and Future Protein Antigens. *J. Pediatr.*

Pharmacol. Ther. **21**, 27–35 (2016).

37. Seabright, G. E., Doores, K. J., Burton, D. R. & Crispin, M. Protein and Glycan Mimicry in HIV Vaccine Design. *J. Mol. Biol.* **431**, 2223–2247 (2019).

38. Kumar, R., Qureshi, H., Deshpande, S. & Bhattacharya, J. Broadly Neutralizing Antibodies in HIV-1 Treatment and Prevention. *Ther. Adv. Vaccines Immunother.* **6**, 61–68 (2018).

39. Amin, M. N. *et al.* Synthetic Glycopeptides Reveal the Glycan Specificity of HIV-Neutralizing Antibodies. *Nat. Chem. Biol.* **9**, 521–526 (2013).

40. Horiya, S., MacPherson, I. S. & Krauss, I. J. Recent Strategies Targeting HIV Glycans in Vaccine Design. *Nat. Chem. Biol.* **10**, 990–999 (2014).

41. Kim, B.-M., Kim, H., Raines, R. T. & Lee, Y. Glycosylation of Onconase Increases its Conformational Stability and Toxicity for Cancer Cells. *Biochem. Biophys. Res. Commun.* **315**, 976–983 (2004).

42. Jefferis, R. Variable Domain-Linked Oligosaccharides of a Human Monoclonal IgG: Structure and Influence on Antigen Binding. *Nat. Rev. Drug Discov.* **8**, 226–34 (2009).

43. van de Bovenkamp, F. S., Hafkenscheid, L., Rispens, T. & Rombouts, Y. The Emerging Importance of IgG Fab Glycosylation in Immunity. *J. Immunol.* **196**, (2016).

44. Leibiger, H., Wustner, D., Stigler, R.-D. & Marx, U. Variable Domain-Linked Oligosaccharides of a Human Monoclonal IgG: Structure and Influence on Antigen Binding. *Biochem. J.* **338**, 529 (1999).

45. Courtois, F., Agrawal, N. J., Lauer, T. M. & Trout, B. L. Rational Design of Therapeutic mAbs Against Aggregation Through Protein Engineering and Incorporation of Glycosylation Motifs Applied to Bevacizumab. *MAbs* **8**, 99–112 (2016).

46. Jacquemin, M. *et al.* Variable Region Heavy Chain Glycosylation Determines the Anticoagulant Activity of a Factor VIII Antibody. *J. Thromb. Haemost.* **4**, 1047–1055 (2006).

47. Goletz, S., Danielczyk, A. & Stoeckl, L. FAB-GLYCOSYLATED ANTIBODIES. (2012).

48. Zheng, K., Bantog, C. & Bayer, R. The Impact of Glycosylation on Monoclonal Antibody Conformation and Stability. *MAbs* **3**, 568–76 (2011).

49. Wright, A. & Morrison, S. L. Effect of C2-Associated Carbohydrate Structure on Ig Effector Function: Studies with Chimeric Mouse-Human IgG1 Antibodies in Glycosylation Mutants of Chinese Hamster Ovary Cells. *J. Immunol.* **160**, 3393–402 (1998).

50. Scallon, B. J., Tam, S. H., McCarthy, S. G., Cai, A. N. & Raju, T. S. Higher Levels of Sialylated Fc Glycans in Immunoglobulin G Molecules can Adversely Impact Functionality. *Mol. Immunol.* **44**, 1524–1534 (2007).

51. Shinkawa, T. *et al.* The Absence of Fucose but Not the Presence of Galactose or Bisecting N-acetylglucosamine of Human IgG1 Complex-Type Oligosaccharides Shows the Critical Role of Enhancing Antibody-Dependent Cellular Cytotoxicity. *J. Biol. Chem.* **278**, 3466–73 (2003).

52. Thomann, M., Reckermann, K., Reusch, D., Prasser, J. & Tejada, M. L. Fc-Galactosylation

Modulates Antibody-Dependent Cellular Cytotoxicity of Therapeutic Antibodies. *Mol. Immunol.* **73**, 69–75 (2016).

53. Li, T. *et al.* Modulating IgG Effector Function by Fc Glycan Engineering. *Proc. Natl. Acad. Sci.* **114**, 3485–3490 (2017).

54. Kelly, R. M. *et al.* Modulation of IgG1 Immunoeffector Function by Glycoengineering of the GDP-Fucose Biosynthesis Pathway. *Biotechnol. Bioeng.* **115**, 705–718 (2018).

55. Washburn, N. *et al.* Controlled Tetra-Fc Sialylation of IVIg Results in a Drug Candidate with Consistent Enhanced anti-Inflammatory Activity. *Proc. Natl. Acad. Sci. U. S. A.* **112**, E1297–E1306 (2015).

56. Lübbers, J., Rodríguez, E. & van Kooyk, Y. Modulation of Immune Tolerance via Siglec-Sialic Acid Interactions. *Front. Immunol.* **9**, (2018).

57. Bas, M. *et al.* Fc Sialylation Prolongs Serum Half-Life of Therapeutic Antibodies. *J. Immunol.* **202**, 1582–1594 (2019).

58. Byrne, B., Donohoe, G. G. & O'Kennedy, R. Sialic Acids: Carbohydrate Moieties that Influence the Biological and Physical Properties of Biopharmaceutical Proteins and Living Cells. *Drug Discov. Today* **12**, 319–326 (2007).

59. Yu, M. *et al.* Production, Characterization and Pharmacokinetic Properties of Antibodies with N-linked Mannose-5 Glycans. *MAbs* **4**, 475–487 (2012).

60. Kuriakose, A., Chirmule, N. & Nair, P. Immunogenicity of Biotherapeutics: Causes and Association with Posttranslational Modifications. *J. Immunol. Res.* **2016**, 1–18 (2016).

61. Joshi, L. The Market For Glycoprotein Drugs. **22**, 1513–1519 (2004).

62. Chung, C. H. *et al.* Cetuximab-Induced Anaphylaxis and IgE Specific for Galactose-α-1,3-Galactose. *N. Engl. J. Med.* **358**, 1109–1117 (2008).

63. Chung, A. W. *et al.* Identification of Antibody Glycosylation Structures that Predict Monoclonal Antibody Fc-Effector Function. *AIDS* **28**, 2523–2530 (2014).

64. Peschke, B., Keller, C. W., Weber, P., Quast, I. & Lünemann, J. D. Fc-Galactosylation of Human Immunoglobulin Gamma Isotypes Improves C1q Binding and Enhances Complement-Dependent Cytotoxicity. *Front. Immunol.* **8**, (2017).

65. Nimmerjahn, F., Anthony, R. M. & Ravetch, J. V. Agalactosylated IgG antibodies depend on cellular Fc receptors for in vivo activity. *Proc. Natl. Acad. Sci.* **104**, 8433–8437 (2007).

66. Dashivets, T. *et al.* Multi-Angle Effector Function Analysis of Human Monoclonal IgG Glycovariants. *PLoS One* **10**, e0143520 (2015).

67. Karsten, C. M. *et al.* Anti-Inflammatory Activity of IgG1 Mediated by Fc Galactosylation and Association of FcγRIIB and Dectin-1. *Nat. Med.* **18**, 1401–1406 (2012).

68. Chung, C. *et al.* Integrated Genome and Protein Editing Swaps α -2,6 Sialylation for α -2,3 Sialic Acid on Recombinant Antibodies from CHO. *Biotechnol. J.* **12**, 1600502 (2017).

69. Jones, A. J. S. *et al.* Selective Clearance of Glycoforms of a Complex Glycoprotein Pharmaceutical Caused by Terminal N-Acetylglucosamine is Similar in Humans and Cynomolgus Monkeys. *Glycobiology* **17**, 529–540 (2007).

70. Liu, L. Antibody Glycosylation and Its Impact on the Pharmacokinetics and Pharmacodynamics of Monoclonal Antibodies and Fc-Fusion Proteins. *J. Pharm. Sci.* **104**, 1866–1884 (2015).

71. Jefferis, R. Glycosylation of Recombinant Antibody Therapeutics. *Biotechnol. Prog.* **21**, 11–16 (2008).

72. Scott, A. M., Allison, J. P. & Wolchok, J. D. Monoclonal Antibodies in Cancer therapy. *Cancer Immun.* **12**, 14 (2012).

73. Khozin, S. Personalized Medicine: On the Brink of Revolutionizing Cancer Care. (2015).

74. Zhang, P. *et al.* Challenges of Glycosylation Analysis and Control: an Integrated Approach to Producing Optimal and Consistent Therapeutic Drugs. *Drug Discov. Today* **21**, 740–765 (2016).

75. Jimenez del Val, I., Nagy, J. M. & Kontoravdi, C. A Dynamic Mathematical Model for Monoclonal Antibody N-linked Glycosylation and Nucleotide Sugar Donor Transport within a Maturing Golgi Apparatus. *Biotechnol. Prog.* **27**, 1730–1743 (2011).

76. Kontoravdi, C. & Jimenez del Val, I. Computational Tools for Predicting and Controlling the Glycosylation of Biopharmaceuticals. *Curr. Opin. Chem. Eng.* **22**, 89–97 (2018).

77. Manabe, S. *et al.* Characterization of Antibody Products Obtained through Enzymatic and Nonenzymatic Glycosylation Reactions with a Glycan Oxazoline and Preparation of a Homogeneous Antibody–Drug Conjugate via Fc N -Glycan. *Bioconjug. Chem.* **30**, 1343–1355 (2019).

78. Lu, R.-M. *et al.* Development of Therapeutic Antibodies for the Treatment of Diseases. *J. Biomed. Sci.* **27**, 1 (2020).

79. Mastrangeli, R., Palinsky, W. & Bierau, H. Glycoengineered Antibodies: Towards the Next-Generation of Immunotherapeutics. *Glycobiology* **29**, 199–210 (2018).

80. Zong, H. *et al.* Producing Defucosylated Antibodies with Enhanced In Vitro Antibody-Dependent Cellular Cytotoxicity via FUT8 Knockout CHO-S Cells. *Eng. Life Sci.* **17**, 801–808 (2017).

81. Fan, Y. *et al.* Amino Acid and Glucose Metabolism in Fed-Batch CHO Cell Culture Affects Antibody Production and Glycosylation. *Biotechnol. Bioeng.* **112**, 521–535 (2015).

82. Wong, N. S. C. *et al.* An Investigation of Intracellular Glycosylation Activities in CHO Cells: Effects of Nucleotide Sugar Precursor Feeding. *Biotechnol. Bioeng.* **107**, 321–336 (2010).

83. Dumont, J., Euwart, D., Mei, B., Estes, S. & Kshirsagar, R. Human Cell Lines for Biopharmaceutical Manufacturing: History, Status, and Future Perspectives. *Crit. Rev. Biotechnol.* **36**, 1110–1122 (2016).

84. Beck, A. & Reichert, J. M. Marketing Approval of Mogamulizumab. *MAbs* **4**, 419–425 (2012).

85. Goh, J. B. & Ng, S. K. Impact of Host Cell Line Choice on Glycan Profile. *Crit. Rev. Biotechnol.* **38**, 851–867 (2018).

86. Ren, W.-W. *et al.* Glycoengineering of HEK293 Cells to Produce High-Mannose-Type N-glycan Structures. *J. Biochem.* **166**, 245–258 (2019).

87. Steentoft, C., Bennett, E. P. & Clausen, H. Glycoengineering of Human Cell Lines using Zinc Finger Nuclease Gene Targeting: SimpleCells with Homogeneous GalNAc O-Glycosylation Allow Isolation of the O-glycoproteome by One-Step Lectin Affinity Chromatography. *Methods Mol. Biol.* **1022**, 387–402 (2013).

88. Meuris, L. *et al.* GlycoDelete Engineering of Mammalian Cells Simplifies N-glycosylation of Recombinant Proteins. *Nat. Biotechnol.* **32**, 485–9 (2014).

89. Goehring, A. *et al.* Screening and Large-Scale Expression of Membrane Proteins in Mammalian Cells for Structural Studies. *Nat. Protoc.* **9**, 2574–2585 (2014).

90. Kato, K. *et al.* Expression, Purification, Crystallization and Preliminary X-ray Crystallographic Analysis of Enpp1. *Acta Crystallogr. Sect. F Struct. Biol. Cryst. Commun.* **68**, 778–782 (2012).

91. Croset, A. *et al.* Differences in the Glycosylation of Recombinant Proteins Expressed in HEK and CHO Cells. *J. Biotechnol.* **161**, 336–348 (2012).

92. Sanchez-Garcia, L. *et al.* Recombinant Pharmaceuticals from Microbial Cells: a 2015 update. *Microb. Cell Fact.* **15**, 33 (2016).

93. Matsushita, T. Engineered Therapeutic Antibodies with Enhanced Effector Functions: Clinical Application of the Potelligent® Technology. *Korean J. Hematol.* **46**, 148 (2011).

94. Ferrara, C. *et al.* Modulation of Therapeutic Antibody Effector Functions by Glycosylation Engineering: Influence of Golgi Enzyme Localization Domain and co-Expression of Heterologous β1, 4-N-Acetylglucosaminyltransferase III and Golgi α-Mannosidase II. *Biotechnol. Bioeng.* **93**, 851–861 (2006).

95. Chang, M. M. *et al.* Small-Molecule Control of Antibody N-Glycosylation in Engineered Mammalian Cells. *Nat. Chem. Biol.* **15**, 730–736 (2019).

96. Byrne, G. *et al.* CRISPR/Cas9 Gene Editing for the Creation of an MGAT1-Deficient CHO Cell Line to Control HIV-1 Vaccine Glycosylation. *PLOS Biol.* **16**, e2005817 (2018).

97. Wong, N. S. C., Yap, M. G. S. & Wang, D. I. C. Enhancing Recombinant Glycoprotein Sialylation Through CMP-Sialic Acid Transporter over Expression in Chinese Hamster Ovary Cells. *Biotechnol. Bioeng.* **93**, 1005–1016 (2006).

98. Vogl, T., Hartner, F. S. & Glieder, A. New Opportunities by Synthetic Biology for Biopharmaceutical Production in Pichia pastoris. *Curr. Opin. Biotechnol.* **24**, 1094–101 (2013).

99. North, S. J. *et al.* Glycomics Profiling of Chinese Hamster Ovary Cell Glycosylation Mutants Reveals N-glycans of a Novel Size and Complexity. *J. Biol. Chem.* **285**, 5759–5775 (2010).

100. Spadiut, O., Capone, S., Krainer, F., Glieder, A. & Herwig, C. Microbials for the Production of Monoclonal Antibodies and Antibody Fragments. *Trends Biotechnol.* **32**, 54–60 (2014).

101. Lao, M.-S. & Toth, D. Effects of Ammonium and Lactate on Growth and Metabolism of a Recombinant Chinese Hamster Ovary Cell Culture. *Biotechnol. Prog.* **13**, 688–691 (1997).

102. Bertolini, L. R. *et al.* The Transgenic Animal Platform for Biopharmaceutical Production. *Transgenic Res.* **25**, 329–343 (2016).

103. Chen, W. C. & Murawsky, C. M. Strategies for Generating Diverse Antibody Repertoires Using Transgenic Animals Expressing Human Antibodies. *Front. Immunol.* **9**, 460 (2018).

104. Brüggemann, M., Osborn, M. J., Ma, B. & Buelow, R. Strategies to Obtain Diverse and Specific Human Monoclonal Antibodies From Transgenic Animals. *Transplantation* **101**, 1770–1776 (2017).

105. Osborn, M. J. *et al.* High-Affinity IgG Antibodies Develop Naturally in Ig-Knockout Rats Carrying Germline Human IgH/Igκ/Igλ Loci Bearing the Rat C H Region. *J. Immunol.* **190**, 1481–1490 (2013).

106. Jakobovits, A., Amado, R. G., Yang, X., Roskos, L. & Schwab, G. From XenoMouse Technology to Panitumumab, the First Fully Human Antibody Product from Transgenic Mice. *Nat. Biotechnol.* **25**, 1134–1143 (2007).

107. Balen, B. & Krsnik-Rasol, M. N-Glycosylation of Recombinant Therapeutic Glycoproteins in Plant Systems. *Food Technol. Biotechnol.* **45**, 1–10 (2007).

108. Maksimenko, O. G., Deykin, A. V, Khodarovich, Y. M. & Georgiev, P. G. Use of Transgenic Animals in Biotechnology: Prospects and Problems. *Acta Naturae* **5**, 33–46 (2013).

109. Laukens, B., De Wachter, C. & Callewaert, N. Engineering the Pichia pastoris N-Glycosylation Pathway Using the GlycoSwitch Technology. in *Methods in molecular biology (Clifton, N.J.)* **1321**, 103–122 (2015).

110. Jacobs, P. P., Geysens, S., Vervecken, W., Contreras, R. & Callewaert, N. Engineering complex-type N-glycosylation in Pichia pastoris using GlycoSwitch technology. *Nat. Protoc.* **4**, 58–70 (2009).

111. Tang, H. *et al.* N-hypermannose Glycosylation Disruption Enhances Recombinant Protein Production by Regulating Secretory Pathway and Cell Wall Integrity in Saccharomyces cerevisiae. *Sci. Rep.* **6**, 25654 (2016).

112. Vervecken, W. *et al.* In Vivo Synthesis of Mammalian-Like, Hybrid-Type N-Glycans in Pichia pastoris. *Appl. Environ. Microbiol.* **70**, 2639–2646 (2004).

113. Arico, C., Bonnet, C. & Javaud, C. N-Glycosylation Humanization for Production of Therapeutic Recombinant Glycoproteins in Saccharomyces cerevisiae. *Methods Mol. Biol.* 45–57 (2013).

114. Ahmad, M., Hirz, M., Pichler, H. & Schwab, H. Protein Expression in Pichia pastoris: Recent Achievements and Perspectives for Heterologous Protein Production. *Appl. Microbiol. Biotechnol.* **98**, 5301–5317 (2014).

115. Hamilton, S. R. *et al.* Production of Complex Human Glycoproteins in Yeast. *Science (80-.).* **301**, 1244–6 (2003).

116. Li, H. *et al.* Optimization of Humanized IgGs in Glycoengineered Pichia pastoris. *Nat.*

Biotechnol. **24**, 210–5 (2006).

117. Hamilton, S. R. *et al.* Humanization of Yeast to Produce Complex Terminally Sialylated Glycoproteins. *Science (80-.).* **313**, 1441–1443 (2006).

118. Laukens, B. *et al.* Off-Target Glycans Encountered along the Synthetic Biology Route Toward Humanized N -glycans in Pichia pastoris. *Biotechnol. Bioeng.* **117**, 2479–2488 (2020).

119. Senchenkova, S. N. *et al.* Structure and genetics of the O-antigens of Escherichia coli O182–O187. *Carbohydr. Res.* **435**, 58–67 (2016).

120. Yates, L. E., Mills, D. C. & DeLisa, M. P. Bacterial Glycoengineering as a Biosynthetic Route to Customized Glycomolecules. *Adv. Biochem. Eng. Biotechnol.* (2018).

121. Harding, C. M. & Feldman, M. F. Glycoengineering Bioconjugate Vaccines, Therapeutics, and Diagnostics in E. coli. *Glycobiology* **29**, 519–529 (2019).

122. Wacker, M. *et al.* Substrate Specificity of Bacterial Oligosaccharyltransferase Suggests a Common Transfer Mechanism for The Bacterial and Eukaryotic Systems. *Proc. Natl. Acad. Sci.* **103**, 7088–7093 (2006).

123. Szymanski, C. M. M. *et al.* Evidence for a System of General Protein Glycosylation in Campylobacter jejuni. *Mol. Microbiol.* **32**, 1022–1030 (1999).

124. Thibault, P. *et al.* Identification of the Carbohydrate Moieties and Glycosylation Motifs in Campylobacter jejuni Flagellin. *J. Biol. Chem.* **276**, 34862–34870 (2001).

125. Wacker, M. *et al.* N-Linked Glycosylation in Campylobacter jejuni and Its Functional Transfer into E. coli. *Science (80-.).* **298**, (2002).

126. Valderrama-Rincon, J. D. D. *et al.* An engineered eukaryotic protein glycosylation pathway in Escherichia coli. *Nat. Chem. Biol.* **8**, 434–436 (2012).

127. Cortina, M. E. *et al.* A Bacterial Glycoengineered Antigen for Improved Serodiagnosis of Porcine Brucellosis. *J. Clin. Microbiol.* **54**, 1448–1455 (2016).

128. Huttner, A. *et al.* Safety, Immunogenicity, and Preliminary Clinical Efficacy of a Vaccine against Extraintestinal Pathogenic Escherichia coli in Women with a History of Recurrent Urinary Tract Infection: a Randomised, Single-Blind, Placebo-controlled phase 1b trial. *Lancet Infect. Dis.* **17**, 528–537 (2017).

129. Hatz, C. F. R. *et al.* Safety and Immunogenicity of a Candidate Bioconjugate Vaccine Against Shigella Dysenteriae type 1 Administered to Healthy Adults: A Single Blind, Partially Randomized Phase I Study. *Vaccine* **33**, 4594–4601 (2015).

130. Kowarik, M. *et al.* Definition of the Bacterial N-Glycosylation Site Consensus Sequence. *EMBO J.* **25**, 1957–1966 (2006).

131. Yavuz, E., Maffioli, C., Ilg, K., Aebi, M. & Priem, B. Glycomimicry: Display of Fucosylation on the Lipo-Oligosaccharide of Recombinant Escherichia coli K12. *Glycoconj. J.* **28**, 39–47 (2011).

132. Ollis, A. A. *et al.* Substitute Sweeteners: Diverse Bacterial Oligosaccharyltransferases with Unique N-glycosylation Site Preferences. *Sci. Rep.* **5**, 15237 (2015).

133. Lin, L. *et al.* Sequential Glycosylation of Proteins with Substrate-Specific N - Glycosyltransferases. *ACS Cent. Sci.* **6**, 144–154 (2020).

134. Strutton, B. *et al.* Engineering Pathways in Central Carbon Metabolism Help to Increase Glycan Production and Improve N-Type Glycosylation of Recombinant Proteins in E. coli. *Bioengineering* **6**, 27 (2019).

135. Ferrer-Miralles, N., Domingo-Espín, J., Corchero, J., Vázquez, E. & Villaverde, A. Microbial Factories for Recombinant Pharmaceuticals. *Microb. Cell Fact.* **8**, 17 (2009).

136. Montero-Morales, L. & Steinkellner, H. Advanced Plant-Based Glycan Engineering. *Front. Bioeng. Biotechnol.* **6**, (2018).

137. Steinkellner, H. & Castilho, A. N-Glyco-Engineering in Plants: Update on Strategies and Major Achievements. *Methods Mol. Biol.* **1321**, 195–212 (2015).

138. Gasdaska, J. R., Sherwood, S., Regan, J. T. & Dickey, L. F. An Afucosylated anti-CD20 monoclonal Antibody with Greater Antibody-Dependent Cellular Cytotoxicity and B-Cell Depletion and Lower Complement-Dependent Cytotoxicity than Rituximab. *Mol. Immunol.* **50**, 134–141 (2012).

139. Qiu, X. *et al.* Reversion of Advanced Ebola Virus Disease in Non Human Primates with ZMapp. *Nature* **514**, 47–53 (2014).

140. Chen, Q. & Davis, K. R. The Potential of Plants as a System for the Development and Production of Human Biologics. *F1000Research* **5**, 912 (2016).

141. Dicker, M. & Strasser, R. Using Glyco-Engineering to Produce Therapeutic Proteins. *Expert Opin. Biol. Ther.* **2598**, 1–16 (2015).

142. Diamos, A. G. *et al.* Vaccine Synergy with Virus-Like Particle and Immune Complex Platforms for Delivery of Human Papillomavirus L2 Antigen. *Vaccine* **37**, 137–144 (2019).

143. Castilho, A. *et al.* In Planta Protein Sialylation through Overexpression of the Respective Mammalian Pathway. *J. Biol. Chem.* **285**, 15923–15930 (2010).

144. Burnett, M. J. B. & Burnett, A. C. Therapeutic Recombinant Protein Production in Plants: Challenges and Opportunities. *PLANTS, PEOPLE, PLANET* **2**, 121–132 (2020).

145. Khan, A. H., Bayat, H., Rajabibazl, M., Sabri, S. & Rahimpour, A. Humanizing Glycosylation Pathways in Eukaryotic Expression Systems. *World J. Microbiol. Biotechnol.* **33**, 4 (2017).

146. Amann, T., Schmieder, V., Faustrup Kildegaard, H., Borth, N. & Andersen, M. R. Genetic Engineering Approaches to Improve Posttranslational Modification of Biopharmaceuticals in Different Production Platforms. *Biotechnol. Bioeng.* **116**, 2778–2796 (2019).

147. Kato, T. *et al.* N-Glycan Modification of a Recombinant Protein via Coexpression of Human Glycosyltransferases in Silkworm Pupae. *Sci. Rep.* **7**, 1409 (2017).

148. Hollister, J., Grabenhorst, E., Nimtz, M., Conradt, H. & Jarvis, D. L. Engineering the Protein N-Glycosylation Pathway in Insect Cells for Production of Biantennary, Complex N-Glycans †. *Biochemistry* **41**, 15093–15104 (2002).

149. Geisler, C. & Jarvis, D. L. Innovative Use of a Bacterial Enzyme Involved in Sialic Acid Degradation to Initiate Sialic Acid Biosynthesis in Glycoengineered Insect Cells. *Metab. Eng.* **14**, 642–652 (2012).

150. Mabashi-Asazuma, H., Kuo, C.-W., Khoo, K.-H. & Jarvis, D. L. A novel Baculovirus Vector for the Production of Nonfucosylated Recombinant Glycoproteins in Insect Cells. *Glycobiology* **24**, 325–340 (2014).

151. Geisler, C., Mabashi-Asazuma, H. & Jarvis, D. L. An Overview and History of Glyco-Engineering in Insect Expression Systems. *Methods Mol. Biol. Mol. Biol.* **1321**, 131–52 (2015).

152. Li, C. & Wang, L.-X. Chemoenzymatic Methods for the Synthesis of Glycoproteins. *Chem. Rev.* **118**, 8359–8413 (2018).

153. Overkleeft, H. S. & Seeberger, P. H. *Chemoenzymatic Synthesis of Glycans and Glycoconjugates*. *Essentials of Glycobiology* (Cold Spring Harbor Laboratory Press, 2015). doi:10.1101/GLYCOBIOLOGY.3E.054

154. Wang, L.-X. & Amin, M. N. Chemical and Chemoenzymatic Synthesis of Glycoproteins for Deciphering Functions. *Chem. Biol.* **21**, 51–66 (2014).

155. Tang, F., Wang, L.-X. & Huang, W. Chemoenzymatic Synthesis of Glycoengineered IgG Antibodies and Glycosite-Specific Antibody–Drug Conjugates. *Nat. Protoc.* **12**, 1702–1721 (2017).

156. Giddens, J. P. & Wang, L.-X. Chemoenzymatic Glyco-engineering of Monoclonal Antibodies. in *Methods in Molecular Biology* 375–387 (2015). doi:10.1007/978-1-4939-2760-9_25

157. Liu, C.-P. *et al.* Glycoengineering of Antibody (Herceptin) through Yeast Expression and In Vitro Enzymatic Glycosylation. *Proc. Natl. Acad. Sci.* **115**, 720–725 (2018).

158. Huang, W., Giddens, J., Fan, S.-Q., Toonstra, C. & Wang, L.-X. Chemoenzymatic Glycoengineering of Intact IgG Antibodies for Gain of Functions. *J. Am. Chem. Soc.* **134**, 12308–12318 (2012).

159. Giddens, J. P., Lomino, J. V., DiLillo, D. J., Ravetch, J. V. & Wang, L.-X. Site-Selective Chemoenzymatic Glycoengineering of Fab and Fc Glycans of a Therapeutic Antibody. *Proc. Natl. Acad. Sci.* **115**, 12023–12027 (2018).

160. Tang, F. *et al.* One-pot N-glycosylation Remodeling of IgG with Non-Natural Sialylglycopeptides Enables Glycosite-Specific and Dual-payload Antibody–Drug Conjugates. *Org. Biomol. Chem.* **14**, 9501–9518 (2016).

161. Li, X., Fang, T. & Boons, G. Preparation of Well-Defined Antibody–Drug Conjugates through Glycan Remodeling and Strain-Promoted Azide–Alkyne Cycloadditions. *Angew. Chemie Int. Ed.* **53**, 7179–7182 (2014).

162. Schwarz, F. *et al.* A Combined Method for Producing Homogeneous Glycoproteins with Eukaryotic N-Glycosylation. *Nat. Chem. Biol.* **6**, 264–266 (2010).

163. Wei, Y. *et al.* Glycoengineering of Human IgG1-Fc through Combined Yeast Expression and In Vitro Chemoenzymatic Glycosylation. *Biochemistry* **47**, 10294–10304 (2008).

164. Liu, L. *et al.* Streamlining the Chemoenzymatic Synthesis of Complex N-glycans by a Stop and Go Strategy. *Nat. Chem.* **11**, 161–169 (2019).

165. Rising, T. W. D. F. *et al.* Synthesis of N-Glycan Oxazolines: Donors for Endohexosaminidase Catalysed Glycosylation. *Carbohydr. Res.* **341**, 1574–1596 (2006).

166. Murakami, M. *et al.* Chemical Synthesis of Erythropoietin Glycoforms for Insights Into the Relationship Between Glycosylation Pattern and Bioactivity. *Sci. Adv.* **2**, e1500678 (2016).

167. Thomann, M. *et al.* In vitro glycoengineering of IgG1 and its effect on Fc receptor binding and ADCC activity. *PLoS One* **10**, (2015).

168. Brühlmann, D. *et al.* Generation of Site-Distinct N-Glycan Variants for In Vitro BioactivityTesting. *Biotechnol. Bioeng.* **116**, 1017–1028 (2019).

169. Warnock, D. *et al.* In Vitro Galactosylation of Human IgG at 1 kg Scale Using Recombinant Galactosyltransferase. *Biotechnol. Bioeng.* **92**, 831–842 (2005).

170. Tayi, V. S. & Butler, M. Solid-Phase Enzymatic Remodeling Produces High Yields of Single Glycoform Antibodies. *Biotechnol. J.* **13**, 1700381 (2018).

171. Li, C., Li, T. & Wang, L.-X. Chemoenzymatic Defucosylation of Therapeutic Antibodies for Enhanced Effector Functions Using Bacterial α-Fucosidases. *Methods Mol. Biol.* **1827**, 367–380 (2018).

172. Hamilton, B. S. *et al.* A Library of Chemically Defined Human N-Glycans Synthesized from Microbial Oligosaccharide Precursors. *Sci. Rep.* **7**, (2017).

173. Gurramkonda, C. *et al.* Improving the Recombinant Human Erythropoietin Glycosylation Using Microsome Supplementation in CHO Cell-Free System. *Biotechnol. Bioeng.* **115**, 1253–1264 (2018).

174. Guarino, C. & DeLisa, M. P. A Prokaryote-Based Cell-Free Translation System that Efficiently Synthesizes Glycoproteins. *Glycobiology* **22**, 596–601 (2012).

175. Jaroentomeechai, T. *et al.* Single-Pot Glycoprotein Biosynthesis Using a Cell-Free Transcription-Translation System Enriched with Glycosylation Machinery. *Nat. Commun.* **9**, 2686 (2018).

176. Kightlinger, W. *et al.* A Cell-Free Biosynthesis Platform for Modular Construction of Protein Glycosylation Pathway. *Nat. Commun.* **10**, 5404 (2019).

177. Liu, H., Nowak, C., Shao, M., Ponniah, G. & Neill, A. Impact of Cell Culture on Recombinant Monoclonal Antibody Product Heterogeneity. *Biotechnol. Prog.* **32**, 1103–1112 (2016).

178. Brühlmann, D. *et al.* Tailoring Recombinant Protein Quality by Rational Media Design. *Biotechnol. Prog.* **31**, 615–629 (2015).

179. Hossler, P., Khattak, S. F. & Li, Z. J. Optimal and Consistent Protein Glycosylation in Mammalian Cell Culture. *Glycobiology* **19**, 936–949 (2009).

180. Shi, H. H. & Goudar, C. T. Recent Advances in the Understanding of Biological Implications and Modulation Methodologies of Monoclonal Antibody N-linked High Mannose Glycans.

Biotechnol. Bioeng. **111**, 1907–1919 (2014).

181. Gramer, M. J. *et al.* Modulation of Antibody Galactosylation through Feeding of Uridine, Manganese Chloride, and Galactose. *Biotechnol. Bioeng.* **108**, 1591–1602 (2011).

182. Kotidis, P. *et al.* Model-Based Optimization of Antibody Galactosylation in CHO Cell Culture. *Biotechnol. Bioeng.* **116**, 1612–1626 (2019).

183. Gu, X. & Wang, D. I. C. Improvement of Interferon-γ Sialylation in Chinese Hamster Ovary Cell Culture by Feeding of N-Acetylmannosamine. *Biotechnol. Bioeng.* **58**, 642–648 (1998).

184. Rillahan, C. D. *et al.* Global Metabolic Inhibitors of Sialyl- and Fucosyltransferases Remodel the Glycome. *Nat. Chem. Biol.* **8**, 661–668 (2012).

185. Buettner, M. J., Shah, S. R., Saeui, C. T., Ariss, R. & Yarema, K. J. Improving Immunotherapy Through Glycodesign. *Front. Immunol.* **9**, (2018).

186. Qiu, L. *et al.* Combining Synthetic Carbohydrate Vaccines with Cancer Cell Glycoengineering for Effective Cancer Immunotherapy. *Cancer Immunol. Immunother.* **61**, 2045–2054 (2012).

187. Sou, S. N. *et al.* How Does Mild Hypothermia Affect Monoclonal Antibody Glycosylation? *Biotechnol. Bioeng.* **112**, 1165–1176 (2015).

188. Jedrzejewski, P. *et al.* Towards Controlling the Glycoform: A Model Framework Linking Extracellular Metabolites to Antibody Glycosylation. *Int. J. Mol. Sci.* **15**, 4492–4522 (2014).

189. Sou, S. N. *et al.* Model-Based Investigation of Intracellular Processes Determining Antibody Fc-Glycosylation Under Mild Hypothermia. *Biotechnol. Bioeng.* **114**, 1570–1582 (2017).

190. Grainger, R. K. & James, D. C. CHO Cell Line Specific Prediction and Control of Recombinant Monoclonal Antibody N -Glycosylation. *Biotechnol. Bioeng.* **110**, 2970–2983 (2013).

191. Spahn, P. N. *et al.* A Markov Chain Model for N-Linked Protein Glycosylation – Towards a Low-Parameter Tool for Model-Driven Glycoengineering. *Metab. Eng.* **33**, 52–66 (2016).

192. Liang, C. *et al.* A Markov Model of Glycosylation Elucidates Isozyme Specificity and Glycosyltransferase Interactions for Glycoengineering. *Curr. Res. Biotechnol.* **2**, 22–36 (2020).

193. Spahn, P. N., Hansen, A. H., Kol, S., Voldborg, B. G. & Lewis, N. E. Predictive Glycoengineering of Biosimilars Using a Markov Chain Glycosylation model. *Biotechnol. J.* **12**, 1600489 (2017).

194. Harris, R. J. Heterogeneity of Recombinant Antibodies: Linking Structure to Function. *Dev. Biol. (Basel).* **122**, 117–27 (2005).

195. Liu, L. Pharmacokinetics of Monoclonal Antibodies and Fc-Fusion Proteins. *Protein Cell* **9**, 15–32 (2018).

196. Martin, J. G. *et al.* Toward an Artificial Golgi: Redesigning the Biological Activities of Heparan Sulfate on a Digital Microfluidic Chip. *J. Am. Chem. Soc.* **131**, 11041–8 (2009).

197. Ono, Y. *et al.* Sequential Enzymatic Glycosyltransfer Reactions on a Microfluidic Device: Synthesis of a Glycosaminoglycan Linkage Region Tetrasaccharide. *Lab Chip* **8**, 2168–73 (2008).

198. Heinzler, R., Fischöder, T., Elling, L. & Franzreb, M. Toward Automated Enzymatic Glycan Synthesis in a Compartmented Flow Microreactor System. *Adv. Synth. Catal.* **361**, 4506–4516 (2019).

199. Xu, D. & Esko, J. D. A Golgi-on-a-Chip for Glycan Synthesis. *Nat. Chem. Biol.* **5**, 612–613 (2009).

200. Klymenko, O. V., Shah, N., Kontoravdi, C., Royle, K. E. & Polizzi, K. M. Designing an Artificial Golgi Reactor to Achieve Targeted Glycosylation of Monoclonal Antibodies. *AIChE J.* **62**, 2959–2973 (2016).

201. Almo, S. C. & Love, J. D. Better and Faster: Improvements and Optimization for Mammalian Recombinant Protein Production. *Curr. Opin. Struct. Biol.* **26**, 39–43 (2014).

202. Dohi, K., Isoyama-Tanaka, J., Tokuda, T. & Fujiyama, K. Recombinant Expression and Characterization of N-Acetylglucosaminyltransferase I Derived from Nicotiana tabacum. *J. Biosci. Bioeng.* **109**, 388–391 (2010).

203. Fujiyama, K. *et al.* Human N-Acetylglucosaminyltransferase I. Expression in Escherichia coli as a Soluble Enzyme, and Application as an Immobilized Enzyme for the Chemoenzymatic Synthesis of N-Linked Oligosaccharides. *J. Biosci. Bioeng.* **92**, 569–574 (2001).

204. Strasser, R. *et al.* Molecular Cloning and Characterization of cDNA Coding for 1,2N-Acetylglucosaminyltransferase I (GlcNAc-TI) from Nicotiana tabacum. *Glycobiology* **9**, 779–785 (1999).

205. Chen, R., Pawlicki, M. A., Hamilton, B. S. & Tolbert, T. J. Enzyme-Catalyzed Synthesis of a Hybrid N-Linked Oligosaccharide using N-Acetylglucosaminyltransferase I. *Adv. Synth. Catal.* **350**, 1689–1695 (2008).

206. Varki, A. *et al. Essentials of glycobiology*.

207. Fiaux, H. *et al.* Functionalized Pyrrolidine Inhibitors of Human Type II α-mannosidases as Anti-Cancer Agents: Optimizing the Fit to the Active Site. *Bioorg. Med. Chem.* **16**, 7337–7346 (2008).

208. van den Elsen, J. M. H. Structure of Golgi alpha-Mannosidase II: a Target for Inhibition of Growth and Metastasis of Cancer Cells. *EMBO J.* **20**, 3008–3017 (2001).

209. Rose, D. R. *Structure, Mechanism and Inhibition of Golgi α-Mannosidase II*. *Curr. Opin. Struct. Biol.* **22**, 558–562 (2012).

210. Bydlinski, N. *et al.* The Contributions of Individual Galactosyltransferases to Protein Specific N-Glycan Processing in Chinese Hamster Ovary Cells. *J. Biotechnol.* **282**, 101–110 (2018).

211. Berger, E. . & Rohrer, J. Galactosyltransferase—Still Up and Running. *Biochimie* **85**, 261–274 (2003).

212. Ayyar, B. V., Arora, S. & Ravi, S. S. Optimizing Antibody Expression: The Nuts and Bolts. *Methods* **116**, 51–62 (2017).

213. Andréll, J. & Tate, C. G. Overexpression of Membrane Proteins in Mammalian Cells for Structural Studies. *Mol. Membr. Biol.* **30**, 52–63 (2013).

214. Oh-eda, M. *et al.* Overexpression of the Golgi-Localized Enzyme α-Mannosidase IIx in Chinese Hamster Ovary Cells Results in the Conversion of Hexamannosyl- N -Acetylchitobiose to Tetramannosyl- N -Acetylchitobiose in the N-Glycan-Processing Pathway. *Eur. J. Biochem.* **268**, 1280–1288 (2001).

215. Opat, A. S., Houghton, F. & Gleeson, P. A. Medial Golgi but not Late Golgi Glycosyltransferases Exist as High Molecular Weight Complexes. Role of Luminal Domain in Complex Formation and Localization. *J. Biol. Chem.* **275**, 11836–45 (2000).

216. Paschinger, K. *et al.* A Deletion in the Golgi alpha-Mannosidase II Gene of Caenorhabditis elegans Results in Unexpected Non-Wild-Type N-Glycan Structures. *J. Biol. Chem.* **281**, 28265–77 (2006).

217. Li, J., Zhang, J., Lai, B., Zhao, Y. & Li, Q. Cloning, Expression, and Characterization of Capra hircus Golgi α-Mannosidase II. *Appl. Biochem. Biotechnol.* **177**, 1241–1251 (2015).

218. Palacpac, N. Q. *et al.* Stable Expression of Human β1,4-Galactosyltransferase in Plant Cells Modifies N-linked Glycosylation Patterns. *Proc. Natl. Acad. Sci.* **96**, 4692–4697 (1999).

219. Malissard, M. *et al.* Recombinant Soluble beta-1,4-Galactosyltransferases Expressed in Saccharomyces cerevisiae. Purification, Characterization and Comparison with Human Enzyme. *Eur. J. Biochem.* **239**, 340–348 (1996).

220. Ito, T. *et al.* Highly Oriented Recombinant Glycosyltransferases: Site-specific Immobilization of Unstable Membrane Proteins by Using Staphylococcus aureus Sortase A. *Biochemistry* **49**, 2604–2614 (2010).

221. Barbosa, O. *et al.* Strategies for the One-Step Immobilization–Purification of Enzymes as Industrial Biocatalysts. *Biotechnol. Adv.* **33**, 435–456 (2015).

222. Kim, D. & Herr, A. E. Protein Immobilization Techniques for Microfluidic Assays. *Biomicrofluidics* **7**, (2013).

223. Mohamad, N. R., Marzuki, N. H. C., Buang, N. A., Huyop, F. & Wahab, R. A. An Overview of Technologies for Immobilization of Enzymes and Surface Analysis Techniques for Immobilized Enzymes. *Biotechnol. Biotechnol. Equip.* **29**, 205–220 (2015).

224. Nishiguchi, S. *et al.* Highly efficient oligosaccharide synthesis on water-soluble polymeric primers by recombinant glycosyltransferases immobilised on solid supports. *Chem. Commun. (Camb).* 1944–5 (2001). doi:10.1039/b104896c

225. Rabouille, C. *et al.* The Drosophila GMII gene encodes a Golgi alpha-mannosidase II. *J. Cell Sci.* **112 (Pt 1**, 3319–3330 (1999).

226. Fairhead, M. & Howarth, M. Site-Specific Biotinylation of Purified Proteins Using BirA. *Methods Mol. Biol.* **1266**, 171–184 (2015).

227. Wahab, R. A., Elias, N., Abdullah, F. & Ghoshal, S. K. On the Taught New Tricks of Enzymes Immobilization: An All-Inclusive Overview. *React. Funct. Polym.* **152**, 104613 (2020).

228. Riz, I., Hawley, T. S. & Hawley, R. G. Lentiviral Fluorescent Protein Expression Vectors for Biotinylation Proteomics. *Methods Mol. Biol.* **699**, 431–47 (2011).

229. Kay, B. K., Thai, S. & Volgina, V. V. High-Throughput Biotinylation of Proteins. *Methods Mol. Biol.* **498**, 185–96 (2009).

230. Cull, M. G. & Schatz, P. J. Biotinylation of proteins in vivo and in vitro using small peptide tags. *Methods Enzym.* **326**, 430–40 (2000).

231. Schachter, H., Reck, F. & Paulsen, H. Use of Synthetic Oligosaccharide Substrate Analogs to Map the Active Sites of N-Acetylglucosaminyltransferases I and II. *Methods Enzymol.* **363**, 459–475 (2003).

232. Wu, Z. L., Ethen, C. M., Prather, B., MacHacek, M. & Jiang, W. Universal Phosphatase-Coupled Glycosyltransferase Assay. *Glycobiology* **21**, 727–733 (2011).

233. Dotz, V. *et al.* Mass Spectrometry for Glycosylation Analysis of Biopharmaceuticals. *TrAC Trends Anal. Chem.* **73**, 1–9 (2015).

234. Shibatani, S., Fujiyama, K., Nishiguchi, S., Seki, T. & Maekawa, Y. Production and Characterization of Active Soluble Human l,4-Galactosyltransferase in Escherichia coli as a Useful Catalyst in Synthesis of the Gal GlcNAc Linkage. *J. Biosci. Bioeng.* **91**, 85–87 (2001).

235. Numao, S., Kuntz, D. A., Withers, S. G. & Rose, D. R. Insights into the Mechanism of Drosophila melanogaster Golgi α-Mannosidase II through the Structural Analysis of Covalent Reaction Intermediates. *J. Biol. Chem.* **278**, 48074–48083 (2003).

236. Scholle, M. D., Collart, F. R. & Kay, B. K. In Vivo Biotinylated Proteins as Targets for Phage-Display Selection Experiments. *Protein Expr. Purif.* **37**, 243–252 (2004).

237. Use of Protein Biotinylation In Vivo for Chromatin Immunoprecipitation. *Anal. Biochem.* **325**, 68–76 (2004).

238. Kim, S. G., Shin, S. Y., Park, Y. C., Shin, C. S. & Seo, J. H. Production and Solid-Phase Refolding of Human Glucagon-like Peptide-1 Using Recombinant Escherichia coli. *Protein Expr. Purif.* **78**, 197–203 (2011).

239. Karav, S., Cohen, J. L., Barile, D. & de Moura Bell, J. M. L. N. Recent Advances in Immobilization Strategies for Glycosidases. *Biotechnol. Prog.* **33**, 104–112 (2017).

240. Kweon, D.-H. *et al.* Immobilization of Bacillus macerans Cyclodextrin Glycosyltransferase Fused with Poly-Lysine Using Cation Exchanger. *Enzyme Microb. Technol.* **36**, 571–578 (2005).

241. Rha, C. S. *et al.* Production of Cyclodextrin by Poly-Lysine Fused Bacillus macerans Cyclodextrin Glycosyltransferase Immobilized on Cation Exchanger. *J. Mol. Catal. B Enzym.* **34**, 39–43 (2005).

242. Matte, C. R. *et al.* Characterization of Cyclodextrin Glycosyltransferase Immobilized on Silica Microspheres Via Aminopropyltrimethoxysilane as a 'Spacer Arm'. *J. Mol. Catal. B Enzym.* **78**, 51–56 (2012).

243. Lee, D.-H., Kim, S.-G., Kweon, D.-H. & Seo, J.-H. Folding Machineries Displayed on a Cation-Exchanger for the Concerted Refolding of Cysteine- or Proline-Rich Proteins. *BMC Biotechnol.* **9**, 27 (2009).

244. Hata, Y., Matsumoto, T., Tanaka, T. & Kondo, A. C-Terminal-oriented Immobilization of

Enzymes Using Sortase A-mediated Technique. *Macromol. Biosci.* **15**, 1375–1380 (2015).

245. Rehm, F. B. H., Chen, S. & Rehm, B. H. A. Enzyme Engineering for In Situ Immobilization. *Molecules* **21**, 1370 (2016).

246. Ardèvol, A. & Rovira, C. Reaction Mechanisms in Carbohydrate-Active Enzymes: Glycoside Hydrolases and Glycosyltransferases. Insights from ab Initio Quantum Mechanics/Molecular Mechanics Dynamic Simulations. *J. Am. Chem. Soc.* **137**, 7528–7547 (2015).

247. Biswas, A. & Thattai, M. Promiscuity and Specificity of Eukaryotic Glycosyltransferases. *Biochem. Soc. Trans.* **48**, 891–900 (2020).

248. Sauerzapfe, B. *et al.* Characterization of Recombinant Fusion Constructs of Human β1,4-Galactosyltransferase 1 and the Lipase Pre-Propeptide from Staphylococcus hyicus. *J. Mol. Catal. B Enzym.* **50**, 128–140 (2008).

249. Park, J.-E., Lee, K.-Y., Do, S.-I. & Lee, S.-S. Expression and Characterization of β-1,4-Galactosyltransferase from Neisseria meningitidis and Neisseria gonorrhoeae. *BMB Rep.* **35**, 330–336 (2002).

250. Duncan, M. W., Roder, H. & Hunsucker, S. W. Quantitative Matrix-Assisted Laser Desorption/Ionization Mass Spectrometry. *Briefings Funct. Genomics Proteomics* **7**, 355–370 (2008).

251. Mehta, N. *et al.* Mass Spectrometric Quantification of N-Linked Glycans by Reference to Exogenous Standards. *J. Proteome Res.* **15**, 2969–2980 (2016).

252. Gillmeister, M. P. *et al.* An HPLC-MALDI MS Method for N-Glycan Analyses Using Smaller Size Samples: Application to Monitor Glycan Modulation by Medium Conditions. *Glycoconj. J.* **26**, 1135–1149 (2009).

253. Rohrer, J. S., Basumallick, L. & Hurum, D. C. Profiling N-Linked Oligosaccharides from IgG by High-Performance Anion-Exchange Chromatography with Pulsed Amperometric Detection. *Glycobiology* **26**, 582–591 (2016).

254. Prater, B. D., Connelly, H. M., Qin, Q. & Cockrill, S. L. High-Throughput Immunoglobulin G N-Glycan Characterization Using Rapid Resolution Reverse-Phase Chromatography Tandem Mass Spectrometry. *Anal. Biochem.* **385**, 69–79 (2009).

255. Chen, X. & Flynn, G. C. Analysis of N-Glycans from Recombinant Immunoglobulin G by On-Line Reversed-Phase High-Performance Liquid Chromatography/Mass Spectrometry. *Anal. Biochem.* **370**, 147–161 (2007).

256. Bigge, J. C. C. *et al.* Nonselective and Efficient Fluorescent Labeling of Glycans Using 2-Amino Benzamide and Anthranilic Acid. *Anal. Biochem.* **230**, 229–238 (1995).

257. Szabo, Z., Guttman, A., Rejtar, T. & Karger, B. L. Improved Sample Preparation Method For Glycan Analysis of Glycoproteins by CE-LIF and CE-MS. *Electrophoresis* **31**, 1389–1395 (2010).

258. Agrawal, A. *et al.* Click-Chemistry Enabled Directed Evolution of Glycosynthases for Bespoke Glycans Synthesis. *bioRxiv Biochem.* (2020).

259. Witte, K., Sears, P., Martin, R. & Wong, C. H. Enzymatic Glycoprotein Synthesis: Preparation of

Ribonuclease Glycoforms via Enzymatic Glycopeptide Condensation and Glycosylation. *J. Am. Chem. Soc.* **119**, 2114–2118 (1997).

260. Sears, P. Toward Automated Synthesis of Oligosaccharides and Glycoproteins. *Science (80-.).* **291**, 2344–2350 (2001).

261. Wang, C. *et al.* Engineered Soluble Monomeric IgG1 Fc with Significantly Decreased Non-Specific Binding. *Front. Immunol.* **8**, 1545 (2017).

262. Ying, T., Chen, W., Gong, R., Feng, Y. & Dimitrov, D. S. Soluble Monomeric IgG1 Fc. *J. Biol. Chem.* **287**, 19399–19408 (2012).

263. Nakazawa, K., Furukawa, K., Narimatsu, H. & Kobata, a. Kinetic study of human beta-1,4-galactosyltransferase expressed in E. coli. *J. Biochem.* **113**, 747–53 (1993).

264. Sato, T., Furukawa, K., Bakker, H., Van den Eijnden, D. H. & Van Die, I. Molecular Cloning of a Human cDNA Encoding β-1,4-Galactosyltransferase with 37% Identity to Mammalian UDP-Gal:GlcNAc β-1,4-Galactosyltransferase. *Proc. Natl. Acad. Sci. U. S. A.* **95**, 472-477. (1998).

265. Malissard, M. & Berger, E. G. Improving Solubility of Catalytic Domain of Human Beta-1,4-Galactosyltransferase 1 Through Rationally Designed Amino Acid Replacements. *Eur. J. Biochem.* **268**, 4352–8 (2001).

266. Namdjou, D. J. *et al.* A β-1,4-Galactosyltransferase from Helicobacter pylori is an Efficient and Versatile Biocatalyst Displaying a Novel Activity for Thioglycoside Synthesis. *ChemBioChem* **9**, 1632–1640 (2008).

267. Kanie, Y., Kirsch, A., Kanie, O. & Wong, C. H. Enzymatic Assay of Galactosyltransferase by Capillary Electrophoresis. *Anal. Biochem.* **263**, 240–245 (1998).

268. Heinzler, R., Hübner, J., Fischöder, T., Elling, L. & Franzreb, M. A Compartmented Flow Microreactor System for Automated Optimization of Bioprocesses Applying Immobilized Enzymes. *Front. Bioeng. Biotechnol.* **6**, (2018).

269. Bitter, G. A., Chen, K. K., Banks, A. R. & Lai, P. H. Secretion of Foreign Proteins from Saccharomyces cerevisiae Directed by Alpha-Factor Gene Fusions. *Proc. Natl. Acad. Sci.* **81**, 5330–5334 (1984).

270. Yang, S. *et al.* Enhanced Production of Recombinant Secretory Proteins in Pichia pastoris by Optimizing Kex2 P1' site. *PLoS One* **8**, e75347 (2013).

271. Laukens, B. *et al.* Off-target glycans encountered along the synthetic biology route toward humanized N-glycans in Pichia pastoris. *Biotechnol. Bioeng.* (2020). doi:10.1002/bit.27375

272. Gomathinayagam, S. *et al.* Structural elucidation of an -1,2-Mannosidase Resistant Oligosaccharide Produced in Pichia pastoris. *Glycobiology* **21**, 1606–1615 (2011).

273. Dumont, J. A., Low, S. C., Peters, R. T. & Bitonti, A. J. Monomeric Fc Fusions. *BioDrugs* **20**, 151–160 (2006).

274. Krasnova, L. & Wong, C.-H. Understanding the Chemistry and Biology of Glycosylation with Glycan Synthesis. *Annu. Rev. Biochem.* **85**, 599–630 (2016).

275. Kunert, R. & Reinhart, D. Advances in Recombinant Antibody Manufacturing. *Appl. Microbiol. Biotechnol.* **100**, 3451–3461 (2016).

276. Gammons, C. H. & Seward, T. M. Stability of Manganese (II) Chloride Complexes from 25 to 300°C. *Geochim. Cosmochim. Acta* **60**, 4295–4311 (1996).

277. Shubhakar, A. *et al.* Automated High-Throughput Permethylation for Glycosylation Analysis of Biologics Using MALDI-TOF-MS. *Anal. Chem.* (2016).

278. Szigeti, M. & Guttman, A. Automated N-Glycosylation Sequencing Of Biopharmaceuticals By Capillary Electrophoresis. *Sci. Rep.* **7**, 11663 (2017).

279. Guttman, A. Capillary Electrophoresis in the N-Glycosylation Analysis of Biopharmaceuticals. *TrAC Trends Anal. Chem.* **48**, 132–143 (2013).

280. Baković, M. P. *et al.* High-Throughput IgG Fc N-Glycosylation Profiling by Mass Spectrometry of Glycopeptides. *J. Proteome Res.* **12**, 821–831 (2013).

281. Arnold, J. N., Wormald, M. R., Sim, R. B., Rudd, P. M. & Dwek, R. A. The Impact of Glycosylation on the Biological Function and Structure of Human Immunoglobulins. *Annu. Rev. Immunol.* **25**, 21–50 (2007).

282. Mimura, Y. *et al.* The Influence of Glycosylation on the Thermal Stability and Effector Function Expression of Human IgG1-Fc: Properties of a Series of Truncated Glycoforms. *Mol. Immunol.* **37**, 697–706 (2000).

283. Dekkers, G. *et al.* Multi-Level Glyco-Engineering Techniques to Generate IgG with Defined Fc-Glycans. *Sci. Rep.* **6**, 36964 (2016).

284. Mimura, Y. *et al.* Glycosylation Engineering of Therapeutic IgG Antibodies: Challenges for the Safety, Functionality and Efficacy. *Protein Cell* **9**, 47–62 (2018).

285. Higel, F., Seidl, A., Sörgel, F. & Friess, W. N-glycosylation Heterogeneity and the Influence on Structure, Function and Pharmacokinetics of Monoclonal Antibodies and Fc Fusion Proteins. *Eur. J. Pharm. Biopharm.* **100**, 94–100 (2016).

286. Nigrovic, P. A. Sweets Are Good for You: Fine Tuning Antibodies via Glycosylation. *Arthritis Rheum.* n/a-n/a (2013).

287. Stach, C. S. *et al.* Model-Driven Engineering of N-Linked Glycosylation in Chinese Hamster Ovary Cells. *ACS Synth. Biol.* **8**, 2524–2535 (2019).

288. Mateo, C., Palomo, J. M., Fernandez-Lorente, G., Guisan, J. M. & Fernandez-Lafuente, R. Improvement of Enzyme Activity, Stability and Selectivity via Immobilization Techniques. *Enzyme Microb. Technol.* **40**, 1451–1463 (2007).

289. Hajduk, J. *et al.* Interaction Analysis of Glycoengineered Antibodies with CD16a: a Native Mass Spectrometry Approach. *MAbs* **12**, 1736975 (2020).

290. Raju, T. S., Briggs, J. B., Chamow, S. M., Winkler, M. E. & Jones, A. J. S. Glycoengineering of Therapeutic Glycoproteins: In Vitro Galactosylation and Sialylation of Glycoproteins with Terminal N -Acetylglucosamine and Galactose Residues. *Biochemistry* **40**, 8868–8876 (2001).

291. Basso, A. & Serban, S. Industrial applications of immobilized enzymes—A review. *Mol. Catal.* **479**, 110607 (2019).

292. M. Gaboardi, G. Pallanza, G. Castaldi, M. C. Process for the Preparation of Sofosbuvir.

293. Kallenberg, A. I., van Rantwijk, F. & Sheldon, R. A. Immobilization of Penicillin G Acylase: The Key to Optimum Performance. *Adv. Synth. Catal.* **347**, 905–926 (2005).

294. Wu, J. C. Y., Hutchings, C. H., Lindsay, M. J., Werner, C. J. & Bundy, B. C. Enhanced Enzyme Stability Through Site-Directed Covalent Immobilization. *J. Biotechnol.* **193**, 83–90 (2015).

295. Ha, E.-J. *et al.* One-Step Immobilization and Purification of His-Tagged Enzyme Using poly(2-acetamidoacrylic acid) Hydrogel. *Macromol. Res.* **21**, 5–9 (2013).

296. Taniguchi, T. *et al.* Structures of the Sugar Chains of Rabbit Immunoglobin G: Occurrence of Asparagine-Linked Sugar Chains in Fab Fragment. *Biochemistry* **24**, 5551–5557 (1985).

297. Girardi, E., Holdom, M. D., Davies, A. M., Sutton, B. J. & Beavil, A. J. The Crystal Structure of Rabbit IgG-Fc. *Biochem. J.* **417**, 77–83 (2009).

298. Lu, G., Crihfield, C. L., Gattu, S., Veltri, L. M. & Holland, L. A. Capillary Electrophoresis Separations of Glycans. *Chem. Rev.* **118**, 7867–7885 (2018).

299. Wang, Y., Santos, M. & Guttman, A. Comparative Core Fucosylation Analysis of Some Major Therapeutic Antibody N -Glycans by Direct Infusion ESI-MS and CE-LIF Detection. *J. Sep. Sci.* **36**, 2862–2867 (2013).

300. Yamane-Ohnuki, N. *et al.* Establishment of FUT8 Knockout Chinese Hamster Ovary Cells: An Ideal Host Cell Line for Producing Completely Defucosylated Antibodies with Enhanced Antibody-Dependent Cellular Cytotoxicity. *Biotechnol. Bioeng.* **87**, 614–622 (2004).

301. Vainauskas, S. *et al.* A Novel Broad Specificity Fucosidase Capable of Core α1-6 Fucose Release from N-Glycans Labeled with Urea-Linked Fluorescent Dyes. *Sci. Rep.* **8**, 9504 (2018).

302. Johnson, R. R., Johnson, A. T. C. & Klein, M. L. Probing the Structure of DNA−Carbon Nanotube Hybrids with Molecular Dynamics. *Nano Lett.* **8**, 69–75 (2008).

303. Liang, J., Fieg, G., Keil, F. J. & Jakobtorweihen, S. Adsorption of Proteins onto Ion-Exchange Chromatographic Media: A Molecular Dynamics Study. *Ind. Eng. Chem. Res.* **51**, 16049–16058 (2012).

304. Zhang, L. *et al.* Probing Immobilization Mechanism of alpha-chymotrypsin onto Carbon Nanotube in Organic Media by Molecular Dynamics Simulation. *Sci. Rep.* **5**, 9297 (2015).

305. Sun, X., Feng, Z., Hou, T. & Li, Y. Mechanism of Graphene Oxide as an Enzyme Inhibitor from Molecular Dynamics Simulations. *ACS Appl. Mater. Interfaces* **6**, 7153–7163 (2014).

306. Qi, S. Y., Yao, S. C., Yin, L. H. & Hu, C. Q. A Strategy to Assess Quality Consistency of Drug Products. *Front. Chem.* **7**, (2019).

307. Schiestl, M. *et al.* Acceptable Changes in Quality Attributes of Glycosylated Biopharmaceuticals. *Nat. Biotechnol.* **29**, 310–312 (2011).

308. Berkowitz, S. A., Engen, J. R., Mazzeo, J. R. & Jones, G. B. Analytical Tools for Characterizing Biopharmaceuticals and the Implications for Biosimilars. *Nat. Rev. Drug Discov.* **11**, 527–540 (2012).

309. Schneider, R. *et al.* Immobilization of Galactosyltransferase and Continuous Galactosylation of Glycoproteins in a Reactor. *Glycoconjugate J* **7**, 589–600 (1990).

310. Grilo, A. L. & Mantalaris, A. The Increasingly Human and Profitable Monoclonal Antibody Market. *Trends in Biotechnology* (2019). doi:10.1016/j.tibtech.2018.05.014

311. Haselberg, R., de Jong, G. J. & Somsen, G. W. Low-Flow Sheathless Capillary Electrophoresis–Mass Spectrometry for Sensitive Glycoform Profiling of Intact Pharmaceutical Proteins. *Anal. Chem.* **85**, 2289–2296 (2013).

312. Ma, B. *et al.* Protein Glycoengineering: An Approach for Improving Protein Properties. *Front. Chem.* **8**, (2020).

313. Sambrook, J., G. M. *Molecular Cloning: A Laboratory Manual. 4 ed*. *Cold Spring Harbor Laboratory Press* (2012). doi:10.3724/SP.J.1141.2012.01075

314. Chapman, J., Ismail, A. & Dinu, C. Industrial Applications of Enzymes: Recent Advances, Techniques, and Outlooks. *Catalysts* **8**, 238 (2018).

315. DiCosimo, R., McAuliffe, J., Poulose, A. J. & Bohlmann, G. Industrial Use of Immobilized Enzymes. *Chem. Soc. Rev.* **42**, 6437 (2013).

316. Tamborini, L., Fernandes, P., Paradisi, F. & Molinari, F. Flow Bioreactors as Complementary Tools for Biocatalytic Process Intensification. *Trends Biotechnol.* **36**, 73–88 (2018).

317. Zhu, Y., Chen, Q., Shao, L., Jia, Y. & Zhang, X. Microfluidic immobilized enzyme reactors for continuous biocatalysis. *React. Chem. Eng.* **5**, 9–32 (2020).

318. Bendiak, B. & Schachter, H. Control of glycoprotein synthesis. Purification of UDP-N-acetylglucosamine:alpha-D-mannoside beta 1-2 N-acetylglucosaminyltransferase II from rat liver. *J. Biol. Chem.* (1987).

319. Nishikawa, Y., Pegg, W., Paulsen, H. & Schachter, H. Control of glycoprotein synthesis. Purification and characterization of rabbit liver UDP-N-acetylglucosamine:α-3-D-mannoside β-1,2-N-acetylglucosaminyltransferase I. *J. Biol. Chem.* (1988).

320. Schachter, H. The joys of HexNAc. The synthesis and function of N- and O-glycan branches. *Glycoconjugate Journal* (2000). doi:10.1023/A:1011010206774

321. Sun, L. *et al.* Integrated Device for Online Sample Buffer Exchange, Protein Enrichment, and Digestion. *Anal. Chem.* **82**, 2574–2579 (2010).

322. Bülter, T. & Elling, L. Enzymatic synthesis of nucleotide sugars. *Glycoconj. J.* **16**, 147–59 (1999).

323. Zhai, Y. *et al.* NahK/GlmU fusion enzyme: characterization and one-step enzymatic synthesis of UDP-N-acetylglucosamine. *Biotechnol. Lett.* **34**, 1321–1326 (2012).

324. Ichikawa, Y., Wang, R. & Wong, C. H. Regeneration of sugar nucleotide for enzymatic

oligosaccharide synthesis. *Methods Enzymol.* **247**, 107–27 (1994).

325. Abdul-Hammeda, M., Babalolab, J. O., Breidenc, B. & Sandhoff, and K. Regeneration of Streptavidin-coated Paramagnetic Beads for Multiple uses in Inter-membrane Lipid Transfer Assays. *Ann. Sci. Technol.* **1**, 13–18 (2016).

326. Sheldon, R. A. Enzyme Immobilization: The Quest for Optimum Performance. *Adv. Synth. Catal.* **349**, 1289–1307 (2007).

327. Rakmai, J. & Cheirsilp, B. Continuous production of β-cyclodextrin by cyclodextrin glycosyltransferase immobilized in mixed gel beads: Comparative study in continuous stirred tank reactor and packed bed reactor. *Biochem. Eng. J.* **105**, 107–113 (2016).

328. Boehm, C. R., Freemont, P. S. & Ces, O. Design of a prototype flow microreactor for synthetic biology in vitro. *Lab Chip* **13**, 3426 (2013).

329. Hanefeld, U., Gardossi, L. & Magner, E. Understanding enzyme immobilisation. *Chem Soc Rev* **38**, 453–468 (2009).

330. Royle, K. E. & Polizzi, K. A streamlined cloning workflow minimising the time-to-strain pipeline for Pichia pastoris. *Sci. Rep.* **7**, 15817 (2017).

331. Ciucanu, I. & Kerek, F. A simple and rapid method for the permethylation of carbohydrates. *Carbohydr. Res.* **131**, 209–217 (1984).

332. Ceroni, A. *et al.* GlycoWorkbench: A Tool for the Computer-Assisted Annotation of Mass Spectra of Glycans †. *J. Proteome Res.* **7**, 1650–1659 (2008).

333. North, S. J. *et al.* Mass Spectrometric Analysis of Mutant Mice. in *Methods in Enzymology* 27–77 (2010). doi:10.1016/S0076-6879(10)78002-2

334. Saribas, A. S., Johnson, K., Liu, L., Bezila, D. & Hakes, D. Refolding of human ??-1-2 GlcNAc transferase (GnT1) and the role of its unpaired Cys 121. *Biochem. Biophys. Res. Commun.* **362**, 381–386 (2007).

335. Wagner, R. *et al.* Elongation of the N-glycans of fowl plague virus hemagglutinin expressed in Spodoptera frugiperda (Sf9) cells by coexpression of human ??1,2-N-acetylglucosaminyltransferase I. *Glycobiology* **6**, 165–175 (1996).

336. Strasser, R. *et al.* Molecular basis of N-acetylglucosaminyltransferase I deficiency in Arabidopsis thaliana plants lacking complex N-glycans. *Biochem. J.* **387**, 385–391 (2005).

337. Nishiu, J., Kioka, N., Fukada, T., Sakai, H. & Komano, T. Characterization of rat N-acetylglucosaminyltransferase I expressed in Escherichia coli. *Biosci. Biotechnol. Biochem.* **59**, 1750–2 (1995).

338. Sarkar, M. & Schachter, H. Cloning and expression of Drosophila melanogaster UDP-GlcNAc:α-3-D-mannoside β1,2-N-acetylglucosaminyltransferase I. *Biol. Chem.* (2001). doi:10.1515/BC.2001.028

339. Zhang, W., Betel, D. & Schachter, H. Cloning and expression of a novel UDP-GlcNAc :α-D-mannoside β1,2-N- acetylglucosaminyltransferase homologous to UDP-GlcNAc :α-3-D-mannoside β1,2-N-acetylglucosaminyltransferase I. *Biochem. J* **361**, 153–162 (2002).

340. Akama, T. O. & Fukuda, M. N. N-Glycan Structure Analysis Using Lectins and an α-Mannosidase Activity Assay. in 304–314 (2006). doi:10.1016/S0076-6879(06)16020-6

341. Strasser, R. *et al.* Molecular cloning and characterization of *Arabidopsis thaliana* Golgi α-mannosidase II, a key enzyme in the formation of complex N-glycans in plants. *Plant J.* **45**, 789–803 (2006).

342. Moremen, K. W. & Robbins, P. W. Isolation, Characterization, and Expression of cDNAs Encoding Murine a-Mannosidase II, a Golgi Enzyme That Controls Conversion of High Mannose to Complex N-Glycans. *J. Cell Biol.* **115**, (1991).

343. Hesselink, T. *et al.* Expression of natural human β1,4-GalT1 variants and of non-mammalian homologues in plants leads to differences in galactosylation of N-glycans. *Transgenic Res.* (2014). doi:10.1007/s11248-014-9806-z

344. Geisler, C., Mabashi-Asazuma, H., Kuo, C. W., Khoo, K. H. & Jarvis, D. L. Engineering β1,4-galactosyltransferase I to reduce secretion and enhance N-glycan elongation in insect cells. *J. Biotechnol.* (2015). doi:10.1016/j.jbiotec.2014.11.013

Chapter 8: Appendix

8.1. Appendix specific to Chapter 2

Table 8-1*:* Review of expression and immobilisation systems of GnTI enzyme orthologs.

Enzyme	Structural Features and PTMs	Expression system	Specific / Enzymatic Activity	Immobilisation	Ref.
***Homo sapiens* GnTI** (445 amino acids)	Disulfide bonds 113-143, 237-303	Human GnTI lacking first 103 amino acids (Δ103) in *E. coli* as an MBP fusion protein	0.101 µmol/min/mg (purified enzyme)	Affinity immobilisation of MBP fusion on amylose beads	[203]
		MBP-Δ103 hGnTI in *E. coli* (Top 10 cells). Mutations of the unpaired C121 shown to have an impact on specific activity	7mU/mg (purified enzyme)	N/A	[334]
		His-Δ103 hGnTI in *E. coli* (trxB/gor mutations strain).	0.48 µmol/min/mg (purified enzyme)	N/A	[205]
		hGnTI with N-terminus viral tag epitope in Sf9 insect cells	N/A	N/A	[335]

		hGnTI-Myc in Lec1 CHO cells a with different transmembrane domains.	0.121 nmol/min/mg (enzyme in cell lysate)	N/A	[215]
***Arabidopsis thaliana* GnTI** (444 amino Acids)	N-Linked Glycosylated in Asn 351	Δ24 AtGnTI-His in Sf21 insect cells using the Baculovirus expression system	3.42 µmol/ min/mg (purified enzyme)	N/A	[336]
***Oryctolagus cuniculus* (rabbit) GnTI** (447 amino acids)	Disulfide bonds 115-145, 239-305	Δ29 OcGnTI-His Sf21 insect cells using the Baculovirus expression system	5.7 µmol/ min/mg (purified enzyme)	N/A	[336]
***Rattus norvegicus* GnTI (**447 amino acids)	Disulfide bonds 115-145, 239-305	Δ37 RnGnTI *E. coli* (BL21 cells) as a His-tag fusion protein (N- or C-terminus)	5.30 µmol/min/mg (34.8 ug/ml purified enzyme)	N/A	[337]
***Drosophila melanogaster* GnTI** (458 amino acids)	1 predicted N- site Disulfide bonds 127-250, 157-316	His-Δ25 DmGnTI was expressed in Sf9 insect cells	0.007 µmol/min/min	N/A	[338]
Caenorhabditis elegans GnTI.2 Homologous to **GnTI** (449 amino acids)	Disulfide bonds 100-131, 227-293 N-Linked Glycosylated Asn 2, 8 and 159	*C. elegans* Gly-13 GnTI.2 was expressed as a His tag fusion protein in Sf9 insect cells	0.31 nmol/15h/0.01 ml of resin (purified enzyme)	N/A	[339]
Nicotiana tabacum GnTI (446 amino acids)	1 N-linked glycosylation site Asn 203 Disulfide bonds 7-81, 8-49, 115-309	MBP-Δ29 NtGnTI *E. coli* (Rosetta DE3-Gami) cells	Significant activity of purified enzyme with Km=0.5mM	N/A	[202]
		Δ29 NtGnTI- GST in Sf9 insect cells	Data not shown, higher activity for Man5 than Man3	N/A	[204]
		NtGnTI-MBP in various *E. coli* strains	Qualitative data	N/A	[172]

Table 8-2 *:* Review of expression and immobilisation systems of ManII enzyme orthologs.

Enzyme	Structural Features and PTMs	Expression system	Specific / enzymatic Activity	Immobilisation	Ref.
***Homo sapiens* ManII** (1144 amino acids)	3 N-linked glycosylation sites Asn 78, 93, 1125 2 phosphorylated sites	Protein A-hManII (only catalytic domain) in COS cells	Active Value N/A	Affinity immobilisation on IgG-agarose beads	[214]
***Homo sapiens* ManIIX (MX)** (1139 amino acids)	4 N-linked glycosylation sites Asn 95, 305, 1093, 1131	His_6-hMX (only catalytic domain) in CHO cells	Active Value N/A	N/A	[340]
		Protein A-hMX (only catalytic domain) in COS cells	Active but only on 4-UM-Man Value N/A	Affinity immobilisation on IgG-agarose beads	[214]
***Arabidopsis thaliana* ManII** (1173 amino acids)	9 N-linked glycosylation sites Asn 106, 262, 467, 675, 772, 782, 991, 1098, 1108	His-AtManII in Sf21 insect cells using the Baculovirus expression system	6.38 µmol/ min/mg (purified enzyme)	N/A	[341]
***Drosophila melanogaster* ManII** (1108 amino acids)	Multiple disulfide bonds	Overexpression in S2 insect cells via stable transfection Produced 60mg/ml of purified enzyme	Active Value N/A	N/A	[209]
		Protein A-Δ74 DmManII transiently expressed in CHOP cells	N/A	Affinity immobilisation on IgG-sepharose Beads	[225]
***Capra hircus* ManII** (1144) amino acids)	3 predicted N-linked glycosylation sites Multiple disulfide bonds	ChManII-His_6 was expressed in *P. pastoris*	8.96 µmol/min	N/A	[217]
***Caenorhabditis elegans* ManII** (1145 amino acids)	1 predicted N-linked glycosylation site Multiple disulfide bonds	Δ122Ce ManII expressed in *P. pastoris*	Active Value N/A	N/A	[216]
***Mus musculus* ManII** (1150 amino acids)	3 N-linked glycosylation Sites Asn 78, 93, 1129 2 phosphorylated sites	MmManII was transiently expressed in COS cells	52 .9 µmol/min/mg in salt washed microsomes	N/A	[342]

Table 8-3: Review of expression and immobilisation systems of GalT orthologs.

Enzyme	PTMs	Expression system	Specific / enzymatic Activity	Immobilisation	Ref.
***Homo sapiens* GalT** (398 amino acids)	N-linked glycosylated in Asn 113 Disulfide bonds 130-172, 243-262	hGalT was expressed in *S. cerevisiae* strain BT150 (only catalytic domain)	8.4 U/mg (purified enzyme)	N/A	[219]
		hGalT was expressed in *E. coli*	80.9 nmol/h/mg	N/A	[263]
		MBP-hGalT-LPETG-His_6 was expressed in *E. coli*	Purified and immobilised enzyme retained 100% of its relative specific activity	Sortase-mediated immobilisation (covalent)	[220]
		hGalT in *N. tabacum* BY2 cells	900 pmol/h/mg	N/A	[218]
		His_6- *S. hyicus* lipase pre-propeptide- hGalT (only catalytic domain)	vmax = 1.12 U/mg	Affinity immobilisation on Ni/NTa magnetic beads	[198]
		hGalT-MBP in *E. coli*	Active, value N/A	Covalent immobilisation on CNBr-activated Sepharose beads	[224]
		MBP-hGalT (lacking transmembrane domain) in *E. coli*	Vmax 643 × 103 nmol/mg/h	N/A	[234]
***Gallus Gallus* (chicken) GalT** (362 amino acids)	1 predicted N-linked glycosylation site	GgGalT Beta-1,4-galactosyltransferase 1 was fused to N-terminal fragments of human GalT or rat ST6Gal1 and expressed in *N. tabacum* leaves	Qualitative results-effect of enzyme origin and fusion constructs on overall galactosylation	N/A	[343]
***Danio rerio* (zebrafish) GalT** (350amino acids)	1 predicted N-linked glycosylation site				
***Bos Taurus* (bovine) GalT** (402 amino acids)	N-linked glycosylated in Asn 90 & 117 Disulfide bonds 134-176, 247-266	BtGalT lacking the cytosolic and transmembrane domain (CTD), was N-terminally fused to the CTD of FuT7 and an 8XHis tag while expressed in *Sf9* cells.	0.4-2.4 pmol gal transfer/mg/h	N/A	[344]

Neisseria meningitis (275 amino acids) **&** ***Neisseria gonorrhoeae*** (275 amino acids) **GalT**	No PTMS	GalT-His_6 tag to C-terminus was expressed in *E. coli* BL21 cells	N/A	N/A	[249]

8.2. Appendix specific to Chapter 4

a.

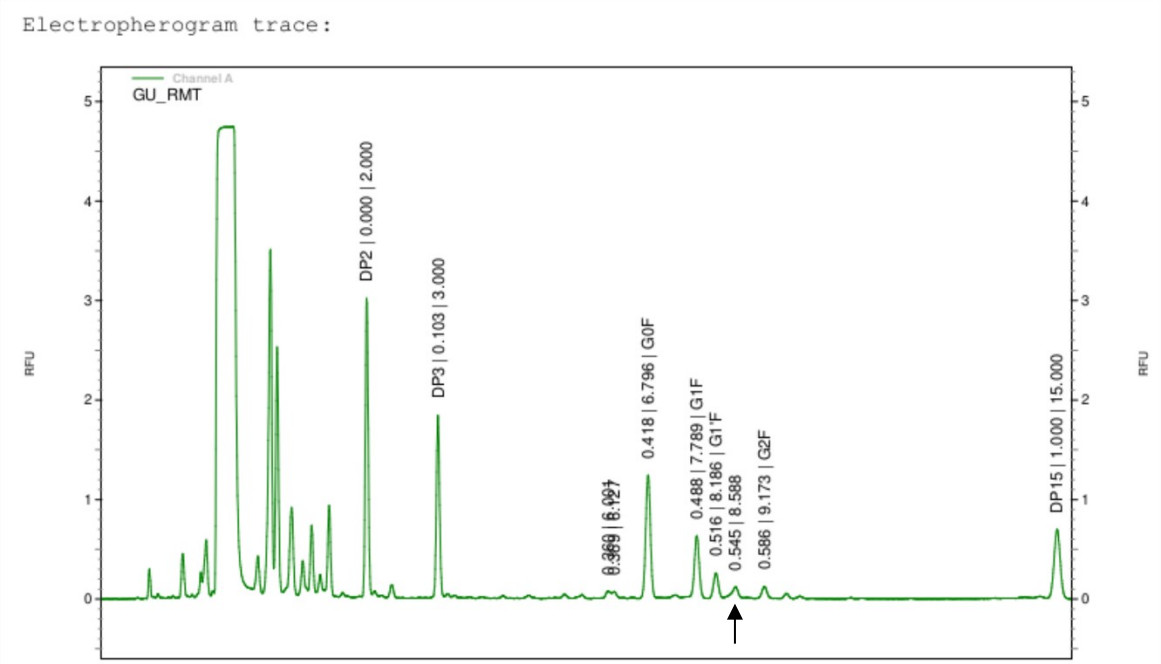

b.

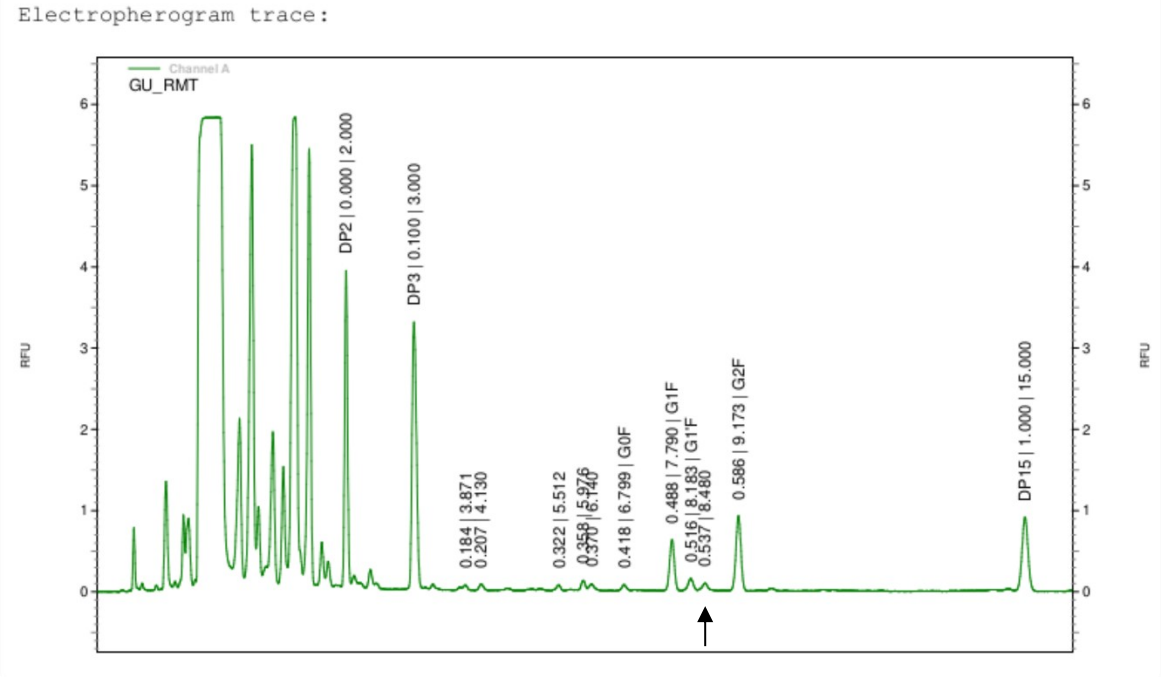

Figure 8-1: CE electropherograms for chIgG treatment with immobilised on magnetic StV beads hGalT. The detected glycoforms are G0F, G1F, G1'F and G2F. G2 is not labelled but its migration time is ~0.54 and the GU value at ~8.5. Thus, the unlabelled peak depicted by the arrow, was determined to belong to G2. a: untreated chIg; b. chIg and hGalT.

a.

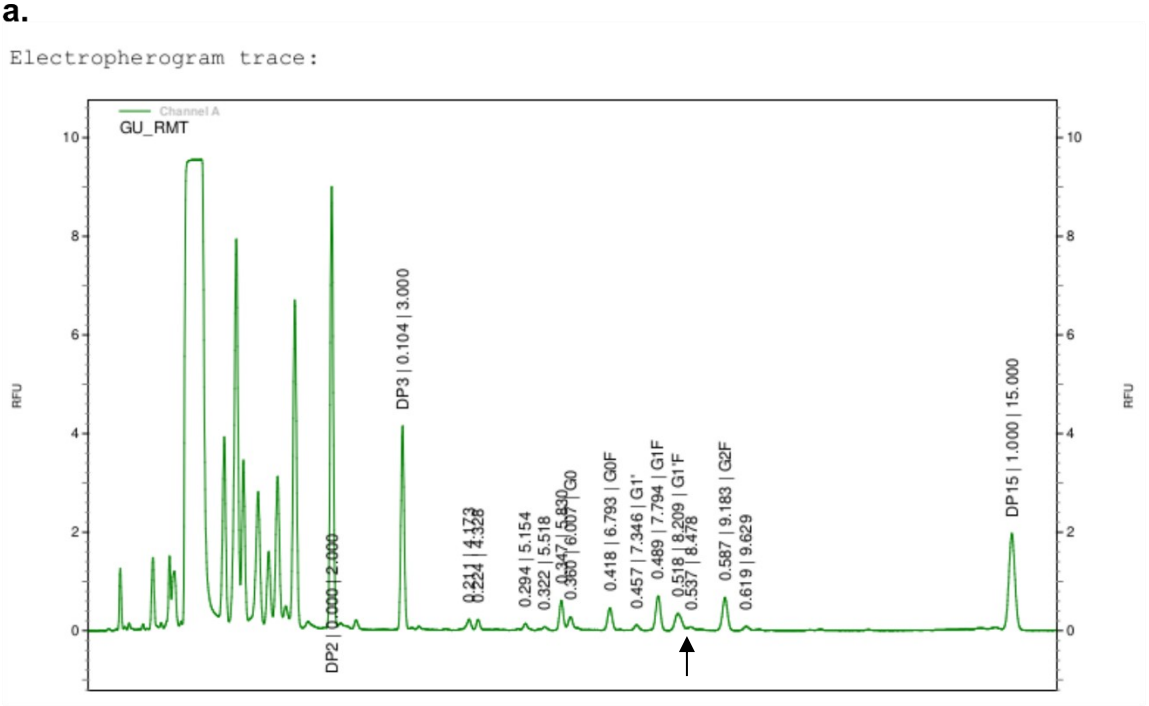

b.

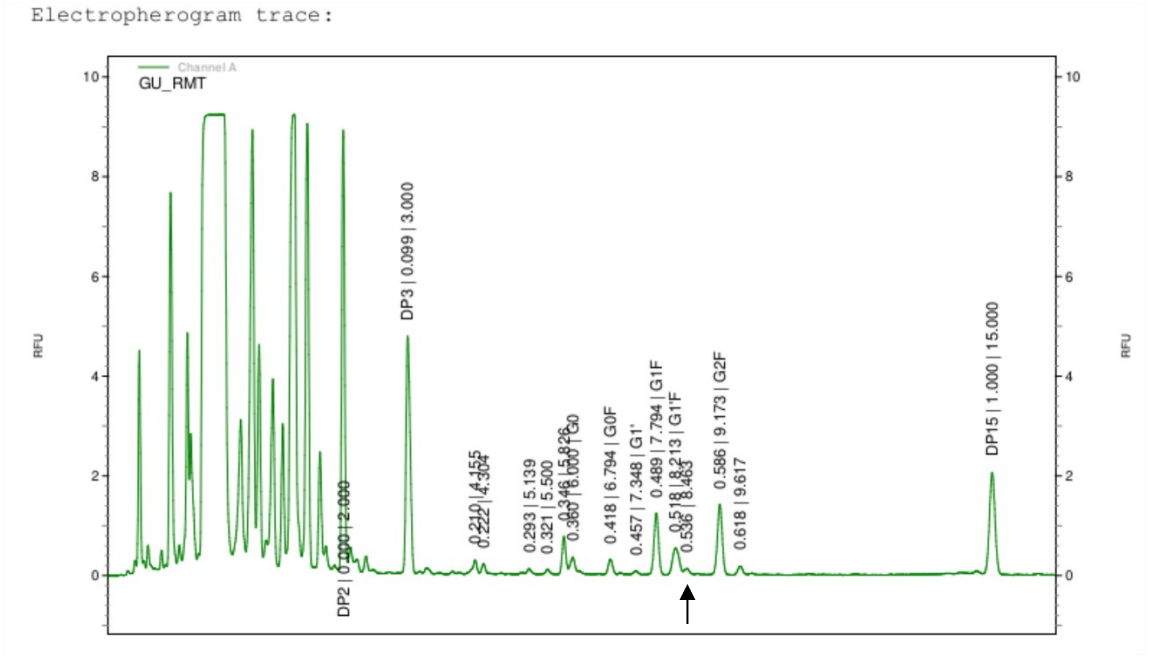

Figure 8-2: CE electropherograms for hIgG treatment with immobilised on magnetic StV beads hGalT. The detected glycoforms are G0, G1', G0F, G1F, G1'F and G2F. The detected glycoforms are G0F, G1F, G1'F and G2F. G2 is not labelled but its migration time is ~0.537 and the GU value at ~8.470. Thus, the unlabelled peak depicted by the arrow, was assumed to belong to G2 a: untreated hIgG; b. hIgG and hGalT.

a.

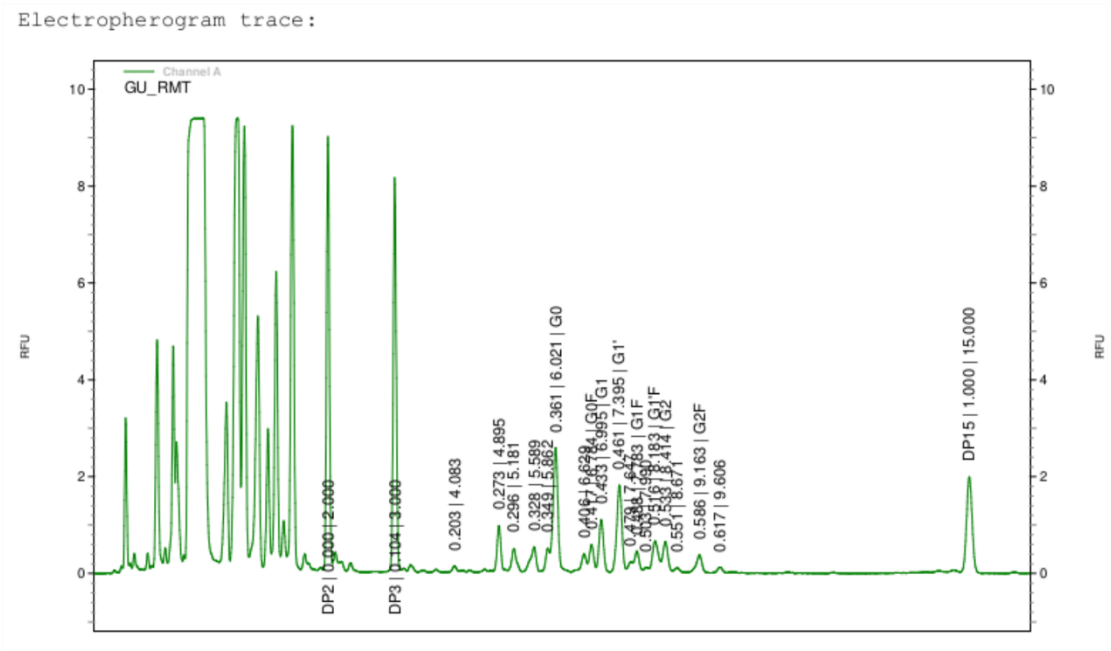

b.

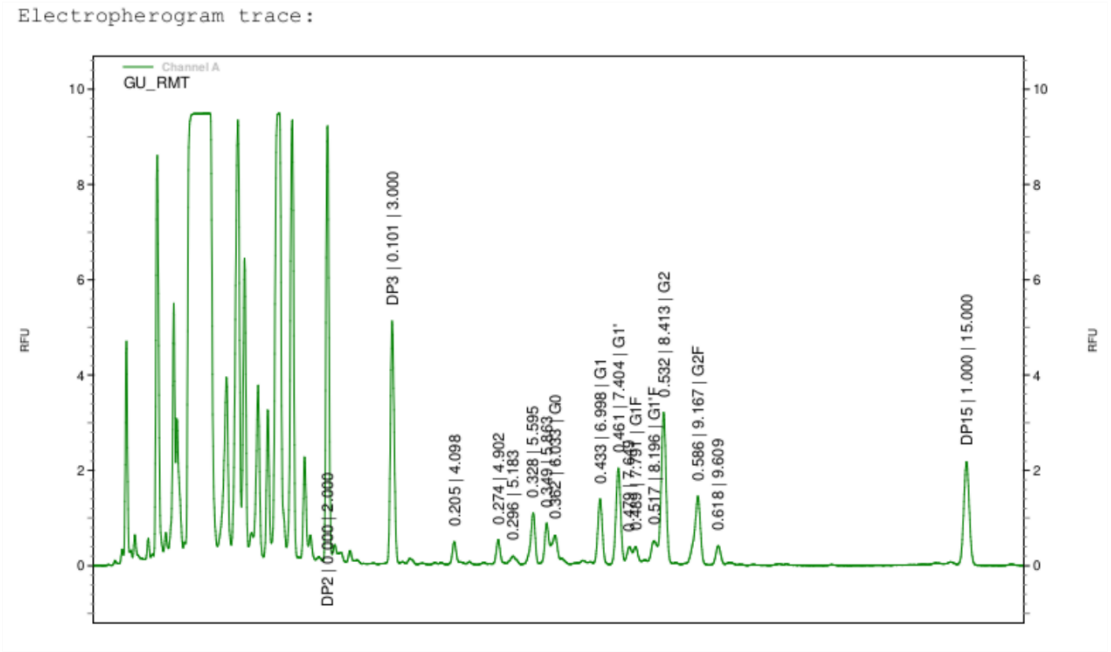

Figure 8-3: CE electropherograms for rIgG treatment with immobilised on magnetic StV beads hGalT. The detected glycoforms are G0, G1, G1', G0F, G1F, G1'F and G2F. a: untreated rIgG; b. rIgG and hGalT.

8.3. Appendix specific to Chapter 6

8.3.1. Nucleotide sequence of Δ29 NtGnTI sequence used in this study.

GCGACGCAATCGGAATATGCGGATCGCTTGGCAGCGGCGATTGAAGCCGAAAACCATTGCACGTCACAGACC
CGCTTACTGATCGATCAAATCAGTCAGCAACAAGGACGCATTGTAGCCCTGGAGGAACAGATGAAACGTCAG
GATCAGGAGTGTCGCCAATTACGTGCTTTGGTTCAGGATCTTGAGTCGAAAGGGATTAAGAAATTGATCGGC
AATGTTCAAATGCCTGTTGCTGCAGTAGTGGTCATGGCCTGCAATCGTGCGGATTACCTCGAGAAAACCATCA
AATCCATCCTGAAGTATCAGATTAGCGTTGCACCGAAATACCCTCTGTTTATCTCCCAAGATGGTTCTCATCCG
GATGTCCGCAAACTGGCGTTAAGCTACGATCAACTGACCTATATGCAGCATCTGGATTTTGAACCGGTGCACA
CTGAACGTCCTGGCGAATTAATCGCGTATTACAAAATTGCACGCCACTACAAATGGGCCCTTGACCAGCTCTTT
TACAAGCACAACTTTAGCCGGGTGATCATTCTTGAGGACGATATGGAAATTGCCCCAGACTTCTTCGACTTCTT
TGAAGCCGGAGCTACTCTGCTGGATCGCGATAAGTCGATTATGGCGATCAGTAGCTGGAACGATAACGGGCA
GATGCAGTTTGTGCAAGATCCCTATGCTTTATATCGCTCAGACTTCTTTCCGGGTCTGGGTTGGATGTTGAGTA
AATCGACATGGGACGAACTGAGCCCGAAATGGCCGAAAGCTTACTGGGATGACTGGTTGCGCCTGAAGGAA
AACCATCGTGGTCGTCAGTTCATTCGCCCGGAAGTGTGTCGTAGCTATAACTTTGGTGAACATGGTAGCAGTC
TGGGCCAGTTCTTTAAACAGTATCTGGAACCCATCAAACTCAATGACGTCCAGGTCGACTGGAAATCCATGGA
TCTTTCTTATCTGCTGGAGGACAATTACGTGAAACACTTTGGCGATCTGGTGAAGAAAGCGAAACCGATTCAT
GGTGCCGACGCAGTGCTGAAAGCGTTTAACATTGATGGGGATGTTCGCATTCAGTACCGTGATCAGCTGGACT
TTGAAGATATTGCACGTCAGTTTGGCATTTTCGAAGAGTGGAAAGATGGCGTACCACGTGCGGCCTATAAAG
GCATCGTAGTGTTCCGCTATCAGACGTCACGCCGGGTTTTCCTCGTCGGCCCAGACTCTCTGCAGCAACTGGG
CAATGAAGATACC

8.3.2. Nucleotide sequence of Δ128 hGalT sequence used in this study.

GCCTGCCCTGAGGAAAGCCCACTGTTGGTGGGCCCAATGCTGATCGAGTTTAACATGCCGGTGGACCTGGAA
CTGGTGGCGAAACAGAACCCGAACGTCAAAATGGGCGGCCGTTACGCACCGCGTGACTGCGTTAGCCCGCAC
AAAGTCGCGATCATTATTCCGTTCCGCAATCGCCAAGAGCATCTGAAGTACTGGCTGTACTATCTGCATCCAGT
TCTGCAACGTCAGCAATTGGACTACGGTATTTACGTTATCAATCAAGCCGGCGACACGATCTTTAATCGTGCTA
AGTTGCTGAATGTTGGTTTTCAAGAAGCGCTGAAAGACTACGACTACACCTGTTTCGTGTTCTCCGACGTTGAC
CTGATTCCGATGAATGATCACAATGCGTACCGCTGTTTTTCTCAGCCGCGTCACATCAGCGTAGCGATGGATAA
GTTTGGTTTCAGCCTGCCGTATGTGCAGTATTTTGGTGGCGTCAGCGCACTGAGCAAGCAACAGTTTCTCACG
ATTAACGGTTTCCCGAACAACTATTGGGGTTGGGGTGGCGAAGATGATGATATCTTCAACCGTCTGGTGTTCC
GTGGTATGAGCATTAGCCGCCCGAACGCTGTGGTTGGCCGTTGCCGTATGATTCGTCATAGCCGCGACAAGA
AAAATGAACCGAATCCTCAGCGTTTCGATCGTATCGCACACACCAAAGAAACTATGTTGAGCGACGGCTTAAA
CAGCCTGACCTATCAAGTCTTGGATGTTCAACGCTATCCGCTGTACACGCAGATTACCGTGGACATTGGCACCC
CGAGC

8.3.3. Nucleotide sequence of Δ103 hGnTI sequence used in this study.

GCGGTGATTCCGATCCTGGTCATTGCGTGTGACCGTTCGACCGTGCGTCGTTGCCTGGATAAACTGTTGCATT
ACCGCCCGTCTGCCGAGCTGTTTCCAATCATTGTTTCTCAAGACTGCGGCCATGAGGAAACCGCTCAAGCGAT
CGCAAGCTATGGTAGCGCGGTTACGCACATCCGCCAGCCGGATCTGTCCAGCATCGCGGTTCCGCCGGATCAC
CGCAAATTCCAAGGTTACTACAAAATTGCGCGTCATTATCGTTGGGCGCTGGGTCAGGTATTTCGCCAGTTTC
GCTTTCCGGCAGCGGTCGTCGTCGAGGATGATCTGGAGGTTGCCCCAGACTTCTTCGAGTACTTCCGTGCGAC
GTATCCGTTGCTGAAGGCAGATCCGTCCCTGTGGTGCGTCAGCGCGTGGAATGATAACGGTAAAGAGCAGAT
GGTGGATGCCAGCCGTCCTGAACTGCTGTACCGTACCGACTTCTTTCCGGGCCTGGGTTGGCTGCTGTTGGCT
GAACTGTGGGCGGAACTGGAGCCGAAGTGGCCGAAAGCATTTTGGGACGATTGGATGCGTCGCCCGGAACA
GCGCCAGGGCCGTGCCTGTATTCGCCCGGAGATTAGCCGCACCATGACGTTTGGTCGCAAGGGCGTGAGCCA
CGGCCAGTTCTTTGACCAGCATCTGAAATTCATTAAGCTGAATCAGCAATTCGTTCACTTCACCCAACTGGACC
TGAGCTACTTGCAACGTGAGGCGTATGATCGTGACTTCTTGGCGCGTGTCTATGGTGCTCCGCAACTGCAAGT
CGAGAAAGTGCGCACGAACGATCGTAAGGAGCTGGGTGAGGTGCGCGTGCAGTACACCGGCCGTGACAGCT
TTAAGGCCTTCGCCAAGGCGCTGGGCGTCATGGACGACCTGAAAAGCGGCGTTCCTCGTGCGGGTTATCGTG
GTATTGTGACCTTTCAGTTCCGTGGTCGTCGCGTTCATCTGGCACCGCCGCTGACCTGGGAAGGCTACGACCC
GAGCTGGAAC